



proceedings

The 8th GOSPEL Workshop. Gas Sensors Based on Semiconducting Metal Oxides: Basic Understanding & Application Fields

20-21 June 2019

Ferrara, Italy

agenda.infn.it/event/17310/

Volume 14 · GOSPEL-2019



mdpi.com/journal/proceedings
ISSN 2504-3900

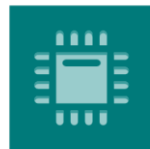
Conference Organizers



**Università
degli Studi
di Ferrara**



Partners



sensors

an Open Access Journal by MDPI

Sponsors



SACMI



FONDAZIONE
BRUNO KESSLER

Previous GOSPEL Workshops

2017: Seoul, Korea

2015: Tübingen (Germany)

2013: Yufuin Sansuikan, Oita, Japan

2011: Tuebingen, Germany

2009: Tuebingen, Germany

2008: Tuebingen, Germany

2007: Tuebingen, Germany

Table of Contents

Welcome Message	1
Steering Committee and Organizing Committee	2
Exhibitors	3
General Information	4
About—Venue	5
About—Social Dinner	8
Guidelines for Authors	9
Scientific Programme	10
Invited Speakers	14
Indexing of Oral Presentations	15
Indexing of Posters Presentations	17
List of All Papers	19

Welcome Message

Dear Colleagues,

It is a pleasure to welcome you to Ferrara for GOSPEL 2019. We are proud to organize the 8th edition of this Workshop series, which is hosted for the first time in Italy.

GOSPEL is an international biannual research meeting dedicated to R&D activities in the field of semiconducting metal-oxide gas sensors. Indeed, research studies on gas sensors based on semiconducting metal oxides are under continuous evolution about both materials and potential applications.

It is a great honor for us to bring such important scientific gathering in our country, which boasts a good number of consolidated research groups on these topics.

Special aim of GOSPEL is to bring together academia and industry and help the latter to identify the new research developments that may be most relevant to it.

We hope that the union between the presentation of scientific studies and exhibitions by startups and technology companies will lead the attendees to a deepened and improved understanding on semiconducting metal-oxide and a state-of-the-art update on applications about gas sensors.

Vincenzo Guidi

Workshop Chair

Steering Committee

Jong-Heun Lee—Korea University, Republic of Korea

Nicolae Barsan—University of Tübingen, Germany

Kengo Shimanoe—Kyushu University, Japan

Kuniyuki Izawa—Figaro Engineering, Japan

Eduard Llobet—Universitat Rovira i Virgili, Spain

Vincenzo Guidi—University of Ferrara, Italy

Geyu Lu—Jilin University, China

Johannes Buehler—Sensirion AG, Switzerland

Nikolay Samotaev—National Research Nuclear University “MEPhI”, Moscow, Russia

Organizing Committee

<https://agenda.infn.it/event/17310/page/2425-organizing-committee>



Vincenzo Guidi
Chair



Cesare Malagù



Barbara Fabbri

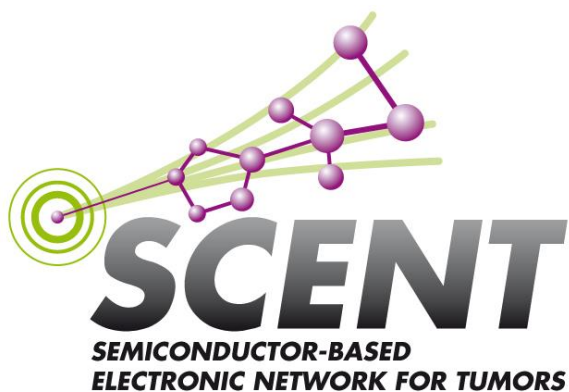


Matteo Valt

Exhibitors



FONDAZIONE
BRUNO KESSLER



General Information

CONFERENCE LANGUAGE

The official conference language is English.

BADGES & VOUCHERS

Badges must always be visibly worn during the scientific sessions, the coffee and lunch breaks as well as the poster session at the conference site.

Please make sure to bring the voucher for the congress dinner and deliver it at the conference staff.

The voucher is valid for one person only and is not transferable.

Attendees who declared restrictions for food (such as vegetarian menu or others) will find a special voucher in their badge to exhibit at their place during the social dinner, in order to support the catering staff.

COFFEE AND LUNCH BREAKS

The conference fee includes admission to the scientific programme, poster sessions and exhibitions, the congress documentation, refreshments and snacks during the coffee and lunch breaks, the participation to the social dinner.

INTERNET AND WLAN

A WLAN code will be provided on site to each attendee and it will be valid during the whole conference. Moreover, the conference area is covered by Eduroam service.

CERTIFICATE OF ATTENDANCE

The certificate of attendance will be provided during registration.

PERSONS WITH SPECIAL NEEDS

Should you require any specific assistance, please let us know how to assist in making your stay at the conference pleasant and comfortable.

EMERGENCY NUMBER:

Emergency telephone number: 112

About—Venue

The 8th GOSPEL Workshop will be held in Ferrara, a historical city in northern-east Italy, founded as a Bizantine castrum in the VI century and undergoing a time of splendor and international attractiveness during the dukedom ruled by the Estense family in the XV-XVI centuries.

Ferrara, with a population of 130.000, is a cyclist and pedestrian-friendly city with a high quality of life. It is also a lively cultural centre.

The Estense Duchy acted as a patron to some of the most important scholars and artists of that time.

In 1995, UNESCO granted the city World Heritage status as an example of a city planned in the Renaissance still keeping its historical centre intact, surrounded by more than 9 kilometres of ancient walls.

Reminiscences of the Middle Ages and the Renaissance live on in palaces, churches and museums.

Yearly events include:

- the Palio: celebrations, parades, flag-throwing competitions and a spectacular horse race in the city center;
- Buskers Festival: the world biggest event dedicated to street performance;
- ‘Internazionale’ Festival: lectures and meetings regarding international politics and economy involving journalists and authors from all over the world;
- 1000 Miglia: a vintage car race throughout Italy

The University of Ferrara, founded in 1391, is one of the oldest universities in Italy. Prominent figures such as Copernicus and Paracelsus studied here.

Today, its twelve Departments offer some fifty-degree programmes, ranging from Architecture to Design, from Medicine to Engineering, from Physics to Biotechnologies and Literature.

The quality of education and research, and the facilities available to students and guests, make Ferrara a top-ranking University in Italy.

The whole city is a dynamic campus, fostering interaction among national and international students.



Source: <https://commons.wikimedia.org>

The Workshop will be organized by the University of Ferrara and the National Institute of Nuclear Physics (INFN, Ferrara), over two full days—20th and 21th of June 2019.

<http://www.unife.it>

Department of Physics and Earth Sciences:

http://fst.unife.it/en?set_language=en

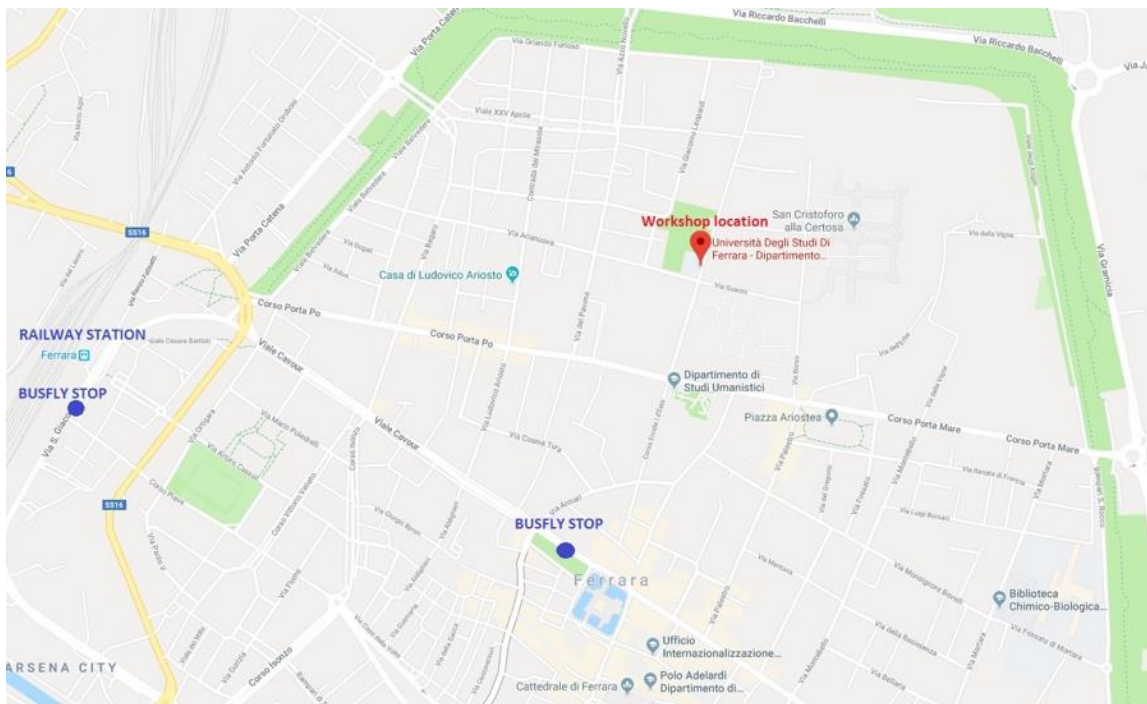
Institute of Nuclear Physics in Ferrara:

<http://www.fe.infn.it/>



Source: <http://www.giuri.unife.it>

All oral contributions will be held in the “Aula Magna” of Palazzo Trotti-Mosti (Juridical Science Department), along the historical Avenue Corso Ercole I D’Este 37, Ferrara.



Coffee breaks, lunches and Posters session will be held in “Sala Acquario” of Palazzo Giordani, Avenue Corso Ercole I D’Este 44-46, placed in front of Palazzo Trotti-Mosti.



Source: <http://www.giuri.unife.it>

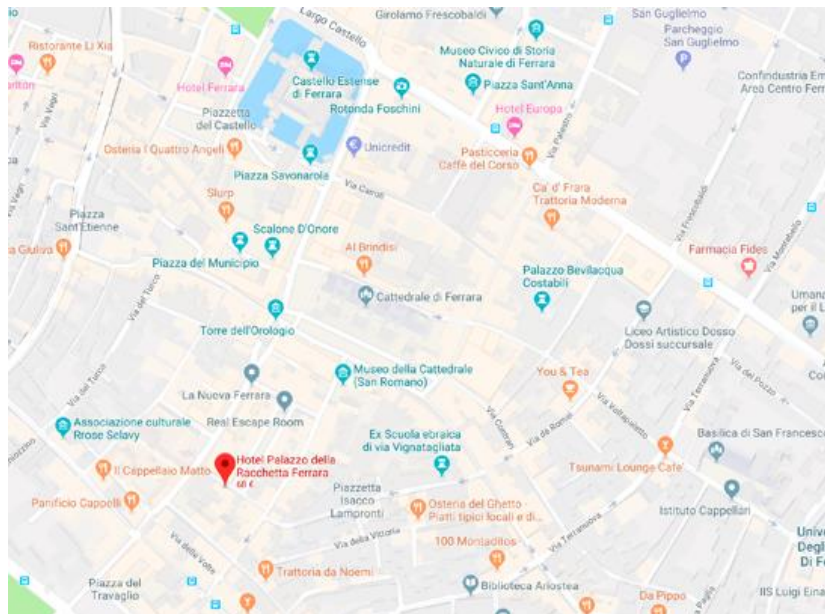
About—Social Dinner

The conference dinner will be held at Racchetta Palace. The palace, probably dates back to the 13th-century, is located on the heart of the medieval centre of Ferrara. The halls can accommodate from 60 to 220 seats. Thanks to restoration activities the halls still maintain a medieval atmosphere: the suitable place for art exhibitions and cultural events.



Address: Via Vaspergolo, 4/6, 44121 Ferrara FE

Website: <http://www.dimoralaracchetta.it/>



Guidelines for Authors

Oral Presentation Guidelines:

Please, note that speakers will have to bring their presentation on USB flash drives. Own laptops can be used only in exceptional cases. Speakers must show up in the room of their session during the break latest 20 minutes before the start of their session to upload their files and check compatibility. Assistants are in the session room for technical support if required. Speakers are advised to embed all fonts in their PowerPoint file and to bring a backup PDF-version of their presentation.

Poster Presentation Guidelines:

The Author can attach posters starting from 8:00 am on 20th June. The posters must remain attached during the entire conference. The poster format is A0 (84.1 cm × 118.9 cm), portrait orientation (height > width); suitable tape will be provided for attaching the posters.

The assigned placement of each poster is marked on the panel with the ID poster number corresponding to the abstract ID number assigned during the submission process.

Posters will be placed in “Sala Acquario” of Palazzo Giordani, Avenue Corso Ercole I D’Este 44-46, placed in front of Palazzo Trotti-Mosti.

8th GOSPEL Workshop

Registration (08:00-09:00)

Opening Ceremony (08:45-09:00)

Session 1 - Fundamental understanding - General (09:00-10:50)

Chair: Eduard Llobet

09:00	Application runs the show: what can we learn about the future from the past?	BARSAN, Nicolae
09:30	Monitoring Surface Stoichiometry, Work Function and Valance Band of Tungsten Oxide (WO ₃), Molybdenum Oxide (MoO ₃) and Tin Oxide (SnO ₂) Thin Films as a Function of Temperature and Oxygen Partial Pressure with Advanced Surface Sensitive Techniques for Chemical Sensing Applications	ENGIN, Ciftiyurek
09:50	How the gas flow affects conductometric sensor performance	GARCIA M. , Gemma
10:10	Heterogeneous integration of metal oxides – towards a CMOS based multi gas sensor device	KOECK, Anton
10:30	Consideration for oxygen adsorption species on SnO ₂ semiconductor gas sensors	SHIMANOE, Kengo

Coffee Break (10:50-11:10)

Session 2 - Advanced materials – Nanomaterials (11:10-13:00)

Chair: Jong-Heun Lee

11:10	Gas Sensors Based on Oxide Semiconductors with Porous Nanostructures	PENG, Sun
11:40	H ₂ S sensing properties of a diode-type device using ZnO nanorods coupled with CuO nanocrystals	KIDA, Tetsuya
12:00	Metal Oxides and Noble Metal Additives in the Nanocrystalline Regime. Enhancement of the Performances of Chemoresistive Gas-Sensors and Novel Interpretation Issues	EPIFANI, Mauro
12:20	Gas sensing optimization of NiO-SCCNTs core-shell nanostructures by atomic layer deposition	PINNA, Nicola
12:40	A Multi-MOx Sensor Approach to Measure Oxidizing and Reducing Gases	DANESH, Ehsan

8th GOSPEL Workshop

Lunch (13:00-14:00)

Session 3 - New devices – MEMS (14:00-15:30)

Chair: Kuniyuki Izawa

14:00	Ultra-Low Power MEMS Gas Sensor Technology and Applications	NISHIUE, Yoshinori
14:30	A flexible room-temperature NH ₃ sensor for ultrasensitive, selective, and humidity-independent gas detection *	LEE, Jong-Heun
14:50	Testing the Reliability of Flexible MOX Gas Sensors Under Strain	LLOBET, Eduard
15:10	Rapid Prototyping of MOX Gas Sensors in Form-factor of SMD Packages	SAMOTAEV, Nikolay

Coffee Break (15:30-15:50)

Session 4 - Fundamental understanding – Photostimulation (15:50-17:20)

Chair: Kengo Shimano

15:50	Micro Light Plates for Photoactivated Micro-Power Gas Sensors	PRADES, J Daniel
16:20	Luminescence Probing of Surface Adsorption Processes Using InGaN/GaN Nanowire Heterostructure Arrays	MÜLLER, Gerhard
16:40	Shining light on indium oxide gas sensors at work: A combined operando Raman / UV-Vis / FT-IR spectroscopic study	HESS, Christian
17:00	The influence of temperature and visible light activation on the NO₂ response of WO₃ nanofibers prepared by electrospinning	PAOLUCCI, Valentina

Poster Session: Poster Session (17:20-18:20)

Social Dinner (19:30-21:30)

8th GOSPEL Workshop

Session 5 - Advanced materials (08:30-10:20)

Chair: Geyu Lu

08:30	Self-heated graphene microchannels for low-power-consumption chemoresistive sensor array	JANG, Ho Won
09:00	Metal oxide decorated graphene for high sensitivity applications *	RODNER, Marius
09:20	Oxide Semiconductor Gas Sensors with Nanoscale Catalytic Overlayer: Toward Highly Selective and Sensitive Gas Detection using Bilayer Design *	LEE, Jong-Heun
09:40	Branch-like NiO-based p-n heterostructures with enhanced gas sensing properties *	ZAPPA, Dario
10:00	Low-power, multiplexed MEMS gas sensor array by local liquid phase reaction*	PARK, Inkyu

GOSPEL 2019 Official Photo (10:20-10:35)

Coffee Break (10:35-10:55)

Award Cerimony (10:55-11:30)

Session 6 - Fundamental understanding - High sensitivity (11:30-13:00)

Chair: Nikolay Samotaev

11:30	Ultra-high sensitive (ppt) gas sensor based on the pulse heating using MEMS technique	SUEMATSU, Koichi
12:00	Nanocrystalline LaCoO ₃ modified by Ag nanoparticles with improved sensitivity to H ₂ S	MARIKUTSA, Artem
12:20	Realizing the Control of Fermi Level and Gas-Sensing Selectivity over Gallium-Doped In ₂ O ₃ Inverse Opal Microspheres	WANG, Tianshuang
12:40	Sub-ppm NO ₂ sensing in temperature cycled mode with Ga doped ZnO thin films deposited by RF sputtering	PRESMANES, Lionel

Lunch (13:00-14:00)

Session 7 - New devices – Applications (14:00-16:10)

Chair: Veronica Sberveglieri

14:00	Metal Oxide Sensors Applied to Industrial and Consumer Applications: Examples and Requirements for Successful Implementation	STENZEL, Adrian
14:30	Application of a micro-machined electronic nose to detect Escherichia coli in human urine samples	SOPRANI, Matteo
14:50	SACMI Electronic Olfactory System based on Semiconducting Metal Oxides	MARZOCCHI, Marco
15:10	Identification of poisonous mushrooms by means of a hand-held electronic nose	LOZANO, Jesus
15:30	MOX sensors to ensure suitable parameters of grated Parmigiano Reggiano Cheese	ABBATANGELO, Marco
15:50	Campilobacter jejuni monitoring, from in vitro to in vivo scenario*	NÚÑEZ-CARMONA, Estefanía

Coffee Break (16:10-16:30)

Session 8 - New devices – Application (16:30-18:20)

Chair: Lionel Presmanes

16:30	Selective detection of hydrogen and hydrogen containing gases with metal oxide gas sensor operating in non-stationary thermal regime	VASILIEV, Alexey
17:00	SnO ₂ -based gas sensor for detection of refrigerant gases	IZAWA, Kuniyuki
17:20	Rare-earth based chemoresistive CO ₂ sensors and their operando investigations	SUZUKI, Takuya
17:40	Comparative Analysis between Blood Test and Breath Analysis using Sensors Array for Diabetic Patients	BYUN, Hyung-Gi
18:00	Selective detection of hydrocarbons in real atmospheric conditions by single MOX sensor in temperature modulation mode	KRIVETSKIY, Valeriy

Workshop Closing (18:20-18:30)

* Document not available in this electronic conference book since author did not agree with online publication. The attendees to GOSPEL 2019 can download the abstract of this scientific contribution at the dedicate link sent by mail.

Invited Speakers

Nicolae Barsan, Institute of Physical Chemistry, University of Tuebingen (ipc)—*Application Runs the Show: What Can We Learn about the Future from the Past?* †

Ho Won Jang, Seoul National University, Department of Materials Science and Engineering—*Self-Heated Graphene Microchannels for Low-Power-Consumption Chemoresistive Sensor Array* †

Yoshinori Nishiue, New Cosmos Electric Co Ltd—*Ultra-Low Power MEMS Gas Sensor Technology and Application* †

Sun Peng, Jilin University, College of Electronic Science and Engineering—*Gas Sensors Based on Oxide Semiconductors with Porous Nanostructures* †

J Daniel Prades, MIND—Departament d'Enginyeria Electrònica i Biomèdica, Universitat de Barcelona—*Micro Light Plates for Photoactivated Micro-Power Gas Sensors* †

Adrian Stenzel, Integrated Device Technology, Inc. (IDT)—*Metal Oxide Sensors Applied to Industrial and Consumer Applications: Examples and Requirements for Successful Implementation* †

Koichi Suematsu, Kyushu University, Faculty of Engineering Sciences—*Ultra-High Sensitive (ppt) Gas Sensor Based on the Pulse Heating Using MEMS Technique* †

Alexey Vasiliev, Kurchatov Institute—Physical and Chemical Technology Center—Moscow—*Selective Detection of Hydrogen and Hydrogen Containing Gases with Metal Oxide Gas Sensor Operating in Non-Stationary Thermal Regime* †

Indexing of Oral Presentations

10	Monitoring Surface Stoichiometry, Work Function and Valance Band of Tungsten Oxide (WO ₃), Molybdenum Oxide (MoO ₃) and Tin Oxide (SnO ₂) Thin Films as a Function of Temperature and Oxygen Partial Pressure with Advanced Surface Sensitive Techniques for Chemical Sensing Applications †
18	Nanocrystalline LaCoO ₃ Modified by Ag Nanoparticles with Improved Sensitivity to H ₂ S †
19*	Oxide Semiconductor Gas Sensors with Nanoscale Catalytic Overlayer: Toward Highly Selective and Sensitive Gas Detection using Bilayer Design
29	H ₂ S Sensing Properties of a Diode-Type Device Using ZnO Nanorods Coupled with CuO Nanocrystals †
31	SnO ₂ -Based Gas Sensor for Detection of Refrigerant Gases †
32*	Metal Oxides and Noble Metal Additives in the Nanocrystalline Regime. Enhancement of the Performances of Chemoresistive Gas-Sensors and Novel Interpretation Issues
33	Shining light on Indium Oxide Gas Sensors at Work: A Combined <i>Operando</i> Raman/UV-Vis/FT-IR Spectroscopic Study †
36*	Metal oxide decorated graphene for high sensitivity applications
37	Realizing the Control of Fermi Level and Gas-Sensing Selectivity over Gallium-Doped In ₂ O ₃ Inverse Opal Microspheres †
41	Rare-Earth Based Chemoresistive CO ₂ Sensors and Their <i>Operando</i> Investigations †
45*	A flexible room-temperature NH ₃ sensor for ultrasensitive, selective, and humidity-independent gas detection
51*	Gas sensing optimization of NiO-SCCNTs core-shell nanostructures by atomic layer deposition
53	Application of a Micro-Machined Electronic Nose to Detect <i>Escherichia Coli</i> in Human Urine Samples †
55	The Influence of Temperature and Visible Light Activation on the NO ₂ Response of WO ₃ Nanofibers Prepared by Electrospinning †
59	Comparative Analysis between Blood Test and Breath Analysis using Sensors Array for Diabetic Patients
60	How the Gas Flow Affects Conductometric Sensor Performance
61	Testing the Reliability of Flexible MOX Gas Sensors under Strain
62	SACMI Electronic Olfactory System Based on Semiconducting Metal Oxides
65	MOX Sensors to Ensure Suitable Parameters of Grated Parmigiano Reggiano Cheese
66*	Campilobacter jejuni monitoring, from in vitro to in vivo scenario
69	Chemically Sensitive Photoluminescence of InGaN/GaN Nanowire Heterostructure Arrays †
70*	Branch-like NiO-based p-n heterostructures with enhanced gas sensing properties

74	Selective Detection of Hydrocarbons in Real Atmospheric Conditions by Single MOX Sensor in Temperature Modulation Mode †
76	Identification of Poisonous Mushrooms by Means of a Hand-Held Electronic Nose †
78	A Multi-MOX Sensor Approach to Measure Oxidizing and Reducing Gases †
79	Rapid Prototyping of MOX Gas Sensors in Form-factor of SMD Packages †
84	Sub-ppm NO ₂ Sensing in Temperature Cycled Mode with Ga Doped ZnO Thin Films Deposited by RF Sputtering †
85	Heterogeneous Integration of Metal Oxides—Towards a CMOS Based Multi Gas Sensor Device †
89	Consideration for Oxygen Adsorption Species on SnO ₂ Semiconductor Gas Sensors †
93*	Low-Power, Multiplexed MEMS Gas Sensor Array by Local Liquid Phase Reaction †

* Document not available in this electronic conference book since author did not agree with online publication. The attendees to GOSPEL 2019 can download the abstract of this scientific contribution at the dedicate link sent by mail.

Indexing of Posters Presentations

14	Flexible Gas Sensor Printed on Polymer Substrate for Acetone Detection in Portable Exhaled Breath Analyzers †
15	Surface Properties of SnO ₂ Nanolayers Deposited by Rheotaxial Growth and Vacuum Oxidation for Potential Gas Sensor Applications †
25	Semiconductor Gas Sensors to Analyze Fecal Exhalation as a Method for Colorectal Cancer Screening
26	Nanostructured Chemoresistive Sensors for Oncological Screening: Preliminary Study with Single Sensor Approach on Human Blood Samples
27	Chemoresistive Nanostructured Sensors for Tumor Pre-Screening
30	Sensing Performance of Al and Sn Doped ZnO for Hydrogen Detection †
34*	Exploration of Au Functionalized Nanocomposites for Highly Selective Gas Sensing †
35	Gas Sensing Mechanism Investigation of LaFeO ₃ Perovskite-Type Oxides via Operando Technique †
38	Optical Gas Sensors Based on Localised Surface Plasmon Resonance †
39	Selective Gas Sensor Based on Metal Oxide Nanostructure †
40	SnO ₂ -Pd as a Gate Material for the Capacitor Type Gas Sensor †
42	Regulating Adsorbed Oxygen Species and Electron Transport for SnO ₂ -Based Gas Sensors through Surface Modification and Structural Design †
47*	Gas Sensing Properties of CuO-ZnO Core-shell Nanowires
48*	Hierarchical and hollow Fe ₂ O ₃ nano-boxes derived from metal-organic frameworks with excellent sensitivity to H ₂ S
49	Light-Assisted Low Temperature Formaldehyde Detection at Sub-ppm Level Using Metal Oxide Semiconductor Gas Sensors †
50	High Temperature Resistive Gas Sensors Based on ZnO/SiC Nanocomposites †
56	Elaboration and Characterization of SnS Thin Film for Gas Sensors Application †
57	Elaboration and Characterization of CuO Thin Films by Spray Pyrolysis Method for Gas Sensors Applications
58*	Effect of compensating acceptor doping with Ni on the gas sensing of In ₂ O ₃
63*	Nickel-decorated black phosphorus for sub-ppm NO ₂ detection at room temperature
64	Work Function Measurements in Single-Crystalline In ₂ O ₃ for Conduction Modelling †
67	Investigation of the Film Thickness Influence on the Sensor Response of In ₂ O ₃ -Based Sensors for O ₃ Detection at Low Temperature and Operando DRIFT Study †
68	Gas Sensing with Porphyrin Functionalized Metal Oxide Nanostructures †
71*	Application of SiC MISFET Metal/Oxide Gas sensor for SO ₂ Detection

72	Synergistic Effect of Nanocrystalline SnO ₂ Sensitization by Bimetallic Au and Pd Modification via Ingle Step Flame Spray Pyrolysis Technique †
75	Towards the Miniaturization of Electronic Nose as Personal Measurement Systems †
77	A Novel Modular System for Breath Analysis Using Temperature Modulated MOX Sensors †
80*	Ionogel-based gas sensors for formaldehyde and benzene detection
81	Elaboration and Characterization of SnO ₂ Doped TiO ₂ Gas Sensors Deposited through Dip and Spin Coating Methods †
82	Influence of oxygen vacancies in gas sensors based on tin dioxide nanostructure: A first principles study
83	Morphological Control of Metal Oxide for Semiconductor-Based GasSensor †
90	ZnO Nanostructures for Gas Sensing Applications: From Tetrapods-Based Chemoresistive Devices to Carbon Fiber Integration †
91*	Optimization of Silicon and Quartz MEMS Microheater for Chemoresistive Gas Sensors

* Document not available in this electronic conference book since author did not agree with online publication. The attendees to GOSPEL 2019 can download the abstract of this scientific contribution at the dedicate link sent by mail.

Invited Oral Presentations

Application Runs the Show: What Can We Learn about the Future from the Past? [†]

Nicolae Barsan

Institute of Physical Chemistry, University of Tuebingen, Auf der Morgenstelle 15, D-72076 Tuebingen, Germany; nb@ipc.uni-tuebingen.de

[†] Presented at the 8th GOSPEL Workshop. Gas Sensors Based on Semiconducting Metal Oxides: Basic Understanding & Application Fields, Ferrara, Italy, 20–21 June 2019.

1. History and Current Status

SMOX-based sensors appeared as a response to a very serious safety issue in Japan, namely gas explosion accidents related to leakages of piped and bottled cooking gas. The first commercial gas sensors were self-supported beads; there were two Pt coils, one of them used as heater and with a DC resistance measurement between the two coils. The power consumption was more than 1 W [1].

SMOX-based sensors application fields were extended because of their inherent advantages—high sensitivity, low cost, good stability—and as a consequence the performance requirements evolved. At the beginning of the 1990s, the regulation of the air intake for car cabins was becoming extremely important and, because of cost issues, the miniaturization drive was gaining practical relevance [2]. Together with the additional trend of getting all household devices battery operated [3], the resulting market pull determined the appearance of the current state of the art gas sensors that are realized by depositing porous sensing layers realized by using pre-processed powders onto ceramic and MEMS substrates [4,5].

2. Future Trends

As in the past, the developments in the field are determined by the needs of the applications to be solved. Shifting from mains connected domestic gas alarms to battery operated ones will surely continue as will continue the integration of more sensors with the target to detect more gases and provide extended functionality such as fire detection and/or indoor air quality. There are already commercial devices that use SMOX gas sensors for the latter; they measure the total volatile organic compounds TVOC concentration and are giving a CO₂ equivalent output [6]. One can imagine that success in this field will make possible the large scale integration of SMOX sensors in a host of household products with the biggest prize being the integration into mobile devices such as smart phones. There are companies that are making this approach quite central to their development strategy [7]. There are also reports about successful integration of SMOX sensors in cooking hoods as fire alarms [8].

Another type of applications that are rising a lot of interest are the ones related to breath analysis, especially for the detection of diseases [9]. It was proven that it is possible to use gas sensors for measuring the NO content of alveolar air and by that to get important information about inflammatory processes in the lungs and adjust medication [10]; there are though a couple of caveats: the used gas sensor is a highly specific electrochemical cell and the sampling technique increases the complexity and the price of the instrument. Moreover, the application it serves is really well documented and even standardized [11]. Such a success is not easy to emulate because one of the intrinsic weaknesses of the SMOX sensors is their lack of selectivity. This is the reason why a lot of efforts are made for obtaining selective sensors and it is expected that this will be one of the main direction for the future R&D activities.

In what concerns the transducers, besides the approach towards miniaturization of the MEMS substrates it is expected that activities focused on the use of additives technologies and plastics will amplify with the goal of decreasing even more the costs of the gas sensors to such an extent that disposable devices will be available [2]. It was already shown that it is possible to integrate different sensing principles on foils [12]—the various transducers were obtained by using MEMS, which is a non-additive technology—so the next steps will be in the direction of developing processes compatible to roll to roll production. Such transducers will need sensing layers deposition methods that do not require high temperatures annealing.

One can conclude that, because of the application pull, the drive is towards further miniaturization, see Figure 1, and increased selectivity and sensitivity in order to make possible their integration in a host of mobile and household devices and help make possible the Internet of Things (IoT).

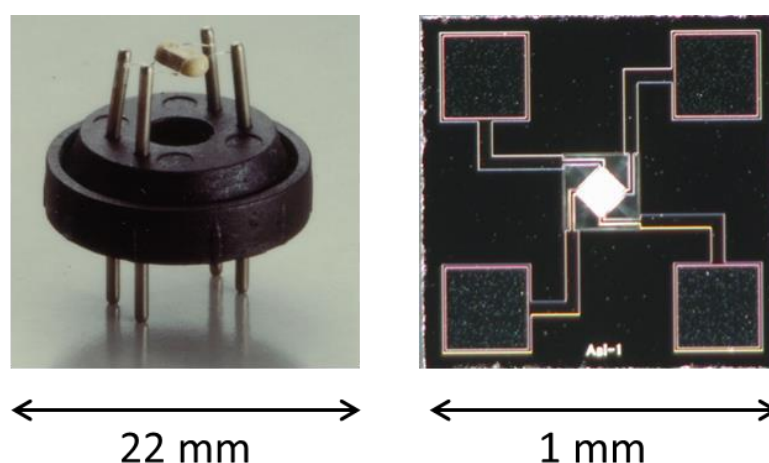


Figure 1. First and last generation of methane Figaro gas sensors (courtesy of Figaro Eng.).

References

1. Ihokura, K.; Watson, J. *Stannic Oxide Gas Sensors, Principles and Applications*; CRC Press: Boca Raton, FL, USA; Ann Arbor, MN, USA; London, UK; Tokyo, Japan, 1994; 187p.
2. Briand, D.; Courbat, J. Micromachined Semiconductor Gas Sensors. In *Semiconductor Gas Sensors*; Jaaniso, R., Tan, O.K., Eds.; Woodhead Publishing Series in Electronic and Optical Materials; Woodhead Publishing Limited: Oxford, UK; Cambridge, UK; Philadelphia, PA, USA; New Delhi, India, 2013; Chapter 6, pp. 220–260.
3. Tanihira, T.; Yoshioka, K.; Shinnishi, K.; Izawa, K.; Kaneyasu, K. Development of CH₄ Sensor Using MEMS Technology for Battery Operated Town Gas Leak Detector. *Sens. Lett.* **2011**, *9*, 414–417.
4. Simon, I.; Barsan, N.; Weimar, U.; Bauer, M. Micromachined metal oxide gas sensors: opportunities to improve sensor performance *Sens. Actuators B* **2001**, *73*, 1–26.
5. Available online: https://www.fujielectric.com/company/research_development/theme/mems_sensor.html (accessed on 1 May 2019).
6. Available online: <http://ams.com/eng/Products/Chemical-Sensors/Air-Quality-Sensors> (accessed on 1 May 2019).
7. Available online: <https://www.sensirion.com/en/environmental-sensors/gas-sensors/> (accessed on 1 May 2019).
8. Ulmer, H. In Proceedings of the 4th GOSPEL Workshop on: Gas Sensors Based on Semiconducting Metal Oxides: Basic Understanding & Applications, Tuebingen, Germany, 6–7 June 2011.
9. Di Natale, C.; Paolesse, R.; Martinelli, E. Capuano R; Solid-state gas sensors for breath analysis: A review. *Anal. Chim. Acta* **2014**, *824*, 1–7.
10. Available online: <https://www.niox.com/en/> (accessed on 1 May 2019).



11. Available online: <https://www.atsjournals.org/doi/10.1164/ajrccm.160.6.ats8-99> (accessed on 1 May 2019).
12. Oprea, A.; Courbat, J.; Briand, D.; Barsan, N.; Weimar, U.; De Rooij, N.F. Environmental monitoring with a multisensor platform on polyimide foil. *Sens. Actuators B* **2012**, *171–172*, 190–197.



© 2019 by the authors. Licensee MDPI, Basel, Switzerland. This article is an open access article distributed under the terms and conditions of the Creative Commons Attribution (CC BY) license (<http://creativecommons.org/licenses/by/4.0/>).

Abstract

Self-Heated Graphene Microchannels for Low-Power-Consumption Chemoresistive Sensor Array [†]

Ho Won Jang ^{1,*} and Soo Young Kim ²

¹ Department of Materials Science and Engineering, Seoul National University, Seoul 08826, Korea

² School of Chemical Engineering and Materials Science, Chung-Ang University, Seoul 06974, Korea; sooyoungkim@cau.ac.kr

* Correspondence: hwjang@snu.ac.kr

[†] Presented at the 8th GOSPEL Workshop. Gas Sensors Based on Semiconducting Metal Oxides: Basic Understanding & Application Fields, Ferrara, Italy, 20–21 June 2019.

The Internet of Everything (IoE) refers to billions of objects having intelligent connections with processed data. Sensors hold the key to the IoE as they detect and assess the internal and external states of objects. In particular, gas sensors contribute greatly to make people's lives better via transmitting information about gas species in ambient air. 2D materials such as graphene and transition metal disulfides are being extensively studied for gas-sensing applications due to their high sensitivity at room temperature, transparency, and flexibility. However, they have drawbacks such as low selectivity and irreversible sensing behaviors. To overcome these drawbacks, the chemoresistive sensing properties of the 2D materials have been modified by diverse approaches such as introducing extrinsic defects, functionalization, and noble metal decoration. Here, we present unprecedented gas detection using self-activated graphene microchannels with surface decoration. Joule heating by applying voltages in graphene microchannels is very effective to make the materials operate at elevated temperatures and enhance gas sensing properties such as response and recovery. Compared to pristine graphene sensors, the noble-metal-decorated graphene sensors exhibit highly improved gas-sensing properties upon exposure to various gases (Figure 1). In particular, an unexpected substantial enhancement in H₂ detection is found, which has never been reported for Au decoration on any types of chemoresistive materials. We show 2 × 2 gas sensors array based on metal-decorated graphene microchannels that operate with low power consumption without additional heaters. The discovery of such a new functionality in the existing material platform holds the key to diverse research areas based on metal nanoparticles/2D material heterostructures.

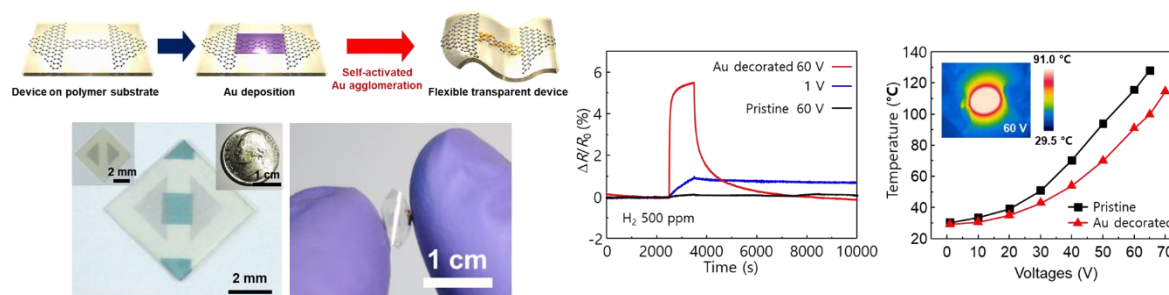


Figure 1. Transparent and flexible Au-decorated graphene microchannel gas sensor (Ref: Kim et al., *Nanoscale* **2019**, *11*, 2966-2973).



© 2019 by the authors. Licensee MDPI, Basel, Switzerland. This article is an open access article distributed under the terms and conditions of the Creative Commons Attribution (CC BY) license (<http://creativecommons.org/licenses/by/4.0/>).

Abstract

Ultra-Low Power MEMS Gas Sensor Technology and Application [†]

Yoshinori Nishiue

New Cosmos Electric CO., LTD. 2-5-4 Mitsuyanaka, Yodogawaku, OSAKA, 532-0036, Japan;
nishiue.yoshinori@new-cosmos.co.jp

[†] Presented at the 8th GOSPEL Workshop. Gas Sensors Based on Semiconducting Metal Oxides: Basic Understanding & Application Fields, Ferrara, Italy, 20–21 June 2019.

The semiconductor type sensor developed by New Cosmos is a very unique sensor depending on its principle and structure. This sensor is called a hot wire type semiconductor sensor (CH). By integrating the detection element and the heater, the two terminals have a simple structure. Therefore, it is excellent in mass production. The resistance is as low as several ohms, and it has high sensitivity and brings about large output change.

The biggest disadvantage of this sensor was its high power consumption. It was not suitable for battery operation. In 2012, we succeeded in miniaturizing the CH sensor using the MEMS technology, and completed the Ultra-Low power MEMS CH sensor (MCH) (Figure 1).

In the U.S., urban gas piping infrastructure is deteriorating due to age and environmental factors. There is a growing need to monitor this aging infrastructure to prevent dangerous explosion risks. Many of the locations where monitoring is required do not have electricity to power a traditional gas detector. The ultra-low power MEMS sensor technology is enabling utility companies to install these products in places where they previously could not be installed. This is enhancing public safety.

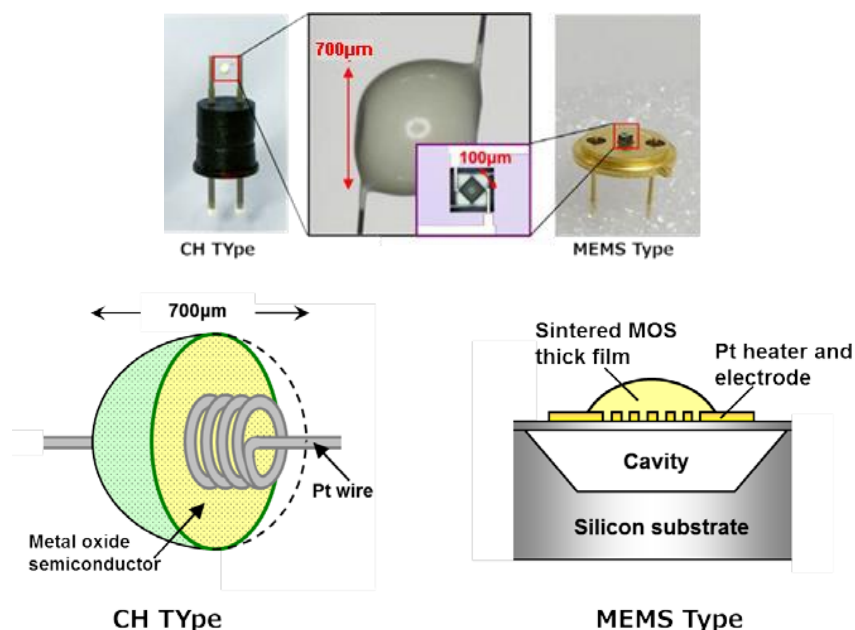


Figure 1. Structural drawing CH & MEMS TYPE.



Figure 2. Final Product.

- 5 year sensor life
- 5 year battery life
- GTI tested for nuisance alarm immunity
- UL1484 certified and FCC certified
- Alarms at methane concentration of 10% LEL
- Provides 85 dB audible alarm
- Communicates through wireless mesh network
- First of its kind device worldwide.

Until now, it was not possible to monitor gas leaks in areas without AC power. The MEMS technology has allowed for a battery powered methane detector, and it is now possible to monitor for gas leak hazards in more locations. Additionally, the wireless technology notifies authorities of emergencies immediately. This product (Figure 2) is currently being installed in New York City, and has already detected several potentially dangerous leaks. This has enhanced the safety of the residents of New York City and is helping New Cosmos achieve our goal of eliminating injury and property damage due to gas accidents in the world.



© 2019 by the authors. Licensee MDPI, Basel, Switzerland. This article is an open access article distributed under the terms and conditions of the Creative Commons Attribution (CC BY) license (<http://creativecommons.org/licenses/by/4.0/>).

Abstract

Gas Sensors Based on Oxide Semiconductors with Porous Nanostructures [†]

Peng Sun

College of Electronic Science and Engineering, State Key Laboratory on Integrated Optoelectronics, 2699 Qianjin Street, Changchun 130012, China; pengsun@jlu.edu.cn

[†] Presented at the 8th GOSPEL Workshop. Gas Sensors Based on Semiconducting Metal Oxides: Basic Understanding & Application Fields, Ferrara, Italy, 20–21 June 2019.

Abstract

Gas sensor as a device composed of sensing material coupled with signal transducer, has been acknowledged as an analytical tool for detection and quantification of inflammable, explosive or toxic gases. The gas sensors based on nanostructured oxide semiconductor endowed with excellent sensing properties have exhibited great potential application in the fields of environmental monitoring, resource exploration, medical welfare, etc. It is well known that the sensing mechanism of sensor employing oxide semiconductors is mainly that the interactions between the surface adsorbed oxygen species and target gases lead to a change in the electrical conductivity. Therefore, the gas sensing properties of oxide semiconductors are closely related with their composition, crystalline size, and microstructure. In this regard, design and preparation of oxides with novel architectures will be increasingly important in the construction of high performance gas sensors. Due to high specific surface area, low density, and good surface permeability, porous nanostructures oxide semiconductor sensing materials have attracted growing interest in recent years. In our work, we successfully prepared various porous nanostructures oxides and their composites to the construction of high performances gas sensors with enhanced sensitivity, selectivity, as well as lowered detection limit. The subsequent gas sensing measurements explicitly revealed that these oxides and composites manifested superior sensing behaviors (like much higher sensitivity and faster response speed), which can be ascribed to the porous architectures and the synergistic effects.



© 2019 by the authors. Licensee MDPI, Basel, Switzerland. This article is an open access article distributed under the terms and conditions of the Creative Commons Attribution (CC BY) license (<http://creativecommons.org/licenses/by/4.0/>).

Extended Abstract

Micro Light Plates for Photoactivated Micro-Power Gas Sensors [†]

Olga Casals ¹, Nicolai Markiewicz ^{1,2,3}, Cristian Fabrega ¹, Isabel Gràcia ⁴, Carles Cané ⁴, Hutomo Suryo Wasisto ^{2,3}, Andreas Waag ^{2,3} and J. Daniel Prades ^{1,*}

¹ MIND-IN²UB, Department of Electronic and Biomedical Engineering, Universitat de Barcelona, Barcelona, E-08028, Spain; ocasals@el.ub.edu (O.C.); n.markiewicz@tu-braunschweig.de (N.M.); cfabrega@el.ub.edu (C.F.)

² IHT-LENA, Technische Universität Braunschweig, Braunschweig, D-38106, Germany; h.wasisto@tu-braunschweig.de (H.S.W.); a.waag@tu-braunschweig.de (A.W.)

³ Epitaxy Competence Center (ec²), Technische Universität Braunschweig, Germany

⁴ IMB-CNM (CSIC), Institut de Microelectrònica de Barcelona, Cerdanyola del Vallès, E-08193, Spain; isabel.gracia@imb-cnm.csic.es (I.G.); carles.cane@imb-cnm.csic.es (C.C.)

* Correspondence: dprades@el.ub.edu

[†] Presented at the 8th GOSPEL Workshop. Gas Sensors Based on Semiconducting Metal Oxides: Basic Understanding & Application Fields, Ferrara, Italy, 20–21 June 2019.

Abstract: In this contribution we present a highly miniaturized device that integrates a photoactive material with a highly efficient LED light source. This so-called micro light plate configuration (μ LP) allows for maximizing the irradiance impinging on the photoactive material, with a minimum power consumption, excellent uniformity and accurate control of the illumination. We demonstrate that, with the μ LP approach, very efficient low power gas sensors can be built, and provide a detailed analysis of the rationales behind such improvement, as well as a quantitative model and a set of design rules to implement it in further integrated applications. As a demonstrator, we will describe a NO₂ gas sensor operating in the part per billion range (ppb) with microwatt (μ W) power consumption. These are the best figures reported to date in conductometric metal-oxides (MOX) sensors operated with light (instead of heat) at room temperature.

1. Motivation

Conventional conductometric MOX-based gas sensors operate at relatively high temperatures (few hundred °C) to activate the interaction between the target gas molecules and the sensor material. This leads to important power needs, with values of ~ 10 mW for the most optimized/miniaturized “micro-hot-plate” configurations [1]. Light is known as an alternative path to achieve such activation [2], but most implementations to date are bulky and based on discrete components, lacking power efficiency and optimized irradiance/response ratios (Figure 1a). Here, we present the new “micro-light-plate” (μ LP) approach [2]: a sensor configuration built around a miniaturized LED (Figure 1a). This represents one of the few efforts made to date to produce wafer-scale integrated illuminated sensors [3,4], and the one rendering the best performances, by more than 3 orders of magnitude (from tens of mW to tens of μ W) [5].

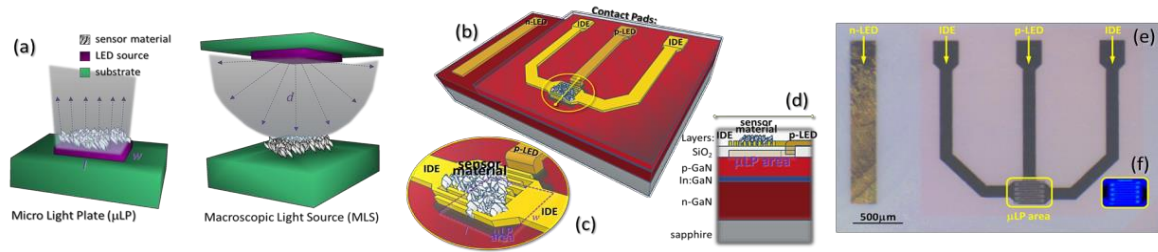


Figure 1. (a) Comparison between the Micro Light Plate (μ LP) proposed in this work and the conventional light spreading scenario (Macroscopic Light Source). (b) Schematic view of the μ LP devices. (c) Detailed view of the μ LP area containing the active LED region, the IDEs, and the sensor material. (d) Cross section of the device structure across the μ LP area. (a–d) Adapted from Ref. [2], with the permission of AIP Publishing. (e) Optical microscopy image of the actual μ LP devices as fabricated, and (f) with the LED lit on.

2. Methods

In the μ LP (Figure 1b–d), the sensor material is placed directly on top of a planar LED structure (InGaN, 455 nm peak emission), only separated by a few hundred nanometers (350 nm) to insulate it electrically (SiO_2). Consequently, almost all the light emitted by the LED impinges on the sensor MOX, allowing for very well controlled, uniform and high irradiances, with reduced electrical power consumption. For demonstration purposes, the sensor material we choose were ZnO nanoparticles deposited on the μ LP on top of a pair of Interdigitated Electrodes (IDE) made of Au (Figure 1b–f). Theory showed that, in order to achieve an optimum performance in terms of power consumption, the LED emission area must match the area of the sensor material (in size and shape). In our case, the active area was a rectangle of $190 \mu\text{m} \times 250 \mu\text{m}$.

3. Results

Figure 2a shows an example of the resistance records measured in the presence of NO_2 in increasing concentrations, from 25 ppb to 1 ppm. Figure 2b summarizes the responses obtained under different irradiance levels, showing a complex bell-shaped response that is fully explained by the balance between the adsorption and desorption of oxidizing molecules from the surface by the action of the impinging photons [6]. Remarkably, at the lowest concentrations investigated, responses above 20% were obtained, with just 30 μW of electrical power applied to the LED in the μ LP. At the optimum irradiance levels, peak responses of more than 90% to 25 ppb were found. In these conditions, with a noise-to-signal level of 3%, even concentrations below 1 ppb could theoretically be detected.

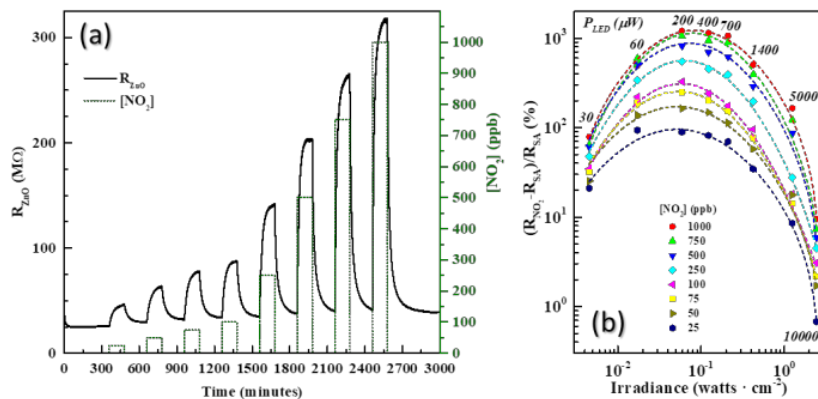


Figure 2. (a) Resistance record of the response to NO_2 and (b) summary of the responses obtained under different irradiance levels (and thus power consumption). Electrical power applied to the LED at each irradiance level is indicated in italics labels. Lines corresponds to qualitative fittings to existing models in the literature [6]. Data taken from Ref. [5].

References

1. Elmi, I.; Zampolli, S.; Cozzani, E.; Mancarella, F.; Cardinali, G.C. Development of ultra-low-power consumption MOX sensors with ppb-level VOC detection capabilities for emerging applications. *Sens. Actuators B Chem.* **2008**, *135*, 342.
2. Prades, J.D.; Wasisto, H.S.; Markiewicz, N.; Cané, C.; Fabrega, C.; Waag, A.; Casals, O.; Gràcia, I. Micro light plates for low-power photoactivated (gas) sensors. *Appl. Phys. Lett.* **2019**, *114*, 053508.
3. Espid, E.; Taghipour, F. UV-LED Photo-activated Chemical Gas Sensors: A Review. *Crit. Rev. Solid State Mater. Sci.* **2017**, *42*, 416.
4. Wang, C.Y.; Cimalla, V.; Kups, T.; Röhligh, C.C.; Stauden, T.; Ambacher, O.; Kunzer, M.; Passow, T.; Schirmacher, W.; Pletschen, W.; et al. Integration of In₂O₃ nanoparticle based ozone sensors with GaInN/GaN light emitting diodes. *Appl. Phys. Lett.* **2007**, *91*, 1.
5. Casals, O.; Markiewicz, N.; Fabrega, C.; Gracia, I.; Cané, C.; Wasisto, H.S.; Waag, A.; Prades, J.D. A Parts Per Billion (ppb) Sensor for NO₂ with Microwatt (μ W) Power Requirements based on Micro Light Plates. *ACS Sens.* **2019**, *4*, 822.
6. Prades, J.D.; Jimenez-Diaz, R.; Manzanares, M.; Hernandez-Ramirez, F.; Cirera, A.; Romano-Rodriguez, A.; Mathur, S.; Morante, J.R. A model for the response towards oxidizing gases of photoactivated sensors based on individual SnO₂ nanowires. *Phys. Chem. Chem. Phys.* **2009**, *11*, 10881.



© 2019 by the authors. Licensee MDPI, Basel, Switzerland. This article is an open access article distributed under the terms and conditions of the Creative Commons Attribution (CC BY) license (<http://creativecommons.org/licenses/by/4.0/>).

Metal Oxide Sensors Applied to Industrial and Consumer Applications: Examples and Requirements for Successful Implementation [†]

Debra J. Deininger

IDT, a Renesas Company, 2605 Trade Centre Ave, Suite C, Longmont, CO 80503, USA;
Debra.Deininger@idt.com; Tel.: +1-303-669-8194

[†] Presented at the 8th GOSPEL Workshop. Gas Sensors Based on Semiconducting Metal Oxides: Basic Understanding & Application Fields, Ferrara, Italy, 20–21 June 2019.

1. Abstract

Metal Oxide (MOx) sensors have been the subject of intense research and development over the years, and are widely used in industrial and commercial sensing applications. This talk will review the application of such gas sensors for industrial and consumer applications, with a focus on the requirements for successful implementation.

MOx sensors have several advantages over other competing sensor technologies in industrial and consumer applications. These sensors offer a highly reliable platform with long lifetimes, which is able to withstand temperature and humidity extremes without damage. Furthermore, MOx sensors can be produced with excellent economies of scale, especially when modern manufacturing methods are leveraged for silicon micro-hotplates.

The successful implementation of MOx sensors in industrial and consumer applications requires consideration of both the application and the technology. The most important items are discussed here.

2. Application of MOx Sensors to Industrial and Commercial Applications—Keys to Success

There are three key aspects to consider when matching MOx sensors to applications: (1) understanding the full application requirements, (2) designing the sensor, including selection of MOx materials and processing, and (3) developing the product, including the design of supporting electronics, calibration (if used) and algorithms to transduce the raw sensor signal (resistance) into useful information. The key to success is balancing the application requirements with both the benefits and limitations of the underlying technology. If the requirements and technology are well matched, then the end user/product is provided with useful and reliable information than benefits the person/product.

3. Understanding the Application

The most important key to success in the deployment of MOx sensors is always to understand the application. MOx sensors are fundamentally non-selective, so the first and most critical factors to understand are what gas(es) are expected to be in the environment and at what concentrations they should be detected, and equally important, what gas(es) are expected to be in the environment at concentrations that should not trigger a response. The environmental conditions, including temperature, humidity and barometric pressure should also be considered. The necessary information can be acquired from customer interactions, first-hand experience, literature review, or a combination of all of these sources.

Another thing to consider is what the desired information output is, and how the end user or product will act upon the information. Is an absolute measurement of concentration required, or would relative concentration or rate of change be more useful? Will the sensor be used in a numeric display, or to trigger a warning or mechanical device? What are the response time, accuracy and precision requirements? Over-specification of requirements, or defining accuracy and precision more tightly than actually required should be avoided, as this will drive unnecessary system costs, while under-specification leads to disappointed or unhappy customers, which should also be equally avoided.

4. MOx Materials Selection and Design

Following a clear definition of the application and requirements, the MOx sensor design begins. There are a range of interesting materials and fabrication methods that have been promoted in the literature by commercial sensor developers. While sensitivity to the target gas(es) is required, there are some important additional criteria that also need to be established.

First, the sensors must be validated under the expected application conditions, including all gases and environmental variations uncovered in the application review. Sufficient quantities of sensors must be characterized under the expected application conditions to establish both sensor reproducibility and stability. In consumer and industrial applications, expectations of performance are measured in years, so particular attention to long-term stability and potential drift and failure modes is required.

The MOx material and deposition process, as well as the sensor substrate must be designed and characterized for reproducibility in high volume manufacturing. As gas testing is not a standard industrial process for most sensor and semiconductor manufacturers, particular attention should be focused on selection of final test method and conditions, including sensor calibration, if implemented.

5. Product Development

The final aspect of development to be considered is the development of a final product. While a stable and reliable MOx material and sensor is a necessary requirement for a good product, it is not sufficient to enable the final product.

The electronics used to control the MOx sensor heater, and to measure the resistance, should be considered, including the necessity for design of accurate heater control and the ability to measure large variations in resistance, depending on the MOx material used.

The sensor response will need to be converted from resistance to information, such as ppm, air quality level, or perhaps rate and magnitude of signal change if the sensor is used in a process control application. Methods of managing sensor aging and drift, coupled with the model used to convert between resistance and concentration, will greatly affect results.

6. Example Implementations

The oral presentation will cover two examples of sensor implantation in real world applications, air quality and breath measurements. The above factors will be discussed in the context of real-world data and decision making.

Funding: This research received no external funding.

Acknowledgments: The author thanks her employer, IDT, and the talented team of individuals working in the gas sensor development team for support.

Conflicts of Interest: The author declares no conflict of interest.



© 2019 by the authors. Licensee MDPI, Basel, Switzerland. This article is an open access article distributed under the terms and conditions of the Creative Commons Attribution (CC BY) license (<http://creativecommons.org/licenses/by/4.0/>).

Ultra-High Sensitive (ppt) Gas Sensor Based on the Pulse Heating Using MEMS Technique [†]

Koichi Suematsu ^{1,*}, Wataru Harano ², Yuki Hiroyama ², Ken Watanabe ¹ and Kengo Shimano ¹

¹ Department of Advanced Materials Science and Engineering, Faculty of Engineering Sciences, Kyushu University, Kasuga, Fukuoka 816-8580, Japan; watanabe.ken.331@m.kyushu-u.ac.jp (K.W.); shimano.kengo.695@m.kyushu-u.ac.jp (K.S.)

² Department of Molecular and Material Science, Interdisciplinary Graduate School of Engineering Science, Kyushu University, Kasuga, Fukuoka, 816-8580, Japan; 2ES17131E@s.kyushu-u.ac.jp (W.H.); hiroyama.yuki.356@s.kyushu-u.ac.jp (Y.H.)

* Correspondence: suematsu.koichi.682@m.kyushu-u.ac.jp

[†] Presented at the 8th GOSPEL Workshop. Gas Sensors Based on Semiconducting Metal Oxides: Basic Understanding & Application Fields, Ferrara, Italy, 20–21 June 2019.

1. Introduction

High sensitivity and low limit of detection to volatile organic compounds (VOCs) gases are typical properties on the resistive-type semiconductor gas sensors using SnO₂-based materials. In this few decades, semiconductor gas sensors were improved on the point of not only the sensitivity but also both compact and low power consumption by using the micro gas sensors equipped with the microheater and microelectrode using the MEMS (Micro Electronic Mechanical System) technique. Recently, we proposed the micro gas sensor driven in repeating mode of instantaneous heating and cooling (pulse-driving) [1,2]. According to the pulse-driving mode, VOCs gases can introduce into the sensing layer during cooling period, and it improves the utilize efficiency of the sensing layer. Thus, in this study, we aimed to improve the sensor response in low concentration of VOCs gases, SnO₂ based gas sensor was driven under pulse-driving mode with monotonic and two-step heating.

2. Gas Detection Using Monotonic Pulse-Driving Mode

The gas sensing layer repeatedly passes heater-on and -off phases in pulse-driving mode. In the monotonic pulse-driving mode, VOCs gas molecules are diffusing and accumulating into the inside of the sensing layer during heater-off phase, and reacting at deep inside of the sensing layer during heater-on phase. The model of gas diffusion and reaction are schematically described in Figure 1. According to the gas diffusion models, gas diffuses entirely in the sensing layer during heater-off phase. In other words, pulse-driving mode can improve the utilization efficiency of the sensing layer regardless of the porosity of sensing layer. Therefore, it allows to improve the sensor response to VOCs gases. In our recent work, we proposed that SnO₂ based gas sensor can detect 200 ppt toluene by using the monotonic pulse-driving mode when heater-on temperature is set at 250 °C [2].

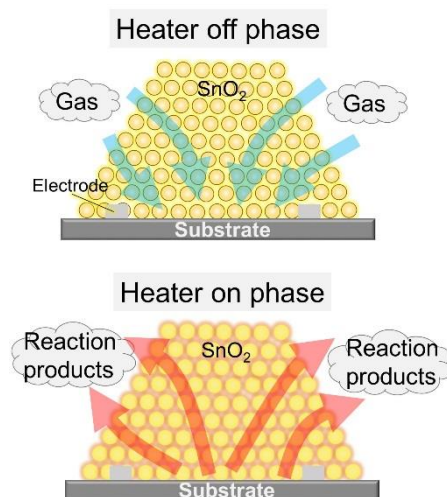


Figure 1. Schematic images of gas diffusion in the sensing layer during heater-on and -off phases.

3. Two-Step Pulse-Driving Mode for Gas Detection

Next, we introduced the two-step pulse-driving as described in Figure 2a to improve the sensor response to VOCs gas using pulse-driving mode. Here, heater temperatures at first step, sensor treatment, was set at 250–400 °C, and second step, sensor operation, was set at 250 °C, respectively. The transient electrical resistance curves in first and second heating period using SnO₂ nanoparticles sensor were shown in Figure 2b. Here, the result that first step temperature was set at 250 °C is same as the result using monotonic pulse-driving mode. It is clear that the electrical resistance at 250 °C in second step are increased with increasing the temperature in first step. According to our previous literature, infinitesimal impurities including in the atmosphere such as coming from the gas cylinder inhibit the oxygen adsorption and decrease the electric resistance in air atmosphere [3]. Additionally, detection process of VOCs gases such as toluene produced incomplete combustion products, and it also plays a role of inhibitor of oxygen adsorption in air atmosphere. Such impurities may reduce the oxygen adsorption amount on the particles surface. Thus, in two-step pulse-driving, the impurities on the particles surface is removed by heating in first-step, and the VOCs gases can be detected in second-step on the pure particles surface. The sensor response to 1–8 ppb toluene using both monotonic pulse-driving and two-step pulse-driving modes are shown in Figure 3. Here, heater temperature of first- and second-step were set at 400 and 250 °C in two-step pulse-driving, respectively, and it was set at 250 °C in monotonic pulse-driving. According to the results, the sensor response toward extremely low concentration of toluene was clearly higher by two-step pulse-driving than monotonic pulse-driving mode. Thus, it is clear that surface condition of particles prepared by first-step heating improved the sensor response to toluene.

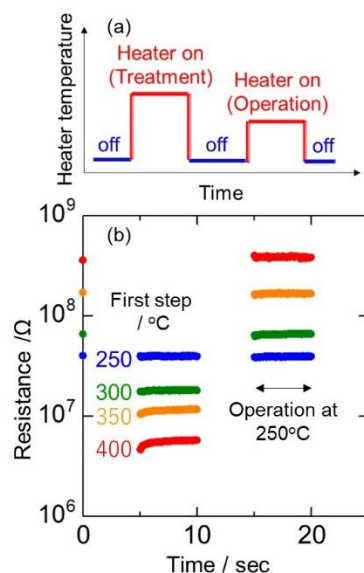


Figure 2. (a) Temperature profile of two-step pulse-driving and (b) the electrical resistances in first- and operation-step.

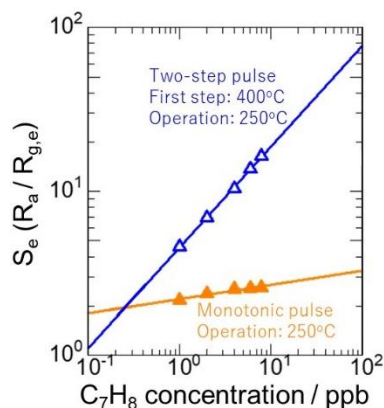


Figure 3. Toluene concentration dependence of the sensor response using monotonic and two-step pulse-driving mode.

References

1. Suematsu, K.; Shin, Y.; Ma, N.; Oyama, T.; Sasaki, M.; Yuasa, M.; Kida, T.; Shimano, K. Pulse-Driven Micro Gas Sensor Fitted with Clustered Pd/SnO₂ Nanoparticles. *Anal. Chem.* **2015**, *87*, 8407–8415.
2. Suematsu, K.; Harano, W.; Oyama, T.; Shin, Y.; Watanabe, K.; Shimano, K. Pulse-Driven Semiconductor Gas Sensors toward ppt Level Toluene Detection. *Anal. Chem.* **2018**, *90*, 11219–11223.
3. Suematsu, K.; Yuasa, M.; Kida, T.; Yamazoe, N.; Shimano, K. Determination of Oxygen Adsorption Species on SnO₂: Exact Analysis of Gas Sensing Properties Using a Sample Gas Pretreatment System. *J. Electrochem. Soc.* **2014**, *161*, B123–B128.



© 2019 by the authors. Licensee MDPI, Basel, Switzerland. This article is an open access article distributed under the terms and conditions of the Creative Commons Attribution (CC BY) license (<http://creativecommons.org/licenses/by/4.0/>).

Extended Abstract

Selective Detection of Hydrogen and Hydrogen Containing Gases with Metal Oxide Gas Sensor Operating in Non-Stationary Thermal Regime [†]

Alexey Shaposhnik ¹, Pavel Moskalev ¹ and Alexey Vasiliev ^{2,*}

¹ Chemistry Chair, Voronezh State Agrarian University, Michurin str., 1, Voronezh 394087, Russia; a.v.shaposhnik@gmail.com (A.S.); moskalefff@gmail.com (P.M.)

² National Research Center, Kurchatov Institute, Kurchatov sq., 1, Moscow 123182, Russia

* Correspondence: a-a-vasiliev@yandex.ru

[†] Presented at the 8th GOSPEL Workshop. Gas Sensors Based on Semiconducting Metal Oxides: Basic Understanding & Application Fields, Ferrara, Italy, 20–21 June 2019.

The main disadvantage of metal oxide (MOX) gas sensors is their insufficient selectivity leading to the dominating application for the quantitative analysis of one-component systems with certain composition, for example, CH₄-air or H₂-air. The application of non-stationary working regimes (modulation of gas flow, temperature, switch on-off of any chemical converter, etc.) increases the selectivity, because of an increase in the information about the nature of the analite. This improvement of selectivity is possible due to the revealing of the kinetics of the chemisorption of the analite and of the product desorption, the analite interaction with the surface located oxygen anions, etc.

The most know is the application of the non-stationary temperature regime of the sensor operation. The application of temperature modulation in MOX sensors can solve the selectivity problem, only if some important conditions are met. It is necessary (1) to use gas sensitive layer composition leading to different kinetics of the chemisorption and reaction with surface for different gas analites; (2) to find appropriate temperature regime giving extrama in the curve representing electrical resistance as a function of time; (3) to develop the algorithms of the treatment of multi-dimensional data arrays, because the application of non-stationary regime of the sensors operation leads to very significant increase in information volume about gas medium to be analyzed.

Gas sensing materials based on Pd decorated SnO₂ have at certain temperature regimes characteristic extrema at the curves representing the resistance of the sensing layer as a function of time (and, therefore, temperature, see Figure 1). These extrema are well pronounced at the detection of hydrogen and gases, which can be dehydrogenized at the interaction with the sensing layer (ethanol, acetone, H₂S, etc.). These curves for hydrogen, ethanol, and CO (concentration of all gases is of 100 ppm) are presented in Figure 1. The plots present these functions during two full temperature modulation cycles.

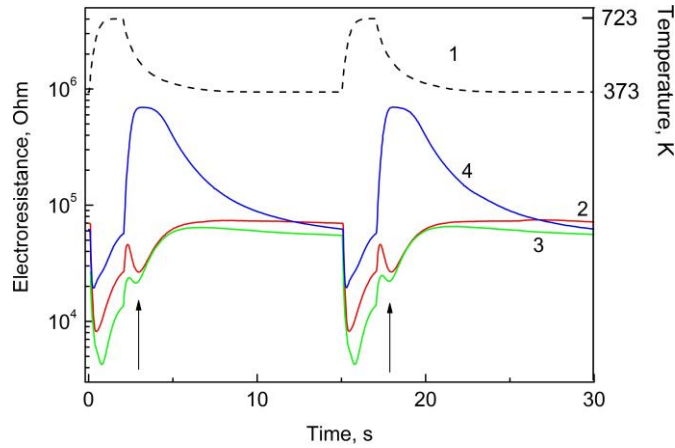


Figure 1. The temperature of the sensor (curve 1) with sensing layer consisting of tin dioxide decorated with Pd and sensing layer resistance at this temperature modulation as a function of time during temperature modulation cycle. (2) 100 ppm of H₂, (3) 100 ppm of ethanol, (4) 100 ppm of CO in air.

The extrema on the curves obtained at the detection of hydrogen and ethanol, which is able to release hydrogen at high working temperature of the sensor, are well pronounced. This extremum marked with arrow in the plot is a result of special mechanism of the reaction of the detected gas with the surface. Indeed, the usual mechanism of the interaction includes the reaction with oxygen anions chemisorbed on the surface.



Such mechanism is typical of the interaction of other reducing gas (for example, CO, methane) with the surface of the semiconductor. Hydrogen, however, can interact with the surface directly, without the participation of oxygen anions.



This mechanism can explain the presence of minimum marked with arrow on the plot presenting sensor resistance as a function of time.

During each measurement cycle (Figure 1), we obtained 575 values of sensor resistance giving, respectively, 575 virtual gas sensors. The multi-dimensional data arrays were treated using Principle Component algorithm. Figure 2 shows the possibility to determine both qualitative and quantitative composition of gas mixtures in both one and two component mixtures.

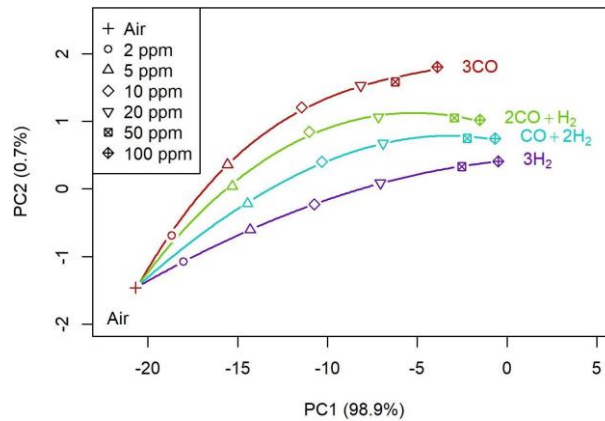


Figure 2. Results of PC analysis of the measurement of 575 virtual sensors. Gas mixtures with the same total concentration and different ratio of CO and H₂ (noted in the plot).

Funding: This work was funded by RFBR according to the research project No. 18-29-24128.

Conflicts of Interest: The authors declare no conflict of interest.



© 2019 by the authors. Licensee MDPI, Basel, Switzerland. This article is an open access article distributed under the terms and conditions of the Creative Commons Attribution (CC BY) license (<http://creativecommons.org/licenses/by/4.0/>).

Oral Presentations

Extended Abstract

Monitoring Surface Stoichiometry, Work Function and Valance Band of Tungsten Oxide (WO₃), Molybdenum Oxide (MoO₃) and Tin Oxide (SnO₂) Thin Films as a Function of Temperature and Oxygen Partial Pressure with Advanced Surface Sensitive Techniques for Chemical Sensing Applications [†]

Engin Ciftiyurek ^{1,*}, Martin Wilken ², David Zanders ², Lukas Mai ², Anjana Devi ² and Klaus D. Schierbaum ¹

¹ Department of Materials Science, Institute for Experimental Condensed Matter Physics, Heinrich Heine University of Duesseldorf, Germany; Klaus.Schierbaum@uni-duesseldorf.de

² Inorganic Materials Chemistry, Ruhr University Bochum, 44801 Bochum, Germany; martin.wilken@rub.de (M.W.); David.Zanders@ruhr-uni-bochum.de (D.Z.) Lukas.Mai@rub.de (L.M.); anjana.devi@rub.de (A.D.)

* Correspondence: engin.ciftiyurek@uni-duesseldorf.de

[†] Presented at the 8th GOSPEL Workshop. Gas Sensors Based on Semiconducting Metal Oxides: Basic Understanding & Application Fields, Ferrara, Italy, 20–21 June 2019.

Atomic layer deposition (ALD) is a chemical vapor deposition (CVD) deposition method in which high-quality, fine functional oxide films in the range of 10–1000 nm can be grown. The low deposition temperature and nonobligatory of heat treatment make it possible to obtain fine grains with high surface area. Despite the fact that few reports in recent years highlighted the importance of thickness/microstructure [1], the role of the defect sites, electronic and surface properties have not been well characterized with varying temperature and oxygen partial pressure [2], additionally understanding on chemisorbed oxygen species and oxygen vacancies (V_o°) which facilitates the replenishment of chemisorbed oxygen ions on the surface [3] are also lacking. This report focus on a correlation of surface electronic, structural and chemical properties with the surface reactivity and sensing behavior of the ALD layers of tungsten oxide (WO₃), molybdenum oxide (MoO₃) and tin oxide (SnO₂) in the thickness range of 20–100 nm by employing advanced synchrotron based surface sensitive spectral-microscopic techniques; near ambient x-ray photoelectron spectroscopy (NAP-XPS), x-ray induced photoelectron emission microscopy (XPEEM), x-ray photoelectron spectroscopy (XPS), ultraviolet photoelectron spectroscopy (UPS) and low energy electron microscopy (LEEM). The characterization work is supported by extensive chemical sensor testing and electrical resistivity measurements.

Depletion layer, dissociative adsorption of oxygen, chemisorption and the continuous replenishment on the surface in the course of catalytic oxidation reactions are prerequisite for an explanation for sensing mechanism, indeed sustained operation for the metal oxide based chemical sensors. This work will focus on the stoichiometry, crystal structure, work-function (Φ), valance band, and surface defect analysis, oxidation state as a function of oxygen partial pressure and temperature and its effect on chemisorbed oxygen ion concentration, thin film processing conditions, microstructure/porosity, depletion layer and Schottky barrier height. Inorganic materials, particularly salts and oxides, are sensitive to photon induced damage, after prolonged high intensity x-ray exposure, on the other hand, it is required high enough intensity and spectral resolution (achievable in synchrotron sources 0.1–0.2 eV) to realize the proposed goals. PM4 with its low dose x-ray ability and SMART with its XPEEM capability end stations, at BESSY II, Berlin and unique

NAP-XPS system at Charles University, Prague, enabled spectra-microscopic characterization with abovementioned techniques. The results are enclosed here briefly in Figure 1.

Figure 1a shows the valence spectrum of WO_3 thin film extends up to the Fermi level starting after 250 °C, indicating a change in the character of the sample surface together with electrical resistivity measurements. Figure 1b shows bright-field image of the 700 °C deposited WO_3 sample. As the figure reveals the formation of continuous thin film with homogeneous grain structure over the surface differentiating with the grain size as the thin film possesses larger grains and obviously higher surface roughness. In LEEM images contrast is determined by work function (Φ) variation over the surface. Surface topography, grain boundaries, porosity and stoichiometry can affect the work function (Φ). The variation in the work function (Φ) from grain to grain is higher in comparison to 600 °C deposited sample. In order to have better understanding on this, XPEEM analysis was conducted (not included here). The Figure 1c shows a valence band spectrum of defective MoO_x taken with 65 eV photons with two different take-off angles. E_{fermi} level followed by valance band minimum, and at larger binding energies, O 2s was seen in the figure. Another feature observable is the 4d and 5s of Mo blended in between 5–12 eV. It is detected that the band gap is not entirely free of states due to the nonstoichiometry of the MoO_x thin film. The oxygen vacancies (V_{O}^{\bullet}) give rise the defect states located around ~3 eV below the E_{fermi} level in 60° in comparison to the 0°. This is attributed to a change in occupancy of the Mo 4d and 5s bands due to reduction from $\text{Mo}^{+6}/\text{Mo}^{+5}$ to Mo^{4+} . The valence band minimum is located at about 1.0 eV below the Fermi level.

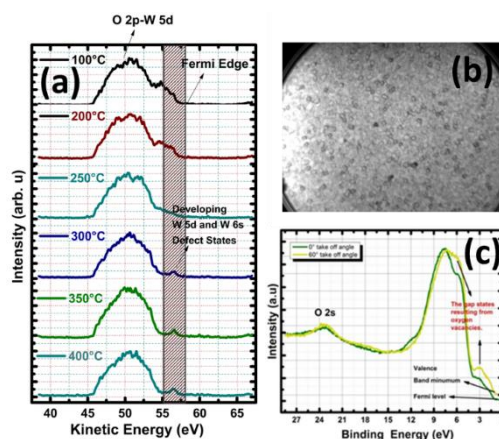


Figure 1. Valence band spectrum of WO_3 25 °C–400 °C (a) LEEM images of 700 °C deposited WO_3 , at FoV of 12.4 μm with 5 eV KE (b), Valence band region of MoO_x ultra-thin film in the vicinity of Fermi level with 60 eV photons at two different electron take-off angles 0° and 60°(c).

References

1. Du, X.; George, S.M. Thickness dependence of sensor response for CO gas sensing by tin oxide films grown using atomic layer deposition. *Sens. Actuator B-Chem.* **2008**, *135*, 152–160.
2. Ciftiyurek, E.; Sabolsyk, K.; Sabolsyk, E. High temperature selective sensing of hydrogen with MgO-modified SrMoO_4 micro-fibers. *Sens. Actuator B-Chem.* **2017**, *249*, 296–310.
3. Azad, A.M.; Akbar, S.A.; Mhaisalkar, S.G.; Birkefeld, L.D.; Goto, K.S. Solid-State Gas Sensors: A Review. *J. Electrochem. Soc.* **1992**, *139*, 3690–3704.
4. Mattinen, M.; Wree, J.; Stegmann, N.; Ciftiyurek, E.; Achhab, M.; King, P.; Mizohata, K.; Räisänen, J.; Schierbaum, K.D.; Devi, A.; Ritala, M.; Leskelä, M. Atomic Layer Deposition of Molybdenum and Tungsten Oxide Thin Films Using Heteroleptic Imido-Amidinato Precursors: Process Development, Film Characterization, and Gas Sensing Properties. *Chem. Mater.* **2018**, *30*, 8690–8701.



© 2019 by the authors. Licensee MDPI, Basel, Switzerland. This article is an open access article distributed under the terms and conditions of the Creative Commons Attribution (CC BY) license (<http://creativecommons.org/licenses/by/4.0/>).

Nanocrystalline LaCoO₃ Modified by Ag Nanoparticles with Improved Sensitivity to H₂S †

Artem Marikutsa *, Valentina Chumakova, Marina Rumyantseva and Alexander Gaskov

Chemistry Department, Moscow State University, Vorobyevy gory 1-3, Moscow 119991, Russia; valentina.chum@yandex.ru (V.C.); roum@inorg.chem.msu.ru (M.R.); gaskov@inorg.chem.msu.ru (A.G.)

* Correspondence: artem.marikutsa@gmail.com; Tel.: +7-495-939-5471

† Presented at the 8th GOSPEL Workshop. Gas Sensors Based on Semiconducting Metal Oxides: Basic Understanding & Application Fields, Ferrara, Italy, 20–21 June 2019.

1. Summary

Nanocrystalline LaCoO₃ was synthesized by sol-gel method and functionalized by Ag nanoparticles via impregnation. An improved sensitivity to H₂S gas was detected for the Ag/LaCoO₃. The nanocomposite sensors showed lower cross-sensitivity to CO and NH₃, in comparison to pure LaCoO₃. The role of Ag nanoparticles in promotion of the H₂S adsorption and oxidation on the surface of LaCoO₃ was elucidated using diffuse reflectance infrared Fourier-transformed (DRIFT) spectroscopy.

2. Motivation and Results

As a semiconductor metal oxide with perovskite structure, LaCoO₃ is of interest for chemical sensors. The hole-type conduction occurs via Co–O framework. The surface of LaCoO₃ nanostructures exhibits different adsorption sites (La³⁺ and Co³⁺) and active sites (chemisorbed oxygen, lattice anions) for gas molecules reception. The sensing mechanisms with LaCoO₃ and its nanocomposites are unclear. In this work we obtained nanocrystalline LaCoO₃ modified by Ag nanoparticles with improved sensitivity and selectivity to H₂S, characterized the microstructure and surface sites of materials, and proposed the sensing routes during gas-solid interaction.

Nanocrystalline LaCoO₃ with particle size 30–80 nm (Figure 1) and specific surface area 5–10 m²/g was obtained by sol-gel synthesis using ethylenediamine as a coordination ligand. The samples were impregnated by Ag nanoparticles with the size increasing in the range 30–60 nm on increasing silver percentage 2–5 wt.%. XPS spectroscopy demonstrated the presence of La³⁺, Co³⁺, O²⁻ ions in the bulk along with a large fraction of chemisorbed oxygen species. Metallic Ag nanoparticles were observed by XPS and XRD. The DC-resistance increased in presence of Ag due to electrons donation into *p*-type LaCoO₃. The Ag/LaCoO₃ nanocomposites demonstrated higher sensitivity to 0.2–5 ppm H₂S at 200 °C, in comparison to pure LaCoO₃ (Figure 2). Cross-sensitivity tests showed about 10-times higher sensor response of Ag/LaCoO₃ to 2 ppm H₂S, as opposed to 20 ppm CO and NH₃ (Figure 3). On DRIFT spectra of the samples Ag/LaCoO₃ exposed to H₂S at 200 °C the evolution of peaks was observed relevant to adsorbed H₂S, Ag₂S and SO₄²⁻ groups (Figure 4a). Thus, the sensing process occurred via H₂S adsorption favored by Ag nanoparticles and oxidation to sulfur oxide and sulfate species on the LaCoO₃ surface. The reaction products, except SO₄²⁻, disappeared during further exposure in air, which accounts for sensor recovery (Figure 4b). The persistent sulfate species were likely inactive by-products that did not affect the sensors behavior.

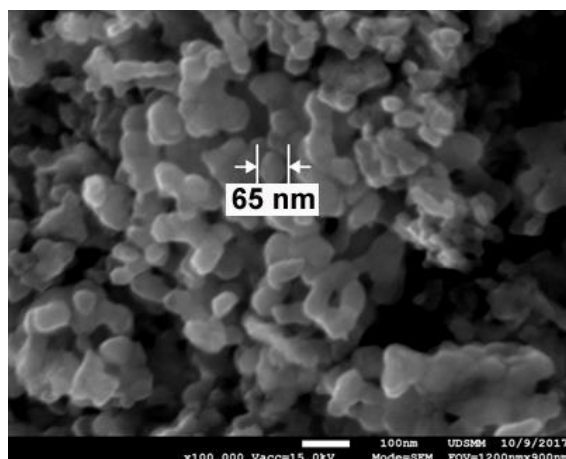


Figure 1. SEM image of LaCoO₃ annealed at 600 °C for 9 h.

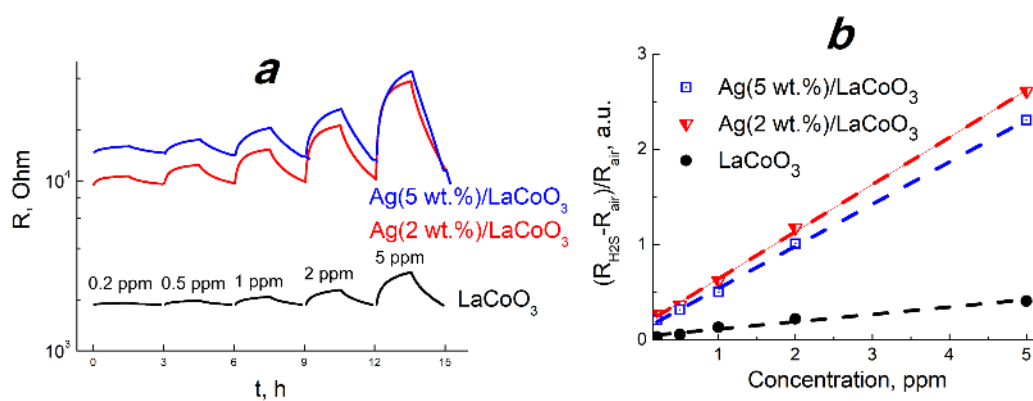


Figure 2. Dynamic response (a) and sensor signals (b) of LaCoO₃ and Ag/LaCoO₃ to 0.2–5 ppm H₂S at 200 °C.

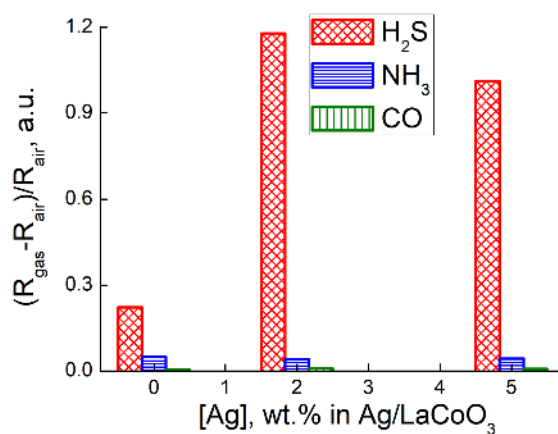


Figure 3. Comparison of sensor signals of LaCoO₃ and Ag/LaCoO₃ to 20 ppm CO, 20 ppm NH₃ and 2 ppm H₂S at 200 °C.

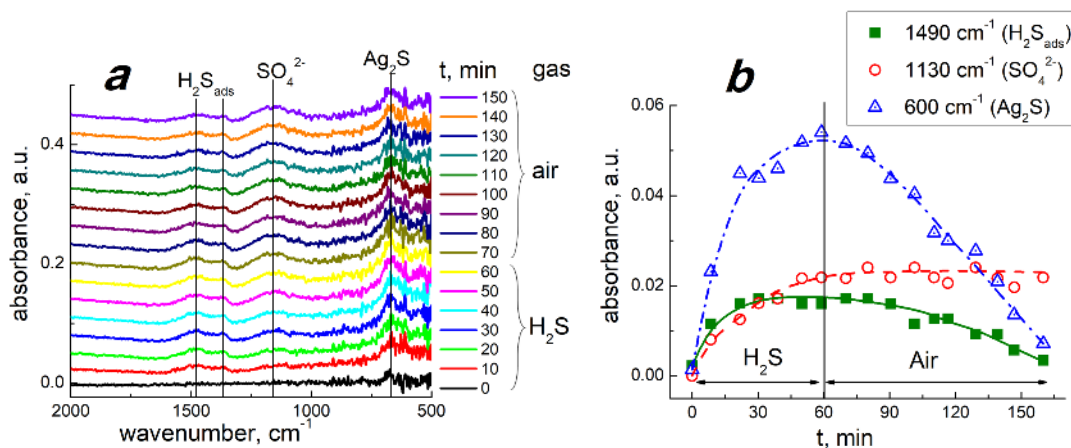


Figure 4. DRIFT spectra of Ag/LaCoO₃ exposed to 20 ppm H₂S at 200 °C for 60 min and to air at 200 °C for further 90 min (a), and absorption intensities of the peaks of adsorbed H₂S, SO₄²⁻ and Ag₂S (b).

Funding: This research was funded by Russian Science Foundation, grant number 18-73-00071.

Acknowledgments: We would like to thank Dr. Fasquelle and Mr. Duponchel from UDSMM lab, Université du Littoral Côte d’Opale, Calais, France for their participation.

Conflicts of Interest: The authors declare no conflict of interest. The funders had no role in the design of the study; in the collection, analyses, or interpretation of data; in the writing of the manuscript, or in the decision to publish the results.



© 2019 by the authors. Licensee MDPI, Basel, Switzerland. This article is an open access article distributed under the terms and conditions of the Creative Commons Attribution (CC BY) license (<http://creativecommons.org/licenses/by/4.0/>).

H₂S Sensing Properties of a Diode-Type Device Using ZnO Nanorods Coupled with CuO Nanocrystals [†]

Tetsuya Kida ^{1,*}, Yuta Kido ² and Takeshi Shinkai ²

¹ Faculty of Advanced Science and Technology, Kumamoto University, Kumamoto, 860-8555, Japan

² Department of Applied Chemistry and Biochemistry, Graduate School of Science and Technology, Kumamoto University, Kumamoto, 860-8555, Japan; kido.yuta.63@gmail.com (Y.K.); s.t_19970101@i.softbank.jp (T.S.)

* Correspondence: tetsuya@kumamoto-u.ac.jp; Tel.: +81-96-342-3679

[†] Presented at the 8th GOSPEL Workshop. Gas Sensors Based on Semiconducting Metal Oxides: Basic Understanding & Application Fields, Ferrara, Italy, 20–21 June 2019.

1. Introduction

Hydrogen sulfide (H₂S) is known as a colorless, flammable and highly toxic gas with strong odor. Therefore, to avoid the risk of its leakage, continuous monitoring of H₂S is extremely important. Semiconductor gas sensor is promising for such applications because of its high sensitivity, selectivity, fast response, and good stability. It has been reported in many papers that CuO/SnO₂ sensor shows a high sensitivity to H₂S since the pioneering work by Tamaki et al. [1] It is believed that sulfidation of CuO with H₂S degrades the PN junction between CuO and SnO₂, resulting in a significant change in electrical resistance. However, the detailed mechanism remains unclear yet. In this study, we fabricated a PN junction film using p-type CuO nanocrystals and n-type ZnO nanorod films to make a sensor device and studied its diode properties under H₂S atmosphere to reveal the sensing mechanism. It was expected that the combination of nanorods and nanocrystals increases the area of junction interfaces, leading to a pronounced change in electrical properties upon gas reaction.

2. Experimental

ZnO nanorods (NRs) were grown on an ITO-coated glass substrate by a seeding method.[2] As seeds, ZnO nanocrystals (NCs) were synthesized by a hot-soap method, in which zinc acetylacetonate and 1,2-hexadecanediol were dissolved in oleylamine and heated at 220 °C for 90 min. The synthesized ZnO NCs were deposited on an ITO-coated glass and annealed in air at 350 °C for 30 min to remove surface capping agents. The ZnO NC film was dipped in an aqueous solution containing Zn(NO₃)₂ and hexamethylenetetramine (HMT), and then heated at 95 °C for 5 h to synthesize ZnO NRs.

Cu₂O nanocrystals (NCs) were also synthesized by a hot-soap method using oleylamine as a high-boiling-point solvent. Typically, Cu (II) acetylacetonate and 1,8-octanediol were added to oleylamine in a three-necked flask. The temperature was raised to 160 °C under an Ar flow and kept at 160 °C for 60 min. The surface ligands, oleylamine, were replaced with 3-mercaptopropyl acid by dispersing NCs in a solution containing water, methanol, and NaOH with pH 12. The ligand exchange reaction was carried out for 30 min.

The Cu₂O NCs were deposited onto the ZnO nanorod film by drop casting and annealed in air at 250 °C for 30 min. Gold electrodes with 100 nm thickness were deposited on the film by thermal evaporation to fabricate a sensor device. IV curves of the device were measured at 50 to 200 °C in air and air containing H₂S with a Keithly 2400 source meter.

3. Results and Discussion

Figure 1 shows a representative SEM image of ZnO NRs deposited on ITO. ZnO NRs grew perpendicular to the substrate to form a porous film. The diameter and the length of the NRs were estimated to be ca. 100 and 700 nm, respectively. Figure 2 shows a TEM image of CuO/Cu₂O NCs. The size of the NCs is 8 to 10 nm with a narrow size distribution. XRD results revealed that Cu₂O was converted into CuO after ligand exchange with an alkaline solution.

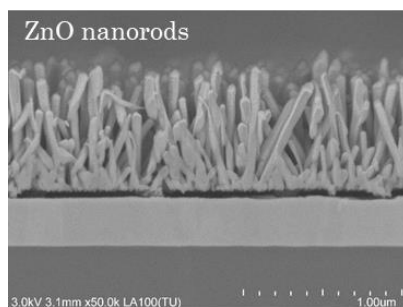


Figure 1. SEM image of ZnO nanorods deposited on an ITO substrate.

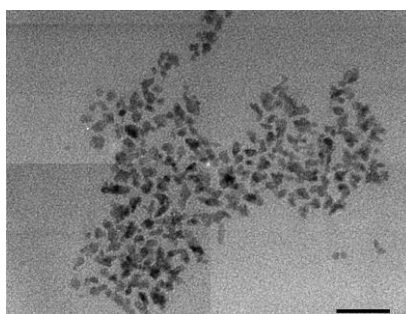


Figure 2. TEM image of CuO nanocrystals synthesized by a hot-soap method. The scale bar is 50 nm.

Figure 3 shows IV curves of the device, in which CuO NCs were deposited onto ZnO NRs, in air and air containing 8 ppm H₂S at 150 °C. The device exhibited a clear rectification behavior in air at 150 °C, indicating that PN junctions were formed between CuO NCs and ZnO NRs. However, such a clear rectification behavior was lost under H₂S atmosphere. The current in the forward and reverse directions significantly reduced after exposure to H₂S. We have recently confirmed that CuO NCs-based sensors respond to H₂S by an increase in electrical resistance due to reaction of adsorbed oxygen with H₂S, representing a typical behavior of p-type semiconductors.[3] Thus, the observed increase in resistance for the present device is possibly due to surface reaction of adsorbed oxygen with H₂S and the resulting annihilation of holes. The rectification of the current recovered by reintroduction of air, which possibly increased the electron concentration in CuO. On the other hand, at higher temperature, the device showed a simple ohmic behavior (no figure), suggesting that complete conversion of CuO into CuS occurred. Thus, the sensing mechanism should be dependent on temperature. The above results demonstrate the feasibility of nanorod/nanocrystal-based PN-junction devices in constructing gas sensors. Currently, a more detailed mechanism is under investigation.

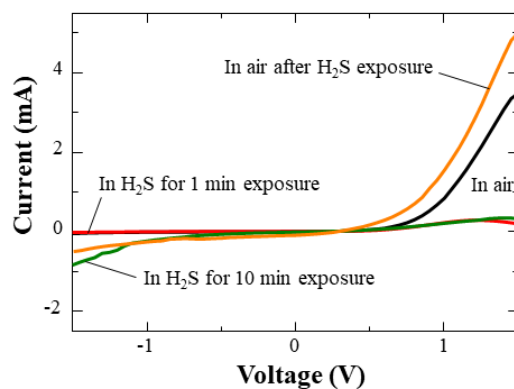


Figure 3. IV curves of the CuO NCs/ZnO NRs device in air and air containing 8 ppm H₂S at 150 °C.

Acknowledgments: This research was funded by a Grant-in-Aid for the Promotion of Joint International Research (15KK0189) from the Ministry of Education, Culture, Sports, Science and Technology of Japan.

Conflicts of Interest: The authors declare no conflict of interest.

References

- ¹ Tamaki, J.; Maekawa, T.; Miura, N.; Yamazoe, N. CuO-SnO₂ element for highly sensitive and selective detection of H₂S. *Sens. Actuators B Chem.* **1992**, *3*, 197–203.
- ² Gaddam, V.; Kumar, R.R.; Parmar, M.; Nayak, M.M.; Rajanna, K. Synthesis of ZnO nanorods on a flexible Phynox alloy substrate: Influence of growth temperature on their properties. *RSC Adv.* **2015**, *5*, 89985–89992.
- ³ Mikami, K.; Kido, Y.; Akaishi, Y.; Quitain, A.; Kida, T. Synthesis of Cu₂O/CuO nanocrystals and their application to H₂S sensing. *Sensors* **2019**, *19*, 211.



© 2019 by the authors. Licensee MDPI, Basel, Switzerland. This article is an open access article distributed under the terms and conditions of the Creative Commons Attribution (CC BY) license (<http://creativecommons.org/licenses/by/4.0/>).

SnO₂-Based Gas Sensor for Detection of Refrigerant Gases [†]

Kuniyuki Izawa

Figaro Engineering Inc., 1-5-11 Senba-nishi, Mino, Osaka 562-8505, Japan; izawa@figaro.co.jp;
Tel.: +81-72-728-2565

[†] Presented at the 8th GOSPEL Workshop. Gas Sensors Based on Semiconducting Metal Oxides: Basic Understanding & Application Fields, Ferrara, Italy, 20–21 June 2019.

The Montreal Protocol on Substances that Deplete the Ozone Layer entered into force in 1989. Since then, replacement of the ozone depleting refrigerants, chlorofluorocarbons (CFCs) and hydrochlorofluorocarbons (HCFCs), with non-chlorine refrigerants, hydrofluorocarbons (HFCs), is seen progressing globally. HFCs have no destruction effect on the ozone layer; however, they are greenhouse gases which have global warming potentials. The Kigali Amendment to the Protocol, which requires gradual reduction of the production and consumption of HFCs in carbon dioxide equivalent (CO_{2e}), was adopted in 2016. The amendment requires a 10% reduction of HFCs in CO_{2e} from the baseline from 2019 and a 40 % reduction from 2024 of economically developed countries. The baseline is calculated from the relevant data in 2011, 2012 and 2013. The amendment has generated a need for immediate actions by manufactures which produce equipment that uses refrigerant. One of the major refrigeration and air conditioning equipment manufacturers, Daikin, states on their website that difluoromethane (HFC32) is the most balanced refrigerant in eco-friendliness (low Global Warming Potential (GWP) value), energy efficiency, safety and economic efficiency for both residential and industrial air conditioners. In a conference hosted by the Japan Refrigeration and Air Conditioning Industry Association (JRA) in August, 2017, Daikin described that HFC32 would make a huge contribution to the achievement of the phasedown timeline of the Kigali Amendment. HFC32 is a promising refrigerant; however, it is classified as a lower flammability substance according to ISO817. There is a trade-off between GWP and flammability of refrigerant gases. Refrigeration and air conditioning equipment manufacturers have been seeking for solutions to ensure safety in using flammable refrigerants. Especially, equipment which uses a large amount of flammable refrigerant, such as multi split air conditioners, is required to have a function to detect refrigerant leakage in accordance with the technical standards, such as JRA4068 and IEC60335–2–40.

For the refrigerant leakage detection, there are two candidate gas sensors in detecting principle, nondispersive infrared (NDIR) gas sensor and metal oxide semiconductor (MOS) gas sensor. While NDIR gas sensors have high accuracy, they are less affordable. Figaro believes that low cost MOS gas sensors are more suitable for the refrigerant leakage detection. Regarding the accuracy, the detection systems require gas sensors to work as a switching device as used in residential gas alarm application, for which MOS gas sensors have been used for almost fifty years, not as a measuring device for indication of gas concentrations.

Figaro has developed a refrigerant gas sensor, TGS2630, to which SnO₂-based sensing material is applied by screen printing method. The structure of TGS2630 is the same as that of Figaro's conventional sensors which are widely used for residential gas alarms, implying TGS2630 has an excellent advantage in cost and productivity (figure 1). Typical sensitivity characteristics of the sensor are shown in figure 2. The sensor has a high sensitivity to HFC32 as well as to 2, 3, 3–tetrafluoro–1–propene (HFO1234yf). HFO1234yf is also classified as a lower flammability substance, but has a very low GWP value. In addition, a filter set underneath the gas inlet reduces the influence of ethanol vapor which is a typical example of the interference gases may exist in our daily living environment. In this presentation, TGS2630 will be introduced with its sensor performances in more detail.

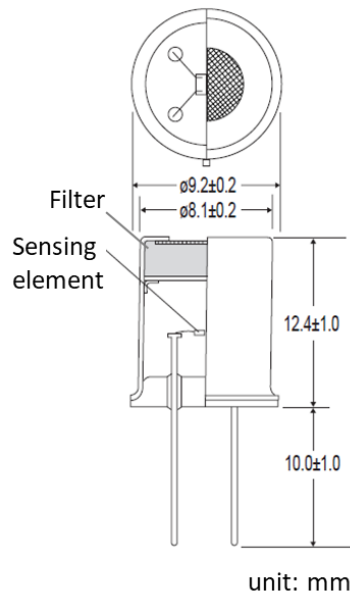


Figure 1. Structure and dimensions of TGS2630.

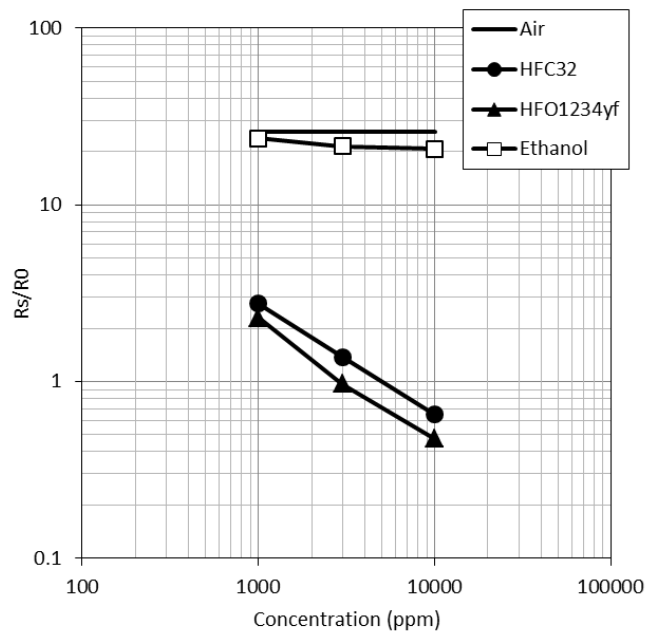


Figure 2. Sensitivity characteristics of TGS2630, R0: sensor resistance at 5000ppm HFC32.

Conflicts of Interest: The author declares no conflict of interest.



© 2019 by the authors. Licensee MDPI, Basel, Switzerland. This article is an open access article distributed under the terms and conditions of the Creative Commons Attribution (CC BY) license (<http://creativecommons.org/licenses/by/4.0/>).

Shining light on Indium Oxide Gas Sensors at Work: A Combined *Operando* Raman/UV-Vis/FT-IR Spectroscopic Study [†]

Sebastian Berka, Viktoriya Fleischer and Christian Hess *

Eduard-Zintl-Institute of Inorganic and Physical Chemistry, Technical University Darmstadt, 64297 Darmstadt, Germany; berka@chemie.tu-darmstadt.de (S.B.); viktoriya336@googlemail.com (V.F.)

* Correspondence: hess@pc.chemie.tu-darmstadt.de; Tel.: +49-6151-16-21975

[†] Presented at the 8th GOSPEL Workshop. Gas Sensors Based on Semiconducting Metal Oxides: Basic Understanding & Application Fields, Ferrara, Italy, 20–21 June 2019.

1. Introduction

Understanding the mode of operation of metal-oxide gas sensors (e.g., SnO₂, In₂O₃) is of great scientific and economic interest. Such a knowledge based approach requires the development and application of spectroscopic tools to monitor the relevant surface and bulk processes under working conditions (*operando* approach) [1,2]. In previous studies on In₂O₃ sensors, we applied combined *operando* Raman/gas-phase FT-IR spectroscopy to ethanol gas sensing [2,3]. In this contribution, we will present recent results on ethanol and CO detection using undoped and Ag doped In₂O₃ gas sensors, demonstrating the advantages of (i) *operando* Surface Enhanced Raman Spectroscopy (SERS) to monitor the metal oxidation state, and (ii) extending the *operando* Raman/FT-IR setup by UV-Vis spectroscopy to reveal the degree of In₂O₃ reduction.

2. Experimental

In₂O₃ was prepared by precipitation of indium (III) nitrate hydrate. AgNO₃ was added to yield a 1 wt% Ag/In₂O₃ sample by calcination. XPS analysis revealed a mixture of metallic (52%) and oxidized (48%) Ag on the surface. For gas sensing experiments an Al₂O₃-transducer substrate with interdigitated Pt-electrodes on one side and a meander Pt-heater on the other side was employed. *Operando* experiments were performed in a Teflon cell equipped with an optical window based on the design shown in Ref. [2]. The exhaust was analyzed by FT-IR spectroscopy. Raman spectra were recorded at 514.5 and 632.8 nm excitation. For details see Refs. [2,3].

3. Results

Previous *operando* Raman studies on undoped In₂O₃ gas sensors have shown that during ethanol (EtOH) gas sensing the sensor signal can be directly correlated with the nature of the adsorbates, the presence of surface hydroxyl groups and the indium oxide oxidation state [2,3]. Turning now to recent results on Ag doped In₂O₃, Figure 1 shows *operando* Raman spectra recorded after switching from air to 250 ppm EtOH/air at 190 °C. At higher wavenumbers, the disappearance of hydroxyl groups at 3639 and 3656 cm⁻¹ (O-H stretch) is accompanied by the formation of acetate based on the bands at 871 cm⁻¹ (C-C stretch) and 2935 cm⁻¹ (C-H stretch) [3]. Interestingly, upon exposure to 250 ppm EtOH/air, the low wavenumber region shows dramatic changes, which are reversible and which can be related to the change in the Ag state during EtOH sensing. In fact, the strong intensity increase in the In₂O₃ phonons (see Figure 1) is attributed to the EtOH surface reduction of oxidized to metallic Ag giving rise to a Raman enhancement based on Surface Enhanced Raman Spectroscopy (SERS), thus enabling the metal oxidation state to be elucidated under working conditions of the gas sensor.

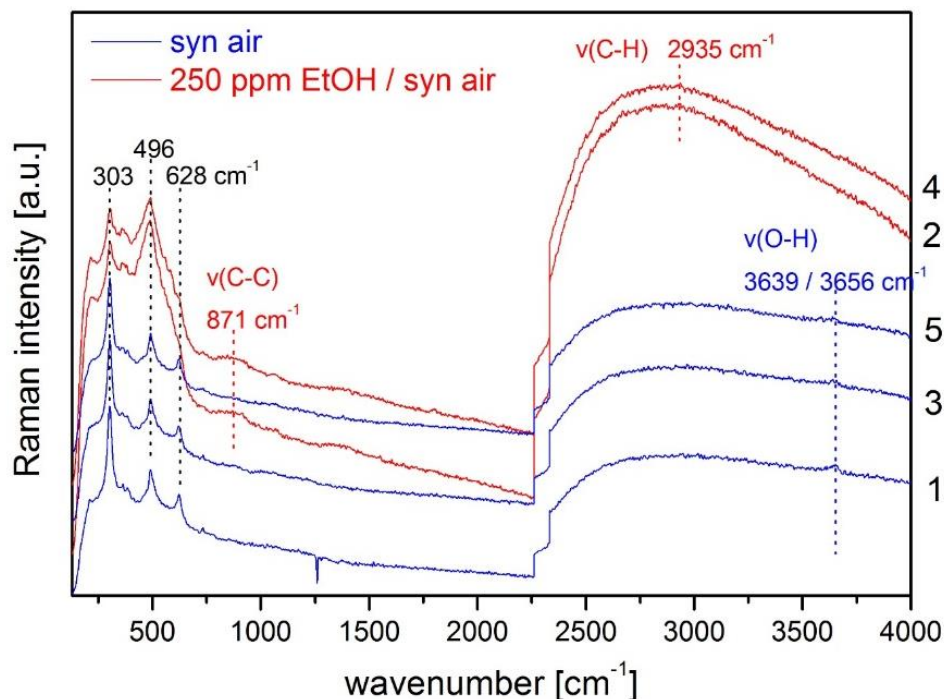


Figure 1. *Operando* Raman spectra during EtOH sensing at 190°C using 1 wt% Ag/In₂O₃.

To extend the information from *operando* experiments by UV-Vis spectroscopy a new *operando* cell was built on the basis of previous cell designs [2]. We illustrate its potential in combined *operando* Raman/UV-Vis/FT-IR spectroscopic experiments on In₂O₃ gas sensors during EtOH and CO gas sensing. For example, in experiments during CO sensing (500 ppm), resistance measurements can be correlated with (i) simultaneous FT-IR gas phase spectra showing changes in the gas-phase composition (CO, CO₂, H₂O), (ii) Raman spectra revealing information on adsorbates (carbonate, formate) and hydroxy species, while in contrast to ceria no super-/peroxide species are observed [4], and (iii) UV-Vis spectra indicating In₂O₃ reduction by increased Vis absorption. Very recent experiments on SnO₂ and CeO₂ gas sensors demonstrate the general applicability of the combined *operando* approach.

4. Conclusions

Our studies highlight the potential of combined *operando* spectroscopic characterization of metal-oxide gas sensors for elucidating their mode of operation on a molecular level.

Funding: This research was funded by the Deutsche Forschungsgemeinschaft (DFG, HE-4515/6-1).

Acknowledgments: The authors thank Sandra Sänze, Ann-Kathrin Elger, and Maximilian Pfeiffer for help with some of the measurements and fruitful discussions, and Karl Kopp for XPS analysis and technical support.

Conflicts of Interest: The authors declare no conflict of interest.

References

- Gurlo, A.; Riedel, R. In situ and *operando* spectroscopy for assessing mechanisms of gas sensors. *Angew. Chem. Int. Ed.* **2007**, *46*, 3826, doi:10.1002/anie.200602597.
- Sänze, S.; Gurlo, A.; Hess, C. Monitoring gas sensors at work: *operando* Raman-FTIR study of ethanol detection by indium oxide. *Angew. Chem. Int. Ed.* **2013**, *52*, 1, doi:10.1002/anie.201207258.
- Sänze, S.; Hess, C. Ethanol gas sensing by indium oxide: an *operando* spectroscopic Raman/FTIR study. *J. Phys. Chem. C.* **2014**, *118*, 25603, doi: 10.1021/jp509068s.

10. Schilling, C.; Ganduglia-Pirovano, M.V.; Hess, C. Experimental and theoretical study on the nature of adsorbed oxygen species on shaped ceria nanoparticles. *J. Phys Chem. Lett.* **2018**, *3*, 6593, doi:10.1021/acs.jpcllett.8b02728.



© 2019 by the authors. Licensee MDPI, Basel, Switzerland. This article is an open access article distributed under the terms and conditions of the Creative Commons Attribution (CC BY) license (<http://creativecommons.org/licenses/by/4.0/>).

Realizing the Control of Fermi Level and Gas-Sensing Selectivity over Gallium-Doped In_2O_3 Inverse Opal Microspheres [†]

Tianshuang Wang, Peng Sun* and Geyu Lu *

State Key Laboratory on Integrated Optoelectronics, College of Electronic Science and Engineering, Jilin University, 2699 Qianjin Street, Changchun 130012, China; wangts_jlu@163.com (T.W.)

* Correspondence: pengsun@jlu.edu.cn (P.S.); luyg@jlu.edu.cn (G.L.)

[†] Presented at the 8th GOSPEL Workshop. Gas Sensors Based on Semiconducting Metal Oxides: Basic Understanding & Application Fields, Ferrara, Italy, 20–21 June 2019.

Herein, formaldehyde sensors based on gallium-doped In_2O_3 inverse opal (IO- $(\text{Ga}_x\text{In}_{1-x})_2\text{O}_3$) microspheres were purposefully prepared by simple ultrasonic spray pyrolysis method combined with self-assembly sulfonated polystyrene spheres template. The well-aligned inverse opal structure, with three different-sized pores, plays dual roles of accelerating the diffusion of gas molecules and providing more active sites. The Ga substitutional doing can alter the electronic energy level structure of $(\text{Ga}_x\text{In}_{1-x})_2\text{O}_3$, leading to the elevation of Fermi level and the modulation of band gap closed to a suitable value (3.90 eV), hence, effectively optimizing the oxidative catalytic activity for preferential CH_2O oxidation and increasing the amount of absorbed oxygen. More importantly, the gas selectivity could be controlled by varying the energy level of adsorbed oxygen. Accordingly, the IO- $(\text{Ga}_{0.2}\text{In}_{0.8})_2\text{O}_3$ microspheres sensor showed high response toward formaldehyde with fast response and recovery speeds, and ultralow detection limit (50 ppb). Our findings finally offer implications for designing Fermi level-tailorable semiconductor nanomaterials for the control of selectivity and monitoring indoor air pollutant.

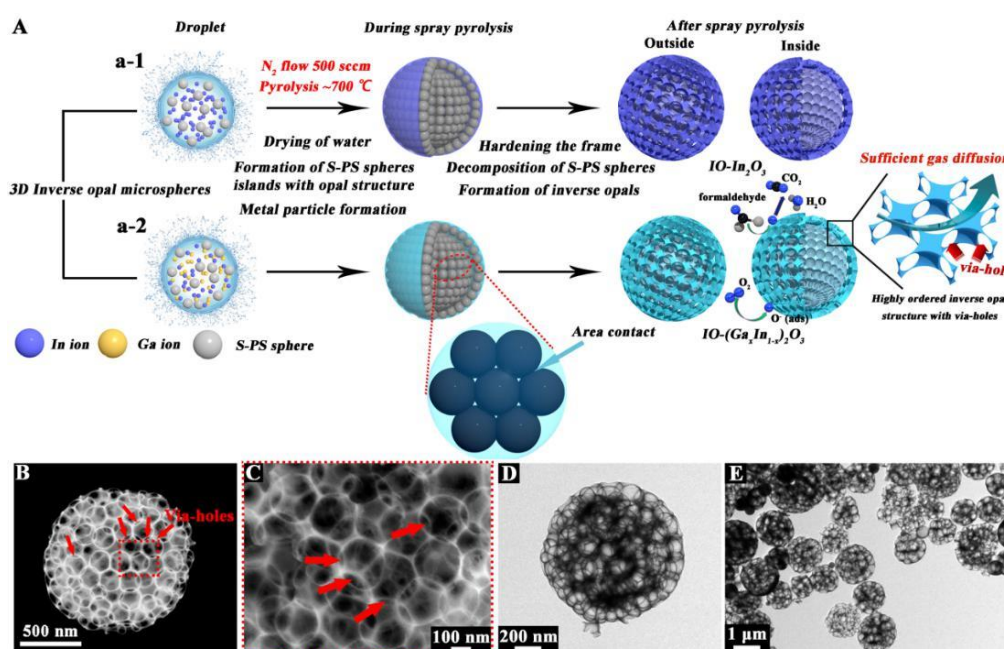


Figure 1. (A) Schemes illustrating the preparation of (a-1) inverse opal- In_2O_3 (IO- In_2O_3) microspheres, (a-2) Ga-doped IO- In_2O_3 microspheres (IO- $(\text{Ga}_{0.2}\text{In}_{0.8})_2\text{O}_3$); (B,C) SEM and (D,E) TEM images of IO- $(\text{Ga}_{0.2}\text{In}_{0.8})_2\text{O}_3$ microspheres.

Figure 1A illustrated the process of fabrication of inverse opal microspheres. As shown in Figure 1B,C, the interconnected and well-aligned 3D inverse opal skeletons were observed in IO-(Ga_{0.2}In_{0.8})₂O₃, and the sample yielded a long-range ordered hexagonal arrangement of the inverse opal microsphere structure. And, it also could be found that the individual inverse opal microsphere was assembled by packed small nanoparticles. Accordingly, due to the closer distance between the adjacent S-PS spheres (increase in contact area), the IO-(Ga_{0.2}In_{0.8})₂O₃ microsphere displayed additional viaholes among the oxide side walls (as indicated by the red arrow in Figure 1C). As shown in Figure 1D,E, a highly aligned inverse opal structure was found in every IO-(Ga_{0.2}In_{0.8})₂O₃ microsphere, and it could be found that the IO morphology remained after Ga doping. Besides, all spherical pores (mean pore size, ~160 nm) reflecting the shape of S-PS spheres were well developed and uniform inside the microspheres, and the oxide side walls formed stably between these pore walls, indicating that the inverse opal structure accumulated by many S-PS spheres could be retained even after decomposition of the S-PS sphere templates.

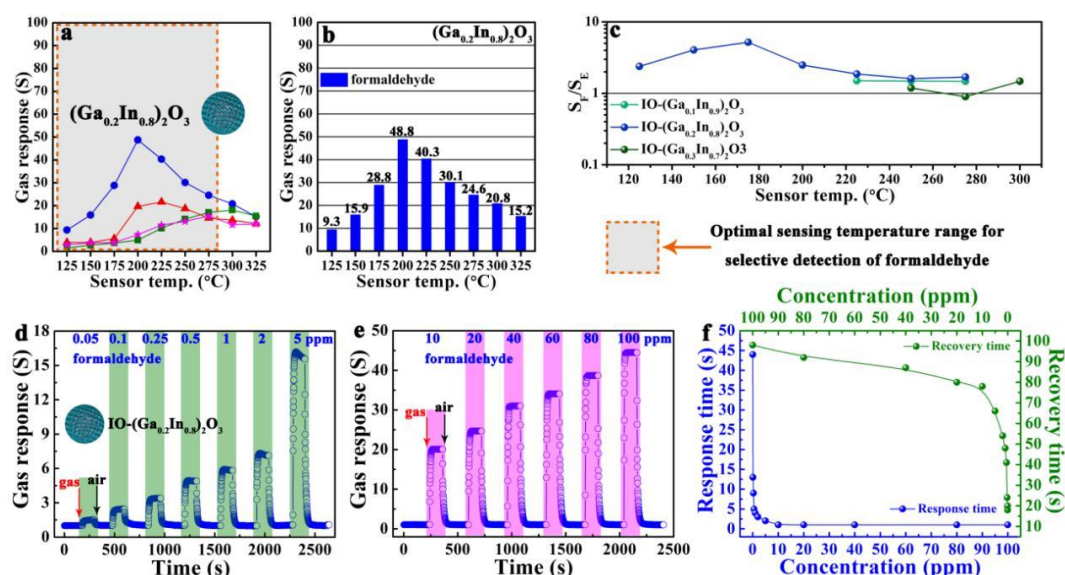


Figure 2. Gas responses (S) of the (a,b) IO-(Ga_{0.2}In_{0.8})₂O₃ sensor to 100 ppm of various gases at 125–325 °C. (c) formaldehyde selectivity ($S_{\text{formaldehyde}}/S_{\text{ethanol}}$, S_f/S_E) of the IO-(Ga_{0.2}In_{0.8})₂O₃ sensor at 125–325 °C. Formaldehyde-sensing characteristics of the IO-(Ga_{0.2}In_{0.8})₂O₃ sensor at 200 °C: (d,e) dynamic sensing transients to 0.05–100 ppm formaldehyde, and (f) response/recovery times toward formaldehyde in the concentration range of 0.05–100 ppm.

As shown in Figure 2a,b, the IO-(Ga_{0.2}In_{0.8})₂O₃ sensor showed the highest formaldehyde response, and reached the maximum ($R_a/R_g = 48.8$ –100 ppm formaldehyde) at the optimal operating temperature of 200 °C. The orange dotted boxes in Figure 2 highlighted the optimal sensing temperature ranges of the IO-(Ga_{0.2}In_{0.8})₂O₃ sensor for selective detection of formaldehyde. The selectivity to formaldehyde over ethanol interference (S_f/S_E) of the IO-(Ga_xIn_{1-x})₂O₃ ($x = 0.1, 0.2,$ and 0.3) sensors were calculated (Figure 2c). Note that the S_f/S_E value of the IO-(Ga_{0.2}In_{0.8})₂O₃ sensor was significantly higher than that of the IO-(Ga_{0.1}In_{0.9})₂O₃ and IO-(Ga_{0.3}In_{0.7})₂O₃ sensors. The gas-sensing transients of the IO-(Ga_{0.2}In_{0.8})₂O₃ sensor toward 0.05–100 ppm formaldehyde at 200 °C are shown in Figure 2d,e. Obviously, the IO-(Ga_{0.2}In_{0.8})₂O₃ sensor possessed excellent response-recovery kinetic characteristics in a broad formaldehyde concentration range. And it can be observed that the IO-(Ga_{0.2}In_{0.8})₂O₃ sensor still had a response of 1.53 when the formaldehyde concentration was as low as 50 ppb. As shown in Figure 2f, for the IO-(Ga_{0.2}In_{0.8})₂O₃ sensor, the response time tended to decrease with increasing formaldehyde concentration, and the sensor showed a long response time at low formaldehyde concentration. However, the recovery time tended to increase when the gas concentration and gas response increased, which emanated mainly from the sluggish surface kinetics of adsorption, dissociation, and ionization of oxygen during the recovery.

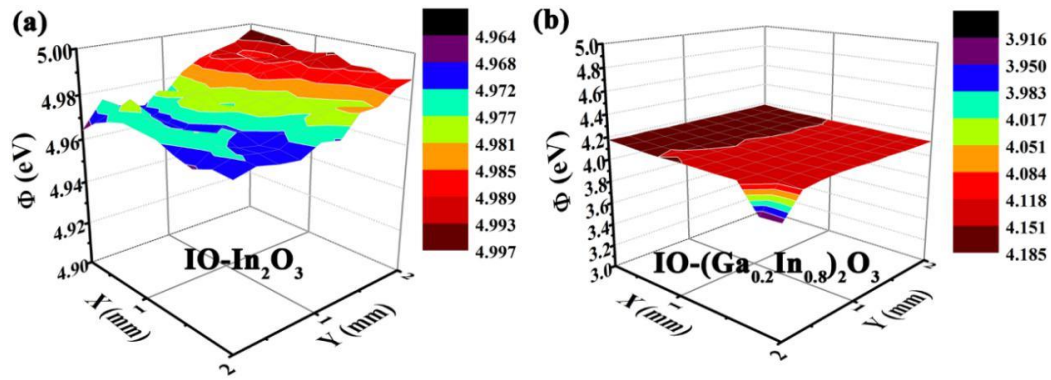


Figure 3. (a,b) work function area scan recorded for IO-(Ga_xIn_{1-x})₂O₃ (x = 0 and 0.2) samples via Kelvin probe measurements.

As shown in Figure 3, the work function area maps recorded for pure In₂O₃ and Ga-doped In₂O₃ are evaluated by employing the Kelvin probe measurements. According to the measured results of the work function values of different IO-(Ga_xIn_{1-x})₂O₃ (x = 0 and 0.2) samples, it can be concluded that the Ga doping will cause the elevation of the Fermi level in Ga-doped In₂O₃ samples.

Funding: This research was funded by the National Key Research and Development Program (No. 2016YFC0207300), National Nature Science Foundation of China (Nos. 61722305, 61833006, 61520106003), Science and Technology Development Program of Jilin Province (No. 20170520162JH), China Postdoctoral Science Foundation funded project Nos. 2017T100208 and 2015M580247, and Graduate Interdisciplinary Research Fund of Jilin University (No. 10183201833).

Conflicts of Interest: The authors declare no conflict of interest.



© 2019 by the authors. Licensee MDPI, Basel, Switzerland. This article is an open access article distributed under the terms and conditions of the Creative Commons Attribution (CC BY) license (<http://creativecommons.org/licenses/by/4.0/>).

Rare-Earth Based Chemoresistive CO₂ Sensors and Their Operando Investigations [†]

Takuya Suzuki ^{1,2,*}, Andre Sackmann ¹, Alexandru Oprea ¹, Udo Weimar ¹ and Nicolae Barsan ¹

¹ Institute of Physical Chemistry, University of Tübingen, 72076 Tübingen, Germany; andre.sackmann@ipc.uni-tuebingen.de (A.S.); alexandru.oprea@ipc.uni-tuebingen.de (A.O.); upw@ipc.uni-tuebingen.de (U.W.); nb@ipc.uni-tuebingen.de (N.B.)

² Corporate R&D Headquarters, Fuji Electric Co. Ltd., 191-8502 Hino-city Tokyo, Japan

* Correspondence: takuya.suzuki@ipc.uni-tuebingen.de

[†] Presented at the 8th GOSPEL Workshop. Gas Sensors Based on Semiconducting Metal Oxides: Basic Understanding & Application Fields, Ferrara, Italy, 20–21 June 2019.

Abstract: Rare-earth oxycarbonates have been proposed as promising chemoresistive materials for CO₂ sensors. In this contribution we present the results of a broad investigation focused on selecting the best candidates in the rare-earth compounds and, in the case of the best performing material, preliminary results dealing with the understanding of sensing by the operando methods.

Keywords: chemoresistive gas sensor; CO₂; rare-earth; oxycarbonate; operando investigation

1. Introduction

CO₂ sensing is of paramount importance for monitoring the state of the atmosphere, controlling indoor air quality, and cultivating crops in greenhouses or plant factories. Obtaining low cost, simple and good performance chemoresistive CO₂ gas sensors has the potential to be a game changer. Rare-earth oxycarbonates Ln₂O₂CO₃ (Ln = La and Nd) have been proposed as promising chemoresistive materials for CO₂ sensors [1–2]. We have been exploring new rare-earth based CO₂ sensitive materials and investigating into the conduction and sensing mechanism by using operando methods [3].

2. Material Synthesis and Sensor Fabrication

Rare-earth oxycarbonates and rare-earth oxides (rare-earth element = La, Ce, Nd, Sm, Gd, Dy, Er, Yb) were produced by the heat treatments of the oxalate hydrate or the acetate hydrate in a flow of ambient air at temperatures between 450 °C and 550 °C for 18 or 72 h. The powders after the heat treatment were mixed with propane-1,2-diol. The resulting pastes were screen printed onto alumina sensor substrates (provided with Pt interdigitated electrodes and Pt heater). The substrates were dried and then heated at the same temperature as its heat treatment.

3. Results and Discussion

3.1. DC Resistance Measurements

Figure 1 shows the comparison of sensor signals at 1,000 ppm CO₂ under standard humidity and operation temperature conditions (20 °C 50% rh, 300 °C) for all (10) sensors. The sensor signal is defined as the relative change of the resistance with respect to the resistance in air (CO₂ = 0 ppm). Every sensor, excepting the CeO₂ and Nd₂O₃ based, was sensitive to CO₂.

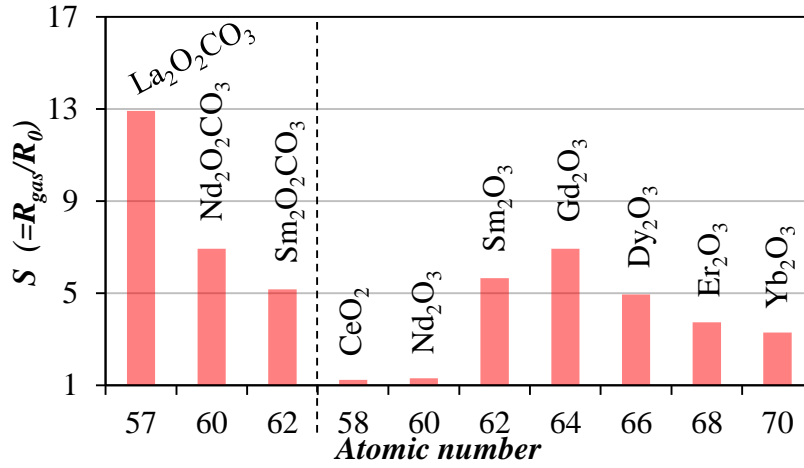


Figure 1. Comparison of sensor signal at 1000 ppm CO₂.

Additional investigations of selectivity and stability indicated that hexagonal $\text{La}_2\text{O}_2\text{CO}_3$ possesses the best properties for a CO₂ sensor so far. The detailed performance is shown in Figure 2.

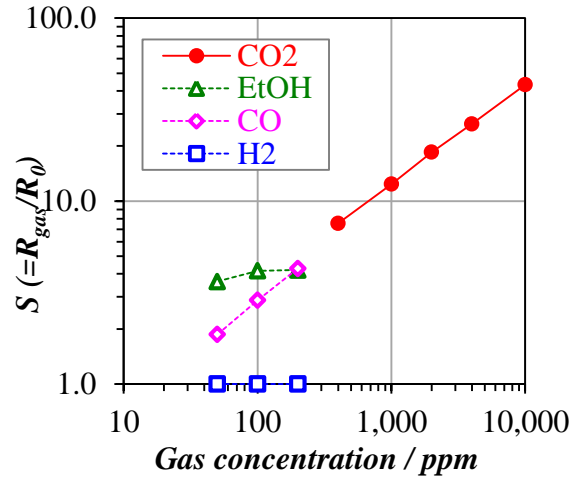


Figure 2. Sensing performance of hexagonal $\text{La}_2\text{O}_2\text{CO}_3$.

3.2. Operando Investigations

To reveal the sensing mechanism, we started by investigating the transduction by focusing on the conduction through the sensitive layer, with the help of operando AC impedance spectroscopy, and the effect of humidity, with the help of operando work function changes measurements; these investigations will be complemented by operando DRIFTS (Diffuse reflectance infrared Fourier transform spectroscopy) experiments; the operando stands for actual gas sensing conditions (e.g., at an operation temperature of 300 °C, with or without gas exposure, humid or dry atmosphere)

Out of the results of AC impedance spectroscopy, presented in Figure 3 as Cole-Cole plots, one can derive an equivalent circuit, see Figure 4. In it, there are two contributions that describe space charge regions – comprising parallel resistive and capacitive contributions. They can either describe electrode contact and intergranular contributions or heterogeneous intergranular contributions. In series, one finds an additional resistive contribution, which could describe the grains bulk. In DC conditions, the resistive contributions that are describing space charge regions, dominate and will show an exponential dependency on the surface barriers, which vary with ambient conditions. The changes of resistive contributions ($R_c + R_{gb}$) are correlated with the changes in the surface barrier height ΔV_s as in Equation (1).

$$(R_c + R_{gb})_0 / (R_c + R_{gb})_{\text{gas}} = \exp(-q\Delta V_s / kT) \quad (1)$$

where $(R_c + R_{gb})_0$ and $(R_c + R_{gb})_{\text{gas}}$ are the values at 0 ppm and at a certain concentration of CO_2 , and q is elementary charge respectively.

The inputs from the AC impedance spectroscopy are allowing to separate the contribution of electron affinity $\Delta\chi$ and band bending $q\Delta V_s$ to the work function changes $\Delta\Phi$ as in (2).

$$\Delta\Phi = q\Delta V_s + \Delta\chi \quad (2)$$

Figure 5 show the preliminary results in the case of the hexagonal $\text{La}_2\text{O}_2\text{CO}_3$ based sensor operated at 300 °C in 20 °C 10% rh. In this case, the work function changes more than 0.6 eV at 4000 ppm CO_2 and the contribution of electron affinity $\Delta\chi$ is larger than that of band bending $q\Delta V_s$.

The electron affinity mainly depends on the surface dipoles which are caused by surface adsorbents such as hydroxyl groups. We will identify the surface adsorbents by operando DRIFTS experiments.

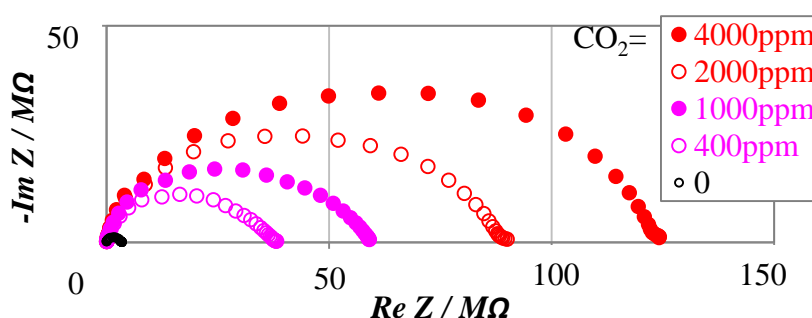


Figure 3. Cole-Cole plots from AC Impedance spectroscopy of hexagonal $\text{La}_2\text{O}_2\text{CO}_3$. (20 °C 10% rh, Operation temperature = 300 °C).

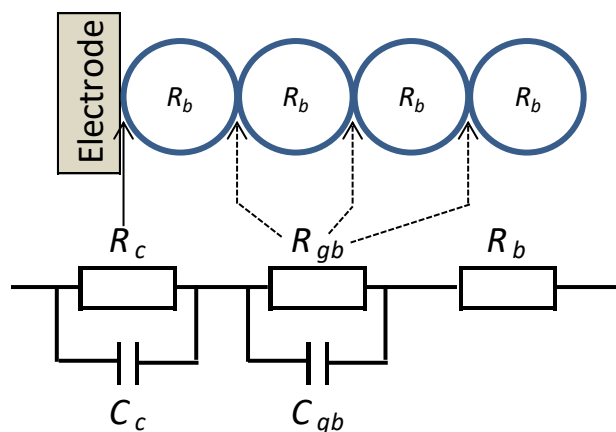


Figure 4. Equivalent circuit composed of the electrode contact ($R_c C_c$), the inter-granular contact ($R_{gb} C_{gb}$), and the bulk (R_b).

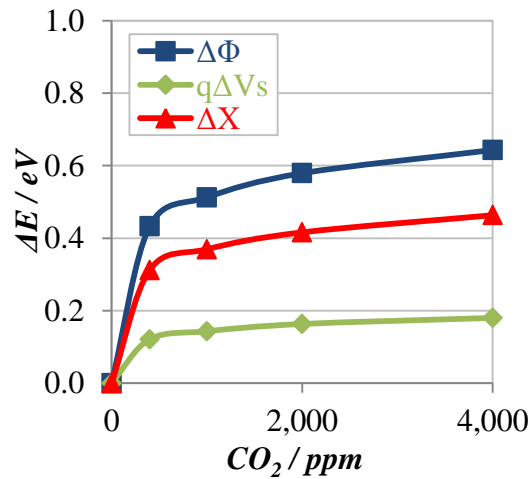


Figure 5. Variation of work function, band bending, and electron affinity with CO₂ concentration.

References

1. Djerdj, I.; Haensch, A.; Koziej, D.; Pokhrel, S.; Barsan, N.; Weimar, U.; Niederberger, M. Neodymium Dioxide Carbonate as a Sensing Layer for Chemoresistive CO₂ Sensing. *Chem. Mater.* **2009**, *21*, 5375–5381.
2. Haensch, A.; Djerj, I.; Niederberger, M.; Barsan, N.; Weimar, U. CO₂ sensing with chemoresistive Nd₂O₂CO₃ sensors-Operando insights. *Procedia Chem.* **2009**, *1*, 650–653.
3. Barsan, N.; Koziej, D.; Weimar, U. Metal oxide-based gas sensor research: How to? *Sens. Actuators B Chem.* **2007**, *121*, 18–35.



© 2019 by the authors. Licensee MDPI, Basel, Switzerland. This article is an open access article distributed under the terms and conditions of the Creative Commons Attribution (CC BY) license (<http://creativecommons.org/licenses/by/4.0/>).

Application of a Micro-Machined Electronic Nose to Detect *Escherichia Coli* in Human Urine Samples [†]

Matteo Soprani ^{1,2,*}, Giulia Zambotti ^{1,2}, Emanuela Gobbi ^{2,3} and Andrea Ponzoni ^{1,2}

¹ Department of Information Engineering, University of Brescia, Via Branze 38, 25123 Brescia, Italy; g.zambotti@unibs.it (G.Z.); a.ponzoni@unibs.it (A.P.)

² National Institute of Optics (INO), National Research Council (CNR), Via Branze 45, 25123 Brescia, Italy; e.gobbi@unibs.it

³ Department of Molecular and Translational Medicine, University of Brescia, Viale Europa 11, 25123 Brescia, Italy

* Correspondence: m.soprani001@unibs.it

[†] Presented at the 8th GOSPEL Workshop. Gas Sensors Based on Semiconducting Metal Oxides: Basic Understanding & Application Fields, Ferrara, Italy, 20–21 June 2019.

1. Introduction

The analysis of volatile organic compounds (VOCs) as disease biomarkers released by the urine, it permits an early and non-invasive diagnosis of Urinary Tract Infections (UTI) [1]. For this purpose, an instrumental method like the electronic nose composed by micromachined metal oxide gas sensors has been taken under consideration. *Escherichia coli* (*E. coli*) is the pathogenic microorganism responsible for up to 80% of the UTI and it is here chosen as benchmark bacterium [2]. The purpose of this research work is to test the capability of the electronic nose approach to recognise the presence of *E. coli*, identificative of a possible UTI disturb [3], in urine samples.

2. Materials and Methods

In the research's work, a device named miniMOx (JLM Innovation, Tübingen, Germany) has been involved. It is equipped with two micromachined metal oxide gas sensors (MOX): TGS8100 (Figaro, Arlington Heights, IL, USA) and CSS801 (AMS, Premstaetten, Austria). The MOX are capable to work with custom temperature modulation protocols controlled through their embedded heaters. This modulation periodically activates and freezes the interaction between gaseous molecules and the metal oxide surface, producing a periodic resistance vs. time curve as a response. In particular, a square wave of a 20 s period was applied. A warm semi-period was settled at voltage of $V_{heaters}$: 2.31 V for 10 s while the cold one at the voltage of $V_{heater} = 1.65$ V for the same amount of time. The resistance vs. time curves obtained were described through the $\Delta R_{cold-hot}$, ΔR_{cold} and ΔR_{hot} parameters. The $\Delta R_{cold-hot}$ represents the subtraction between the sensor's resistance measured at the end of the cold period and the resistance measured at the start of the warm period after 0.2 s. ΔR_{cold} signifies the difference between the sensor's resistance measured at the end of the cold period and after 0.2 s or at the beginning to the same period. ΔR_{hot} respects the warm period. In the end, a Principal Component Analysis algorithm (PCA function on Matlab) was used to elaborate the data acquired with the described parameters. Three representative samples were taken under consideration: urine, urine contaminated with a pathogenic microorganism (*Escherichia coli*) and sterilized water as a control. The analysis' procedure provided to place in contact the miniMOx for a time of 5 min with the head-space released from the samples, interspersed with 10 min for the sensors' recovery in ambient air. In parallel, bacterial counts were performed to monitor the *Escherichia coli* concentration during the whole analysis.

3. Results and Discussion

A summary of the obtained results is reported in the Figure 1.

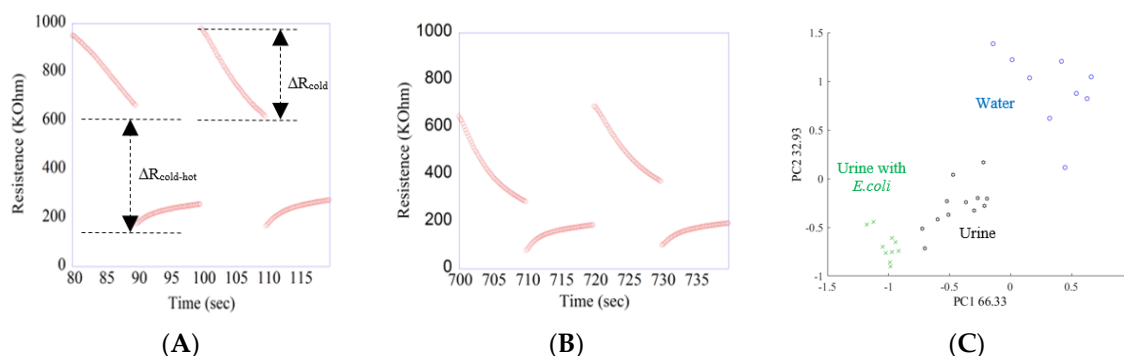


Figure 1. Resistance vs. time curves obtained with the CSS801 sensor. Two cycles of a cold and warm semi-period recorded during the exposition to the VOCs released by urine's samples (A). Two cycles of a cold and warm semi-period recorded during the exposition to the VOCs released by urine contaminated with *E. coli* samples (B). A Principal Component Plot of the MOX sensors response to the VOCs released by water (blue circles), urine (black stars) and urine with *E. coli* (green crosses) (C).

From the Figure 1, it is possible to observe the resistance vs. time curves acquired with the CSS801 sensor during the exposition at the VOCs released by uncontaminated urine (Figure 1A) and urine inoculated with *E. coli* at the initial concentration of 104 CFU/ml (Figure 1B). The resistance values are lower during the warm semi-period and larger during the semi-cold one, mainly due to thermal effect on the MOX semiconductor. The shape of these curves is sensitive to the surrounding atmosphere, with differences that can be properly resumed in terms of $\Delta R_{\text{cold-hot}}$ and ΔR_{cold} . PCA algorithm applied to the parameters explained before, led to results shown in the Figure 1C. The PCA Score Plot represents a scenario with three different clusters. The blue circles for sterilized water, the black stars for the urine and the green crosses for the urine contaminated with *Escherichia coli*. It is possible to understand that there is a separation between the samples among the PC1 and PC2 axes. In particular, there is a separation between the two urine's samples. Since the difference between the two urine's samples is the *E. coli* presence, potentially the pathogenic microorganism is the responsible to the separation itself.

4. Conclusions

The custom measurement protocol developed with the commercial electronic nose miniMOx revealed suitable to discriminate between water, urine and urine with *E. coli* through the analysis of the VOCs released by them. Since *E. coli* causes different kind of diseases in the human body, an early detection of this pathogenic microorganism into the urine could prevent the illnesses development. In conclusion, the miniMOx could be an easy-to-use, low-cost device for the pre-screening diseases through the VOCs released by urine.

Funding: This research was funded by Lombardia Region and CNR through the project FHfFC and by Lombardia Region and Fondazione Cariplo through the project EMPATIA@LECCO.

Conflicts of Interest: The authors declare no conflict of interest. The funding sponsors had no role in the design of the study; in the collection, analyses, or interpretation of data; in the writing of the manuscript, and in the decision to publish the results.

References

1. Mills, G.A.; Walker, V. Headspace solid-phase microextraction profiling of volatile organic compounds in urine: Application to metabolic investigation. *Chromatogr. B Biomed. Sci. Appl.* **2011**, *753*, 259–668.
2. Persaud, K.C.; Pisanelli, A.M.; Evans, P.; Travers, P.J. Monitoring urinary tract infections and bacterial vaginosis. *Sens. Actuator. B Chem.* **2006**, *116*, 116–120.

3. Bernabei, M.; Pennazza, G.; Santonico, M.; Roscioni, C.; Paolesse, R.; Di Natale, C.; D'Amico, A. A preliminary study on the possibility to diagnose urinary tract cancers by an electronic nose. *Sens. Actuator. B Chem.* **2008**, *131*, 1–4.



© 2019 by the authors. Licensee MDPI, Basel, Switzerland. This article is an open access article distributed under the terms and conditions of the Creative Commons Attribution (CC BY) license (<http://creativecommons.org/licenses/by/4.0/>).

The Influence of Temperature and Visible Light Activation on the NO₂ Response of WO₃ Nanofibers Prepared by Electrospinning [†]

Valentina Paolucci ^{1,*}, Seyed Mahmoud Emamjomeh ¹, Umberto Anselmi-Tamburini ² and Carlo Cantalini ¹

¹ Department of Industrial Engineering, University of L'Aquila, Via Gronchi 18, 67100 L'Aquila, Italy; seyedmahmoud.emamjomeh@graduate.univaq.it (S.M.E.); carlo.cantalini@univaq.it (C.C.)

² Department of Chemistry, University of Pavia, Viale Taramelli 12, 27100 Pavia, Italy; tau@unipv.it

* Correspondence: valentina.paolucci2@graduate.univaq.it

[†] Presented at the 8th GOSPEL Workshop. Gas Sensors Based on Semiconducting Metal Oxides: Basic Understanding & Application Fields, Ferrara, Italy, 20–21 June 2019.

Abstract: Aim of this work is to compare the electrical responses to 100–400 ppb NO₂ gas concentrations of WO₃ electrospun nanofibers both activated by thermal (in the temperature range 25–100 °C) and/or visible light at different wavelengths (Red $\lambda = 670$ nm, Green $\lambda = 550$ nm, and Purple-Blue $\lambda = 430$ nm). WO₃ nanofibers were prepared by mixing a W-O sol-gel transparent solution with a polymeric solution made of PVP and DMF, electrospun and subsequently annealed at 450 °C. Regarding gas sensing measurements, Purple Blue light resulted the most effective light source as respect to the others. Light illumination at room temperature revealed to improve both base line recovery and response time, whereas temperature enhances relative response, with a maximum at 75 °C. Light-radiating room temperature gas detection yields a satisfactory response notwithstanding a slight reduction of sensor gas sensitivity. Light induced electrical response mechanisms is presented and discussed.

Keywords: WO₃; nanofibers; light activation; NO₂ sensor

1. Introduction

Thermal activation mode at different operating temperatures (OT) represents so far one of the most common strategies to increase the catalytic activity of metal oxides sensors (MOX) toward gas response [1]. However, drawbacks of the thermal activation mode are yet represented by power consumption and shortened life time of the components. MOX gas response by light activation mode at room temperature has been more recently reported for NiO [2], TiO₂ [3], In₂O₃ [4], and WO₃ [5] respectively. Considering that literature reports have already shown that visible light activation can be easily achieved at room temperature by utilizing WO₃ thick films [5], in this paper we report room temperature NO₂ gas responses of 1D electrospun WO₃ nanofibers thermally and light activated at different wavelengths.

2. Results and Discussion

Figure 1 compares the SEM images for the as deposited (a,b) and annealed (c,d) WO₃ NFs at low (left side) and high magnification (right side), deposited on Si₃N₄ substrates. The formation of a continuous 3D-network of interconnected homogenous nanofibers of around 50 nm diameter is highlighted. After annealing at 450 °C for 1 h, fine nanograins of around 20 nm are visible with a well-developed crystalline structure.

Electrical responses to NO₂ gas were measured in dark conditions and at different visible light sources (Red $\lambda = 670$ nm, Green $\lambda = 550$ nm, and Purple-Blue $\lambda = 430$ nm) in the temperature range 25–100 °C. Figure 2 shows the electrical responses of WO₃ to 400 ppb NO₂ at 25 °C in dark and illuminated conditions. It turns out that the base line resistance (BLR) decreases by switching from dark, red, green and blue light respectively. This behavior can be explained considering that all the investigated light sources yield enough energy to cause the oxygen desorption from the WO₃ surface with associated release of previously-trapped electrons into the conduction band. Furthermore, another evidence coming out from Figure 2 is that by desorbing in dry air, the recovery of the base line is strongly enhanced by light-radiating the sensor surface. To give a figure of the sensor base line recovery ability we introduce the recovery percentage (RP) given by the percentage ratio $(\Delta D/\Delta A) \times 100$, where D and A stands for desorption and adsorption respectively (see Figure 2). It turns out that the RPs increase from 9% (dark), to 38% (Red), 55% (green) and 92% (blue). Figure 3 shows a comparison between the electrical responses of WO₃ nanofibers under dark and purple blue light at different operating temperatures (OT) in the range 25 °C–100 °C and different NO₂ gas concentrations (100 ppb–400 ppb). At 25 °C the base line recovery is very poor when desorbing in dark, but it significantly improves under blue light, as previously demonstrated in Figure 2, thus assigning the best performance to purple blue light. Regarding temperature, under both dark and light conditions, heating resulted to enhance the relative response (RR), with a maximum at 75 °C, and the recovery percentage.

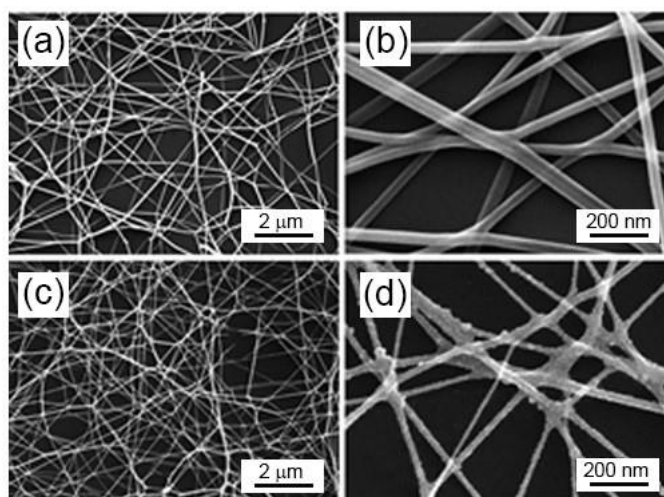


Figure 1. SEM images of electrospun WO₃ nanofibers. Panels (a,b) are respectively low and high magnification of as deposited NFs. Panels (c,d) represent the NFs after 1h annealing at 450 °C.

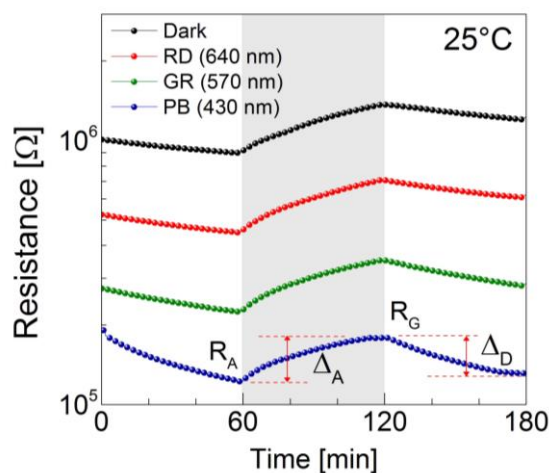


Figure 2. WO₃ nanofibers responses at 25 °C to 400 ppb NO₂ under different illuminating conditions.

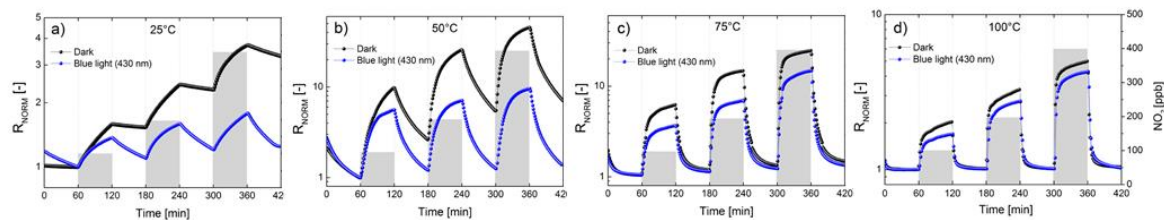


Figure 3. Comparison of the electrical responses in dark conditions and under purple-blue light ($\lambda = 430$ nm) at different temperatures and NO_2 gas concentrations.

However, an inhibiting influence played by light on the relative response is revealed, in particular at 75 °C. We may conclude that light activation mode increases the recovery percentage, whereas thermal activation enhances the relative response. To explain the higher RRs in dark as respect to light illumination conditions, we have to consider again that light is expected to activate the desorption of adsorbed oxygen from WO_3 surface. Considering now that NO_2 sensing is due to the reaction between NO_2 and the oxygen adsorbed on WO_3 surface, by illuminating the sensor surface, less oxygen species are available to react with NO_2 , eventually decreasing the relative response of the sensor.

3. Conclusions

We have prepared WO_3 electrospun nanofibers and tested to sub-ppm NO_2 concentrations by light and thermal activation modes. Room temperature gas sensitivity was comparable in dark and light conditions. A strong enhancement of both base line recovery and response times was displaced under light conditions, suggesting 2D WO_3 fibers to be suitable for ppb NO_2 detection at room temperature.

Funding: This research received no external funding.

Conflicts of Interest: The authors declare no conflict of interest.

References

1. Cantalini, C.; Lozzi, L.; Passacantando, M.; Santucci, S. The comparative effect of two different annealing temperatures and times on the sensitivity and long-term stability of WO_3 thin films for detecting NO_2 . *IEEE Sens. J.* **2003**, *3*, 171–179.
2. Geng, X.; Lahem, D.; Zhang, C.; Li, C.-J.; Olivier, M.-G.; Debliquy, M. Visible light enhanced black NiO sensors for ppb-level NO_2 detection at room temperature. *Sens. Actuators B Chem.* **2019**, *45*, 4253–4261.
3. Zampetti, E.; Macagnano, A.; Bearzotti, A. Gas sensor based on photoconductive electrospun titania nanofibers operating at room temperature, *J. Nanopart. Res.* **2013**, *15*, 1566.
4. Wagner, T.; Kohl, C.-D.; Malagù, C.; Donato, N.; Latino, M.; Neri, G.; Tiemann, M. UV light-enhanced NO_2 sensing by mesoporous In_2O_3 : Interpretation of results by a new sensing model. *Sens. Actuators B Chem.* **2013**, *187*, 488–494.
5. Giberti, A.; Malagù, C.; Guidi, V. WO_3 sensing properties enhanced by UV illumination: An evidence of surface effect. *Sens. Actuators B Chem.* **2012**, *165*, 59–61.



© 2019 by the authors. Licensee MDPI, Basel, Switzerland. This article is an open access article distributed under the terms and conditions of the Creative Commons Attribution (CC BY) license (<http://creativecommons.org/licenses/by/4.0/>).

Comparative Analysis between Blood Test and Breath Analysis using Sensors Array for Diabetic Patients

Hyung-Gi Byun ¹, Joon-Boo Yu ¹, Chong-Yun Kang ², Byoung Kuk Jang ³ and Hae-Ryong Lee ⁴

¹ Division of Electronics, Information & Communication Eng. Kangwon National University, Kangwon-Do, Korea; byun7414@gmail.com (H.-G. B.)

² Center for Electronic Materials, KIST, Seoul, Korea

³ Department of Internal Medicine, Keimyung University Dongsan Medical Center, Daegu, Korea

⁴ SW Contents Lab. ETRI, Daejeon, Korea

† Presented at the 8th GOSPEL Workshop. Gas Sensors Based on Semiconducting Metal Oxides: Basic Understanding & Application Fields, Ferrara, Italy, 20–21 June 2019.

Acetone was one of the volatile organic compounds present in respiration, and acetone contained in the exhalation of diabetic patients was found to be a combustion metabolite of body fat. Degradation of acetyl-CoA due to the metabolism of fatty acids in diabetic patients increase the concentration of acetone in the blood. Acetone in the blood is excreted as urine or breath. It has been studied that acetone released from breathing is 0.3 to 0.9 ppm for healthy people and 1.8 ppm or more for diabetic patients. Therefore, a variety of studies have been conducted to monitor diabetes by measuring the acetone gas released from breathing. Methods for measuring the amount of acetone in the exhalation using a GC-MS, an electrochemical sensor, and a method using an array of gas sensors based on metal oxide types were studied.

In this paper, we have been developed an E-Nose system using a metal oxide sensors array and measured the expiration of the normal and diabetic groups to distinguish diabetic patients from normal subjects. And blood samples from those peoples were analyzed to compare the exhaled breath test results using an E-Nose system.

The E-nose system is composed of sensor array, data acquisition and processing, and clustering part. The sensor array shown as Figure 1 was fabricated as one chip by depositing indium and tungsten with electron beam applying glancing angle deposition method at Korea Institute of Science Technology (KIST), Korea. A chamber was used to maintain the stable operating temperature of the sensor array and solid phase microextraction (SPME) fiber was used for the transfer of the measurement gas. Figure 2 is shown full system which has been used for experimental work.

The subjects were divided into controls and diabetes group, and 12 samples for controls and 11 samples for diabetics were selected. The collection and measurement of expiration and blood test were conducted in Dongsan Medical Center after approval of the Institute Review Board (IRB). The Clinical data for this study was summarized at Table 1.

The PCA results for these data are shown in Figure 3. As shown in Figure 3, diabetic patients and controls are distinguished, but some samples were displayed in different areas. In the blood test, Blood Sugar Test (BST), glucose, and HbA1C were given more information for classification. Throughout the primary results for comparative analysis between blood test and breath analysis using a sensors array, we confirm the clustering between controls and diabetics is possible, but we need more specific blood test information to confirm accuracy of breath analysis.

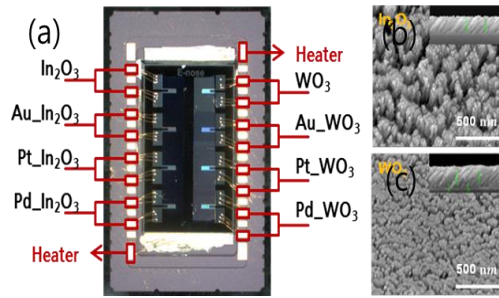


Figure 1. Sensor Array fabricated by KIST.

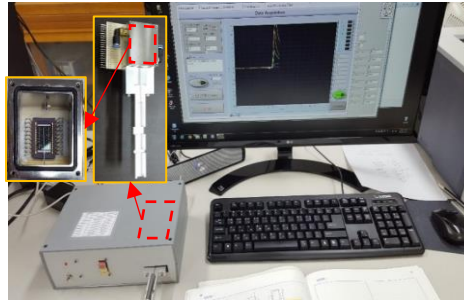


Figure 2. Measurement system using experimental works.

Table 1. Clinical data for the participants in study.

	PLT ($\times 10^3/uL$)	Glucose (mg/dL)	BST (mg/dL)	T.Bilirubin (mg/dL)	ALP (U/L)	AST (U/L)	ALT (U/L)	HbA1C (%)
Standard Values	130–400	<100	<100	0.3–1.0	66–220	0–35	0–35	<6
Average of Control	261	101	102	0.8264	61.7	22.44	20.84	5.232
Average of Diabetes	273	138	132	0.6984	76.8	23.44	21.18	6.452

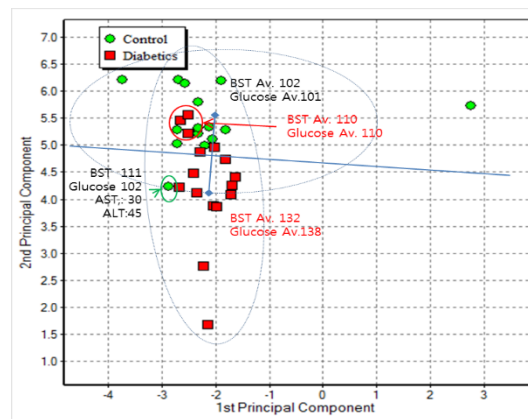


Figure 3. PCA result between diabetics and controls using breath analysis.



© 2019 by the authors. Licensee MDPI, Basel, Switzerland. This article is an open access article distributed under the terms and conditions of the Creative Commons Attribution (CC BY) license (<http://creativecommons.org/licenses/by/4.0/>).

How the Gas Flow Affects Conductometric Sensor Performance

Laura Parellada-Monreal^{1,2}, Alain Martín-Mayor³ and M. Mounir Bou-Ali³ and Gemma García Mandayo^{1,2,*}

¹ Ceit, Manuel Lardizábal 15, 20018 Donostia/San Sebastián, Spain; lparellada@ceit.es

² Ceit and Tecnum, Universidad de Navarra, Manuel Lardizábal 13, 20018 Donostia/San Sebastián, Spain

³ Faculty of Engineering, Mechanical and Industrial Production, Mondragon Unibertsitatea, Loramendi 4, Mondragon 20500 Gipuzkoa, Spain; amartin@eps.mondragon.edu (A.M.-M.); mbouali@mondragon.edu (M.M.B.-A.)

* Correspondence: ggmandayo@ceit.es; Tel.: +34-943-212-800

† Presented at the 8th GOSPEL Workshop. Gas Sensors Based on Semiconducting Metal Oxides: Basic Understanding & Application Fields, Ferrara, Italy, 20–21 June 2019.

1. Introduction

The performance of a metal oxide gas sensor can be affected by different parameters as the fabrication process of the sensitive layer or the post-annealing treatment. Nevertheless, not only the way the material has been obtained is relevant for the sensor performance. The conditions under which the detection is carried out are of great importance, namely the temperature of the material during detection and the gas flow conditions, among others.

The way the flow arrives at the sensor surface is relevant for the sensor response, mainly for the velocity of the response, but also because it can modify the temperature of the sensor. In the experiments to characterize gas sensors, the position of the gas input and output inside the sensor chamber, as well as the magnitude of the gas flow, influence the way the concentration gradient reaches the sensing material.

Moreover, convective flows are generated inside the chamber due to the sensor itself, because it acts as a heat source. As the convective flows can generate random concentration gradients, the response of the sensor will vary depending on the position of the heat source, namely, of the sensor itself.

In this work, the influence of the sensor position inside the chamber and the gas flow are analysed, comparing experimental results with flow dynamic simulations.

2. Simulations and Experimental

In order to investigate the effects of the position of the sensor and the flow of the gas inside the chamber during the sensing process, three cases were simulated and compared to experimental results:

- i. Case I: sensor at the bottom of the test chamber and 200 sccm flow (Figure 1a)
- ii. Case II: sensor at the bottom of the test chamber and 400 sccm flow (Figure 1b).
- iii. Case III: sensor in the middle of the test chamber and 400 sccm flow (Figure 1c).

The temperature of the sensor heater was set at 300 °C and the analyzed pulses were 5 ppm of NO₂ for all the simulations and experiments.

Simulation: a finite volume method based on numerical fluid flow analysis was used to obtain decoupled solution for both the Navier-Stokes equations and the mass diffusion equations (convection-diffusion equations) in the absence of reaction-transport equations and involving a high degree of convection-diffusion discretization schemes, applied to solve the combined effects of both

convection and diffusion. A mass flow inlet with a mass fraction of NO_2 of $7.94418 \cdot 10^{-6}$ (5 ppm of NO_2) relative to air was set and atmospheric pressure was imposed in the outlet.

Experiments: sputtered WO_3 gas sensor on alumina substrate were used for the experiments. The electrical measurements were performed inside a cylindrical sealed stainless steel chamber with a volume of 0.86 l.

3. Results

The comparison of the simulations and the experimental results for the three different cases are shown in Figure 1, where the simulated NO_2 concentration arriving at the sensor (black) and the response of the sensor (blue) are plotted in the left and right axis, respectively.

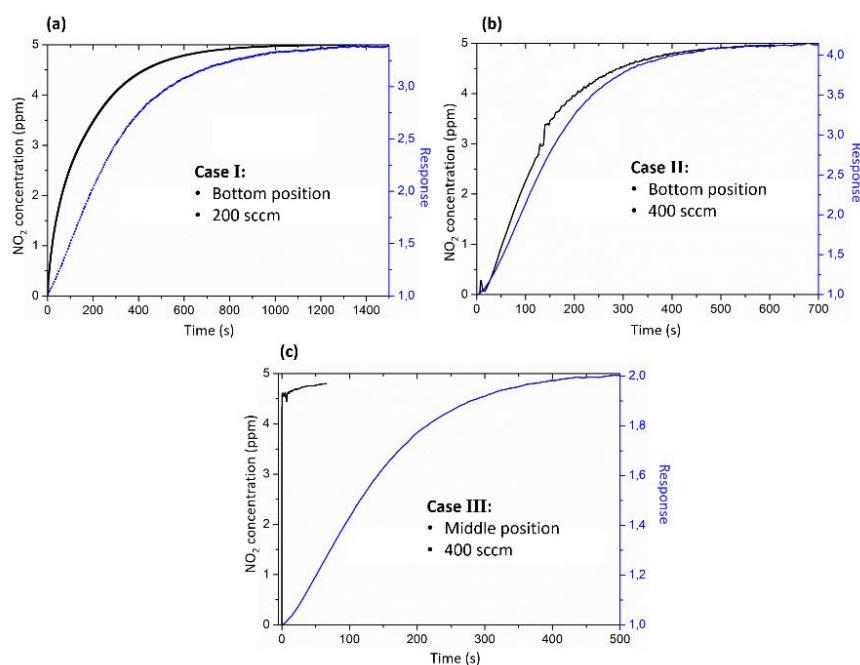


Figure 1. Simulated NO_2 concentration arriving at the sensor surface and response of the sensor for 5 ppm of NO_2 at $300\text{ }^\circ\text{C}$ for: (a) at the bottom of the chamber and with 400 sccm of flow, (b) at the bottom of the chamber and with 200 sccm of flow and (c) at the middle of the chamber and with 400 sccm of flow.

For case I and II, the simulations fits the experimental data and when the flow is increased from 200 to 400 sccm, the time needed to reach the maximum concentration on the sensor surface also decreases by a factor of 2.

If the sensor is placed in the middle of the chamber and the maximum flow is used (case III), the simulations states that in less than one second more than 4.5 ppm of NO_2 arrive at the sensor surface and then increases more slowly up to the maximum concentration introduced in the chamber (5 ppm). By contrast, from the experimental data, the needed time to reach the maximum response is ~ 500 s (the lowest time regarding the three different cases). This substantial difference between the simulation and the experimental results in the case III could be explained by the fact that this type of sensors have a minimum response time to reach the response value. Therefore, although the desired concentration reaches the sensor surface very fast, the sensors would need at least 8 min, in this case, to reach the maximum response, probably due to the time required for the diffusion processes.

Funding: This work was supported by the Ministry of Economy and Competitiveness (MINECO) through the TEMIN-AIR+ project (grant no. TEC2016-79898-C6-3-R) and by the Basque Government under the Micro4fab project (grant no. KK-2016-00030).

Conflicts of Interest: The authors declare no conflict of interest. The funding sponsors had no role in the design of the study; in the collection, analyses, or interpretation of data; in the writing of the manuscript, and in the decision to publish the results.



© 2019 by the authors. Licensee MDPI, Basel, Switzerland. This article is an open access article distributed under the terms and conditions of the Creative Commons Attribution (CC BY) license (<http://creativecommons.org/licenses/by/4.0/>).

Testing the Reliability of Flexible MOX Gas Sensors under Strain [†]

M. Alvarado ¹, A. Romero ¹, J.L. Ramírez ^{1,*}, S. De la Flor ² and E. Llobet ¹

¹ MINOS-EMaS, Departament d'Enginyeria Electrònica, Elèctrica i Automàtica; miriam.alvarado@urv.cat (M.A.); alfonso.romero@urv.cat (A.R.); eduard.llobet@urv.cat (E.L.)

² Departament d'Enginyeria Mecànica, Universitat Rovira i Virgili, Av. Països Catalans 26, 43007 Tarragona, Spain; silvia.delaflores@urv.cat

* Correspondence: joseluis.ramirez@urv.cat

[†] Presented at the 8th GOSPEL Workshop. Gas Sensors Based on Semiconducting Metal Oxides: Basic Understanding & Application Fields, Ferrara, Italy, 20–21 June 2019.

Abstract: We present flexible chemo-resistive sensors based on AACVD grown tungsten trioxide (WO₃) nanowires. The sensor response to gases, before and after a 50-cycle bending test, is reported. Thus, proving that reliable gas sensors, able to withstand repeated bending, have been achieved. Moreover, their integrity and durability have been tested under harsh bending conditions until break down.

1. Background

Flexible sensors are a promising technology for personal environmental monitoring, sports or healthcare and medicine. These applications involve using wearables, which are attached to the body or clothes to sense different variables, including gases. The use of flexible substrates improves the performance in these systems [1]. However, usually, little or no information is given on reliability. Here, metal oxide nanowire gas sensors over polymeric foil, have been developed and their performance after repeated mechanical stress test has been evaluated.

2. Materials and Methods

The sensor architecture consists of one electrode and one coplanar heater over a polymeric substrate (Kapton® 50.5 µm thick) as used in [2]. There is a layer of WO₃ nanowires coating the active area (Figure 1). Electrode and heater patterns were stenciled using silver ink as reported in [3]. The WO₃ layer was grown directly on the flexible substrate via an aerosol assisted chemical vapor deposition in a hot (350 °C) wall reactor. Precursors used were tungsten hexacarbonyl dissolved in a mixture of acetone and methanol, as reported in [4].

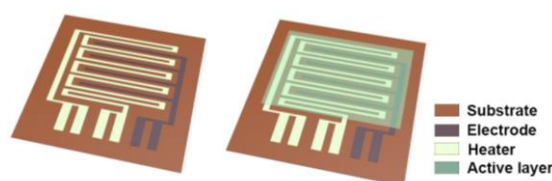


Figure 1. Device layout. Left: electrode and heater. Right: active layer over both elements. Device size 14 × 14 mm².

We made a controlled bending test using an electromechanical universal testing machine (Shimadzu AGS-X 10 kN). Sensors were strained up to 15% and the maximum deflection due to buckling was $d = 3.23$ mm. The test consisted of 50 continuous moves of the upper grip. Each move was 2 mm down and up, at 20 mm/min, producing a curvature radius of approx. 3.1 mm (Figure 2).

Meanwhile, the electrical resistance of the active layer, the stroke and the force applied were measured.

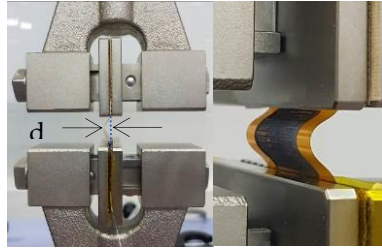


Figure 2. Universal testing machine grips holding the sensor. d = maximum deflection distance.

3. Results

The AACVD process resulted in the direct growth onto the transducer of WO_3 nanowires (150 nm in diameter and 10 microns in length). Sensors were tested against H_2 before and after the bending test. In both cases, three cycles of three H_2 concentrations (250, 500 and 750 ppm) were tested, at a heater mean temperature of 150 °C. Sensor response after the bending test (Figure 3) shows small changes (after bending test baseline electrical resistance increased by 5.5% Figure 4, which can be easily calibrated). An additional test was carried out until the sensing layer was damaged: the electrical resistance increased significantly at zero stroke. This occurred after 200 bending cycles: 100 under compressive strain and 100 under tension strain, with a shift of 4 mm and $d = 4.3$ mm of maximum deflection (curvature radius 3.2 mm).

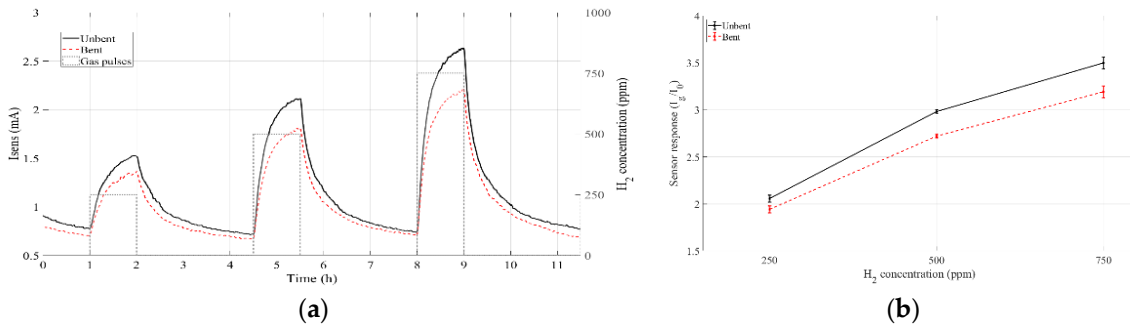


Figure 3. (a) Current through active layer at different concentrations of H_2 (250, 500 and 750 ppm H_2) and (b) Sensor response to H_2 concentration, before and after 50 repeated bending tests.

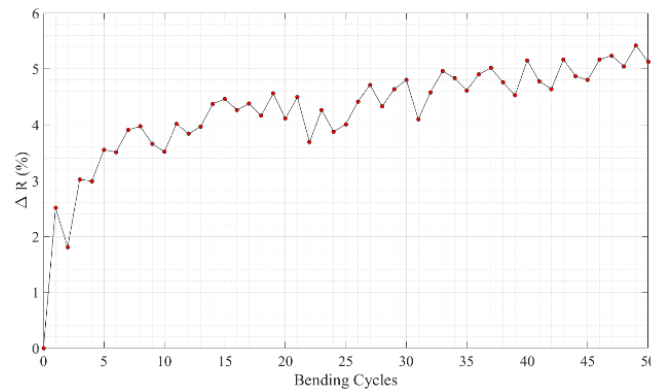


Figure 4. Percentage of sensor resistance increase during 50-cycles bending test.

4. Conclusions

We have proved that is possible to produce reliable flexible sensors with a very affordable technology. After a 50-cycles bending test, under tensile strain, sensor response remains almost unchanged. Moreover, the limits of the physical system have been tested under harsh bending conditions. The sensors could withstand up to 200 bending cycles before losing functionality. This is being developed further via the design of in-house made metal oxide inks for achieving fully printed functional devices. Characterization results will be presented at the conference.

Funding: This research was funded in part by MINECO and FEDER under grant no. TEC2015-71663-R and by AGAUR under grant no. 2017 SGR 418.

Conflicts of Interest: The authors declare no conflict of interest. The funders had no role in the design of the study; in the collection, analyses, or interpretation of data; in the writing of the manuscript, or in the decision to publish the results.

References

1. Nag, A.; Mukhopadhyay, S.C.; Kosel, J. Wearable flexible sensors: A review. *IEEE Sens. J.* **2017**, *17*, 3949.
2. Ramírez, J.L.; Annanouch, F.E.; Llobet, E.; Briand, D. Architecture for the efficient manufacturing by printing of heated, planar, resistive transducers on polymeric foil for gas sensing. *Sens. Actuators B Chem.* **2018**, *258*, 952–960.
3. Alvarado, M.; Navarrete, E.; Romero, A.; Ramírez, J.L.; Llobet, E. Flexible Gas sensors employing octahedral indium oxide films. *Sensors* **2018**, *18*, 999.
4. Vallejos, S.; Umek, P.; Blackman, C. Aerosol assisted chemical vapour deposition control parameters for selective deposition of tungsten oxide nanostructures. *J. Nanosci. Nanotechnol.* **2011**, *11*, 8214–8220.



© 2019 by the authors. Licensee MDPI, Basel, Switzerland. This article is an open access article distributed under the terms and conditions of the Creative Commons Attribution (CC BY) license (<http://creativecommons.org/licenses/by/4.0/>).

Extended Abstract

SACMI Electronic Olfactory System Based on Semiconducting Metal Oxides [†]

Marco Marzocchi * and Oliviero Ossani

SACMI Imola S.C., via Selice Provinciale, 17/A, 40026 Imola (BO), Italy; oliviero.ossani@sacmi.it

* Correspondence: marco.marzocchi@sacmi.it

[†] Presented at the 8th GOSPEL Workshop. Gas Sensors Based on Semiconducting Metal Oxides: Basic Understanding & Application Fields, Ferrara, Italy, 20–21 June 2019.

Electronic Olfactory Systems, also called Electronic Noses, are instruments designed to mimic the sense of smell. This is obtained by using an array of different gas sensors, whose signals are collected and elaborated by a processing unit; the measured signals are then compared to a pre-determined odour training set, in order to obtain odour recognition and quantification.

In SACMI Electronic Noses, an array of six different semiconducting metal oxide gas sensors is used as the sensing element (Figure 1). These sensors are obtained by the deposition of a $1 \times 1 \text{ mm}^2$ layer of sensing material on a $2 \times 2 \text{ mm}^2$ Aluminium Oxide substrate, and are realized through sputtering deposition, with a thickness of 10–100 nm, or by serigraphic deposition, with a thickness of about $10 \mu\text{m}$.

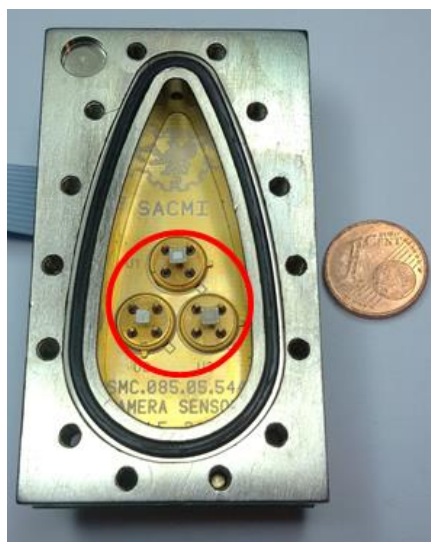


Figure 1. Open sensors chamber showing three gas sensors.

Even though this technology offers a high sensitivity to many odorous compounds and a good stability with time, several problems related to the sensor output need to be addressed to achieve a stable and reproducible instrumental response, namely:

1. Gas flow, temperature, and humidity dependence of sensor response (electrical resistance)
2. Drift of sensor baseline and sensitivity over long times (months/years), especially after inactivity times
3. Non-linear dependence of sensor response vs. gas concentration.

Many hardware and software solutions have been implemented in SACMI Electronic Noses to overcome these limitations:

1. Flow, temperature and humidity control
2. Periodical automatic calibration with reference gas
3. Acquisition of calibration curves using both reference gas and sample gas during training.

As a result, these instruments can be used reliably both in laboratory for quality control measurements and outdoor for continuous environmental monitoring of odour nuisance (Figure 2). In the past years, SACMI Electronic Noses have been applied in food quality control (coffee, olive oil, tomato, etc.), packaging quality control, and monitoring of industrial activities (refineries, waste treatment plants, chemical plants, etc.).



Figure 2. SACMI Electronic Olfactory Systems for outdoor (**left**) and laboratory (**right**) use.

Funding: This research received no external funding.

Acknowledgments: The authors would like to acknowledge Prof. Vincenzo Guidi (University of Ferrara) for his contribution in the development of the semiconducting metal oxides gas sensors used in SACMI Electronic Noses.

Conflicts of Interest: The authors declare no conflict of interest. The funders had no role in the design of the study; in the collection, analyses, or interpretation of data; in the writing of the manuscript, or in the decision to publish the results.



© 2019 by the authors. Licensee MDPI, Basel, Switzerland. This article is an open access article distributed under the terms and conditions of the Creative Commons Attribution (CC BY) license (<http://creativecommons.org/licenses/by/4.0/>).

MOX Sensors to Ensure Suitable Parameters of Grated Parmigiano Reggiano Cheese [†]

Marco Abbatangelo *, Giorgio Duina, Elisabetta Comini and Giorgio Sberveglieri

Department of Information Engineering, University of Brescia, via Branze, 38, 25123 Brescia, BS, Italy; giorgio.duina@unibs.it; elisabetta.comini@unibs.it; giorgio.sberveglieri@unibs.it

* Correspondence: m.abbatangelo@unibs.it

[†] Presented at the 8th GOSPEL Workshop. Gas Sensors Based on Semiconducting Metal Oxides: Basic Understanding & Application Fields, Ferrara, Italy, 20–21 June 2019.

Parmigiano Reggiano (PR) cheese is a long-ripened hard cheese made in Northern Italy registered as a Protected Designation of Origin (PDO) in the European Union. PR is a well-known product for its high content of nutrients and taste. It is present on the market essentially in two formats: trimmed pieces and grated cheeses. When faced with a shortfall of demand of trimmed methods, sales of grated PR have increased by 5.2% [1]. Grated cheese must account specific technical parameters, as established in the procedural guideline [2]. They are inter alia: minimum 12 months of ripening, less than 25% of particles having diameter less than 0.5 mm, and a quantity of rind less than 18% (w/w). However, it can happen that this limit can be exceeded because of process issues (e.g., mixing errors) or fraudulent reasons. This, together with the increase in sales, is the main reason why our attention focused on this kind of product.

In this work, grated PR samples were analyzed by a sensors system with 8 MOX gas sensors inside. Six of them were produced at Sensor Laboratory (University of Brescia, Italy). Three of them were nanowires of MOX (two were tin oxides nanowires sensors using a gold catalyst on the alumina substrate and functionalizing one of them with gold clusters; the third sensor had an active layer of copper oxide nanowires). The other three sensors are prepared with Rheotaxial Growth and Thermal Oxidation (RGTO) thin film technology (one tin oxide functionalized with gold clusters, two pure tin oxide). The last two are commercial MOX sensors produced by Figaro Engineering Inc. (TGS2611 and TGS2602). Headspace of different types of grated PR cheese were analyzed, totalling 452 samples; all of them were provided by Consorzio del Formaggio Parmigiano Reggiano (CFPR). Three characteristic parameters were taken into account: ripening degree (12 months or 24 months), rind working process (i.e., brushed or washed) and rind percentage (lower than 18%, between 18% and 26%, higher than 26%). Sensors' resistances were recorded and their maximum variations for each measure were extracted as features. Data were analyzed using artificial neural networks (ANNs) as classifiers. Given the complexity of the problem due to the different considered variables of the grated PR, a hierarchical approach has been used [3]. The problem was divided in three steps: recognition of ripening degree; then, distinction of rind working process; finally, identification of rind percentage. For each step, a different number of ANNs was used: at the beginning, one ANN sorted samples in 12 months or 24 months classes; in the second step, two ANNs (one for each of the two classes of the previous step) classify the rind working process; at the end, four networks recognize rind percentage in three classes: lower than 18%, between 18% and 26% and higher than 26%. ANNs were trained until they reached the higher classification rate. Results are shown in Table 1. Sensors' array is able to recognize correctly all the samples in 5 out of 7 tasks. However, most misclassified samples are those with 12 months ripening and washed rind and this could be caused by higher quantity of humidity that characterizes these samples.

Table 1. Classification rates of ANNs for each step.

STEP 1	STEP 2	STEP 3		
Ripening (12 months vs. 24 months)	Rind working process for 12 months	Rind percentage (12 months washed)	73.33%	
	Samples (Washed vs. Brushed)	100%	Rind percentage (12 months brushed)	100%
	Rind working process for 24 months	100%	Rind percentage (24 months washed)	100%
	samples (Washed vs. Brushed)	100%	Rind percentage (24 months brushed)	100%

References

1. Available online: https://www.parmigianoreggiano.it/comunicazione/rapporto_annuale_dell_attivita/default.aspx (accessed on 27 May 2019).
2. D.P.C.M. (Decree of the president of the council) (*Estensione della Denominazione di Origine del Formaggio «Parmigiano Reggiano» alla Tipologia «Grattugiato»*; Gazzetta Ufficiale: Italy, 1991; Volume 83).
3. Abbatangelo, M.; Núñez Carmona, E.; Sberveglieri, V.; Zappa, D.; Comini, E.; Sberveglieri, G. Application of a novel S3 nanowire gas sensor device in parallel with GC-MS for the identification of rind percentage of grated Parmigiano Reggiano. *Sensors* **2018**, *18*, 1617, doi:10.3390/s18051617.



© 2019 by the authors. Licensee MDPI, Basel, Switzerland. This article is an open access article distributed under the terms and conditions of the Creative Commons Attribution (CC BY) license (<http://creativecommons.org/licenses/by/4.0/>).

Chemically Sensitive Photoluminescence of InGaN/GaN Nanowire Heterostructure Arrays [†]

Konrad Maier ¹, Andreas Helwig ¹, Gerhard Müller ^{2,*} and Martin Eickhoff ³

¹ Airbus Group Innovations, D-81663 Munich, Germany; maierkonrad@gmail.com (K.M.); andreas.helwig@airbus.com (A.H.)

² Munich University of Applied Sciences and Mechatronics, D-80335 Munich, Germany

³ Institute of Solid-State Physics, University of Bremen, D-28359 Bremen, Germany; eickhoff@ifp.uni-bremen.de

* Correspondence: gerhard.mueller@hm.edu

† Presented at the 8th GOSPEL Workshop: Gas Sensors Based on Semiconducting Metal Oxides—Basic Understanding & Application Fields, Ferrara, Italy, 19–21 June 2019.

1. Background

III-nitride semiconductors (AlGaIn, GaN and InGaIn) have received considerable attention in various fields ranging from high-frequency and high-temperature electronics [1] to LED lighting technologies [2]. Interesting applications also arise in the fields of gas, chemical and biosensors [3,4] and in photo-electrochemical power conversion [5].

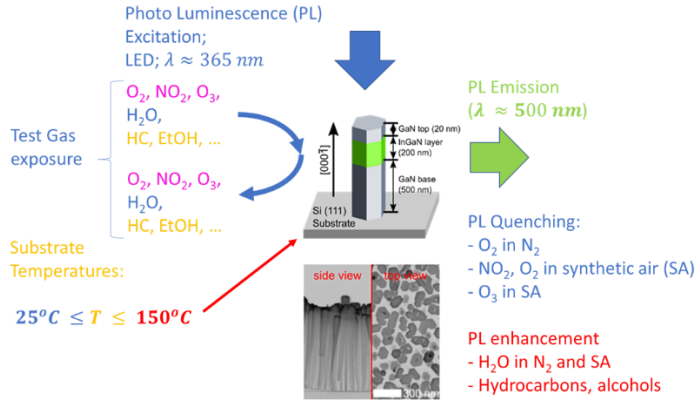
2. Experiment

We have studied the photoluminescence (PL) response of InGaIn/GaN heterostructure nanowire arrays (NWA) while being exposed to different kinds of oxidizing and reducing gases as well as to humidity (Figure 1a) [6–10]. As III-nitrides tend to form thin, native surface oxide layers when exposed to ambient air, their chemical interactions are similar to those on more traditionally studied kinds of metal oxides (MOX). As InGaIn/GaN NWAs exhibit efficient photoluminescence up to temperatures of 200 °C and more, PL measurements can be performed at temperatures approaching those of conventional resistive MOX gas sensors. As localized adsorbate-adsorbent reactions are directly answered by a local PL output, the PL response of InGaIn/GaN NWAs provides a more direct view onto surface adsorption processes than conventional resistive MOX gas sensors.

3. Results

Figure 1b shows that our NWAs exhibit a quenching response when exposed to O₂ in a N₂ background. Quenching responses are also observed when tiny concentrations (ppm and below) of NO₂ and O₃ are admixed to synthetic air (SA) [6,10]. Enhancing responses to water vapor can be observed when H₂O exposures are performed in N₂ (Figure 1c) and when these are maintained for prolonged periods of time and at high illumination levels [7,10]. We attribute this enhancing behavior to the photo-electrochemical generation of passivating H⁺ and OH⁻ fragments. Reducing gas species (e.g. EtOH) give rise to enhancing responses only when the NWAs are operated in SA and at elevated temperatures. No responses to reducing gases are observed when these are applied in inert N₂ backgrounds. Reducing gas species therefore are detected in an indirect manner by consuming quenching oxygen adsorbates and by forming enhancing H₂O ones as these interact with oxygen species co-adsorbed in reactive backgrounds of ambient or synthetic air [8,10].

a) Experiment



Typical gas responses

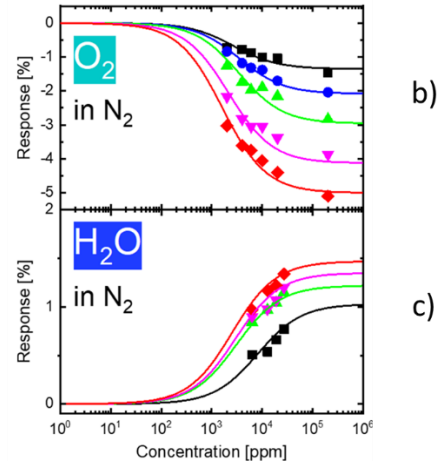


Figure 1. (a) Detection of adsorbate-induced changes in the PL emission response of InGaN/GaN nanowire heterostructure arrays (NWA); (b,c) typical PL response data as a function of the applied gas (vapor) concentration. Full lines represent fits to Langmuir adsorption isotherms (Equation (1)). Differently colored symbols/lines correspond to increasing NWA temperatures (black: 25 °C; red: 150 °C).

A characteristic observed across all kinds of analytes is that the concentration dependence of the PL response, $R_{PL}(p_{gas}, T)$, consistently follows Langmuir isotherms which are easy to interpret regarding adsorbate-specific adsorption energies E_{ads} :

$$R_{PL}(p_{gas}, T) = R_{PL,sat} \frac{p_{gas}}{p_{gas} + P_{00} \exp\left[-\frac{E_{ads}}{k_B T}\right]}; P_{00} \approx 10^{12} Pa. \quad (1)$$

A second important parameter is the position of the gas sensitivity window, i.e., the range of gas partial pressures in which gas-induced changes in the PL response can be observed. A convenient parameter that characterizes this position is the value of $p_{gas} = p_{1/2}$ at which the PL response takes on half of its saturation value $R_{PL,sat}$.

Regarding both parameters, the most important observations are the following:

- (i) For a given NWA operation temperature T , the value of $p_{1/2}$ is exponentially dependent on E_{ads} , i.e. small changes in E_{ads} give rise to huge changes in gas sensitivity [6,10];
- (ii) For a given sensor operation temperature T , the value of E_{ads} for a given adsorbate scales with the electron affinity, E_A , of the adsorbate [6,10]. The value of the electron affinity is defined as the energy gained upon attaching an electron (e^-) to an adsorbate species X : $X + e^- \rightarrow X^-$;
- (iii) For each analyte studied the best-fitting value of E_{ads} is not an adsorbate-specific constant but rather a linear function of the sensor operation temperature. This peculiar behavior can be explained by assuming that test gases compete with background gases for common adsorption sites [9,10].

A full account of our data will be represented in reference [10].

Funding: (M.E.) acknowledges financial support within the LOEWE program of excellence of the Federal State of Hessen (project initiative STORE-E).

Acknowledgments: The authors are grateful to Jörg Schörmann and Jörg Teubert of the University of Gießen for the preparation of InGaN/GaN nanowire arrays.

Conflicts of Interest: The authors declare no conflict of interest. The funders had no role in the design of the study; in the collection, analyses, or interpretation of data; in the writing of the manuscript, or in the decision to publish the results.

References

1. Fletcher, A.S.A.; Nirmal, D. A survey of Gallium Nitride HEMT for RF and high power applications. *Superlattices Microstruct.* **2017**, *109*, 519–537, doi:10.1016/J.SPML.2017.05.042.
2. Chao E. *Analysis of LED Technologies for Solid State Lighting Markets*; Technical Report No. UCB/EECS-2012-138; EECS Department, University of California, Berkeley: Berkeley, CA, USA, 2012. Available online: <https://www2.eecs.berkeley.edu/Pubs/TechRpts/2012/EECS-2012-138.html> (accessed on 18 June 2018).
3. Pearton, S.J.; Kang, B.S.; Kim, S.; Ren, F.; Gila, B.P.; Abernathy, C.R.; Lin, J.; Chu, S.N.G. GaN-based diodes and transistors for chemical, gas, biological and pressure sensing. *J. Phys. Condens. Matter.* **2004**, *16*, R961–R994, doi:10.1088/0953-8984/16/29/R02.
4. Shahbaz, J.; Schneidereit, M.; Thonke, K.; Scholz, F. Functionalized GaN/GaInN heterostructures for hydrogen sulfide sensing. *Jpn. J. Appl. Phys.* **2019**, *58*, SC1028.
5. Winnerl, J.; Hudeczek, R.; Stutzmann, M. Optical Design of GaN Nanowire Arrays for Photocatalytic Applications. *J. Appl. Phys.* **2018**, *123*, 203104.
6. Maier, K.; Helwig, A.; Müller, G.; Becker, P.; Hille, P.; Schörmann, J.; Teubert, J.; Eickhoff, M. Detection of Oxidising Gases Using an Optochemical Sensor System Based on GaN/InGaN Nanowires. *Sens. Actuators B Chem.* **2014**, *197*, 87–94.
7. Maier, K.; Helwig, A.; Müller, G.; Hille, P.; Teubert, J.; Eickhoff, M. Photoluminescence Probing of Complex H₂O Adsorption on InGaN/GaN Nanowires. *Nano Lett.* **2017**, *17*, 615–621.
8. Maier, K.; Helwig, A.; Müller, G.; Eickhoff, M. Photoluminescence Detection of Surface Oxidation Processes on InGaN/GaN Nanowire Arrays. *ACS Sens.* **2018**, *3*, 2254–2260.
9. Maier, K.; Helwig, A.; Müller, G.; Hille, P.; Teubert, J.; Eickhoff, M. Competitive Adsorption of Air Constituents as Observed on InGaN/GaN Nano-Optical Probes. *Sens. Actuators B Chem.* **2017**, *250*, 91–99.
10. Maier, K.; Helwig, A.; Müller, G.; Eickhoff, M. Luminescence Probing of Surface Adsorption Processes Using InGaN/GaN Nanowire Heterostructure Arrays. In *Semiconductor Gas Sensors*; Woodhead Publishing: Cambridge, UK, 2019, in press.



© 2019 by the authors. Licensee MDPI, Basel, Switzerland. This article is an open access article distributed under the terms and conditions of the Creative Commons Attribution (CC BY) license (<http://creativecommons.org/licenses/by/4.0/>).

Selective Detection of Hydrocarbons in Real Atmospheric Conditions by Single MOX Sensor in Temperature Modulation Mode [†]

Valeriy Krivetskiy ^{1*}, Matvey Andreev ¹ and Alexander Efitorov ²

¹ Department of Chemistry, M.V. Lomonosov Moscow State University, Leninskie Gory 1/3, Moscow 119234, Russia; matderevenayv@yandex.ru

² Skobeltsyn Institute of Nuclear Physics (SINP MSU), M.V.Lomonosov Moscow State University, 1(2), Leninskie Gory, GSP-1, Moscow 119991, Russia; a.efitorov@sinp.msu.ru

* Correspondence: vkrivetsky@inorg.chem.msu.ru

[†] Presented at the 8th GOSPEL Workshop. Gas Sensors Based on Semiconducting Metal Oxides: Basic Understanding & Application Fields, Ferrara, Italy, 20–21 June 2019.

Abstract: Selective detection of hydrocarbons—methane and propane—in urban air for industrial safety properties by single metal oxide semiconductor gas sensor has been demonstrated. As sensors were fabricated on the basis of nanocrystalline SnO₂ and alumina micro-hotplates. Sensor working temperature modulation has been applied during raw sensor data collection. Pre-processing of acquired data—scaling, baseline extraction and exclusion of non-valid data points has been demonstrated to be critical procedures before application of machine learning algorithms. The achieved accuracy of 86% for correct gas identification in 40–200 ppm range has been demonstrated.

Keywords: metal oxide; semiconductor; gas sensor; temperature modulation; signal pre-processing; artificial neural networks

1. Introduction

Detection of pipeline hydrocarbons leakage is a valid industrial demand [1]. A deployed network of autonomous miniature micromachined metal oxide semiconductor gas sensors with low power consumption possess a great perspective of practical use in this regard [2,3]. The main obstacle of their high cross sensitivity can be overcome by the implementation of sensor arrays or working temperature modulation in combination of signal processing and nonlinear calibration [4,5]. In this work we demonstrate stable selective detection of propane and methane in low concentrations in the real urban ambient air by the SnO₂-based semiconductor gas sensor.

2. Experimental

Nanocrystalline SnO₂ gas sensitive material has been synthesized by flame spray pyrolysis technique. Gas sensors were fabricated on the basis of 2 × 2 × 0.15 mm alumina micro-hotplates with the use of α -terpineol as a binder. Measurements were carried out in a flow-through sensor cell with the use of outdoor air with the admixture of methane and propane from certified gas bottles. Gas concentrations varied from 40 to 200 ppm. Sets of data were collected during a series of 24 h experiments with variable air temperature and humidity. The measurements were conducted through 2 consecutive months in order to determine the stability of sensor performance. Collected 17 data sets were divided to 10 sets, used for model training and calibration, and 7 sets, used for model testing. The details of sensors working temperature cycle and gas sensor setup are given on Figure 1.

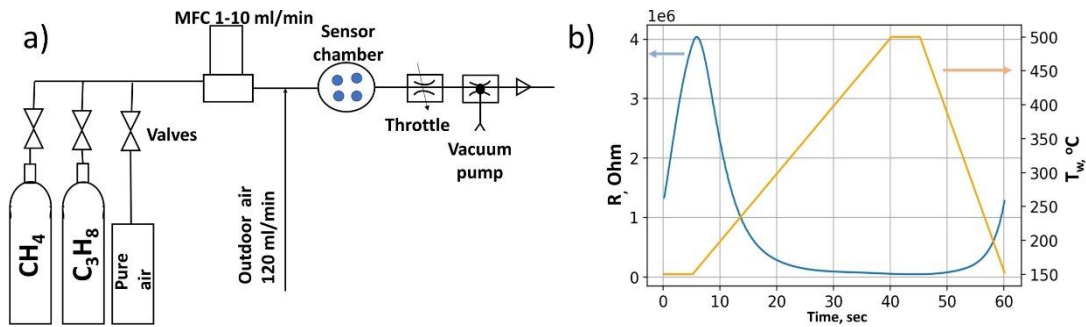


Figure 1. (a) gas sensor setup (b) metal oxide gas sensor working temperature and sensitive layer resistance profile.

3. Results

The obtained gas sensor resistance profiles, recorded during temperature cycles, demonstrate considerable variance due to effects of ambient air humidity and temperature changes. The application of principal component analysis (PCA) to the raw sensor data did not allow to distinguish between methane, propane and air in any acceptable extent (Figure 2a). The use of data pre-processing, represented on Figure 2b (baseline cut-off, data scaling, extraction of data points only from 300–500 °C working temperature region), in combination with machine learning algorithm (artificial neural network with 50 neurons in hidden layer, dropout regularization and sigmoidal activation function) allowed to achieve 86% accuracy of identification of methane vs. propane vs. air in real urban air in 40–200 ppm concentration range.

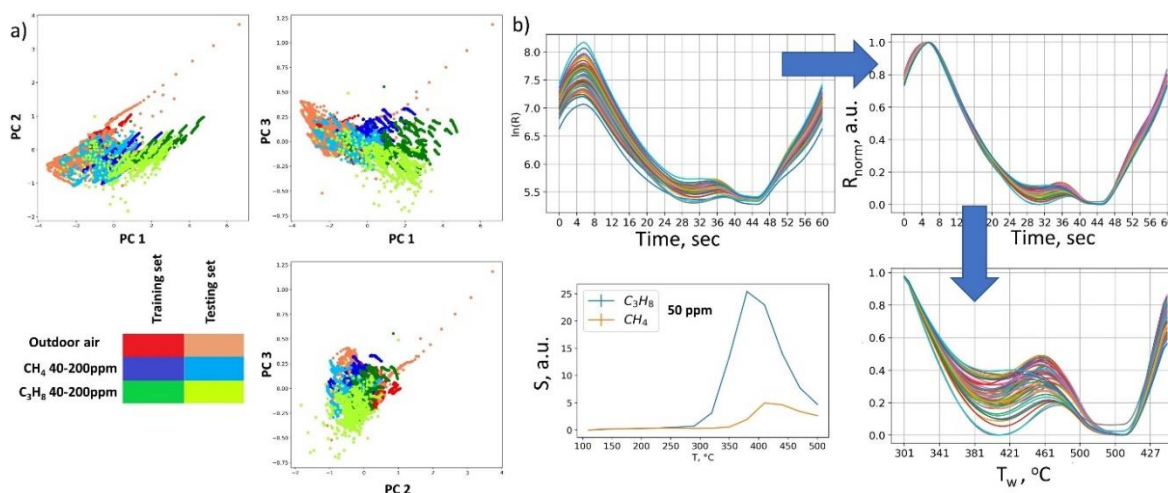


Figure 2. (a) PCA score plots for raw sensor data (b) raw sensor data preprocessing, used for machine learning algorithm.

4. Conclusions

Data preprocessing allows for compensation of metal oxide gas sensor drift effects during operation in real urban air, caused by variations of weather conditions. Application of machine learning algorithms, based on the artificial neural network approach gives the possibility of selective detection of air pollutants even of very close chemical nature. The presented approach demonstrates the applicability of MOX sensors for application in industrial safety tasks, related to flammable and explosive gases leakage.

Acknowledges: The work was funded by Russian Science Foundation grant № 17-73-10491.

References

1. Mujica, L.E.; Ruiz, M.; Mejia, J.M. Leak Detection and Localization on Hydrocarbon Transportation Lines by Combining Real-time Transient Model and Multivariate Statistical Analysis. *Struct. Hlth Monit.* **2015**, 2350–2357, doi: 10.12783/SHM2015/292
2. Santra, S.; Sinha, A.K.; De Luca, A.; Ali, S.Z.; Udrea, F.; Guha, P.K.; Ray, S.K.; Gardner, J.W. Mask-less deposition of Au-SnO₂ nanocomposites on CMOS MEMS platform for ethanol detection. *Nanotechnology* **2016**, 27, 125502.
3. Guha, P.K.; Ali, S.Z.; Lee, C.C.C.; Udrea, F.; Milne, W.I.; Iwaki, T.; Covington, J.A.; Gardner, J.W. Novel design and characterisation of SOI CMOS micro-hotplates for high temperature gas sensors. *Sens. Actuators B Chem.* **2007**, 127, 260–266.
4. Krivetskiy, V.; Efitov, A.; Arkhipenko, A.; Vladimirova, S.; Rummyantseva, M.; Dolenko, S.; Gaskov, A. Selective detection of individual gases and CO/H₂ mixture at low concentrations in air by single semiconductor metal oxide sensors working in dynamic temperature mode. *Sens. Actuators B Chem.* **2018**, 254, 502–513.
5. Collier-Oxandale, A.M.; Thorson, J.; Halliday, H.; Milford, J.; Hannigan, M. Understanding the ability of low-cost MOx sensors to quantify ambient VOCs. *Atmos. Meas. Tech.* **2019**, 12, 1441–1460.



© 2019 by the authors. Licensee MDPI, Basel, Switzerland. This article is an open access article distributed under the terms and conditions of the Creative Commons Attribution (CC BY) license (<http://creativecommons.org/licenses/by/4.0/>).

Identification of Poisonous Mushrooms by Means of a Hand-Held Electronic Nose [†]

Francisco Portalo-Calero *, Jesús Lozano *, Félix Meléndez *, Patricia Arroyo * and José Ignacio Suárez *

Industrial Engineering School, University of Extremadura, Av. Elvas s/n, 06006 Badajoz, Spain

* Correspondence: pacoportalo@unex.es (F.P.); jesusslozano@unex.es (J.L.); felixmv@unex.es (F.M.); parroyoz@unex.es (P.A.); jmarcelo@unex.es (J.I.S.)

† Presented at the 8th GOSPEL Workshop. Gas Sensors Based on Semiconducting Metal Oxides: Basic Understanding & Application Fields, Ferrara, Italy, 20–21 June 2019.

Abstract: This work presents a practical application of an electronic nose to fast and efficient discrimination of different species of Amanita mushrooms. The electronic nose instrument were utilized for investigation of discrimination capability with respect to odour profile of these fungi. The home-made prototype was based on MOS-type chemical sensors and headspace sampling method. Samples were cut into thin sheets, placed in glass vials and maintained at a constant temperature using a thermostatic bath, the headspace of which was subjected to analysis. The data were analysed using multivariate methods: PCA, LDA and Artificial Neural Networks. The obtained results confirmed legitimacy of application of the electronic nose technique to identification and discrimination of fungi species. Results show a correct classification of the fungi species at the level of 80–100%.

1. Introduction

There is no simple test that distinguishes poisonous from nonpoisonous mushrooms, and accurate mushroom identification will require consultation with an experienced mycologist. Although it is estimated that only a few species are lethal, it is not clear how many of the mushrooms worldwide contain potentially toxic compounds. New species are being discovered continuously; for many species, toxicity data are unavailable.

On the other hand, it is known the capacity developed by certain animals to detect volatile substances, and thus find traces of substances emanating from natural products, volatile compounds and biomarkers of different diseases [1], locate explosives [2] and so on. Among the natural aromas that are able to differentiate, are those released by some types of fungi, traditionally used in their harvest once trained for it. This circumstance suggests the possible existence of different odorous nuances between the different species of mushrooms, beyond those currently recognized by human olfaction.

2. Material and Methods

Different mushrooms have been harvested during the autumn months and frozen until the time of analysis. The search location lies between the dehesas of Extremadura (Spain) and the Alentejo (Portugal). The classification was carried out independently by at least two experts. Next, a home-made and home-developed electronic nose (Winose Version 6) was used for the discrimination of the different species. More details of the Winose Version 6 can be found in [3].

3. Results

Two different tests have performed in this work. In both cases, the first step is to get the mushrooms. Once harvested the samples, they were processed and kept frozen. Later a slice of the same mass is cut from the hat of each mushroom to be used as a sample. Using the headspace technique, at least 15 measurements of each sample were made at a constant temperature (30 °C). The measurement cycle consists of 1 min measuring the sample and a recovery phase of 9 min. This process is repeated for all samples. The measurements were made with a flow rate of 150 (L/min) and the operating temperatures of the sensors have been between 300 and 400 °C.

The main objective of the first test is to check the discrimination capability of the developed electronic nose. In this sense, three different types of *Amanita* mushrooms were used: *phalloides*, *caesarea*, and *muscaria*. Once measured and processed the data, Principal Component Analysis (PCA) was made for dimensionality reduction in order to plot in Figure 1. A high degree of discrimination for each of them is observed, and it can be assured that the system offers different answers for each one of the samples, being similar for mushrooms of the same species. The results obtained with the PCA were confirmed with the classification by means of Artificial Neural Networks with Backpropagation Learning Algorithm, in which 97.7% success was obtained in the cross validation using LeaveOneOut method. Only a mistake in the classification of a *Muscaria* was obtained, since it was classified as *Caesarea*.

The second test consists of the detection of two species very similar to the sight and that sometimes it is possible to find in nearby locations. These are species of *Amanita phalloides* and *Agaricus silvicola*. Once measured and pre-processed data (averaged), Figure 2 graphically represented the response of each sensor, clearly indicated the odorous differences perceived by the e-nose between both mushrooms.

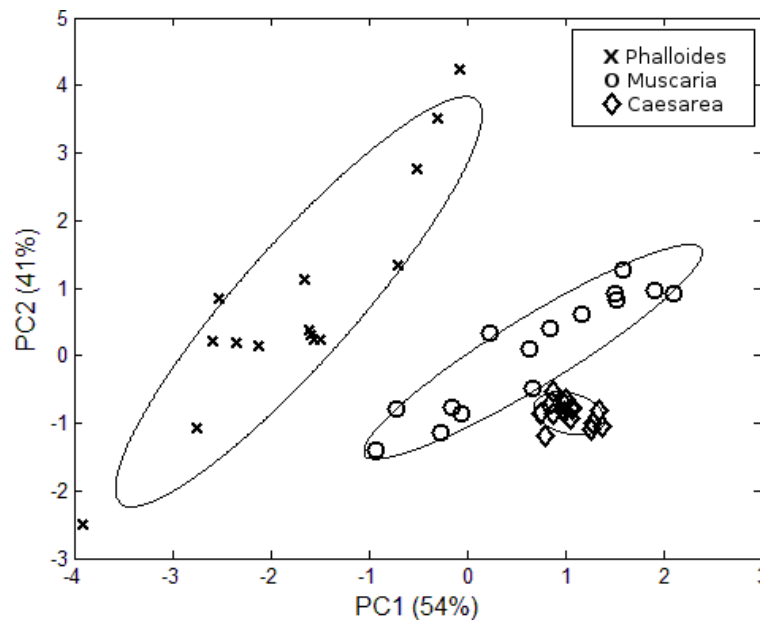


Figure 1. PCA score plot of amanita measurements.

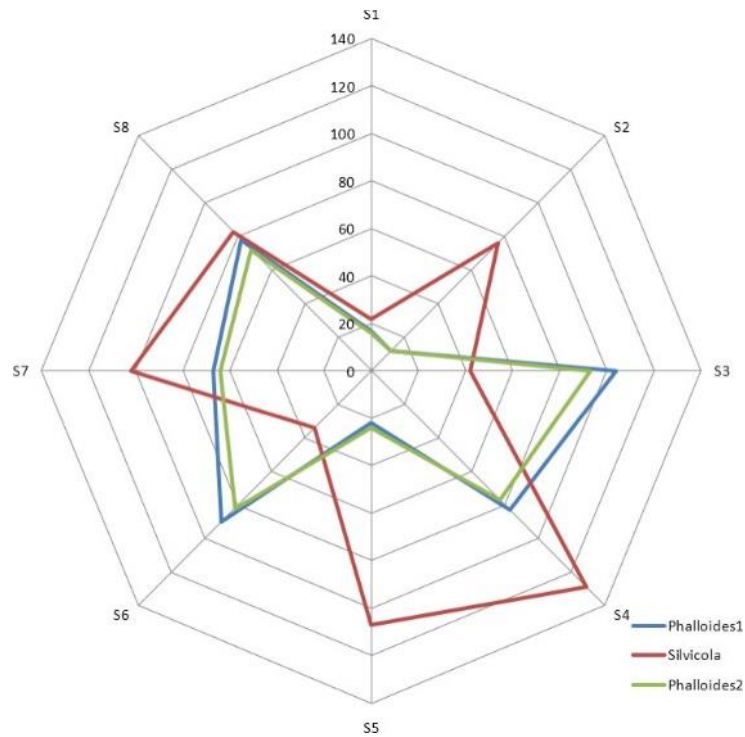


Figure 2. Radial plot of sensors response.

References

1. Sánchez, C.; Santos, J.P.; Lozano, J. Use of Electronic Noses for Diagnosis of Digestive and Respiratory Diseases through the Breath. *Biosensors* **2019**, *9*, 35.
2. Pardo, L.F.M.; Acosta, A.P. Detection of explosives with animal aid: a review of scientific literature. *Logos Sci. Technol. Mag.* **2009**, *1*, 106–118.
3. Santos, J.; Alexandre, M.; Arroyo, P.; Suarez, J.I.; Lozano, J. An Advanced Hand Held Electronic Nose for Ambient Air Applications. *Chem. Eng. Trans.* **2018**, *68*, 235–240.



© 2019 by the authors. Licensee MDPI, Basel, Switzerland. This article is an open access article distributed under the terms and conditions of the Creative Commons Attribution (CC BY) license (<http://creativecommons.org/licenses/by/4.0/>).

Abstract

A Multi-MOx Sensor Approach to Measure Oxidizing and Reducing Gases [†]

Ehsan Danesh ¹, Richard Dudeney ², Jone-Him Tsang ³, Chris Blackman ³, James Covington ⁴, Peter Smith ² and John Saffell ¹

¹ Alphasense Ltd., Sensor Technology House 300 Avenue West, Skyline 120, Great Notley, Essex CM77 7AA, UK; jrs@alphasense.com

² McGowan Sensor Labs Ltd., Culham Innovation Centre, D5 Culham Science Centre, Abingdon, Oxfordshire OX14 3DB, UK; rdudeney@mcgowan-smith.co.uk (R.D.); psmith@mcgowan-smith.co.uk (P.S.)

³ Department of Chemistry, University College London, London WC1H 0AJ, UK; jone-him.tsang.16@ucl.ac.uk (J.-H.T.); c.blackman@ucl.ac.uk (C.B.)

⁴ School of Engineering, University of Warwick, Coventry CV4 7AL, UK; j.a.covington@warwick.ac.uk

* Correspondence: ed@alphasense.com.

† Presented at the 8th GOSPEL Workshop. Gas Sensors Based on Semiconducting Metal Oxides: Basic Understanding & Application Fields, Ferrara, Italy, 20–21 June 2019.

Abstract: This report summarizes our recent work on a *p*-type/*n*-type Multi-MOx gas sensor platform for simultaneously measuring oxidizing and reducing gases.

Keywords: semiconducting metal oxide; *p*-type; gas sensor; air quality; multi-sensor platform

Reliable and real-time measurements of gaseous pollutants (e.g., NO₂ and CO) in both indoor and outdoor air are required to implement worldwide air quality legislation designed to protect human health and the environment. While electrochemical sensors are popular for air quality monitoring due to their fast and linear response, low power consumption and excellent selectivity, some applications operate in environments that extend beyond their capability. Gas sensors based on semiconducting metal oxides (MOx) technology offer advantages such as high sensitivity, low manufacturing cost, miniaturization potential and long lifetime. Commercially available MOx sensors are typically based on *n*-type SnO₂, WO₃ or versions thereof modified by the presence of precious metal catalysts such as Pt or Pd. The shortcomings of these materials i.e., baseline drift, humidity interference and cross-sensitivity to nuisance gases, are well-known. Moreover, exposure to oxidizing and reducing gases have reverse effects on a MOx electrical conductance, governed by its semiconducting characteristics. This introduces a key challenge in interpreting the response of a single MOx sensor exposed to a mixture of oxidizing and reducing gases.

To address the aforementioned shortcomings, Alphasense and partners have adopted a “Multi-MOx” array approach, where *p*-type and *n*-type metal oxide sensing elements are combined on a single ceramic chip. A Platinum heater on the underside of the chip heats the sensor to the desired operating temperature. The sensor discussed here is comprised of:

1. *p*-type CTO (titanium-doped chromium trioxide), a ternary oxide which provides a stable baseline, minimal humidity interference and high sensitivity to reducing gases such as CO, and
2. *n*-type WO₃, a binary oxide with excellent sensitivity to oxidizing gases such as NO₂ and O₃.

In the case of *p*-type CTO, exposure to CO causes a decrease in the charge carrier (hole) concentration in the near-surface region and a decrease in the measured conductance. Whereas, the measured resistance of *n*-type WO₃ increases in exposure to NO₂ due to an increase in the density of charge carriers (electrons) trapped at the oxide surface (see Figure 1). The use of different MOx

materials in conjunction with operating temperature modulation and advanced on-chip filtering can be used to reliably measure both oxidizing and reducing gases.

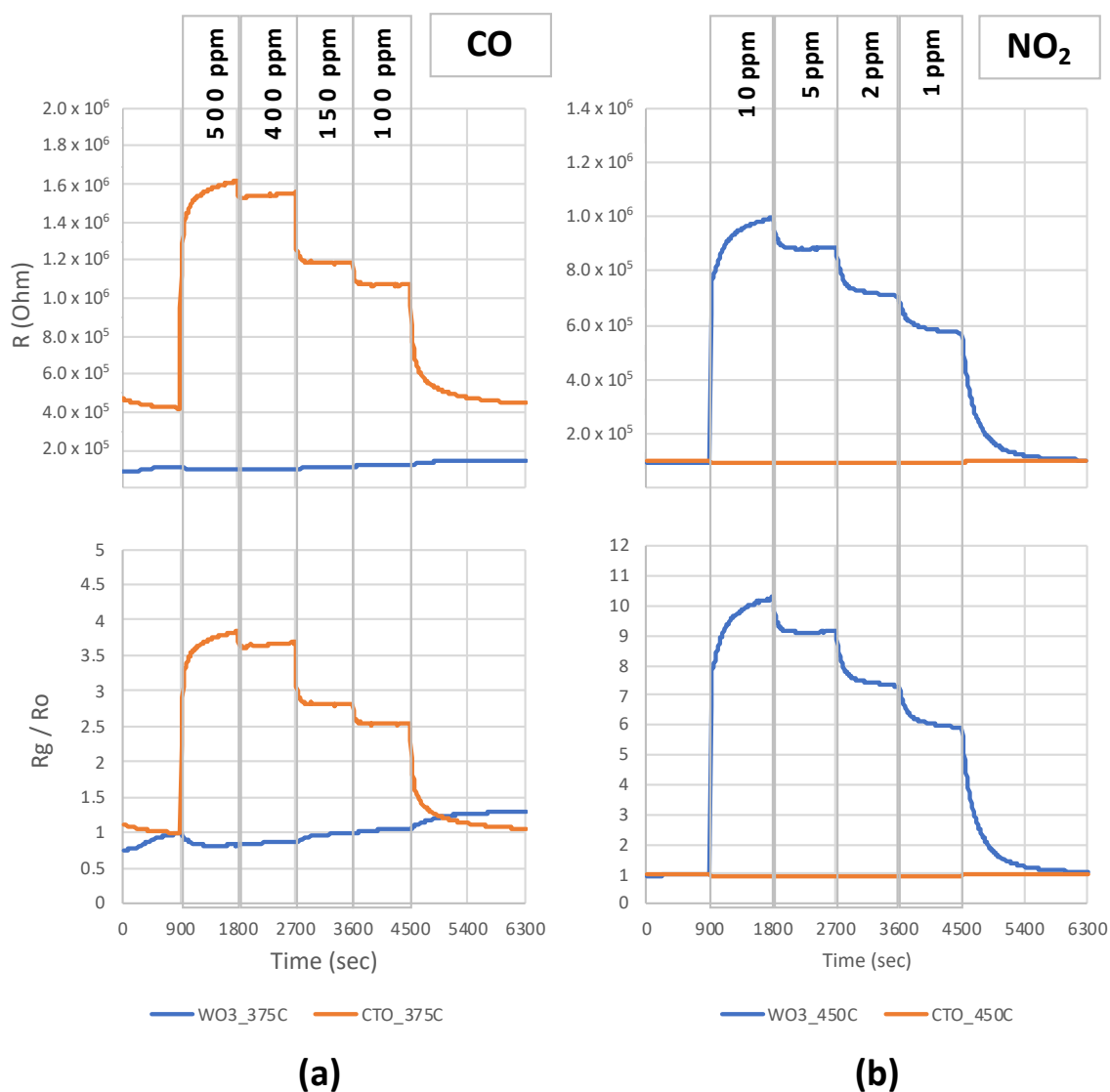


Figure 1. A Multi-MOx sensor response to (a) CO at operating $T = 375\text{ }^{\circ}\text{C}$, and (b) NO_2 at operating $T = 450\text{ }^{\circ}\text{C}$, both in 50% relative humidity air. Top and bottom charts show the raw signal (R) and the corresponding relative response (R_g/R_o), respectively. Blue and orange lines are WO_3 (n -type) and CTO (p -type) sensors signal, respectively.



© 2019 by the authors. Licensee MDPI, Basel, Switzerland. This article is an open access article distributed under the terms and conditions of the Creative Commons Attribution (CC BY) license (<http://creativecommons.org/licenses/by/4.0/>).

Rapid Prototyping of MOX Gas Sensors in Form-factor of SMD Packages [†]

Nikolay Samotaev *, Konstantin Oblov, Anastasiya Gorshkova, Anastasia Ivanova and Maya Etrekova

National Research Nuclear University MEPhI (Moscow Engineering Physics Institute), Kashirskoe highway 31, Moscow 115409, Russia; kyoblov@mephi.ru (K.O.); nastypzspb@mail.ru (A.G.); avivanova@mephi.ru (A.I.); moetrekova@mephi.ru (M.E.)

* Correspondence: nnsamotaev@mephi.ru

† Presented at the 8th GOSPEL Workshop. Gas Sensors Based on Semiconducting Metal Oxides: Basic Understanding & Application Fields, Ferrara, Italy, 20–21 June 2019.

Abstract: By laser micromilling technology it is possible to fabricate custom MEMS microhotplate platform and also SMD package for MOX sensor, that gives complete solution for integration in mobile devices-smart phones, tablets and etc. The 3D design and fabrication of MEMS microhotplates and packages products occurs simultaneously that give opportunity for ultra-fast time making unique solutions for MOX sensors (number of microhotplates, hot spot size on microhotplates, diameter holes in package cap and etc.) without looking at standard solutions (primarily the package type).

1. Introduction

The main idea of our developed technological flow based on laser micromilling is wide flexibility in developing of MEMS and SMD structures. Using of equipments only widely presented on the market and refusing of technological steps needs a clean rooms support. Only semi custom 3D printing type software is especially developed product for laser micromilling system needed for successful development and production of MEMS and SMD structure during our experiments. Software is needed for translation CNC code to 4-axis laser micromilling setup and online measuring of geometrical parameters of MEMS and SMD structure for corrections micromilling procedure during automatic production.

2. Experimental

During our work, an Ytterbium pulsing 20 W fiber laser with a wavelength of 1.064 μm and tunable pulse duration from 50 to 200 ns is used. This laser emitter is installed on the four-coordinate portal complex, which allows the laser scanner to be moved across wide field. The processing of ceramic substrates is carried out in a snap-in fixed in a rotational device, which allows processing of flat substrates on both sides, cylindrical substrates over the entire surface area. Currently, fiber markers are most often used in industry for marking various types of products and are not intended for 3D laser milling, despite the fact that the technical capabilities of any laser marker allow it by using of our developed software. Fabrication of MOX sensors includes the following main steps:

- MEMS microhotplate modeling and both bottom and top parts of the SMD package (Figure 1) in 3D CAD programs with output file in STL format and also 2D modeling of MEMS and SMD metallization topology in DXF format;
- Optionally MEMS microhotplate parameters could be simulated in COMSOL program, which allows to predict approximate thermal characteristics of the MOX sensor;
- 4-axis laser facility is used for monolithic ceramics laser micromilling with help of 3D models of

- bottom and top parts of the SMD package and MEMS microhotplate;
- Platinum metallization deposition according with 2D model of topology, metallization annealing paying attention to specification on jet or screen-print platinum materials (Figure 2);
- Optionally the metallization can be processed with laser according with 2D model;
- MOX gas sensitive layer deposition and annealing on the MEMS microhotplate;
- Assembling separate parts of sensor into one SMD package and adhesion with special glass (Figure 3)

Using described tech flow, experiments were carried out to fabricate a possible minimum size of MEMS microhotplate from Al_2O_3 ceramics. The minimum size of the manufactured microhotplate with 250 mW power consumption at 450 °C with track width was 30 μm and 20 μm thickness in SMD SOT-23 package type (3.0 × 1.4 × 1.0 mm with max dissipating power at 20 °C-350 mW) were achieved. Tests of fabricated MEMS microhotplate present in work [1].

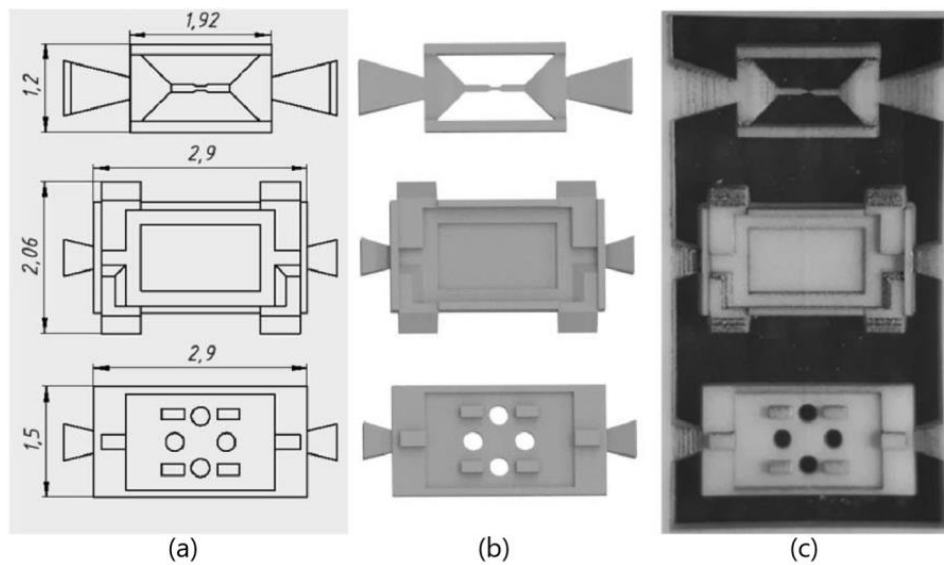


Figure 1. (a) Sketch with dimension in mm for parts of MEMS microhotplate (on top) and SOT-23 package (in bottom); (b) 3D model of sketch as screenshot in CAD program; (c) Parts of MEMS and SMD package after laser micromilling by using 3D models of MEMS.

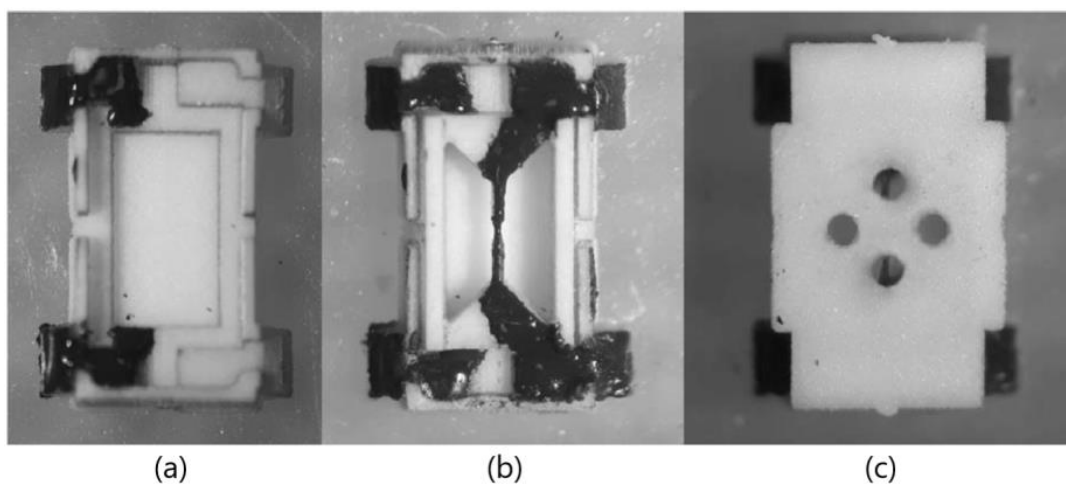


Figure 2. (a) Deposited Pt paste on bottom part of SOT-23 package; (b) Deposited Pt paste on MEMS part inside SOT-23 package; (c) The assembled SOT-23 package before firing.

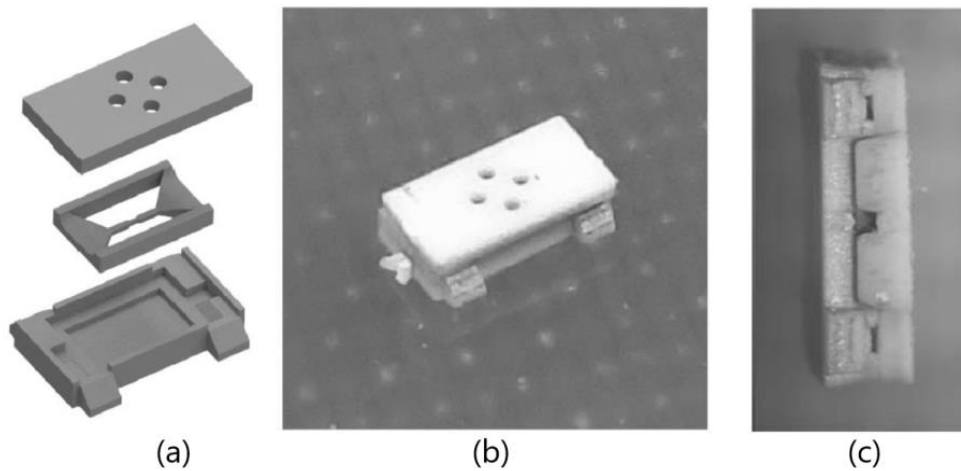


Figure 3. (a) 3D model assembling of SOT-23 package; (b) The top view of SOT-23 assembled package; (c) The side view SOT-23 assembled package.

Advantage of ceramic using as a material for laser micromilling is extension of MOX sensor working temperatures range up to 1000 °C compare with typical 700 °C for silicon technology. Also useful advantage of fully ceramics based MOX sensor is long term stability against harsh environmental conditions including extreme temperature and acid or alkaline gases.

This research was funded by Ministry of Science and Higher Education of Russian Federation under grant number 14.584.21.0054 from 26 November 2018, unique identifier RFMEFI58718X0054.

Reference

1. Samotaev, N.; Oblov, K.; Ivanova, A. Laser micromilling technology as a key for rapid prototyping SMD ceramic MEMS devices. In Proceedings of the MATEC Web of Conferences, Jeju Island, Korea, 19–20 July 2018; Volume 207, Article number 040034.



© 2019 by the authors. Licensee MDPI, Basel, Switzerland. This article is an open access article distributed under the terms and conditions of the Creative Commons Attribution (CC BY) license (<http://creativecommons.org/licenses/by/4.0/>).

Abstract

Sub-ppm NO₂ Sensing in Temperature Cycled Mode with Ga Doped ZnO Thin Films Deposited by RF Sputtering [†]

Lionel Presmanes ^{1,*}, Vignesh Gunasekaran ^{1,2}, Yohann Thimont ¹, Inthuga Sinnarasa ¹, Antoine Barnabe ¹, Philippe Tailhades ¹, Frédéric Blanc ², Chabane Talhi ² and Philippe Menini ²

¹ CIRIMAT, Université de Toulouse, CNRS, INPT, UPS, 118 Route de Narbonne, F-31062 Toulouse CEDEX 9, France; vignesh.gunasekaran@laas.fr (V.G.); thimont@chimie.ups-tlse.fr (Y.T.); sinnarasa@chimie.ups-tlse.fr (I.S.); barnabe@chimie.ups-tlse.fr (A.B.); tailhade@chimie.ups-tlse.fr (P.T.);

² LAAS-CNRS, Université de Toulouse, UPS, INSA, 7 avenue du colonel Roche, F-31031 Toulouse, France; frederic.blanc@laas.fr (F.B.); chabane.talhi@laas.fr (C.T.); philippe.menini@laas.fr (P.M.)

* Correspondence: presmane@chimie.ups-tlse.fr

[†] Presented at the 8th GOSPEL Workshop. Gas Sensors Based on Semiconducting Metal Oxides: Basic Understanding & Application Fields, Ferrara, Italy, 20–21 June 2019.

Abstract: In this work Ga doped ZnO thin films have been deposited by RF magnetron sputtering onto a silicon micro-hotplate and their structural, microstructural and gas sensing properties have been studied. ZnO:Ga thin film with a thickness of 50 nm has been deposited onto a silicon based micro-hotplates without any photolithography process thanks to a low cost and reliable stencil mask process. Sub-ppm sensing (500 ppb) of NO₂ gas at low temperature (50 °C) has been obtained with promising responses R/R₀ up to 18.

1. Results

Micro-hotplates have been prepared using photolithographic process. The system is composed by a heating element and sensing electrodes. They are both integrated in membrane in order to have a localized heating and sensing spot onto which the sensitive thin film is deposited. The microhotplates can operate with low consumption and can heat up to 500 °C with a good stability. This system has been already published in [1]. The use of lift-off process to restrict the deposition of the thin film onto central electrodes can lead to the dissolution and/or contamination of the sensitive layer. That's why the photolithographic method was avoided and a stencil mask process was used (Figure 1).

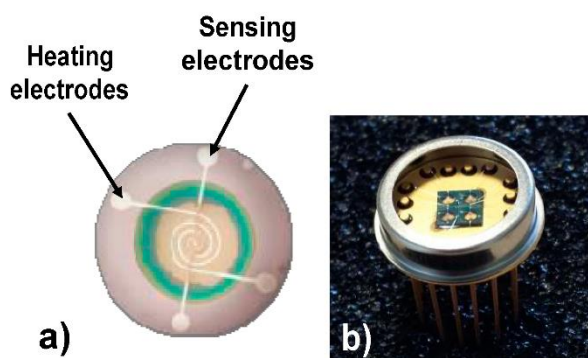


Figure 1. (a) top-view of the membrane; (b) mounted micro-sensor.

The deposition conditions are shown in the Table 1.

Table 1. Deposition parameters of ZnO:Ga thin film by RF-sputtering.

Target Material	ZnO:Ga
Power (W)	(4%at)
Magnetron	30
Argon pressure P (Pa)	Yes
Target to substrate distance	2
d (cm)	7

The measurement protocol used in the test bench is a cycle of heating and cooling steps from 5 mW to 35 mW with a step of 5 mW for 5 min which correspond approximately to 50 °C to 350 °C. The tests were performed with 50% relative humidity. Alternation of air and air with 500 ppb of NO₂ has been applied. In presence of air, the resistance is very low, close to 300 Ω, due the high conductivity of ZnO:Ga. When 500 ppb of NO₂ are injected, the resistance increases strongly up to 7 kΩ at 50 °C. The ratio R/R₀ (where R is the resistance under NO₂ and R₀ the resistance under air) has been calculated using the last points at each temperature step (Figure 2).

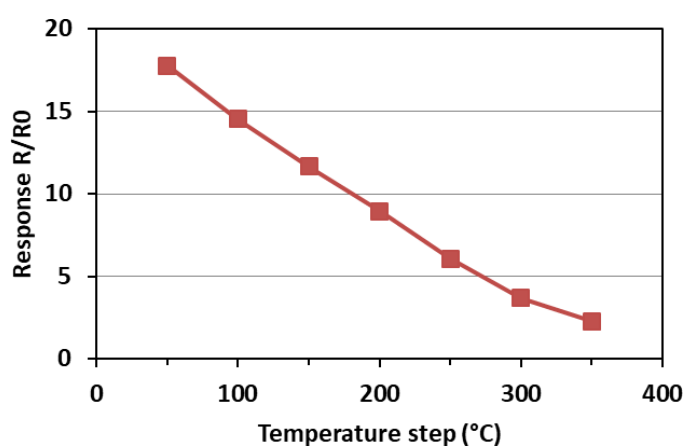


Figure 2. Response of ZnO:Ga vs. temperature step (in cycled temperature mode).

Unlike the results we obtained in isothermal mode, the response in cycled temperature mode is much higher close to room temperature. Promising results with a response up to 18 for 500 ppb of NO₂ at 50 °C (R/R₀ ~ 36/ppm) have been highlighted.

Acknowledgments: This work has received funding from the Program Interreg-Sudoe of the European Union under grant agreement SOE2/P1/E0569 (NanoSen-AQM).

References

1. Presmanes, L.; Thimont, Y.; Younsi, I.E.; Chapelle, A.; Blanc, F.; Talhi, C.; Bonningue, C.; Barnabé, A.; Menini, P.; Tailhades, P. Integration of P-CuO Thin Sputtered Layers onto Microsensor Platforms for Gas Sensing. *Sensors* **2017**, *17*, 1409.



© 2019 by the authors. Licensee MDPI, Basel, Switzerland. This article is an open access article distributed under the terms and conditions of the Creative Commons Attribution (CC BY) license (<http://creativecommons.org/licenses/by/4.0/>).

Heterogeneous Integration of Metal Oxides— Towards a CMOS Based Multi Gas Sensor Device [†]

Anton Köck ^{1,*}, Marco Deluca ¹, Florentyna Sosada-Ludwikowska ¹, Günther Maier ¹
Robert Wimmer Teubenbacher ¹, Martin Sagmeister ², Karl Rohrer ², Ewald Wachmann ²,
Jan Steffen Niehaus ³, Sören Becker ³, Öznur Tokmak ³, Hendrik Schlicke ³, Alexander Blümel ⁴,
Karl Popovic ⁴ and Martin Tscherner ⁴

¹ Materials Center Leoben Forschung GmbH, Roseggerstraße 12, 8700 Leoben, Austria; marco.deluca@mcl.at (M.D.); florentyna.sosada-ludwikowska@mcl.at (F.S.-L.); guenther.maier@mcl.at (G.M.); robert.wimmer-teubenbacher@mcl.at (R.W.T.)

² ams AG, Tobelbader Strasse 30, 8141 Unterpremstaetten, Austria; martin.sagmeister@ams.com (M.S.); karl.rohracher@ams.com (K.R.); ewald.wachmann@ams.com (E.W.)

³ Center for Applied Nanotechnology CAN, Fraunhofer Institute for Applied Polymer Research IAP, Grindelallee 117, 20146 Hamburg, Germany; jan.steffen.niehaus@iap.fraunhofer.de (J.S.N.); soeren.becker@iap.fraunhofer.de (S.B.); oeznur.tokmak@iap.fraunhofer.de (Ö.T.); hendrik.schlicke@iap.fraunhofer.de (H.S.)

⁴ Joanneum Research, Institute for Surface Technologies and Photonics, Franz-Pichler-Strasse 30, 8160 Weiz, Austria; alexander.bluemel@joanneum.at (A.B.); karl.popovic@joanneum.at (K.P.); martin.tscherner@joanneum.at (M.T.)

* Correspondence: anton.koeck@mcl.at

[†] Presented at the 8th GOSPEL Workshop. Gas Sensors Based on Semiconducting Metal Oxides: Basic Understanding & Application Fields, Ferrara, Italy, 20–21 June 2019.

A worldwide unique CMOS based chemical sensor device comprising an array of 8 microhotplates (μ hps) for a total of 16 chemical sensors has been fabricated (Figure 1). Ultrathin (50 nm) SnO₂ films have been heterogeneously integrated on the device by spray pyrolysis technology, photolithography and etching. Subsequently the SnO₂ films are functionalized with metallic nanoparticles (NPs) such as Au, Pt, AuPd, or NiPt in order to improve sensitivity and selectivity. Figure 2 shows the strongly improved response of a NiPt-functionalized SnO₂ sensor towards carbon monoxide (10–200 ppm, 25–75% rh): at an operation temperature of only 150 °C the sensor exhibits a response of more than 90%. Presently different metal oxide films (SnO₂, ZnO, CuO) additionally functionalized with NPs are processed on the μ hp-array chip. This is the approach of choice for realization of a fully CMOS integrated multi-gas sensor device.

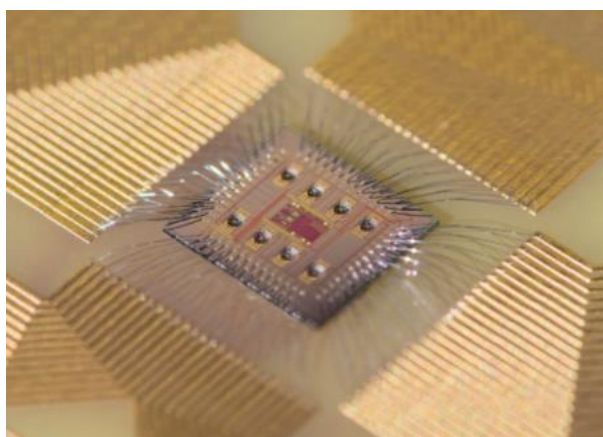


Figure 1. Chemical sensor device comprising an array of 8 μ hps for a total of 16 sensors.

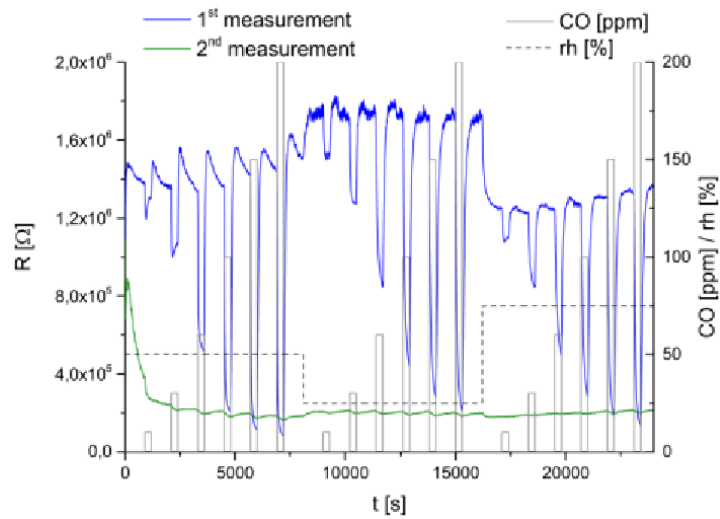


Figure 2. Response of SnO₂ thin film sensor, functionalized with NiPt-NPs towards CO.

Acknowledgments: This work was performed within the EC FP7 project “MSP—Multi Sensor Platform for Smart Building Management” (GA No. 611887), and the Austrian FFG project “FunkyNano—Optimized Functionalization of Nanosensors for Gas Detection by Screening of Hybrid Nanoparticles” (Project No. 858637).



© 2019 by the authors. Licensee MDPI, Basel, Switzerland. This article is an open access article distributed under the terms and conditions of the Creative Commons Attribution (CC BY) license (<http://creativecommons.org/licenses/by/4.0/>).

Abstract

Consideration for Oxygen Adsorption Species on SnO₂ Semiconductor Gas Sensors [†]

Kengo Shimano^{1,*}, Takaharu Mizukami², Koichi Suematsu¹ and Ken Watanabe¹

¹ Department of Advanced Materials Science and Engineering, Faculty of Engineering Sciences, Kyushu University, Kasuga, Fukuoka 816-8580, Japan; suematsu.koichi.682@m.kyushu-u.ac.jp (K.S.); watanabe.ken.331@m.kyushu-u.ac.jp (K.W.)

² Department of Molecular and Material Science, Interdisciplinary Graduate School of Engineering Sciences, Kyushu University, Kasuga, Fukuoka 816-8580, Japan

* Correspondence: shimano.kengo.695@m.kyushu-u.ac.jp.

[†] Presented at the 8th GOSPEL Workshop. Gas Sensors Based on Semiconducting Metal Oxides: Basic Understanding & Application Fields, Ferrara, Italy, 20–21 June 2019.

1. Introduction

Water vapor is the most important factor to influence on gas sensing properties. We can obtain high gas sensor response in dry atmosphere, but the gas response is decreased gradually by introducing water vapor. Such phenomena are strongly related with oxygen adsorption species on SnO₂ particles. Previously we reported that oxygen adsorption species is O²⁻ and O⁻ in dry and wet atmosphere, respectively [1]. However, the effect of treatment before measurement doesn't have discussed. In this study, we investigated pretreatment of neat SnO₂ and Sb-doped SnO₂ for behavior of oxygen adsorption.

2. Experiments

In this study, we used the following equation for analysis of oxygen adsorption species.

$$\frac{R}{R_0} = \frac{1}{2} \cdot \left(c + \frac{3}{a} \cdot (K_1 P_{O_2})^{\frac{1}{2}} \right) + \left\{ \frac{1}{4} \cdot \left(c + \frac{3}{a} \cdot (K_1 P_{O_2})^{\frac{1}{2}} \right)^2 + \frac{6N_D}{a} \cdot (K_2 P_{O_2})^{\frac{1}{2}} \right\}^{\frac{1}{2}} \quad (1)$$

R is electric resistance (Ω) in measurement condition, R_0 electric resistance (Ω) at flat band, a crystalline size (nm), N_D donor density (nm⁻³), P_{O_2} oxygen partial pressure (atm), K_1 and K_2 adsorption equilibrium constants for O⁻ (nm²/atm) and O²⁻ (nm⁸/atm), respectively, and c constant.

We used SnO₂ and Sb(0.1 mol.%)–SnO₂ particles calcined at 600–700 °C in various atmosphere. After the powders were deposited on alumina substrates with Au electrodes by screen-printing, the elements were calcined at 580 °C in oxygen atmosphere for 3 h. After that, the resulting sensor elements were pretreated at 580 °C for 3 h in N₂, 0.3%O₂, 1%O₂ or 100%O₂. The sensor element was cooled to 350 °C with keeping the atmosphere of the pretreatment, and the oxygen partial pressure dependence of the electrical resistance was measured in dry and wet atmosphere ($P_{H_2O} = 0.03$ atm).

3. Results and Discussion

At first, neat SnO₂ calcined at 700 °C in O₂ or N₂ atmosphere was investigated after pretreating at 580 °C for 3 h in 0.3%O₂, 1%O₂ or 100%O₂. Figure 1 shows relationship between amount of oxygen adsorption species and oxygen partial pressure in pretreatment. It was revealed that O²⁻ adsorbs with precedence than O⁻. In addition, by reducing oxygen partial pressure at pretreatment, the amount of O²⁻ adsorption decreased and the amount of O⁻ adsorption increased. Figure 2 shows total amounts of [O²⁻] and [O⁻] against oxygen partial pressure in pretreatment. It is found that the total amount of oxygen adsorption increases by reducing oxygen partial pressure at pretreatment. Furthermore, it is

clear that the control of atmosphere at pretreatment gives a big influence on amounts of oxygen adsorption than the control of atmosphere at the powder calcination.

Second, neat SnO₂ and Sb-doped SnO₂ calcined at 600 °C in O₂ atmosphere was investigated was investigated in wet atmosphere after pretreating at 580 °C for 3 h in N₂ or 100%O₂. Figure 3 shows total amounts of [O²⁻] and [O⁻] against oxygen partial pressure in pretreatment (measured in dry and wet atmosphere). The difference in the total amounts of oxygen adsorption species for dry and wet atmosphere was not observed, although Sb-SnO₂ are more on the total amounts of oxygen adsorption than neat SnO₂. From these results, it is considered that, at the first stage by changing dry to wet atmosphere, the hydroxyl group formation from water vapor may be related with the reduce in electric resistance. However, when the elements are kept for long time in wet atmosphere, the oxygen adsorption species changes O²⁻ to O⁻, and the resulting also gives the reduce in electric resistance, as reported previously [1].

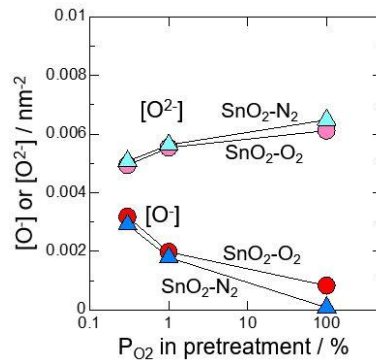


Figure 1. Relationship between amount of oxygen adsorption species and oxygen partial pressure in pretreatment (measured in dry atmosphere).

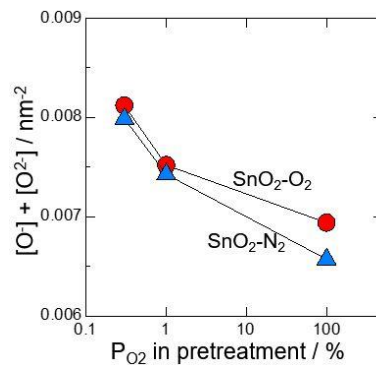


Figure 2. Total amounts of [O²⁻] and [O⁻] against oxygen partial pressure in pretreatment (measured in dry atmosphere).

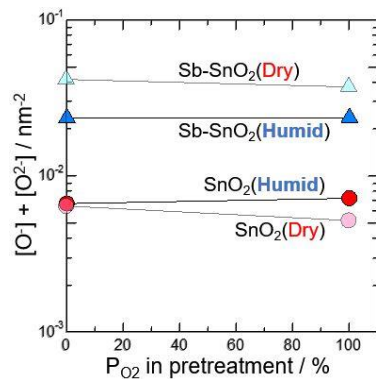


Figure 3. Total amounts of [O²⁻] and [O⁻] against oxygen partial pressure in pretreatment (measured in dry and wet atmosphere).

References

1. Yamazoe, N.; Suematsu, K.; Shimano, K. Extension of receptor function theory to include two types of adsorbed oxygen for oxide semiconductor gas sensors. *Sens. Actuators B Chem.* **2012**, *163*, 128–135.



© 2019 by the authors. Licensee MDPI, Basel, Switzerland. This article is an open access article distributed under the terms and conditions of the Creative Commons Attribution (CC BY) license (<http://creativecommons.org/licenses/by/4.0/>).

Poster Presentations

Extended Abstract

Flexible Gas Sensor Printed on Polymer Substrate for Acetone Detection in Portable Exhaled Breath Analyzers [†]

W. Andrysiewicz ¹, J. Krzeminski ², K. Marszalek ¹, M. Sloma ² and A. Rydosz ^{1,*}

¹ Department of Electronics, AGH University of Science and Technology, Al. Mickiewicza 30, Krakow, Poland; Wojciech.andrysiewicz@agh.edu.pl (W.A.); Konstanty.marszalek@agh.edu.pl (K.M.); artur.rydosz@agh.edu.pl (A.R.)

² Warsaw University of Technology, Faculty of Mechatronics, Institute of Metrology and Biomedical Engineering, Micro- and Nanotechnology Division, 8 sw. A. Boboli st., 02-525 Warsaw, Poland; krzem@mchtr.pw.edu.pl (J.K.); Marcin.Sloma@mchtr.pw.edu.pl (M.S.)

* Correspondence: artur.rydosz@agh.edu.pl, Tel.: +48-126-172-594

[†] Presented at the 8th GOSPEL Workshop. Gas Sensors Based on Semiconducting Metal Oxides: Basic Understanding & Application Fields, Ferrara, Italy, 20–21 June 2019.

1. Introduction

Gas detectors have constantly been developed over the few last decades as a result of industrial demands: for monitoring air quality, in the automotive industry in medicine for the detection of biomarkers in several diseases. Generally, the gas sensors consists of gas sensor substrate with a gas-sensitive layer and package. The gas sensor substrates are usually realized in alumina and silicon technology and gas-sensitive layers are based on the metal oxides. Flexible gas sensor substrates are very promising in the portable exhaled breath analyzers.

2. Material and Methods

Flexible Gas Sensors Substrates

The first stage of the work was the design of the electrode, deposited on the elastic substrate. The shape of the electrode should allow receiving the signal from the sensor in a stable undisturbed manner. Therefore, a tailored design compatible with the whole sensor was developed. The designed sensor substrate consists of a comb-shaped electrode with the sensitive material deposited on the top. The change in the conductivity of the sensitive layer due to the reaction with the detected gas will change the resistance between galvanically separated electrodes. Such a construction of electrodes allows to easily apply various sensitive materials to detect the presence of gases in the atmosphere and enable easy implementation for further high throughput manufacturing of the developed sensor. Large area contact pads allow connecting the external measuring apparatus to the sensor in a reliable manner, which will increase the reliability of the solution. Figure 1 shows the designed comb-shaped electrodes.

Printed electrodes exhibit a slight non-linearity at the edge of the paths visible in Figure 2, resulting from the limitations of aerosol printing deposition. Obtained lines are homogeneous and parallel. Both the edges and corners of the contact pads were printed correctly.

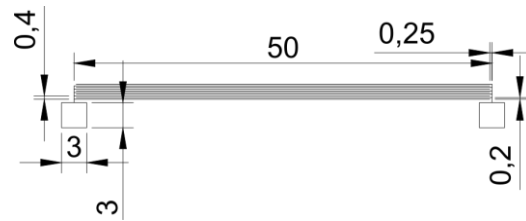


Figure 1. The designed comb-shaped electrode with dimensions in millimeters. Two contact pads 3×3 mm with 50 mm pitch, are used to connect external measuring systems. Each electrode has 5 lines with $250 \mu\text{m}$ pitch.

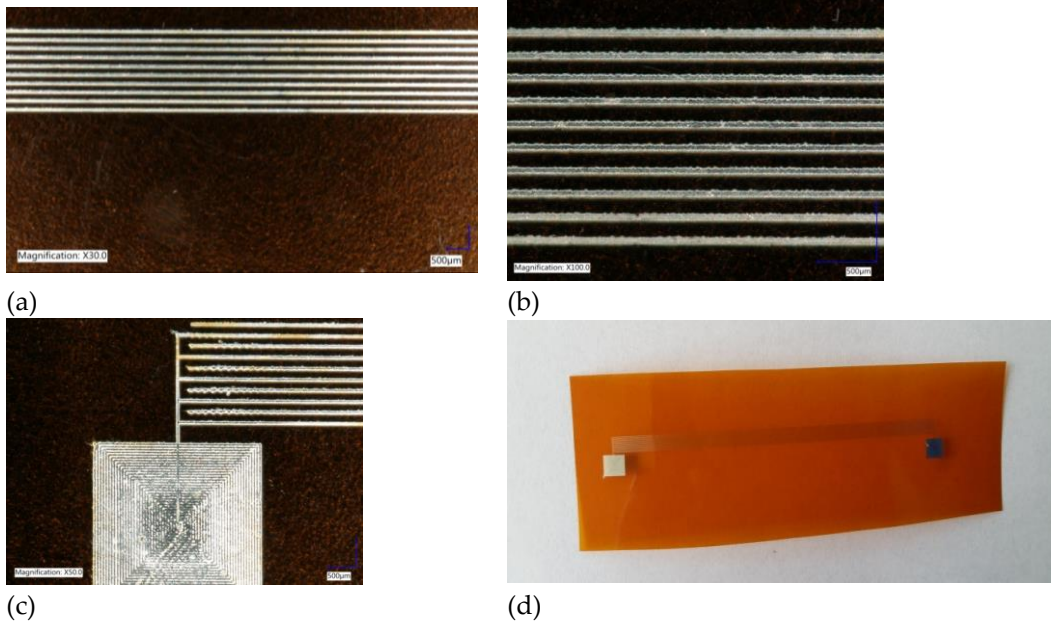


Figure 2. Micrographs of the printed sensor electrodes and contact pads; (a) general view with Magnification $\times 30.0$; (b) zoom to electrodes with Magnification $\times 100.0$; (c) zoom to contact pad with Magnification $\times 100.0$; (d) photograph of the sensor substrate.

3. Conclusions

Presented results demonstrate that aerosol jet printed electrodes on flexible substrates are suitable for the fabrication of gas sensors. Further perspectives are based on the patent application [1]. Flexible electronics is extremely fast developed field due to applications in screen, monitors mobiles and a few more. In our case it is applied for portable device for diabetes diagnostics. Design of multi sensors matrix on elastic substrate is a key problem for construction of such device describe in [1]. Such elastic device could be fix to a body or cloth of a patient and collects necessary data it means level of diabetic markers. Figure 3 shows a possible realization that is currently patent pending [1].

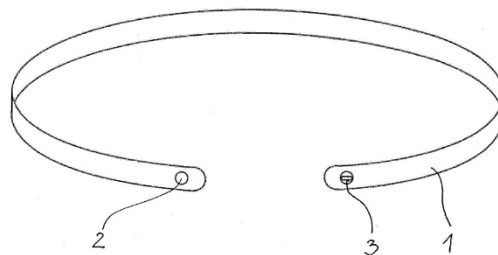


Figure 3. Drawing of the flexible exhaled breath analyzer based on the developed gas sensor substrates: (1) substrate, (2) gas-inlet port, (3) electronic port [1].

Funding: This research is part of the “Functional heterophase materials for structural electronics” project carried out within the First TEAM/2016-1/7 programme of the Foundation for Polish Science co-financed by the European Union under the European Regional Development Fund and partially funded by the National Science Centre, Poland 2017/26/D/ST7/00355.

Acknowledgments: This research is part of the “functional heterophase materials for structural electronics” project carried out within the First TEAM/2016-1/7 programme of the Foundation for Polish Science co-financed by the European Union under the European Regional Development Fund and partially funded by the National Science Centre, Poland 2017/26/D/ST7/00355.

Conflicts of Interest: The authors declare no conflict of interest.

Reference

1. Rydosz, A.; Marszalek, K. Portable device for detection of biomarkers in exhaled air and method of biomarker detection in exhaled air. EP18190345.1, 2018.



© 2019 by the authors. Licensee MDPI, Basel, Switzerland. This article is an open access article distributed under the terms and conditions of the Creative Commons Attribution (CC BY) license (<http://creativecommons.org/licenses/by/4.0/>).

Surface Properties of SnO₂ Nanolayers Deposited by Rheotaxial Growth and Vacuum Oxidation for Potential Gas Sensor Applications [†]

Barbara Lyson-Sypien ^{1,*}, Monika Kwoka ¹ and Maciej Krzywiecki ²

¹ Silesian University of Technology, Faculty of Automatic Control, Electronics and Computer Science, Institute of Electronics, 44-100 Gliwice, Poland; Monika.Kwoka@polsl.pl

² Silesian University of Technology, Institute of Physics - Center for Science and Education, 44-100 Gliwice, Poland; Maciej.Krzywiecki@polsl.pl

* Correspondence: barbara.lyson-sypien@polsl.pl; Tel.: +48-509-528-427.

[†] Presented at the 8th GOSPEL Workshop. Gas Sensors Based on Semiconducting Metal Oxides: Basic Understanding & Application Fields, Ferrara, Italy, 20–21 June 2019.

1. Aim

Within this work the advantages of Rheotaxial Growth and Vacuum Oxidation i.e. maximal extension of internal surfaces, small degree of nanograins agglomeration and reduced influence of undesired contaminations together with exceedingly well—promising features of SnO₂ in terms of gas detection, have driven us to study RGVO SnO₂ nanolayers for potential gas sensing applications. Moreover, the influence of doping SiO₂ substrate with Cr and Al on the surface chemistry and morphology of RGVO SnO₂ nanolayers is under investigation.

2. Results

For the purpose of the better understanding the surface chemical properties, with the special empathizes on nonstoichiometry, carbon contaminations, the relative concentrations of the main components and bondings, the XPS technique was applied. Figure 1a demonstrates XPS survey spectra with the main core level lines for RGVO SnO₂ nanostructures deposited on SiO₂ substrates for as deposited and additionally oxidized samples. As it can be clearly seen, the spectra contain well recognized peaks related to O1s, Sn3d, and Sn4d (basic components of the expected SnO₂). The contribution of adventitious C contamination has not been detected neither in the case of raw samples nor after additional oxidation. The inset to Figure 1a shows the respective O–Sn3d spectral window required for the quantitative analysis of the surface chemistry performed in the subsequent part of the paper. In the case of RGVO SnO₂ nanolayers deposited on SiO₂ substrate modified with Cr and Al additives (also as deposited and after additional oxidation) the only visible XPS core level peaks also belong to the expected SnO₂ compound (Figure 1b). There is no contribution from Cr nor Al that can be treated as an indirect proof of the continuous SnO₂ nanolayer formation. The results of the calculation of the atomic relative concentrations [O]/[Sn] are presented in Table 1. As it can be seen, SnO₂ nanolayers are highly nonstoichiometric—namely oxygen deficient. This leads to conclusion that the obtained oxides are the mixture of SnO₂ with significant contribution of SnO phase which is present in both: RGVO SnO₂ samples obtained on pure as well as on doped substrates. A slight increase in [O]/[Sn] can be observed each time in the case of the samples that underwent additional oxidation. Moreover the atomic relative concentration [O]/[Sn] is higher for nanolayers deposited on the substrates covered with Cr and Al.

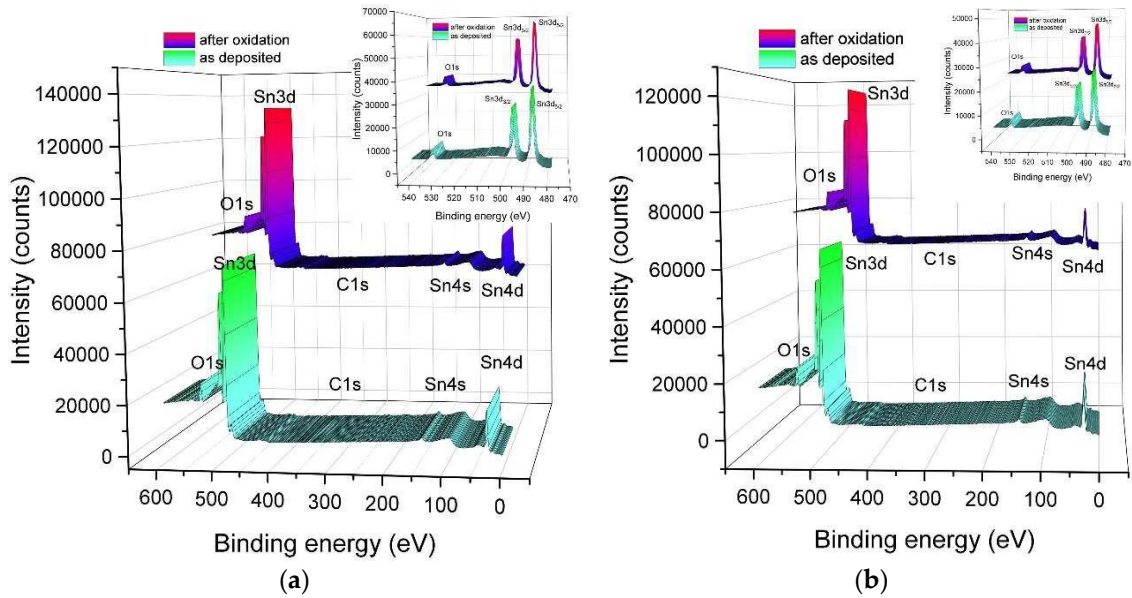


Figure 1. XPS survey spectra with the main core level lines of: (a) RGVO SnO₂ nanolayers deposited on SiO₂ substrate both as deposited and after additional oxidation, together with the corresponding O – Sn3d spectral window (in the inset); (b) RGVO SnO₂ nanolayers deposited on SiO₂ substrate modified with Cr and Al additives both as deposited and after additional oxidation, together with the corresponding O–Sn3d spectral window (in the inset).

Table 1. The results of XPS investigation: relative intensity (RI) of XPS lines and the atomic relative concentrations (ARC) of the main components for RGVO SnO₂ nanolayers.

Samples	XPS Lines RI		ARC	
Substrates	RGVO SnO ₂	O1s (a.u.)	Sn3d5/2 (a.u.)	[O]/[Sn]
Pure SiO ₂	As-deposited	47	340	0.90
	After oxidation	48	336	0.93
SiO ₂ covered with Cr and Al	As-deposited	46	328	0.95
	After oxidation	50	320	1.02

Figure 2 shows the AFM data of RGVO SnO₂ nanolayers containing the 3D image, average grain height distribution and the respective depth profile. As it can be seen from AFM data, that RGVO SnO₂ nanolayers exhibit the grain type surface morphology. The lateral grain dimension is in the range of 15–50 nm, whereas their height is at the level of several nm with distribution of maximum at ~5 nm, what finally causes that these nanolayers are of high flatness in a large surface area up to several μm.

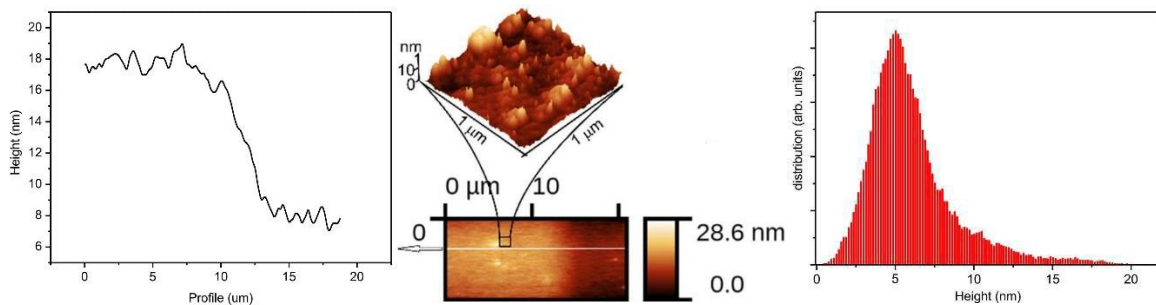


Figure 2. AFM data of RGVO SnO₂ nanolayers including the main image, average height distribution and the layer's edge profile.

Funding: This research was funded by the research grant of National Science Centre, Poland grant decision DEC-2016/20/S/ST5/00165 and partially realized within the Statutory Funding of Institute of Electronics, Silesian University of Technology, Gliwice, BK as well as BKM.

Conflicts of Interest: The authors declare no conflict of interest.



© 2019 by the authors. Licensee MDPI, Basel, Switzerland. This article is an open access article distributed under the terms and conditions of the Creative Commons Attribution (CC BY) license (<http://creativecommons.org/licenses/by/4.0/>).

Semiconductor Gas Sensors to Analyze Fecal Exhalation as a Method for Colorectal Cancer Screening

G. Zonta ^{1,2,*}, M. Astolfi ^{1,2}, A. Gaiardo ^{1,2,4}, S. Gherardi ², A. Giberti ^{2,3}, V. Guidi ¹, N. Landini ^{1,2} and C. Malagù ^{1,2}

¹ University of Ferrara, Via Savonarola 9 - 44121 Ferrara, Italy; michele.astolfi@unife.it (M.A.); andrea.gaiardo@unife.it (A.G.); guidi@fe.infn.it (V.G.); nicolo.landini@unife.it (N.L.); malagu@fe.infn.it (C.M.)

² SCENT S.r.l., Via Quadrifoglio 11—44124 Ferrara, Italy; gherardi@fe.infn.it (S.G.); giberti@fe.infn.it (A.G.);

³ MIST E-R s.c.r.l., Via P. Gobetti 101, 40129 Bologna, Italy

⁴ MNF—Micro Nano Facility, Bruno Kessler Foundation, Via Sommarive 18, 38123 Trento, Italy

* Correspondence: giulia.zonta@unife.it; Tel.: +39-0532-974-286.

† Presented at the 8th GOSPEL Workshop. Gas Sensors Based on Semiconducting Metal Oxides: Basic Understanding & Application Fields, Ferrara, Italy, 20–21 June 2019.

1. Introduction

Colorectal cancer (CRC) preventive screening is fundamental to identify tumors before their possible degeneration. The current screening method employed on population aging between 50–69 years by Italian National Health Service is fecal occult blood test (FOBT). This test leads to a lot of false positives (more than 60%) and to non-operative colonoscopies.

Our patented device, named SCENT A1 [1] and described in our publications [2–4], is capable to identify CRC with an economic, in-vitro, non-invasive technique. The device is composed of a set of five chemoresistive MOX sensors that, by smelling the odor of fecal samples, can distinguish between populations of healthy and CRC-affected patients. The odor of fecal exhalations is strongly different if the tumor is present, also depending on its dimensions and degeneration stage, due to the presence of specific tumor biomarkers produced by peroxidation of the cell membrane or by metabolic alterations. Here the results obtained so far in the clinical validation Protocol, started in May 2016, that involves S. Anna Hospital of Ferrara, UNIFE, Ospedale del Delta of Lagosanto, AUSL of Ferrara and the startup SCENT S.r.l.

2. Experimental Section

All screening users in Ferrara who resulted positive to FOBT can participate in the project bringing an additional sample of frozen feces to be analyzed with SCENT A1. Up to now, over 500 fecal samples have already been measured with the device, already resulted positive for FOBT, 100 of which were already compared with colonoscopy. The technique employed for data analysis is support vector machine (SVM) by dividing the samples into three categories (low-risk adenomas, LR, healthy subjects, NEG, and high-risk adenomas plus carcinomas), see Figure 1. Here this method correctly classified the 90% of NEG, the 100% of CRC and the 57% of LOW. A new approach, that employs the information of only two sensors, to simplify the system and improve the algorithm efficiency, is the k-fold cross validation test. This method ensures an immediate double-blind check. It emerges that, by performing SCENT A1 test with the data compared so far, the percentage of colonoscopies saved is 79%. If the results over a sufficiently large statistics will be confirmed, the goal would be to combine FOBT with SCENT A1 test in the countries where FOBT is employed as a screening on population.

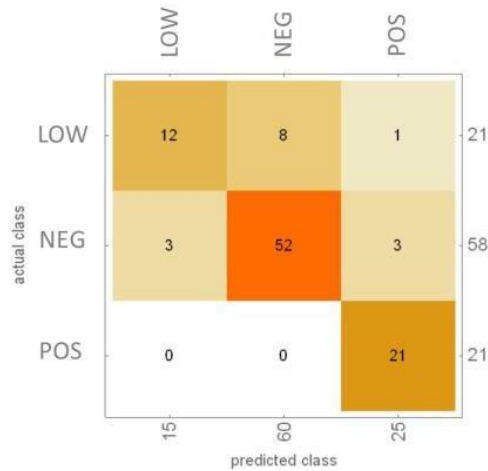


Figure 1. Confusion matrix with 100 samples.

Funding: This research was supported by LILT (Lega Italiana Lotta Tumori) section of Ferrara for the Design Work Plan Call for Health Research 2016 “Programma 5 per mille anno 2014”.

Acknowledgments: The authors would like to thank SCENT S.r.l. for the operational contribution in the research.

Conflicts of Interest: The authors declare no conflict of interest.

References

1. SCENT A1. Italian patent number: RM20144000595, European extension: 3210013; patent of SCENT S.r.l.
2. Landini, N.; Zonta, G.; Malagù, C. *Detection of Tumor Markers on Feces with Nanostructured Sensors*; Scholars' Press: Saarbrücken, Germany, 2015; ISBN-13 978-3-639-76538-0.
3. Zonta, G.; Anania, G.; Fabbri, B.; Gaiardo, A.; Gherardi, S.; Giberti, A.; Landini, N.; Malagù, C.; Scagliarini, L.; Guidi, V. Preventive screening of colorectal cancer with a device based on chemoresistive sensors. *Sens. Actuators B* **2016**, *238*, 1098–1110.
4. Zonta, G.; Anania, G.; Feo, C.; Gaiardo, A.; Gherardi, S.; Giberti, A.; Guidi, V.; Landini, N.; Palmonari, C.; Ricci, L.; et al. Use of gas sensors and FOBT for the early detection of colorectal cancer. *Sens. Actuators B* **2018**, *262*, 884–891.



© 2019 by the authors. Licensee MDPI, Basel, Switzerland. This article is an open access article distributed under the terms and conditions of the Creative Commons Attribution (CC BY) license (<http://creativecommons.org/licenses/by/4.0/>).

Nanostructured Chemoresistive Sensors for Oncological Screening: Preliminary Study with Single Sensor Approach on Human Blood Samples

N. Landini ^{1,2,*}, G. Anania ³, M. Astolfi ¹, B. Fabbri ¹, A. Gaiardo ^{1,4}, S. Gherardi ², A. Giberti ⁷, V. Guidi ^{1,5}, G. Rispoli ⁶, L. Scagliarini ³, M. Valt ^{1,4}, G. Zonta ¹ and C. Malagù ¹

¹ Department of Physics and Earth Sciences, University of Ferrara, Via Saragat 1/C, 44122 Ferrara, Italy; stlmhl@unife.it (M.A.); fbbbr@unife.it (B.F.); grdnldr@unife.it (A.G.); gduvncn@unife.it (V.G.); vltmtt1@unife.it (M.V.); zntgli@unife.it (G.Z.); malagu@fe.infn.it (C.M.)

² SCENT S.r.l, Via Quadrifoglio 11, 44124 Ferrara, Italy; gherardi@fe.infn.it

³ Department of Morphology, Surgery and Experimental Medicine, University of Ferrara, Via Luigi Borsari 46, 44121 Ferrara, Italy; ang@unife.it (G.A.); scglcu@unife.it (L.S.)

⁴ Bruno Kessler Foundation, Via Sommarive 18, 38123 Trento, Italy

⁵ CNR-INO – Istituto Nazionale di Ottica, Largo Enrico Fermi 6, 50124 Firenze, Italy

⁶ Department of Life Sciences and Biotechnology, University of Ferrara, Via Luigi Borsari 46, 44121 Ferrara, Italy; rsg@unife.it

⁷ MIST E-R s.c.r.l., Via P. Gobetti 101, 40129 Bologna, Italy; giberti@fe.infn.it

* Correspondence: lndncl@unife.it

† Presented at the 8th GOSPEL Workshop. Gas Sensors Based on Semiconducting Metal Oxides: Basic Understanding & Application Fields, Ferrara, Italy, 20–21 June 2019.

1. Introduction

The demand for reliable devices to detect tumor biomarkers in human body is constantly increasing. The reasons behind that lays on the advantage of early intervention on pathologies, allowing a greater chance of healing and survival for the patient, compared to taking action in the malignant state of a pathology not diagnosed in time. Consequentially, also the expenses for the National Health Systems drop consistently while the efficiency of intervention form physicians and surgeons increases, having a reduction on the malignant and terminal cases. Chemoresistive semiconductor sensors, fast responding devices commonly used for pollution and alimentary screening, can be the brand new choice as sensing units for medical devices aimed to this kind of approach, as multiple studies from the team proved their reliability for screening applications on different organic samples [1–6]. Four different sensors have been tested on a collection of blood samples, both from healthy and tumor affected individuals (colorectal and gastric cancer) ranging between 21 and 91 years of age, and the responses compared to recognize recurrent patterns from which the two populations could be distinguished. The trial protocol and the informed consent form for this research were presented, accepted and retrospectively registered from the Ethical Committee of the District of Ferrara, with trial number 170484, on 13 July 2017.

2. Application and Results

The following sensors have been used for the detection of the markers, emanated from human blood samples kept at room temperature:

- TiTaV—composed by titanium, tantalum and vanadium oxides
- STN—composed by tin, titanium and niobium oxides
- ST 25 650 +1%Au—composed by tin oxides and titanium and gold
- W11—composed by tungsten oxide

Each sensor was put to his best working temperature, defined by laboratory tests on the tumor markers previously studied, chosen from literature [1–3]. The responses are defined as the average value between three output voltages measured by the sensor from the same sample, as shown in the following formula:

$$R = \frac{V_{\text{sensA}} + V_{\text{sensB}} + V_{\text{sensC}}}{3}$$

The volatile compounds exhaled from the 7 mL volume of blood were carried by the flow of filtered environmental air (to avoid contaminations and moist alteration) through the sensor chambers, where they reacted with the semiconductor film and

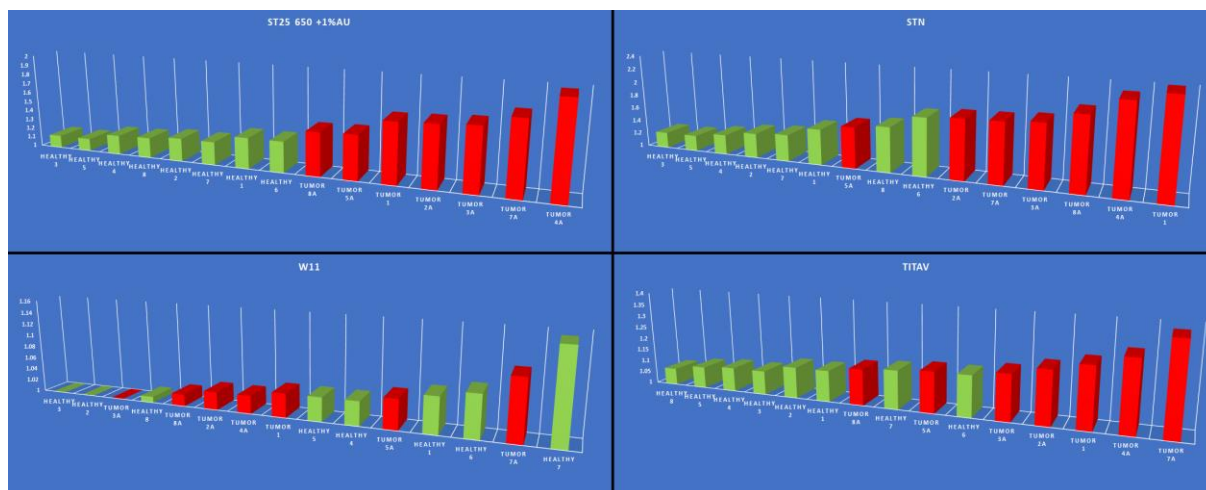


Figure 1. Tests results from ST25 650 + 1%Au, STN, W11 and TiTaV on multiple blood samples.

As shown in Figure 1 from our results, three out of four sensors showed a recognizable trend, correlating the amplitude of the response with the markers of oncological interest, even if the responses were quantitatively smaller compared to other researches underwent in the past. The team is now gathering further data to increase the statistic pool and try PCA [6] and machine learning approach as in other studies, in order to define if these sensors are good choices for setting an array as sensitive core for a post-screening device, aimed to give fast responses from simple blood sampling for the follow up of patients that needed surgeries to heal from colorectal malignant neoplasms.

References

1. Zonta, G.; Fabbri, B.; Giberti, A.; Guidi, V.; Landini, N.; Malagù, C. Detection of Colorectal Cancer Biomarkers in the Presence of Interfering Gases. *Sens. Actuators B* **2014**, *87*, 596–599.
2. Malagù, C.; Fabbri, B.; Gherardi, S.; Giberti, A.; Guidi, V.; Landini, N.; Zonta, G. Chemoresistive Gas Sensors for the Detection of Colorectal Cancer Biomarkers. *Sensors* **2014**, *14*, 18982–18992, doi:10.3990/s141018982.
3. Malagù, C.; Landini, N. Simulation of Intestinal Gaseous Environment in Order to Verify the Capability of Nanostructured Chemoresistive Sensors to Detect Colorectal Tumor Markers (Benzene, 1-Iodo-Nonane, Decanal). *J. Mol. Biomark. Diagn.* **2015**, *S2*, 012, doi:10.4172/2155-9929.S2-012.
4. Zonta, G.; Anania, G.; Fabbri, B.; Gaiardo, A.; Gherardi, S.; Giberti, A.; Landini, N.; Malagu, C.; Scagliarini, L.; Guidi, V. Preventive screening of colorectal cancer with a device based on chemoresistive sensors. *Sens. Actuators B* **2017**, *238*, 1098–1101.
5. Zonta, G.; Anania, G.; Feo, C.; Gaiardo, A.; Gherardi, S.; Giberti, A.; Guidi, V.; Landini, N.; Palmonari, C.; Ricci, L.; et al. Use of gas sensors and FOBT for the early detection of colorectal cancer. *Sens. Actuators B Chem.* **2018**, *262*, 884–891.

6. Landini, N.; Anania, G.; Fabbri, B.; Gaiardo, A.; Gherardi, S.; Guidi, V.; Rispoli, G.; Scagliarini, L.; Malagù, G.Z.C. Neoplasms and metastasis detection in human blood exhalations with a device composed by nanostructured sensors. *Sens. Actuators B Chem.* **2018**, *271*, 203–214.



© 2019 by the authors. Licensee MDPI, Basel, Switzerland. This article is an open access article distributed under the terms and conditions of the Creative Commons Attribution (CC BY) license (<http://creativecommons.org/licenses/by/4.0/>).

Chemoresistive Nanostructured Sensors for Tumor Pre-Screening

Michele Astolfi ^{1,2}, Giulia Zonta ^{1,2}, Nicolò Landini ^{1,2}, Sandro Gherardi ^{2,*}, Giorgio Rispoli ¹, Gabriele Anania ¹, Mascia Benedusi ¹, Vincenzo Guidi ¹, Caterina Palmonari ^{1,3}, Paola Secchiero ¹, Veronica Tisato ¹, Matteo Valt ¹ and Cesare Malagù ^{1,2}

¹ University of Ferrara, Via Savonarola 9, 44121 Ferrara, Italy

² SCENT S.r.l., Via Quadrifoglio 11, 44124 Ferrara, Italy

³ Department of Public Health (AUSL), UO Igiene Pubblica, Via Fausto Beretta, 7, 44121 Ferrara, Italy

* Correspondence: stlmhl@unife.it

† Presented at the 8th GOSPEL Workshop. Gas Sensors Based on Semiconducting Metal Oxides: Basic Understanding & Application Fields, Ferrara, Italy, 20–21 June 2019.

1. Introduction

One of the greatest goals in medicine is early-stage detection of tumors, to allow physicians and surgeons to apply the available therapies, which are usually successful on small volume cancers only. Our purpose is to identify the presence of a cancer by detecting the volatile organic compounds (VOC's) exhaled by cancer cells that are different by the ones exhaled by healthy cells, through a chemoresistive sensor array. In this study, a fast-responding, reliable and reproducible sensing technique proved to discriminate cancer cells from the healthy ones, making it a good cancer screener with a very low invasiveness. The measures have been performed on cancer and healthy tissues coming from human colon and rectum, with the aim of extending the study to the other type of tumors. Neoplastic tissues exhibit altered metabolic processes with respect to the metabolism of healthy cells, therefore the chemicals (metabolites) expelled during cellular respiration depend upon the cell health status. In this study, a device named SCENT B1 [1] is used with the aim to discriminate between normal and malignant tissues, by using an array containing four nanostructured chemoresistive metal-oxide sensors (nanograins with average size of 40–50 nm) manufactured in the Sensor Laboratory of the University of Ferrara.

Concurrently to the tissues investigation, samples containing different kind of immortalized cells have been investigated using the same sensor array, with the target of discriminating the different immortalized cell types and of analyzing the sensor responses depending on the cell concentration (after 24, 48, 72 h of incubation).

2. Experimental Section

The voltage output of each sensor is directly proportional to its conductance and, in turn, it depends upon the chemicals interacting with its surface [2,5]. Figure 1 shows the ratio G/G_0 , where

G_0 is the difference between the sensor conductance with and without the metabolites expelled by the cells of a tissue.

All four sensors gave larger responses (although with different amplitudes) to tumor tissue with respect to the healthy one. Smaller responses were given by the DMEM only (Figure 1).

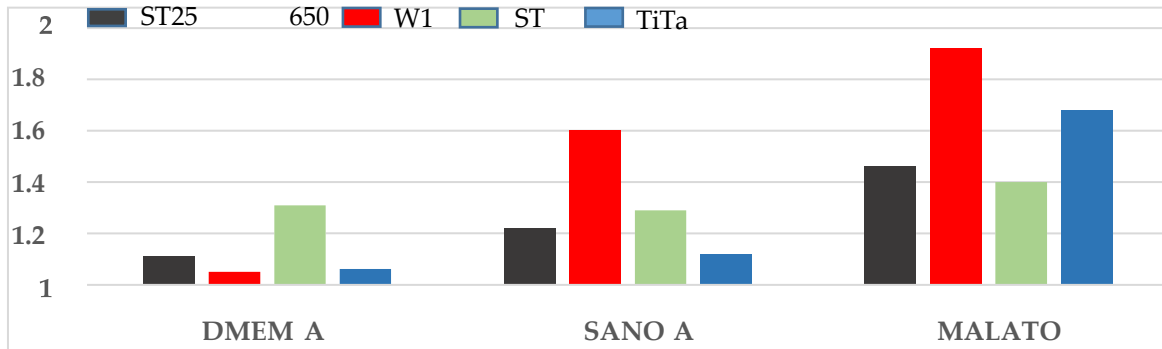


Figure 1. Histogram of the responses of four different sensors to the cell samples exhalations.

These results are consistent with the stronger metabolism of tumor cells with respect to the healthy ones, because the former emits larger amounts of VOCs [3].

In Figure 2 a histogram of the responses of four different sensors to cell sample exhalations with different initial plating concentrations 250k, 500k and 1M. It is evident that the device is capable of distinguishing different cell samples at different concentrations.

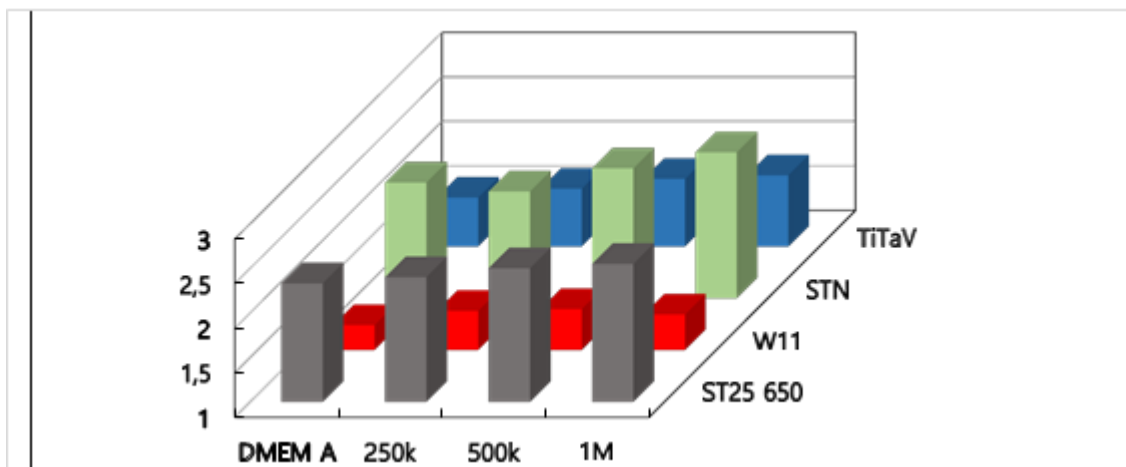


Figure 2. 3D Histogram of the responses of four different sensors to cell sample exhalations with different initial plating concentrations 250k, 500k and 1M.

Acknowledgments: This research was funded by the research grant of National Science Centre, Poland grant decision DEC-2016/20/S/ST5/00165 and partially realized within the Statutory Funding of Institute of Electronics, Silesian University of Technology, Gliwice, BK as well as BKM.

References

1. SCENT B1, Italian Patent Number: 102015000057717.
2. Zonta, G.; Anania, G.; Fabbri, B.; Gaiardo, A.; Gherardi, S.; Giberti, A.; Guidi, V.; Landini, N.; Malagù, C. Detection of colorectal cancer biomarkers in the presence of interfering gases. *Sens. Actuators B Chem.* **2015**, *218*, 289–295.
3. Altomare, D.F.; di Lena, M.; Porcelli, F.; Trizio, L.; Travaglio, E.; Tutino, M.; Dragonieri, S.; Memeo, V.; de Gennaro, G. Exhaled volatile organic compounds identify patients with colorectal cancer. *Br. J. Surg.* **2013**, *100*, 144–150.
4. Chan, E.C.Y.; Koh, P.K.; Mal, M.; Cheah, P.Y.; Eu, K.W.; Backshall, A.; Cavill, R.; Nicholson, J.K.; Keun, H.C. Metabolic Profiling of Human Colorectal Cancer Using High-Resolution Magic Angle Spinning Nuclear Magnetic Resonance (HR-MAS NMR) Spectroscopy and Gas Chromatography Mass Spectrometry (GC/MS). *J. Proteom. Res.* **2009**, *8*, 352–361.

5. Zonta, G.; Anania, G.; Fabbri, B.; Gaiardo, A.; Gherardi, S.; Giberti, A.; Landini, N.; Malagù, C.; Scagliarini, L.; Guidi, V. Preventive screening of colorectal cancer with a device based on chemoresistive sensors. *Sens. Actuators B Chem.* **2017**, *238*, 1098–1101.



© 2019 by the authors. Licensee MDPI, Basel, Switzerland. This article is an open access article distributed under the terms and conditions of the Creative Commons Attribution (CC BY) license (<http://creativecommons.org/licenses/by/4.0/>).

Sensing Performance of Al and Sn Doped ZnO for Hydrogen Detection [†]

Zahira. El khalidi ^{1,4,*}, Bouchaib. Hartiti ^{1,4}, Maryam Siadat ², Elisabetta. Comini ³, Salah. Fadili ⁴ and Philippe Thevenin ²

¹ Senior Assoc. ICTP-UNESCO-IAEA, 34100 Trieste, Italy; Bhartiti@gmail.com

² LMOPS Laboratory, University of Lorraine Metz, 57000 Metz, France; maryam.siadat@univ-lorraine.fr (M.S.); philippe.thevenin@univ-lorraine.fr (P.T.)

³ Dipartimento di Ingegneria dell'informazione, Università degli Studi di Brescia, 25100 Brescia, Italy; elisabetta.comini@unibs.it

⁴ MAC & PM Laboratory, FST Mohammedia, Hassan II Casablanca University Casablanca, 20430 Casablanca, Morocco; safadili@yahoo.fr

* Correspondence: elkhalidizahira@gmail.com; +212-663-130-999

[†] Presented at the 8th GOSPEL Workshop. Gas Sensors Based on Semiconducting Metal Oxides: Basic Understanding & Application Fields, Ferrara, Italy, 20–21 June 2019.

Abstract: Chemical gas sensors were studied long ago and nowadays, for the advantageous role they provide to the environment, health condition monitoring and protection. The recent studies focus on the semiconductors sensing abilities, especially of non toxic and low cost compounds. The present work describes the steps to elaborate and perform a chemical sensor using intrinsic and doped semiconductor zinc oxide. First, we synthesized pure oxide using zinc powder, then, two other samples were established where we introduced the same doping percentage of Al and Sn respectively. Using low cost spray pyrolysis, and respecting the same conditions of preparation. The obtained samples were then characterized by X Ray Diffraction (XRD) that revealed the hexagonal wurzite structure and higher crystallite density towards the direction (002), besides the appearance of the vibration modes related to zinc oxide, confirmed by Raman spectroscopy. SEM spectroscopy showed that the surface morphology is ideal for oxidizing/reduction reactions, due to the porous structure and the low grain sizes, especially observed for the sample Sn doped ZnO. The gas testing confirms these predictions showing that the highest response is related to Sn doped ZnO compared to ZnO and followed by Al doped ZnO. The films exhibited responses towards: CO, acetone, methanol, H₂, ammonia and NO₂. The concentrations were varied from 10 to 500 ppm and the working temperatures from 250 to 500 °C, the optimal working temperatures were 350 and 400 °C. Sn doped ZnO showed a high response towards H₂ gas target, with a sensitivity reaching 200 at 500 ppm, for 400 °C.

Keywords: binary materials; Sn and Al doped ZnO; porous surface; gas sensors; H₂

Conflicts of Interest: The authors declare no conflict of interest.



© 2019 by the authors. Licensee MDPI, Basel, Switzerland. This article is an open access article distributed under the terms and conditions of the Creative Commons Attribution (CC BY) license (<http://creativecommons.org/licenses/by/4.0/>).

Gas Sensing Mechanism Investigation of LaFeO₃ Perovskite-Type Oxides via Operando Technique †

A. A. Alharbi, U. Weimar and N. Bârsan *

Institute of Physical and Theoretical Chemistry (IPTC), University of Tuebingen, Auf der Morgenstelle 15, D-72076 Tuebingen, Germany; abdulaziz.alharbi@ipc.uni-tuebingen.de (A.A.A.); upw@ipc.uni-tuebingen.de (U.W.)

* Correspondence: nb@ipc.uni-tuebingen.de; Tel.: +49-7071-29-78761

† Presented at the 8th GOSPEL Workshop. Gas Sensors Based on Semiconducting Metal Oxides: Basic Understanding & Application Fields, Ferrara, Italy, 20–21 June 2019.

1. Summary

Gas sensor based on perovskites, such as LaFeO₃ (LFO), have been used successfully to detect various target gases [1,2]. Despite the importance of understanding the underlying mechanism for future development of gas sensing materials, there is only little known on their gas sensing mechanism. Here, we investigated the gas sensing mechanism during ethylene and CO₂ exposure under operando conditions. The changes in the active sites at the surface, which are responsible for the gas response, have been observed. Our work has demonstrated a correlation between the gas sensing behaviour of LFO material and the changes in its surface chemistry during gas exposure in operando conditions. This work aims to gain more insight into the underlying mechanism.

2. Experimental Results

IR spectra of LFO sensor have been obtained through a series of Operando diffuse reflectance infrared Fourier transform spectroscopy (DRIFTS) experiments. This in operando technique combined with measurements of the resistance change of the sensor during the gas exposures which deliver significant information about the chemistry change on the surface and thus helps to interpret the gas sensing mechanism.

The DRIFTS spectra and DC resistance results of LFO sensor exposed to different ethylene concentration in dry condition at 200 °C are shown in Figure 1. The spectra were referenced to the spectra which were recorded in dry air. As the gas concentration is increasing, a systematic increase in the resistance can be observed in correlation with changes of some bands in the IR spectra. After the end of gas exposure, the change in the resistance and the spectra features started to decrease with time back to the original state, as shown in Figure 2. The recovery speed for the surface species is correlated to the changes of the resistance. Isotope labeling exchange experiments combined with experiments performed in N₂ backgrounds have been used for interpreting the spectra: The bands at 2953 and 2851 cm⁻¹ together with 1580 and 1373 cm⁻¹ could be assigned to formates. The highest intensity band at 1580 cm⁻¹ is considered to have two components, one that refers to formates and another to carbonates. Spectra for the LFO sensor exposed to 500 ppm C₂H₄ and CO₂, separately, in dry conditions at 200 °C and 250 °C are shown in Figures 3 and 4 respectively. The sensor only showed a good response to ethylene at 200 °C whereas no responses have been observed to CO₂ at both temperatures.

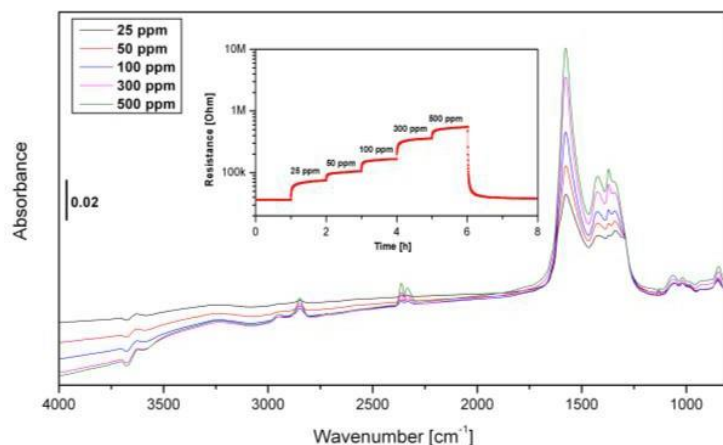


Figure 1. Drifts spectra of LFO sensor exposed to 25, 50, 100, 300 and 500 ppm C_2H_4 in dry air conditions at 200 °C. All spectra were referenced to the dry air spectrum measured prior to C_2H_4 exposure. Inset figure shows the DC resistance measurement.

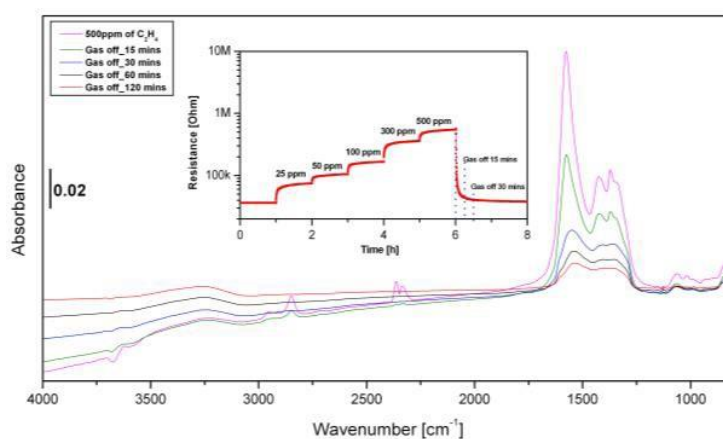


Figure 2. Drifts spectra of LFO sensor exposed to 500 ppm C_2H_4 in dry air followed by clean dry air for 15, 30, 60 and 120 min at 200 °C. All spectra were referenced to the dry air spectrum measured prior to C_2H_4 exposure. The inset figure shows the DC resistance.

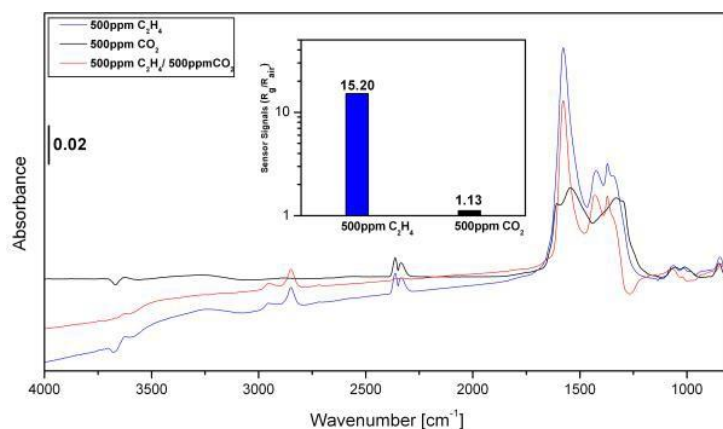


Figure 3. Drifts spectra of LFO sensor exposed to 500 ppm C_2H_4 (blue line) and CO_2 (black line) in dry air conditions at 200 °C. All spectra were referenced to the dry air spectrum measured prior to C_2H_4 exposure, except for the C_2H_4 spectrum (red line) which was referenced to CO_2 . The inset figure shows the sensor signals of C_2H_4 and CO_2 in same conditions.

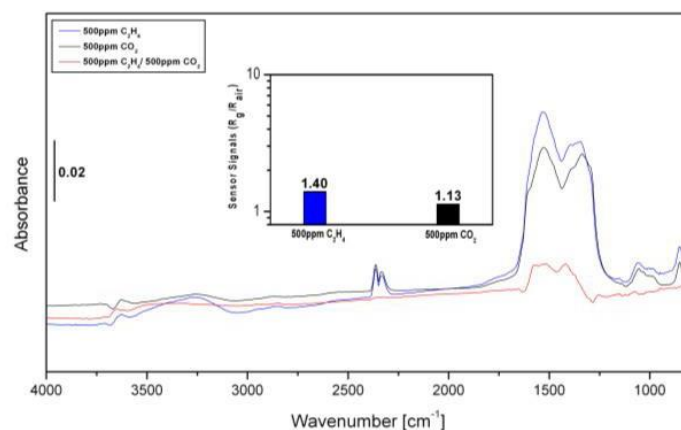


Figure 4. Drifts spectra of LFO sensor exposed to 500 ppm C₂H₄ (blue line) and CO₂ (black line) in dry conditions at 250 °C. All spectra were referenced to the dry air spectrum measured prior to C₂H₄ exposure, except for the C₂H₄ spectrum (red line) which was referenced to CO₂. The inset figure shows the sensor signals of C₂H₄ and CO₂ in same conditions.

The DRIFTS spectra reveal that the presence of formates on the surface during gas exposure results in determine the sensor signals. When the target gas exposure was stopped, a direct reduction of the resistance accompanied with the disappearance of formate bands was recorded, while corresponding to other surface species bands remained at the sensor surface. At 250 °C, ethylene preferred to form other types of carbonates on the surface of LFO rather than formates and that caused a huge reduction in the gas response from around 15 at 200 °C to only 1.5 at 250 °C. Therefore, we think that there is a correlation between the presence of formates on the surface and the gas response of LFO sensor.

Our findings indicate that the formation of formates at the surface of LFO sensor during gas exposure plays a key role in the gas sensing mechanism. This is a significant step in understanding the origin of gas response and helps the development of practical sensors.

Acknowledgments: We acknowledge the financial support of King Abdulaziz City for Science and Technology (KACST), Saudi Arabia for funding a PhD student.

Conflicts of Interest: The authors declare no conflict of interest

References

1. Chu, X.; Siciliano, P. CH₃SH-sensing characteristics of LaFeO₃ thick-film prepared by co-precipitation method. *Sens. Actuators B. Chem* **2003**, *94*, 197–200.
2. Song, P.; Wang, Q.; Zhang, Z.; Yang, Z. Synthesis and Gas Sensing Properties of Biomorphic LaFeO₃ Hollow Fibers Templated from Cotton. *Sens. Actuators B. Chem* **2010**, *147*, 248–254.



© 2019 by the authors. Licensee MDPI, Basel, Switzerland. This article is an open access article distributed under the terms and conditions of the Creative Commons Attribution (CC BY) license (<http://creativecommons.org/licenses/by/4.0/>).

Optical Gas Sensors Based on Localised Surface Plasmon Resonance †

Michele Rigon ¹, Enrico Della Gaspera ² and Alessandro Martucci ^{1,*}

¹ Dipartimento di Ingegneria Industriale, Università di Padova, Via Marzolo 9, 35131 Padova, Italy; michele.rigon.4@phd.unipd.it

² RMIT University, School of Science, Melbourne, VIC, Australia; enrico.dellagaspera@rmit.edu.au

* Correspondence: alex.martucci@unipd.it

† Presented at the 8th GOSPEL Workshop. Gas Sensors Based on Semiconducting Metal Oxides: Basic Understanding & Application Fields, Ferrara, Italy, 20–21 June 2019.

Gas species recognition through fully optical devices is currently a raising trend over the well-established conductometric approach, as it opens new possibilities especially for *in situ* recognition of flammable and/or toxic species such as CO, H₂ NO₂ or volatile organic compounds (VOC).

Au nanoparticles (NPs) dispersed in an oxide matrix represent an effective design for a gas sensor's active material owing to their catalytic and localized surface plasmon resonance (LSPR) properties. Noble metal NPs can exhibit catalytic properties and hence modify the chemical interactions between the oxide surface and the target analyte, thereby improving the sensing process. Moreover, if the metal NPs show a LSPR peak in the visible range (like Au), the nanocomposites can be used as selective optical gas sensors. The variation in the dielectric constant around the LSPR peaks will differ for different gas species, leading to a diverse variation in the optical properties at different wavelengths.

TiO₂ thin films with embedded Au and/or Pt NPs have been obtained by synthesizing high-quality metal and metal oxide colloids and directly spinning a nanocrystalline ink made of colloidal solutions on glass substrates. These TiO₂-Au samples showed fast and reversible changes in optical absorption when exposed to H₂ and CO species at 200–350 °C, with high sensitivities. More impressively, TiO₂-Au-Pt films showed room-temperature response to H₂ and VOC.

Thin films composed of Au NPs dispersed inside a TiO₂-NiO mixed oxide matrix were obtained spin coating a sol-gel solution on a glass substrate and subsequently thermal annealing. These samples show high response to H₂S down to few ppm and almost no interference in response is observed during simultaneous exposure to CO or H₂. For mechanistic studies, experimental evidence using reaction product analysis and thin film surface characterization suggests a direct catalytic oxidation of H₂S over the Au-TiO₂-NiO nanocomposite film.

More recently, we demonstrate the application of ZnO doped with gallium (GZO), aluminum (AZO) and silicon (SZO) nanocrystals as novel plasmonic sensors for the detection of hazardous gases. GZO, AZO and SZO nanocrystals are obtained by non-aqueous colloidal heat-up synthesis with high transparency in the visible range and strong LSPR in the near IR range, tunable with dopant concentration (up to 20% mol nominal). Thanks to the strong sensitivity of the LSPR to chemical and electrical changes occurring at the surface of the nanocrystals, such optical features can be used to detect the presence of toxic gases. By monitoring the changes in the dopant-induced plasmon resonance in the near infrared, we demonstrate that GZO, AZO and SZO thin films prepared depositing an assembly of highly doped ZnO colloids are able to optically detect both oxidizing and reducing gases at mild (<100 °C) operating temperatures.



© 2019 by the authors. Licensee MDPI, Basel, Switzerland. This article is an open access article distributed under the terms and conditions of the Creative Commons Attribution (CC BY) license (<http://creativecommons.org/licenses/by/4.0/>).

Extended Abstract

Selective Gas Sensor Based on Metal Oxide Nanostructure [†]

Vardan Galstyan *, Nicola Poli and Elisabetta Comini *

Sensor Lab, Department of Information Engineering, University of Brescia, Via Valotti 9, 25133 Brescia, Italy; nicola.poli@unibs.it

* Correspondence: vardan.galstyan@unibs.it (V.G.); elisabetta.comini@unibs.it (E.C.)

[†] Presented at the 8th GOSPEL Workshop. Gas Sensors Based on Semiconducting Metal Oxides: Basic Understanding & Application Fields, Ferrara, Italy, 20–21 June 2019.

Hydrogen sulfide (H₂S) is a colorless, highly flammable and toxic gas. It is produced due to industrial activities including petroleum refineries, natural gas plants, sewage treatment plants and tanneries. Its presence causes eye irritation, fatigue, headache, poor memory, dizziness, olfactory paralysis and respiratory distress. An increase in the concentration of H₂S up to 700 ppm causes human death. Therefore, the monitoring of H₂S levels in ambient, particularly in areas at hazardous waste sites is needed [1].

Metal oxides are very attractive materials for the fabrication of chemical sensors due to their ability to interact with different gaseous compounds. In this aspect, the preparation of nanoscale oxide materials seems to be more efficient to improve their functional performance and open new perspectives for their application in chemical gas sensors. Recent years, the ZnO nanomaterials have been studied for the detection of ZnO owing to its high electron mobility and thermal stability. However, it is still a challenge to achieve high response and selectivity of ZnO towards H₂S.

Herein, we present the synthesis and study of the gas sensing properties of ZnO nanomaterial for the detection of H₂S. ZnO nanomaterial was prepared by combination of electrochemical anodization and thermal decomposition methods [1]. First, metallic zinc films were deposited on alumina substrates by means of radio-frequency (13.56 MHz) magnetron sputtering. The sputtering power and the time were 75 W and 35 min, respectively. To improve the adhesion of metallic films the temperature of the alumina substrates was kept at 300 °C during the sputtering process. Then, the metallic films were electrochemically anodized in a Teflon cell using a two-electrode system. The electrolyte solution was oxalic acid dihydrate (C₂H₂O₄·2H₂O) containing ethanol. We have investigated the materials structural, morphological and sensing properties. Figure 1a reports the XRD spectrum of the nanomaterial. As can be seen, the fabricated material is crystalline ZnO. The morphological (Figure 1b) analyses were carried out by scanning electron microscope (SEM). The prepared materials have a nonosized structure, which consists of nanoparticles connected to each other and forming chains with the length of a few microns. Figure 2 reports the gas sensing response variation of the ZnO depending on the concentration of H₂S. The selectivity of the prepared ZnO was studied towards 20 ppm of ammonia (NH₃) and acetone (C₃H₆O) at the optimal operating temperature of 400 °C (Figure 3).

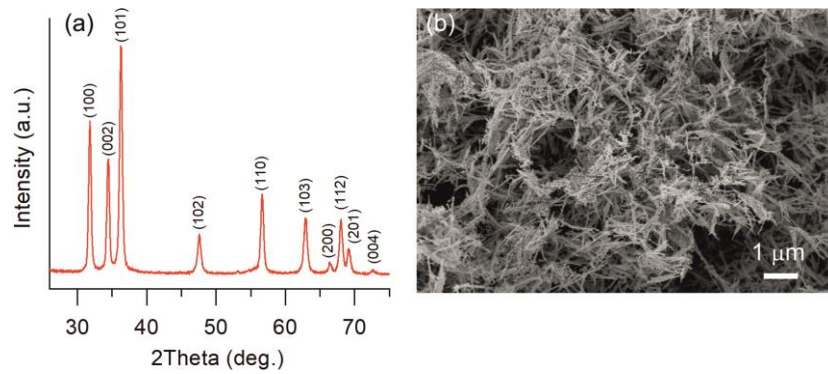


Figure 1. (a) XRD pattern of the ZnO nanostructure, (b) SEM images of the ZnO.

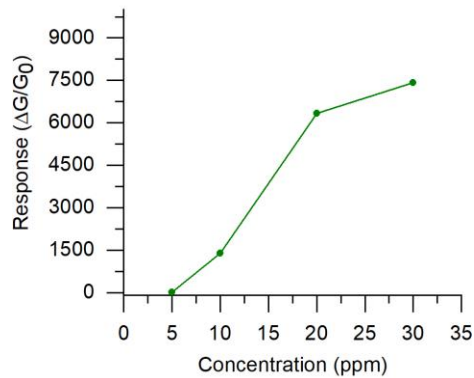


Figure 2. Gas sensing response variation of the ZnO depending on the concentration of H_2S (5, 10, 20 and 30 ppm) at 400 °C.

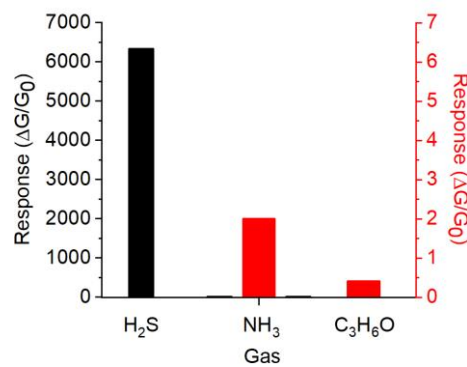


Figure 3. Response of the ZnO towards 20 ppm of H_2S , NH_3 and C_3H_6O at 400 °C.

Reference

- Galstyan, V.; Poli, N.; Comini, E. Highly Sensitive and Selective H_2S Chemical Sensor Based on ZnO Nanomaterial. *Appl. Sci.* **2019**, *9*, 1167, doi:10.3390/app9061167.



© 2019 by the authors. Licensee MDPI, Basel, Switzerland. This article is an open access article distributed under the terms and conditions of the Creative Commons Attribution (CC BY) license (<http://creativecommons.org/licenses/by/4.0/>).

SnO₂-Pd as a Gate Material for the Capacitor Type Gas Sensor †

Nikolay Samotaev *, Konstantin Oblov, Arthur Litvinov and Maya Etrekova

National Research Nuclear University MEPHI (Moscow Engineering Physics Institute), Kashirskoe highway 31, Moscow 115409, Russia; kyoblov@mephi.ru (K.O.); avlitvinov@mephi.ru (A.L.); moetrekova@mephi.ru (M.E.)

* Correspondence: nnsamotaev@mephi.ru

† Presented at the 8th GOSPEL Workshop. Gas Sensors Based on Semiconducting Metal Oxides: Basic Understanding & Application Fields, Ferrara, Italy, 20–21 June 2019.

Abstract: The article describes the result of the use SnO₂-Pd thin films as a gate for structure measured ppb range of NO₂ gas by the capacitive method. The technological aspects of fabrication SnO₂-Pd gate and one comparison by metrological parameters with the classical Pd gate field effect sensor are discussed. The use of SnO₂-Pd material allows improvement in sensitivity of NO₂ by an order of magnitude compare the classical Pd based gate field effect sensors.

Keywords: field-effect sensor; metal oxide sensor; gas sensitivity

1. Introduction

Using of SnO₂ material for fabrication field effect gas sensors based on Schottky diode effect firstly describing in work [1], somewhat later, a study of the sensitivity of field-effect sensors to NO₂ began [2]. But still remains an important issue measurement of sub-ppb concentrations of NO₂ in such areas as medicine, environmental control and explosives detection. Materials based on SnO₂ are widely used to measure NO₂ by resistive type MOX sensors, but MOX sensors margin of stable sensitivity is limited by sub-ppm range. The further increase in sensitivity to NO₂ is possible in the technological combination of well proven material using nowadays in MOX sensors and high sensitivity of field-effect sensors.

2. Experimental

In [3] was shown that the characteristics of field-effect sensors strongly depend on the composition metal-dielectric transition layer, which is determined by the materials of metal gate and insulator dielectric and methods of their deposition. For a new capacity type sensor manufacturing n-type silicon substrate with a 0.1 μm SiO₂ layer thickness was used. Layer of SnO₂ is additionally deposited through the shadow mask on the SiO₂ film by the method of magnetron sputtering. This method of deposition allows you to form films with a high effective surface area. The Pd film with a thickness of 100 nm was coated SnO₂ film through the shadow mask by pulse laser deposition method. The Pd-SnO₂-SiO₂-Si structure was basis of capacitor type gas sensor which photo present on Figure 1 and cross-section scheme of structure on Figure 2, respectively. In parallel with the SnO₂-Pd based sensor, a similar series of capacity sensors without SnO₂ layer, only with a 100 nm Pd gate, was made for comparing changes of gas-sensitive characteristics.

Figure 3 presents the capacitance-voltage characteristic for Pd gate sensor at different heating temperatures. The capacitance-voltage characteristics for SnO₂-Pd and Pd base sensors at temperatures of 170 °C, 140 °C and 100 °C was study and present in Figure 4. Also sensitivity to NO₂ at different temperatures present on Figures 5 and 6. On Figures 4 and 5 can be seen that the slope of the characteristic decreases with increasing temperature, therefore, the sensitivity of the sensor should decrease; this effect is explained by the shift of C-V characteristic during exposed to gas. The

Figure 5 shows the time responding capacity sensor with SnO₂-Pd gate to 108 ppb NO₂ at different temperature and possible to see decreasing response time and sensitivity during increasing working temperature of sensor. This behavior is standard for the field effect sensor.



Figure 1. Capacitor sensor’s photo assembled with film resistive heater and thermistor. Package type is TO-8 (11 mm in diameter).

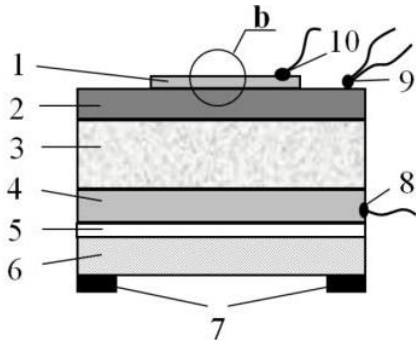


Figure 2. Capacitor sensor: 1—SnO₂/Pd gate; 2—SiO₂ film; 3—Si substrate; 4—Al electrode; 5—insulator; 6—heater; 7, 8, 10—the electric contacts; 9—thermistor.

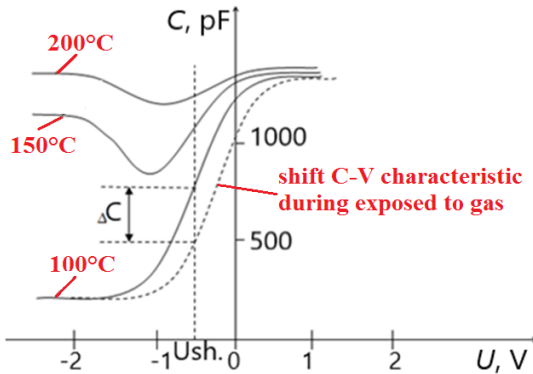


Figure 3. Scheme of capacitance-voltage characteristic for Pd gate sensor at different heating temperatures and shift C-V characteristic during exposed to gas.

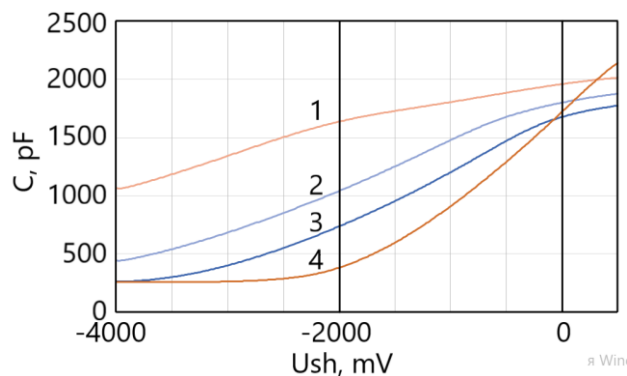


Figure 4. The capacitance-voltage characteristics for capacity sensor at temperatures: 1—170 °C, 2—140 °C, 3—100 °C, 4—pure Pd gate at 100 °C.

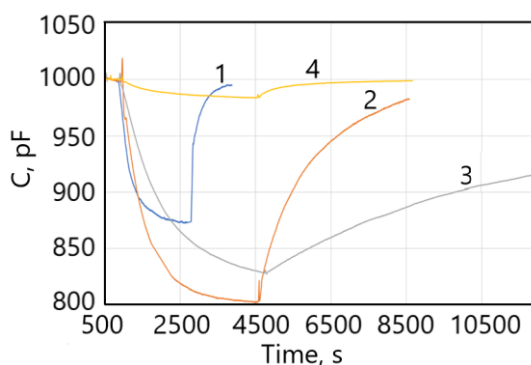


Figure 5. Responses capacitor sensor to 108 ppb NO₂ concentration at temperatures: 1—170 °C, 2—140 °C, 3—100 °C, 4—pure Pd gate at 100 °C.

T, °C	Gate Structure	
	Pd-SnO ₂	Pd
	Response, pF	
100	172	20
140	195	-
170	130	-

Figure 6. The response of capacity sensors to 108 ppb NO₂ concentration at different temperatures.

The using of the new type SnO₂-Pd gate in capacity type sensor gives possible to raise sensitivity by almost ten times but disadvantage for such approach is increasing response and relaxation times of the sensor. Possible approach for improving response and relaxation times is using pulse temperature mode increasing diffusion rate through the gate present in work [4]. Extrapolation of present measurement results suggests stable detection NO₂ concentrations by the Pd-SnO₂-SiO₂-Si structure in the region of 1 ppb and less.

Funding: This work was supported by the Russian Science Foundation (Grant Agreement 18-79-10230 of 08.08.2018).

Conflicts of Interest: The authors declare no conflict of interest.

References

1. Shivaraman, M.S.; Lundström, I.; Svensson, C.; Hammarsten, H. Hydrogen sensitivity of palladium-thin-oxide-silicon schottky barriers. *Electron. Lett.* **1976**, *12*, 483–484.
2. Fogelberg, J.; Dannelun, H.; Lundström, I.; Petersson, L.-G. A hydrogen sensitive palladium metal-oxide-semiconductor device as sensor for dissociating NO in H₂-atmospheres. *Vacuum* **1990**, *41*, 705–708.
3. Zhovannik, E.V.; Nikolaev, I.N.; Stavkin, D.G.; Shevlyuga, V.M.; Imamov, R.M.; Lomov, A.A. Studies of transient region between laser-deposited palladium and (111)Si. *Kristallografiya* **1996**, *41*, 935–939.
4. Samotaev, N.; Litvinov, A.; Etrekova, M. Improving Detection Chlorine by Field Effect Gas Sensor with Using Temperature Pulse Mode. In Proceedings of the IMCS 2018, Vienna, Austria, 15–19 July 2018; pp. 474–475.



© 2019 by the authors. Licensee MDPI, Basel, Switzerland. This article is an open access article distributed under the terms and conditions of the Creative Commons Attribution (CC BY) license (<http://creativecommons.org/licenses/by/4.0/>).

Abstract

Regulating Adsorbed Oxygen Species and Electron Transport for SnO₂-Based Gas Sensors through Surface Modification and Structural Design [†]

Liupeng Zhao, Sufang Zhang, Qi Yu, Tianshuang Wang, Yan Zeng, Peng Sun *, Fangmeng Liu, Xu Yan, Xiaohong Chuai, Xishuang Liang, Yuan Gao, Fengmin Liu, Zhongqiu Hua and Geyu Lu *

State Key Laboratory on Integrated Optoelectronics, College of Electronic Science and Engineering, Jilin University, 2699 Qianjin Street, Changchun 130012, China; 1838211801@qq.com (L.Z.)

* Correspondence:

[†] Presented at the 8th GOSPEL Workshop. Gas Sensors Based on Semiconducting Metal Oxides: Basic Understanding & Application Fields, Ferrara, Italy, 20–21 June 2019.

Abstract: The adsorption and desorption of oxygen molecule on the surface of oxide semiconductors are the basis for sensing reactions between the surface oxygen species and the target gases molecules. Combined with experiments and theoretical calculations, we found that antimony impurities were conducive to the promotion of oxygen adsorption and dissociation on the surface of SnO₂. However, the narrow Debye length had an adverse effect on sensing properties of Sb doped SnO₂. Herein, we designed a core-shell structure composed of inner Sb-doped SnO₂ nanospheres and the outer Co-doped SnO₂ nanoparticles enclosing the core. The shell is like a lock gate which can regulate the electron transport of the core. Gas sensing devices were fabricated from the pure, single doped SnO₂ and core-shell composites, and their gas sensing performances were tested for response to ethanol. The sensors based on core-shell composites exhibited excellently enhanced sensitivity to ethanol, giving a response of 72.4–100 ppm, which was about 3-times higher than that of the pure SnO₂. This work highlights the possibility of structural design for achieving high gas response by adjusting the surface adsorbed oxygen properties of oxide semiconductors.

Keywords: adsorbed oxygen species; oxygen dissociation; core-shell; doped SnO₂



© 2019 by the authors. Licensee MDPI, Basel, Switzerland. This article is an open access article distributed under the terms and conditions of the Creative Commons Attribution (CC BY) license (<http://creativecommons.org/licenses/by/4.0/>).

Light-Assisted Low Temperature Formaldehyde Detection at Sub-ppm Level Using Metal Oxide Semiconductor Gas Sensors [†]

Marina Rumyantseva ^{1,*}, Abulkosim Nasriddinov ^{1,2}, Valeriy Krivetskiy ¹ and Alexander Gaskov ¹

¹ Chemistry Department, Moscow State University, 1-3 Leninskie gory, Moscow, 119991, Russia; naf_1994@mail.ru (A.N.); vkrivetsky@gmail.com (V.K.); gaskov@inorg.chem.msu.ru (A.G.)

² Faculty of Materials Science, Moscow State University, 1-73 Leninskie gory, Moscow, 119991, Russia

* Correspondence: roum@inorg.chem.msu.ru

[†] Presented at the 8th GOSPEL Workshop. Gas Sensors Based on Semiconducting Metal Oxides: Basic Understanding & Application Fields, Ferrara, Italy, 20–21 June 2019.

1. Introduction

Formaldehyde HCOH is a toxic compound that, in trace concentrations, causes serious diseases of the respiratory tract, gastrointestinal tract and eyes. The biochemical oxidation of HCOH in human tissues occurs with the formation of CO₂ and formic acid, which with prolonged exposure is the cause of asthma, pulmonary edema, and cancer. The main problem in the HCOH detection is the need to determine very low concentrations: 0.5 mg/m³ (0.4 ppm) and 0.1 mg/m³ (81 ppb) in the air of the working and living area, respectively. A promising alternative for the HCOH quantification is the development of gas analyzers based on an array of metal oxide semiconductor sensors that exhibit the specific temperature dependence of the sensor signal when detecting different gases. It is currently shown that the use of such sensor arrays allows the detection of trace concentrations of individual substances, including various VOCs, in gas mixtures, as well as the recognition of gas mixture components. Such an analysis is relevant not only for environmental control and safety systems, but also promising for the development of new express methods for analyzing food quality, water purity, and medical diagnostics. However, the use of a dynamic temperature regime implies cyclic heating up to 500 °C, which leads to a significant increase in energy consumption and degradation of the sensitive layer. An alternative to dynamic thermal heating can be periodic photoactivation by UV or visible light with subsequent analysis of the photoconductivity rise and fall curves using a mathematical algorithm. This becomes possible when nanocomposites based on nanocrystalline semiconductor metal oxides and photocatalysts providing low-temperature decomposition/oxidation of target gas molecules are used as sensitive materials.

2. Experimental

Nanocomposites SnO₂/TiO₂ modified with Pt, Ag and Au nanoparticles were obtained by wet chemical synthesis. SnO₂ xH₂O xerogel was precipitated from H₂SnCl₆ solution. To obtain the SnO₂/TiO₂ composites, the SnO₂ xH₂O xerogel and Ti(OPr)₄ alcohol solution were stirred at RT till full hydrolysis of titanium precursor. The resulting solid phase was impregnated with Pt(acac)₂, AgNO₃ and previously formed Au sol and then annealed at 300 °C for 24 h. The composition and microstructure of the samples were characterized by EDX, XRD, HRTEM and single-point BET methods. The surface sites were investigated using thermal analysis, FTIR and XPS. The sensor measurements were carried out in the temperature range 50–300 °C in the flow cell shielded from the background light. DC measurements were carried out to monitor the electrical conductance of the sample during exposure to HCOH/air gas mixtures (0.06–0.6 ppm HCOH in dry air) in dark conditions and under constant and periodic lighting. Miniature LEDs with λ_{max} = 365 nm (UV),

$\lambda_{\max} = 470$ nm (blue), $\lambda_{\max} = 535$ nm (green) and $\lambda_{\max} = 630$ nm (red) inserted into the cell were used as illumination sources.

3. Results

Figure 1a shows the change in the samples resistance at periodic changing the composition of the gas phase: “dry air–0.6 ppm HCHO in dry air”, in the temperature range 300–50 °C in dark conditions. From the obtained data the values of the sensor response S were calculated as $S = R_{\text{air}}/R_{\text{gas}}$, where R_{air} and R_{gas} are the values of the nanocomposite resistance in pure air and in the presence of HCHO, respectively (Figure 1b). The best sensor response in dark conditions was obtained for Au@SnO₂/TiO₂ sample at 100 °C. The constant illumination of the samples during the measurements at 100 °C leads to a decrease in the sensor response (Figure 1c), and this decrease in the signal value grows with increasing radiation energy from red to UV light. However, the use of periodic illumination (Figure 1d) makes it possible to obtain the dependences of photoconductivity on the concentration of HCHO for their further description using a mathematical signal processing algorithm. Such a replacement of the dynamic temperature regime with periodic illumination will allow the quantitative determination of HCHO in gas mixtures with a significant reduction in energy consumption.

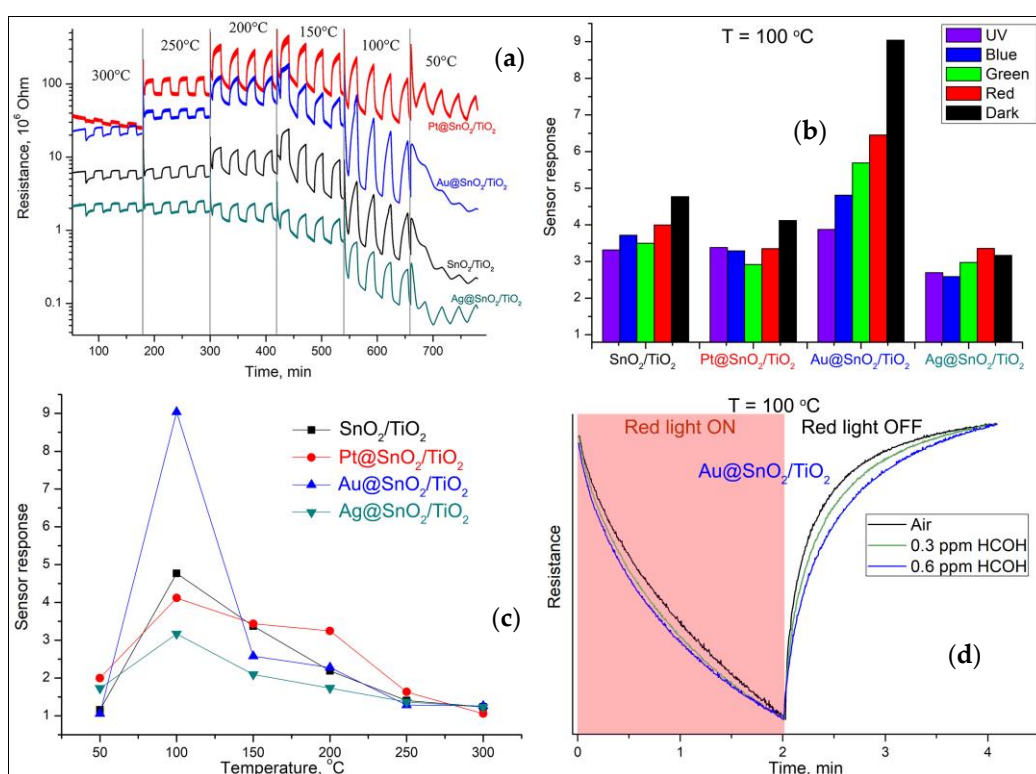


Figure 1. (a) Change in the samples resistance at periodic changing the composition of the gas phase; (b) Temperature dependences of sensor response to 0.6 ppm HCHO in dark conditions; (c) Influence of constant illumination on sensor response to 0.6 ppm HCHO at 100°C; (d) Change in the resistance of Au@SnO₂/TiO₂ nanocomposites at 100°C during one “Light ON/OFF” cycle in dry air containing 0, 0.3 or 0.6 ppm HCHO.

Funding: This research was funded by the Russian Ministry of Education and Sciences (Agreement No. 14.613.21.0075, RFMEFI61317X0075).

Conflicts of Interest: The authors declare no conflict of interest. The funders had no role in the design of the study; in the collection, analyses, or interpretation of data; in the writing of the manuscript, and in the decision to publish the results.



© 2019 by the authors. Licensee MDPI, Basel, Switzerland. This article is an open access article distributed under the terms and conditions of the Creative Commons Attribution (CC BY) license (<http://creativecommons.org/licenses/by/4.0/>).

High Temperature Resistive Gas Sensors Based on ZnO/SiC Nanocomposites [†]

Vadim Platonov ¹, Marina Rumyantseva ^{1,2}, Alexander Gaskov ^{1,2,*}

¹ Chemistry Department, Moscow State University, 1-3 Leninskie gory, Moscow 119991, Russia; agnes1992@yandex.ru (V.P.); roum@inorg.chem.msu.ru (M.R.)

² Saint Petersburg State University, Institute of Chemistry, 7/9 Universitetskaya nab., Saint Petersburg 199034, Russia

* Correspondence: gaskov@inorg.chem.msu.ru

[†] Presented at the 8th GOSPEL Workshop. Gas Sensors Based on Semiconducting Metal Oxides: Basic Understanding & Application Fields, Ferrara, Italy, 20–21 June 2019.

1. Introduction

The work is aimed at creating ZnO/SiC composites for resistive type gas sensors towards main components of exhaust gases CO and NH₃ in temperature range 400–550 °C. The highly dispersed silicon carbide SiC was used to enhance the stability of nanostructured ZnO at high temperature. In this work we prepared the ZnO/SiC nanocomposite materials by mixing and heat treatment of electrospun ZnO nanofibers and nanocrystalline silicon carbide of 3C-SiC polytype.

2. Materials Synthesis

Nanocrystalline SiC and ZnO were prepared separately by electrospinning of polymer solutions followed by heat treatment to polymer removing and materials crystallization. For SiC fabrication the solution of polycarbosilane (PCS) and polyvinylpyrrolidone (PVP, M = 1,300,000) in chloroform was used as a precursor. The electrospinning was carried out at the conditions of 3 mL/h solution feed rate, with 150 mm distance and 6 kV voltage between the needle and metal collector. The 3C-SiC nanofibers of a cubic structure were obtained from amorphous SiC using the spark plasma sintering method (SPS) on a Spark Plasma Sintering System LABOX-625 at a temperature of 1600 °C for 1 h under vacuum. For ZnO fabrication the zinc acetate (Zn(CH₃COO)₂ · 2H₂O) was used as a precursor. The electrospinning of polymer solution was carried out at the conditions of 1 mL/h solution feed rate, with 125 mm distance and 12 kV voltage between the needle and metal collector. The fibrous material was heated at 550 °C (5 h) in air.

3. Material Characterizations

The effect of silicon carbide on the structure and electrical properties of composite materials was studied using different techniques: SEM-EDX, XRD, XPS, FTIR. The FTIR absorption spectra of ZnO/SiC nanocomposites contain intense peaks with absorption maxima at 900 cm⁻¹ and 1067 cm⁻¹, corresponding to the stretching vibrations of the Si–C and Si–O bonds. This indicates the formation of amorphous SiO₂ shell on the surface of SiC nanoparticles, which does not appear on the diffraction patterns. XPS spectra reveal interactions between SiC and ZnO nanoparticles. The formation of silicon oxide was observed in the photoelectron spectrum in the O1s region, containing two components at 532.9 (O1) and 536 (O2) eV and Si2p region contains three components at 100.6 (Si1), 103.0 (Si2), 106.3 (Si3) eV. The formation of nanocomposites is accompanied by a significant increase in the electrical resistance of the material in comparison with ZnO nanofibres.

4. Sensor Measurements

The ZnO/SiC nanocomposites containing 0, 15, 30, 45 and 100 mol% SiC were prepared by mixing components in a single homogeneous paste with using a solution of α -terpineol in ethanol as a binder. The sensors were fabricated by thick films technology via drop-deposition of the paste onto alumina microhotplates provided with vapor-deposited Pt contacts (0.3×0.2 mm) separated by 0.2 mm gap and with embedded Pt-meanders. The paste was dried at room temperature in ambient air and then calcined at 250 °C in purified air for 20 h to remove the binder. Sensor properties (Figure 1) were investigated as resistance response towards 20 ppm NH_3 (a,b) and 20 ppm CO (c,d) in dry air (a,c) and at relative humidity $\text{RH}_{25} = 30\%$ (b,d). In both cases, the formation of ZnO/SiC nanocomposites leads to an increase in the sensor response compared to the bare ZnO nanofibres. Nanocomposites containing 15 and 30 mol% SiC demonstrate the highest values of the sensor response. A further increase in the SiC content leads to an increase in resistance and a decrease in the sensor response of the nanocomposites.

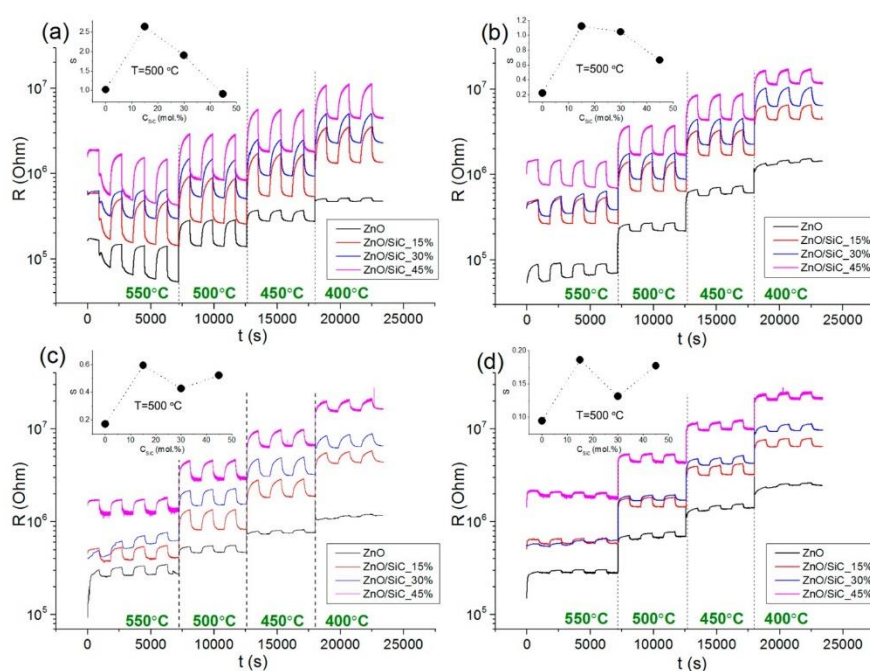


Figure 1. Change in the resistance of ZnO/SiC nanocomposites to 20 ppm NH_3 (a,b) and 20 ppm CO (c,d) in dry air (a,c) and at relative humidity $\text{RH}_{25} = 30\%$ (b,d).

5. Conclusions

ZnO/SiC nanocomposites based on ZnO nanofibers (wurtzite) and nanocrystalline SiC (3C polytype), obtained by the electrospinning method, were investigated as sensitive materials for high-temperature gas sensors of the resistive type. The introduction of SiC results in the magnification in the sensitivity of zinc oxide nanofibers towards reducing gases CO and NH_3 in the temperature range of 400–550 °C. This effect is accompanied by the increase in the activation energy of conductivity in this temperature range. The results obtained are interpreted in the context of the assumption of the formation of an n - n heterojunction at the ZnO/SiC interface, resulting in the electrons transfer from SiC to ZnO. Growth in the concentration of electrons in the near-surface layer of ZnO leads to an increase in the concentration of chemisorbed oxygen on its surface, which is confirmed by XPS. In turn, this determines an increase in the activation energy of conductivity and causes a magnification in the sensor response of ZnO/SiC nanocomposites compared with ZnO nanofibres.

Funding: The work was financially supported by RFBR grant No. 18-03-00091 and in part by a grant from the St. Petersburg State University—Event 3-2018 (id: 26520408)

Conflicts of Interest: The authors declare no conflict of interest. The funders had no role in the design of the study; in the collection, analyses, or interpretation of data; in the writing of the manuscript, and in the decision to publish the results.



© 2019 by the authors. Licensee MDPI, Basel, Switzerland. This article is an open access article distributed under the terms and conditions of the Creative Commons Attribution (CC BY) license (<http://creativecommons.org/licenses/by/4.0/>).

Elaboration and Characterization of SnS Thin Film for Gas Sensors Application [†]

Youssef Nouri ^{1,*}, Bouchaib Hartiti ¹, Abdelkrim Batan ^{1,2}, François Reniers ³,
Claudine Buess-Herman ³, Tiriana Segato ⁴, Salah Fadili ¹, Maryam Siadat ⁵
and Philippe Thévenin ⁵

¹ MEEM & DD Group, Hassan II University of Casablanca, FSTM BP 146 Mohammedia 20650, Morocco.;
bhartiti@gmail.com (B.H.); kbaatan@gmail.com (A.B.)

² FST Errachidia, Equipe Sciences des Matériaux, University Moulay Ismail, BP 509 Boutalamine 52000
Errachidia, Morocco

³ Analytical and Interfacial Chemistry, Faculty of Sciences, Université Libre de Bruxelles, CP255, Bd
Triomphe, B-1050 Brussels, Belgium; *Francois.Reniers@ulb.ac.be* (F.R.); *cbuess@ulb.ac.be* (C.B.-H.)

⁴ Materials engineering, characterization, synthesis and recycling, Ecole polytechnique de Bruxelles,
Université Libre de Bruxelles, Campus du Solbosch, CP 165/63, avenue F.D. Roosevelt 50, 1050 Bruxelles,
Belgium; *Tiriana.Segato@ulb.ac.be* (T.S)

⁵ LCOMS Laboratory, University of Lorraine, 57000 Metz, France;
philippe.thevvepnin@univ-lorraine.fr (P.T.)

* Correspondence: *nouriysf01@gmail.com*; Tel: +212 6 556 599 06

[†] Presented at the 8th GOSPEL Workshop. Gas Sensors Based on Semiconducting Metal Oxides:
Basic Understanding & Application Fields, Ferrara, Italy, 20–21 June 2019.

The tin sulfide (SnS) has p-type conductivity, high absorption coefficient ($\geq 10^4 \text{ cm}^{-1}$), band gap energy in the range of 1.1–1.7 eV and crystallized on the cubic and orthorhombic phase [1]. The semiconductor SnS thin film is used for gas sensor and photovoltaic applications [2,3]. SnS-based layers are promising candidates for gas sensor applications compared to other layered materials such as graphene and phosphorene. For example, SnS thin film performance in chemical sensors for the detection of acetone and ethanol shows: a response of (~190%) with a fast response time of (2 s) and a recovery time of (9 s) for acetone, and a response (~130%), with a fast response time (2 s) and a recovery time (9 seconds) for ethanol, the concentration used is 10 ppm respectively [2]. The present work describes the preparation and characterization of thin films of tin (II) sulfide (SnS) by the chemical spray pyrolysis method for gas sensors applications. The layers obtained were characterized by X-ray photoelectron spectra (XPS), XPS analysis shows the existence of the constituent elements of SnS. And X-ray diffraction (XRD) that revealed the appearance of the orthorhombic phase of tin sulfide Fig.1, this phase was confirmed by vibratory modes measured by Raman spectroscopy. The optical properties such as optical conductivity, refractive-reflectivity index, extinction coefficient, and band gap energy were determined using the absorbance and transmittance data, determined by the UV-visible spectrophotometer.

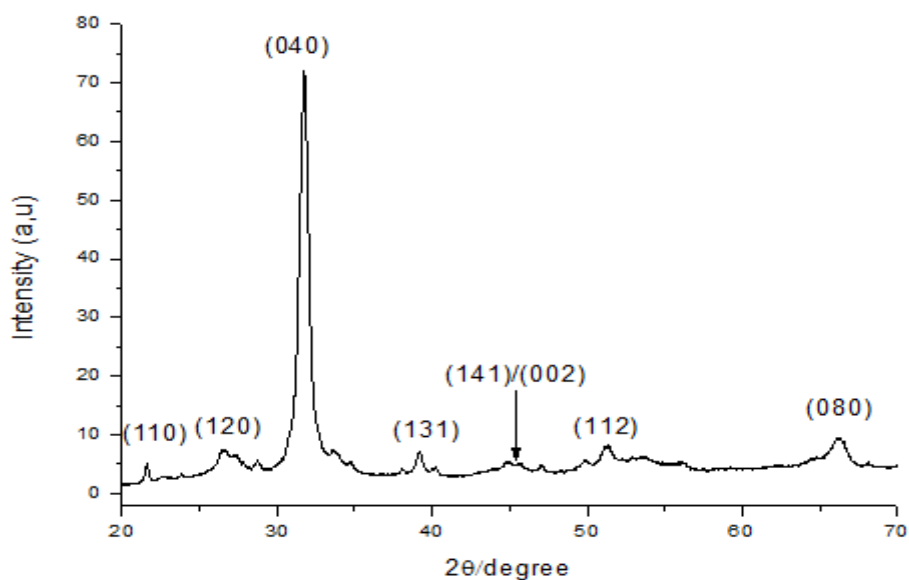


Figure 1. X-Ray diffraction patterns of SnS thin films deposited at various substrate temperatures.

Keywords: SnS; Spray pyrolysis; thin films; gas sensors; response time

Funding: This research received no external funding.

Conflicts of Interest: The authors declare no conflict of interest.

References

11. Nair, P.K.; Garcia-Angelmo, A.R.; Nair, M.T.S. Cubic and orthorhombic SnS thin-film absorbers for tin sulfide solar cells. *Phys. status solidi* **2016**, *213*, 170–177.
12. Afsar, M.F.; Rafiq, M.A.; Tok, A.I.Y. Two-dimensional SnS nanoflakes: synthesis and application to acetone and alcohol sensors. *RSC Adv.* **2017**, *7*, 21556–21566.
13. Di Mare, S.; Menossi, D.; Salavei, A.; Artegiani, E.; Piccinelli, F.; Kumar, A.; Mariotto, G.; Romeo, A. SnS Thin Film Solar Cells: Perspectives and Limitations. *Coatings* **2017**, *7*, 34.
14. Hu, F.; Tan, C.; Ye, H.; Chen, X.; Zhang, G. SnS monolayer as gas sensors: Insights from a first-principles investigation. In Proceedings of 2017 18th International Conference on Thermal, Mechanical and Multi-Physics Simulation and Experiments in Microelectronics and Microsystems (EuroSimE), Dresden, Germany, 3–5 April 2017. DOI: 10.1109/EuroSimE.2017.7926281.



© 2019 by the authors. Licensee MDPI, Basel, Switzerland. This article is an open access article distributed under the terms and conditions of the Creative Commons Attribution (CC BY) license (<http://creativecommons.org/licenses/by/4.0/>).

Elaboration and Characterization of CuO Thin Films by Spray Pyrolysis Method for Gas Sensors Applications

Maha HINNA ^{1,*}, Bouchaib HARTITI ¹, Abdelkrim BATAN ^{1,2}, François RENIERS ³, Claudine BUESS-HERMAN ³, Tiriana SEGATO ⁴, Naoual BELOUAGGADIA ¹, Salah FADILI ¹, Maryam SIADAT ⁵ and Philippe THÉVENIN ⁶

¹ MEEM & DD Group, Hassan II University of Casablanca, FSTM 28800 Mohammedia, Morocco; bhartiti@gmail.com (B.H.); kbatan@gmail.com (A.B.); n.belouaggadia@gmail.com (N.B.); safadili@yahoo.fr (S.F.)

² Materials Science Team, Department of Chemistry, Faculty of Sciences and Techniques Errachidia, University Moulay Ismail, Postcode Errachidia, Morocco.

³ Analytical and Interfacial Chemistry, Department of Chemistry, Faculty of Sciences, Free University of Brussels, 1050 Brussels, Belgium; Francois.Reniers@ulb.ac.be (F.R.); Claudine.Buess-Herman@ulb.ac.be (C. B.-H.)

⁴ 4MAT Laboratory, Polytechnic School of Brussels, Free University of Brussels, 1050 Brussels, Belgium; Tiriana.Segato@ulb.ac.be (T.S.)

⁵ LCOMS Laboratory, Department of physics, University of Lorraine, 57000 Metz, France; maryam.siadat@univ-lorraine.fr

⁶ LMOPS Laboratory, Department of physics, University of Lorraine, 57000 Metz, France; philippe.thevenin@univ-lorraine.fr

* Correspondence: maha.hinna@gmail.com; Tel: +21-266-005-0071

† Presented at the 8th GOSPEL Workshop. Gas Sensors Based on Semiconducting Metal Oxides: Basic Understanding & Application Fields, Ferrara, Italy, 20–21 June 2019.

Abstract: Metal oxide semiconductor gas sensors are used in a various applications in environmental, industrial and medical field, for instance. They are relatively inexpensive compared to other sensing technologies, robust, lightweight, long lasting and benefit from high material sensitivity and quick response times [1]. Copper oxide (CuO) thin film has been promisingly proposed for chemical sensing applications. Particularly, it has been recommended as a sensitive layer for monitoring harmful and combustible gases [1–3]. It is an attractive material because of nontoxic, inexpensive, abundance advantages, and its fabrication is easy. In this work, we have synthesized CuO thin films by Spray pyrolysis method. The effect of the temperature deposition is investigated: to say 350, 400, and 450 °C while the deposition duration was kipped to 15 min. The samples were analyzed by X-ray diffraction, Raman spectroscopy, XPS analysis, UV-visible transmission and four points probe method.

Keywords: CuO; Spray Pyrolysis; Deposition Temperature effect; Gas Sensors

1. Experimental

The solution for CuO was prepared by dissolving copper chloride (II) (CuCl₂) in distilled water; the solution has been stirred at 60 °C during 30 min. The ordinary glass substrates were cleaned with diluting nitric acid, acetone, ethanol, and distilled water. Spray pyrolysis was employed to deposit the CuO solution on the ordinary glass substrates, during 15 min at different temperatures including 350, 400, and 450 °C. The prepared films were analyzed using an X-ray diffractometer, spectroscopy Raman, XPS analysis, UV-visible spectrometer and 4-point probe method to the calculated sheet resistance and resistivity.

2. Characterization

The crystalline phase of the films was characterized by X-Ray diffraction DRX. In the Figure 1 we have the X-Ray diffraction spectrum of copper oxide (CuO) at various substrate temperatures deposition. In the other side, we have Raman spectrum of CuO whose mentions the Ag(1), Bg(1), and Bg(2) modes located at 290, 338, and 626 (Figure 2). The Raman spectroscopy confirms the CuO phase formation proved by DRX data.

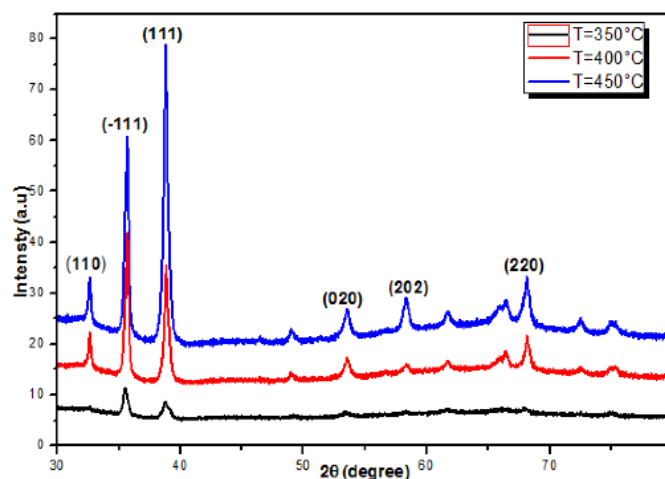


Figure 1. X-Ray diffraction patterns of CuO thin films deposited at various substrate temperatures.

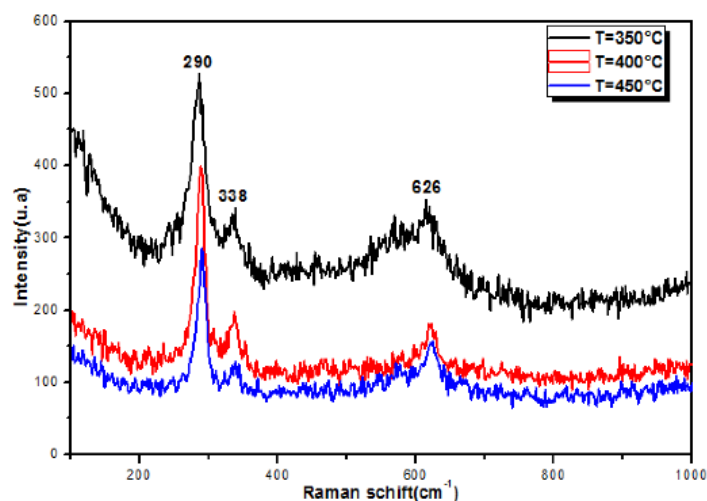


Figure 2. Spectra of CuO thin films deposited at 350 °C, 400 °C and 450 °C.

3. Conclusions

The X-ray diffraction peaks at (110), (-111), (-202), (020), (-113) and (220) planes indicate the formation of CuO thin films. Raman scattering measurements confirm the existence of CuO by peaks at 290, 338 and 626 cm⁻¹. XPS analysis also shows peaks indicating the presence of copper and oxygen. Band gap has been calculated according to the transmission measurements. We observe that the gap decreases while the substrate deposition temperature increases, and in contrary, the sheet resistance of these films increases when the substrate deposition temperature increases. These results make CuO thin films elaborated using spray pyrolysis set up, favourable for gas sensors applications.

Acknowledgments: This research is performed with the support of the Franco-Moroccan PHC Toubkal program.

Conflicts of Interest: The authors declare no conflict of interest.

References

1. Dhas, C.R.; Alexander, D.; Christy, A.J.; Jeyadheepan, K.; Raj, A.M.E.; Raja, C.S. Preparation and Characterization of CuO Thin Films Prepared by Spray Pyrolysis Technique for Ethanol Gas Sensing Application. *Asian J. Appl. Sci.* **2014**, *7*, 671–684.
2. Kim, S.J.; Anwar, M.S.; Heo, S.N.; Koo, B.H. Effect of Zinc Nitrate Concentration on the Optical and Morphological Properties of ZnO Nanorods for Photovoltaic Applications. *J. Nanosci. Nanotechnol.* **2016**, *16*, 6119–6123.
3. Gopalakrishna, D.; Vijayalakshmi, K.; Ravidhas, C. Effect of pyrolytic temperature on the properties of nano-structured CuO optimized for ethanol sensing applications. *J.Mater. Sci. Mater. Electron.* **2013**, *24*, 1004–1011.



© 2019 by the authors. Licensee MDPI, Basel, Switzerland. This article is an open access article distributed under the terms and conditions of the Creative Commons Attribution (CC BY) license (<http://creativecommons.org/licenses/by/4.0/>).

Work Function Measurements in Single-Crystalline In₂O₃ for Conduction Modelling †

Federico Schipani ¹, Alexandru Oprea ¹, Udo Weimar ¹, Alexandra Papadogianni ²,
Oliver Bierwagen ² and Nicolae Barsan ^{1,*}

¹ Institute of Physical Chemistry, University of Tübingen, Auf der Morgenstelle 15, 72076 Tübingen, Germany; federico.schipani@ipc.uni-tuebingen.de (F.S.); alexandru.oprea@ipc.uni-tuebingen.de (A.O.); upw@ipc.uni-tuebingen.de (U.W.)

² Paul-Drude-Institute für Festkörperelektronik, Leibniz-Institut im Forschungsverbund Berlin e.V., Hausvogteiplatz 5–7, 10117 Berlin, Germany; papadogianni@pdi-berlin.de (A.P.); bierwagen@pdi-berlin.de (O.B.)

* Correspondence: nb@ipc.uni-tuebingen.de

† Presented at the 8th GOSPEL Workshop. Gas Sensors Based on Semiconducting Metal Oxides: Basic Understanding & Application Fields, Ferrara, Italy, 20–21 June 2019.

To date, there are only a few studies on the gas sensing properties of single crystalline sensors. The preferred study of polycrystalline materials is mainly due to the considerably larger sensor signals, which are caused by the presence of grain boundaries [1]. However, the high quality and controlled growth of single-crystalline materials has the promise to help the fundamental understanding of sensing: the electrical measurements of crystals under in-operando temperatures and different gas atmospheres are an avenue for directly extracting fundamental electronic behaviour of each material that is essential for building an accurate model of sensor behaviour. Due to the recent advance in the development of in-operando investigation methods, it seems now possible to combine them with controlled single crystalline model sample.

Indium oxide is a wide-bandgap semiconducting material with a direct bandgap of around 2.8–2.9 eV. It has been extensively used as a transparent conductive oxide (TCO) in electronics, for photovoltaic devices, light emitting diodes and chemical sensors [3,6]. Nevertheless, the knowledge about sensing with In₂O₃ based devices is still insufficient.

Here, we present results of investigations performed on an approximately 440 nm thick crystalline In₂O₃ film grown by plasma-assisted molecular beam epitaxy (PA-MBE) on a YSZ substrate. Combined DC resistance and work function change measurements performed at an operation temperature of 300 °C in various atmospheres were used in order to obtain information about the conduction mechanisms and electronic properties of the material in the same manner that was previously employed for the study of polycrystalline samples [2].

The work function and resistance changes are measured with the Kelvin Probe technique, which is a non-contact, non-destructive method that uses a vibrating reference electrode and measures the changes of the contact potential difference (CPD) between the sample and the electrode. Variations in the CPD induced by changes in the gas atmosphere represent relative work function variations of the sample [2]. The work function in a semiconductor can be expressed by

$$\varphi = \chi + (E_c - E_f) + V_s, \quad (1)$$

where V_s is the surface band bending, χ represents the electron affinity, which we assume constant when no humidity is present, and $(E_c - E_f)$ is the difference between the conduction band in the bulk and the Fermi level.

In Figure 1 the dependence of the sample conductance on work function changes is presented. Experimental results will be interpreted using two approaches. First, all changes will be attributed to V_s (surface processes), meaning that no bulk electron concentration changes are allowed in the model.

Next, all changes will be attributed to bulk-related processes, where only the bulk electron concentration changes ($E_C - E_F$) and no band bending at the surface is present.

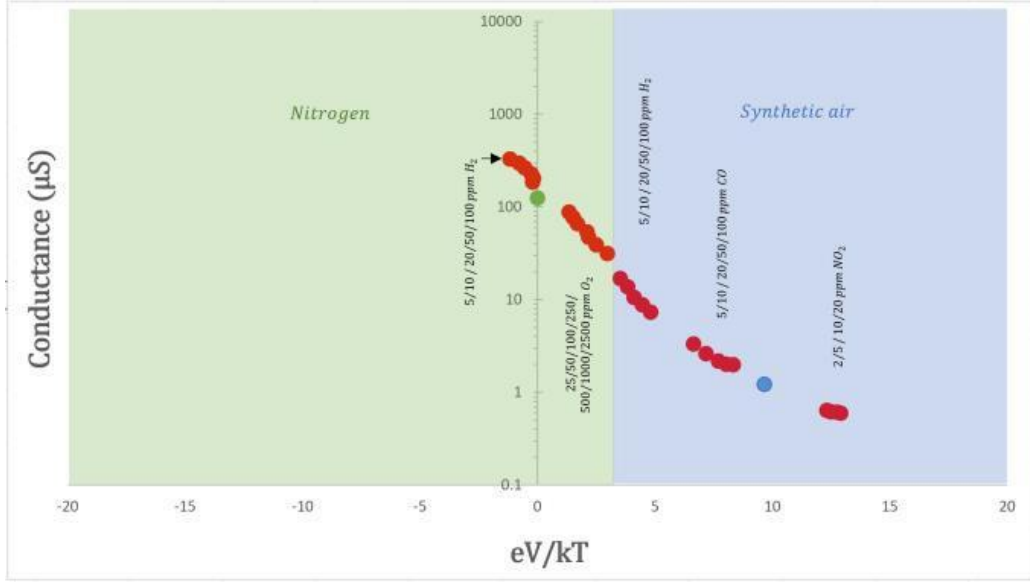


Figure 1. Conductivity against relative work function changes measured at 300 °C with no humidity present. The ϕ measured in nitrogen is taken as the flat band condition. The green and blue area represent the carrier gas present.

The total conductance of a compact layer is the sum of the part of the layer influenced by surface processes and the conductance of the layer that is left unchanged, the bulk.

$$G_{total} = G_s + G_b = \frac{e\mu W}{L} [Z_0 n_s + (D - Z_0) n_b] \quad (2)$$

In Equation (2), L is the length of the layer, W its width, D its thickness and Z_0 the thickness of the surface layer and μ the mobility.

Room temperature experiments indicate that a large downwards band bending is present, which is causing the appearance of a surface electron accumulation layer (SEAL) [4] that cannot be described using Boltzmann statistic. For that reason, a numerical conduction model using Fermi-Dirac statistics, which are valid for all electron densities, has been developed. This was solved with an iterative process to find equilibrium concentration of electrons in the bulk (n_b) and surface properties such as band bending and surface density of electrons (n_s). The fitting parameters (fitting not shown here) would imply a bulk electron concentration of $n_b = 5.6 \times 10^{19} \text{ m}^{-3}$, which would be very low and not realistic.

On the other hand, if we apply a flat band approach, where all changes in conductivity and work function are due to variations of ($E_C - E_F$), the results also cannot be fully explained. From the experimentally measured conductance in pure nitrogen and pure synthetic air (green and blue points in Figure 1), the bulk electron concentration found is $n_b = 4.7 \times 10^{23} \text{ m}^{-3}$ and $n_b = 4.7 \times 10^{21} \text{ m}^{-3}$ respectively. From this, the difference between the Fermi Level and the conduction band can be estimated, using the effective density of states $N_C = 5.9 \times 10^{24} \text{ m}^{-3}$ and Equation (3):

$$(E_C - E_F) = \left(\frac{k_B T}{e}\right) \ln\left[\frac{N_C}{n_b}\right] \quad (3)$$

Here, this difference is $(E_C - E_F) = 0.125$ eV in pure nitrogen and $(E_C - E_F) = 0.350$ eV in synthetic air. These results indicate that the experimental changes in conductance (a factor 100 from nitrogen to synthetic air) and work function differences (approximately 0.5 eV) are neither purely due to bulk changes nor purely surface dominated and implies that the atmosphere changes affect both bulk and surface electron concentration.

Acknowledgments: The work of F. Schipani was supported by a Georg Forster Fellowship from the Alexander von Humboldt Foundation.

References

1. Barsan, N.; Weimar, U. Conduction model of metal oxide gas sensors. *J. Electroceram.* **2001**, *7*, 143–167.
2. Prea, A.; Bârsan, N.; Weimar, U. Work function changes in gas sensitive materials: Fundamentals and applications. *Sens. Actuators B Chem.* **2009**, *142*, 470–493.
3. Zhang, D.; Liu, Z.; Li, C.; Tang, T.; Liu, X.; Han, S.; Zhou, C. Detection of NO₂ down to ppb levels using individual and multiple In₂O₃ nanowire devices. *Nano Lett.* **2004**, *4*, 1919–1924.
4. Rombach, J.; Papadogianni, A.; Mischo, M.; Cimalla, V.; Kirste, L.; Ambacher, O.; Bierwagen, O. The role of surface electron accumulation and bulk doping for gas-sensing explored with single-crystalline In₂O₃ thin films. *Sens. Actuators B Chem.* **2016**, *236*, 909–916.
5. Barsan, N.; Koziej, D.; Weimar, U. Metal oxide-based gas sensor research: How to? *Sens. Actuators B Chem.* **2007**, *12*, 18–35.
6. Roso, S.; Degler, D.; Llobet, E.; Barsan, N.; Urakawa, A. Temperature-dependent NO₂ sensing mechanisms over indium oxide. *ACS Sens.* **2017**, *2*, 1272–1277.



© 2019 by the authors. Licensee MDPI, Basel, Switzerland. This article is an open access article distributed under the terms and conditions of the Creative Commons Attribution (CC BY) license (<http://creativecommons.org/licenses/by/4.0/>).

Extended Abstract

Investigation of the Film Thickness Influence on the Sensor Response of In₂O₃-Based Sensors for O₃ Detection at Low Temperature and Operando DRIFT Study †

Daniele Ziegler ^{1,*}, Paola Palmero ¹, Jean-Marc Tulliani ¹, Anna Staerz ², Alexandru Oprea ², Udo Weimar ² and Nicolae Barsan ²

¹ Politecnico di Torino, Department of Applied Science and Technology, INSTM R.U PoliTO-LINCE Laboratory, Corso Duca degli Abruzzi, 24, 10129 Torino, Italy; paola.palmero@polito.it (P.P.); jeanmarc.tulliani@polito.it (J.-M.T.)

² Institute of Physical and Theoretical Chemistry (IPTC), University of Tuebingen, Auf der Morgenstelle 15, D-72076 Tuebingen, Germany; anna.staerz@ipc.uni-tuebingen.de (A.S.); alexandru.oprea@ipc.uni-tuebingen.de (A.O.); upw@ipc.uni-tuebingen.de (U.W.); nb@ipc.uni-tuebingen.de (N.B.)

* Correspondence: daniele.ziegler@polito.it

† Presented at the 8th GOSPEL Workshop. Gas Sensors Based on Semiconducting Metal Oxides: Basic Understanding & Application Fields, Ferrara, Italy, 20–21 June 2019.

Industrial pollution and traffic emissions emit dangerous amounts of O₃, NO₂, VOCs and PM into environment, bringing higher incidence of morbidity and mortality in respiratory sicknesses [1]. Among tropospheric pollutant species, monitoring the O₃ concentration is remarkably important for its toxicity. The aftereffects of O₃ exposure indeed are upper respiratory irritation, rhinitis, cough, headache, occasional nausea, and vomiting [2]. In 2015, the United States Environmental Protection Agency (EPA), reinforced the National Ambient Air Quality Standards (NAAQS) for O₃ at ground-level not to exceed 70 ppb to improve the protection of human health [3].

This work presents n-type In₂O₃ as sensitive material to detect O₃ between 0.1 and 1 ppm at low temperatures (75 °C–150 °C). In₂O₃ powders were synthesized by hydrothermal route [4], with the goal to achieve a finer crystallite size, higher specific surface area and lower degree of agglomeration compared to commercial In₂O₃ (Sigma Aldrich, St. Louis, MO, USA). Those characteristics are essential to enhance the sensor performances [5].

In the synthesis, In₂O₃ nanostructures were realized by hydrothermal method using indium nitrate as indium precursor, soda as mineralizer and CTAB as capping agent, according to previous literature [6]. The mixture was maintained for 24 h at 70 °C and then for 12 h at 120 °C. Subsequently, powders were calcined at 400 °C for 30 min obtaining In₂O₃ [4].

In₂O₃ powders were characterized by laser granulometry, Thermal Analysis, X-ray Diffraction, N₂ adsorption, Field Emission-Scanning Electron Microscopy and High-Resolution Transmission Electron Microscopy.

Sensors were fabricated by screen-printing technique onto α -alumina substrates with Pt electrodes and a backside Pt heater. Inks for screen-printing were realized by mixing In₂O₃ powders with ethylene glycol monobutyl ether (Emflow), as organic vehicle and polyvinyl butyral (PVB) acting as temporary binder. After screen-printing deposition sensors were dried at 80 °C overnight and fired at 500 °C for 1 h in air. For obtaining different layer thicknesses in the range 10–100 μ m, the first layer was dried and then a new layer was printed onto it.

Films were characterized by Scanning Electron Microscopy, electrical measurements and *operando* diffuse reflectance infrared Fourier transform (DRIFT) spectroscopy.

Sensors were tested towards different amounts of O₃, NO₂ and H₂ under 0, 30% and 60% of RH (relative humidity) to study the selectivity of the as-realized chemical sensors for O₃ detection. Best results were achieved at 150 °C towards O₃, with the sensor selectivity for O₃ increasing by increasing the working temperature from 75 °C to 150 °C. Both oxidant gases (O₃ and NO₂) showed best performance at higher RH amounts, whereas for H₂ the trend was opposite, probably due to the competition between H₂ and H₂O for the same adsorption sites on the In₂O₃ surface. At 150 °C, under 1 ppm O₃, the variation of film resistance is 5 orders of magnitude, while it was only equal to 2 orders of magnitude under 1 ppm of NO₂. Under 30% RH, the influence of sensor thickness is much higher under O₃ compared to NO₂ and a logical trend was noticed in which by changing one order of magnitude the sensor thickness, the sensor response varies of more than 3 orders of magnitude under 1 ppm O₃. Under NO₂, only a small influence of the sensing film thickness on the sensor response was detected. Finally, the interference with H₂ is negligible as the sensor response towards H₂ is independent from the film thickness, as expected. Calibration curves of In₂O₃ sensor towards O₃, NO₂ and H₂ at 150 °C and 30% RH in the range 10–100 μm of thickness are displayed in Figure 1.

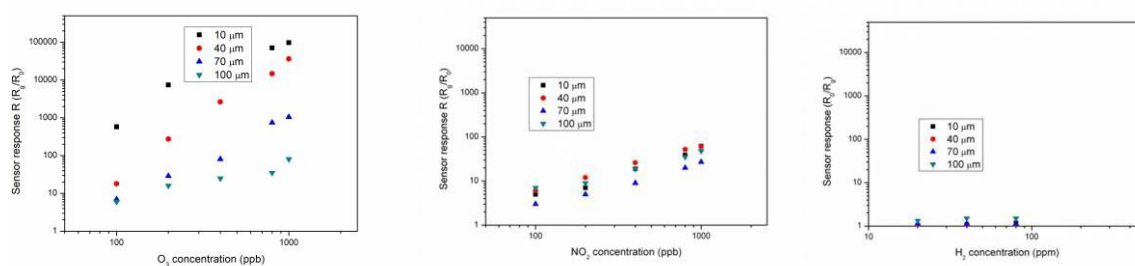


Figure 1. Comparison between 10, 40, 70 and 100 μm thick In₂O₃ sensor response towards O₃ (left), NO₂ (center) and H₂ (right) at 150 °C and 30% RH.

By DRIFTS, the aim is to clarify the interaction of NO₂ and O₃ with In₂O₃ surface establishing tightly the relationship between surface structure and adsorbed species with the gas sensing response.

Considering the NO₂-In₂O₃ interaction, the OH groups, most likely due to adsorbed water on the In₂O₃ surface, play a key role in the NO₂ adsorption. NO₂ withdraw more electrons from In₂O₃ in the presence of water forming nitrites and resulting in the measured increased in electrical resistance. This is confirmed by the higher increase in electrical resistance under humid atmospheres. OH groups are consumed when NO₂ is adsorbed onto the surface in the form of nitrites and in this process, H bonds are broken.

In the interaction of O₃ with In₂O₃ surface, signals related to peroxide formation during O₃ adsorption and decomposition were detected as well as peaks due to physisorbed O₃ still present at 150 °C. Furthermore, bands generated by carbonate-like species formed through reactions of O₃ with residual carbonaceous impurities from the synthesis route were recognized.

To conclude, in this work the role of the film thickness under O₃, NO₂ and H₂ exposure was studied for In₂O₃ sensor realized by screen printing technique. Finally, by operando DRIFT a complex sensing mechanism has been evidenced for In₂O₃ sensors, involving OH groups and adsorbed water in the mechanism of NO₂ adsorption and peroxide formation and O₃ physisorption during O₃ exposure.

References

1. Brunekreef, B.; Holgate, S.T. Air pollution and health. *Lancet* **2002**, *360*, 1233–1242, doi:10.106/S0140-6736(02)11274-8.
2. Gottschalk, C.; Libra, J.A.; Saupe, A. *Ozonation of Water and Waste Water—A Practical Guide to Understanding Ozone and Its Applications*; Wiley: Weinheim, Germany, 2000.
3. 2015 National Ambient Air Quality Standards (NAAQS) for Ozone. Available online: <https://www.epa.gov/ozone-pollution/2015-national-ambient-air-quality-standards-naaqs-ozone> (accessed on 7 April 2019).

4. Shinde, D.V.; Ahn, D.Y.; Jadhav, V.V.; Lee, D.Y.; Shrestha, N.K.; Lee, J.K.; Lee, H.Y.; Maneb, R.S.; Han, S.H. A coordination chemistry approach for shape controlled synthesis of indium oxide nanostructures and their photoelectrochemical properties. *J. Mater. Chem. A* **2014**, *2*, 5490–5498.
5. Korotcenkov, G.; Brinzari, V.; Cerneavschi, A.; Ivanov, M.; Golovanov, V.; Cornet, A.; Morante, J.; Cabot, A.; Arbiol, J. The influence of film structure on In_2O_3 gas response. *Thin Solid Films* **2004**, *460*, 315–323.
6. Yan, T.; Wang, X.; Long, J.; Liu, P.; Fu, X.; Zhang, G.; Fu, X. Urea-based hydrothermal growth, optical and photocatalytic properties of single-crystalline $\text{In}(\text{OH})_3$ nanocubes. *J. Colloid Interface Sci.* **2008**, *325*, 425–431.



© 2019 by the authors. Licensee MDPI, Basel, Switzerland. This article is an open access article distributed under the terms and conditions of the Creative Commons Attribution (CC BY) license (<http://creativecommons.org/licenses/by/4.0/>).

Gas Sensing with Porphyrin Functionalized Metal Oxide Nanostructures [†]

Gabriele Magna ¹, Mounika Muduganti ¹, Roberto Paolesse ² and Corrado Di Natale ^{1,*}

¹ Department of Electronic Engineering, University of Rome Tor Vergata, 00133 Rome, Italy; magna.gabriele@gmail.com (G.M.); mounika.nano@gmail.com (M.M.); dinatale@uniroma2.it (C.D.N.)

² Department of Chemical Science and Technology, University of Rome Tor Vergata, 00133 Rome, Italy; roberto.paolesse@uniroma2.it

* Correspondence: dinatale@uniroma2.it.

[†] Presented at the 8th GOSPEL Workshop. Gas Sensors Based on Semiconducting Metal Oxides: Basic Understanding & Application Fields, Ferrara, Italy, 20–21 June 2019.

In the last years we have been interested to study the interplay of light and gas sensitivity in hybrid materials formed by porphyrins grafted onto ZnO nanostructures. First results shown that the conductivity of the hybrid material is sensitive to the visible light and to donor-acceptor gases such as amines and alcohols [1]. Surface photovoltage studies of the sensing properties of these materials suggests that the adsorption of volatile compounds may modulate, either positively or negatively, the photovoltaic properties of the dye-semiconductor hybrid [2].

The standard procedure to functionalize ZnO surface requires the addition of a carboxylic group functionalized porphyrin to a solution where the ZnO nanostructure is dipped. However, most of the gas sensing properties depend on the surface arrangement of the porphyrin layer. Thus, changes in the molecular film formation procedure may result in different sensors. This feature prompts the development of alternative routes for the hybrid film formation. One-pot methods, where porphyrin is directly added to the ZnO synthesis solution have been introduced, thus in spite of the same components (ZnO and porphyrin) the materials show different morphology and different sensitivity [3].

Further evidence of the importance of the molecular film morphology was obtained with porphyrins coated ZnO nanoparticles spotted on quartz microbalances (QMBs). In this study, a minimal array formed by the same porphyrin deposited onto three surfaces was considered. The same porphyrin (Zinc tetraphenylporphyrin) was spotted on the bare gold pad of the QMB and on ZnO nanoparticles. The coating of nanoparticles was obtained functionalizing the nanoparticles and with the one-pot procedure. Results show that changes in surface arrangements are enough to distinguish different volatile compounds and to recognize complex samples such as the headspace of cell cultures and vegetable oils [4].

A more recent exploitation of porphyrins grafted onto metal oxide nanostructures has been obtained for the development of an enantioselective QMB sensor [5]. The choice of QMB not only enables simple and fast sensors preparation but, more importantly, the non-selectivity of the mass transduction allows to explore the totality of the interactions occurring between the volatile compounds and the sensor, offering the opportunity to put in evidence the importance of chiral selective interactions respect to all the others.

Enantioselectivity is the capability of a sensor to show different sensitivities respect to chiral pairs of the same molecule. One of the main difficulties in chiral gas sensors is to transfer the chirality from single receptors to the solid-state material forming the sensing layer.

The molecular grafting on nanostructured material is a viable route to circumvent this problem. This property has been exploited by preparing a nanostructured film where chiral molecules are arranged on the surface of ZnO particles. The system retains chirality features and offers an optimal accessibility to the volatile compounds. We considered the inherently chiral porphyrin derivative

where a (L)-proline unit imparts the chiral features to a porphyrin macrocycle. Hydrothermally grown ZnO nanoparticles were functionalized in toluene solution of ZnPL.

Figure 1 compares the response of sensors coated with chiral porphyrin and chiral porphyrin grafted onto nanoparticles. Sensors were exposed to the enantiomers of S- and R-limonene, both at concentration of 375 ppm in air. Figure 2 shows the sensor response as a function of concentration. The enantioselectivity is preserved in the whole investigated range of observation.

The sensing properties of layers of porphyrins onto ZnO nanostructures offer a further degree of freedom for the design of sensor arrays extending the properties and the capabilities of porphyrin based sensor array in particular for medical diagnosis, the quality and control of foods and the detection of compounds signaling harmful or dangerous substances.

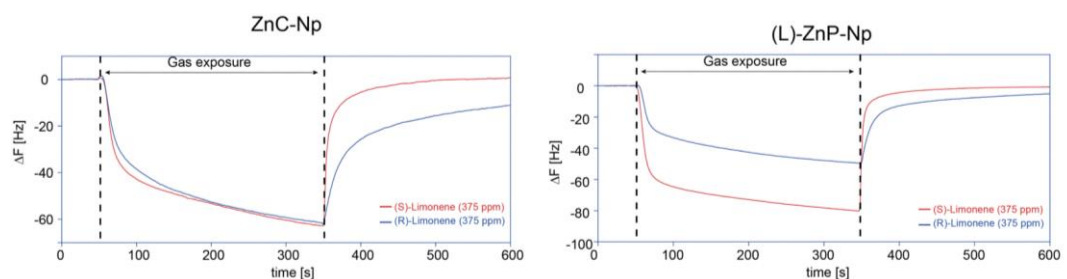


Figure 1. Time evolution of the sensor signal (change of QMB frequency) of chiral porphyrin on gold (left) and ZnO nanoparticles (right) exposed to the two enantiomers of limonene.

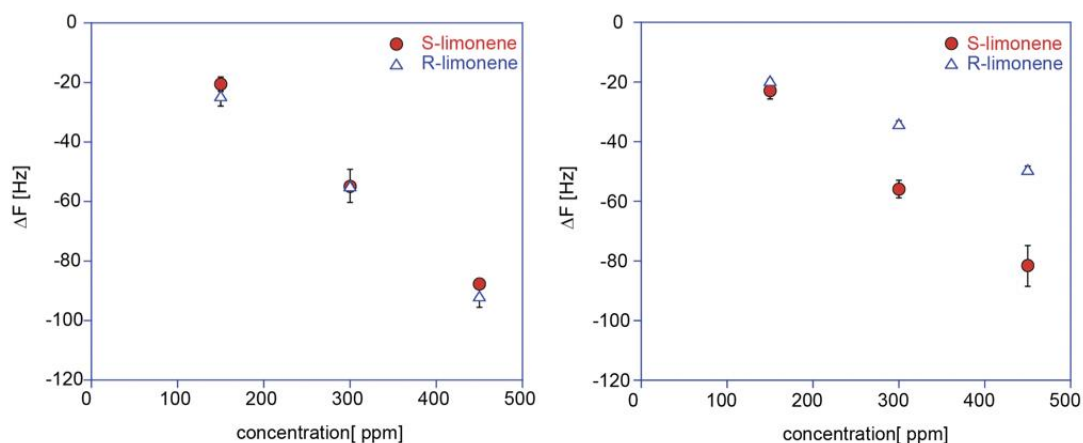


Figure 2. Response curve to limonene enantiomers of chiral porphyrin on gold (left) and ZnO nanoparticles (right).

References

1. Sivalingam, Y.; Martinelli, E.; Catini, A.; Magna, G.; Pomarico, G.; Basoli, F.; Paolesse, R.; Di Natale, C. Gas-Sensitive Photoconductivity of Porphyrin-Functionalized ZnO Nanorods. *J. Phys. Chem. C* **2012**, *116*, 9151–9157.
2. Sivalingam, Y.; Magna, G.; Pomarico, G.; Catini, A.; Martinelli, E.; Paolesse, R.; Di Natale, C. The influence of gas adsorption on photovoltage in porphyrin coated ZnO nanorods. *J. Mater. Chem.* **2012**, *22*, 20032–20037.
3. Magna, G.; Sivalingam, Y.; Martinelli, E.; Pomarico, G.; Basoli, F.; Paolesse, R.; Di Natale, C. The influence of film morphology and illumination conditions on the sensitivity of porphyrins-coated ZnO nanorods. *Anal. Chim. Acta* **2014**, *810*, 86–93.
4. Magna, G.; Zor, S.D.; Catini, A.; Capuano, R.; Basoli, F.; Martinelli, E.; Paolesse, R.; Di Natale, C. Surface arrangement dependent selectivity of porphyrins gas sensors. *Sens. Actuators B* **2017**, *251*, 524–532.

5. Stefanelli, M.; magna, G.; Zurlo, F.; Caso, F.; di Bartolomeo, E.; Antonaroli, S.; Venanzi, M.; Paolesse, R.; Di Natale, C.; Monti, D. Chiral Selectivity of Porphyrin–ZnO Nanoparticle Conjugates. *ACS Appl. Mater. Interfaces* **2019**, *11*, 12077–122087, doi:10.1021/acsami.8b22749.



© 2019 by the authors. Licensee MDPI, Basel, Switzerland. This article is an open access article distributed under the terms and conditions of the Creative Commons Attribution (CC BY) license (<http://creativecommons.org/licenses/by/4.0/>).

Synergistic Effect of Nanocrystalline SnO₂ Sensitization by Bimetallic Au and Pd Modification via Ingle Step Flame Spray Pyrolysis Technique [†]

Valeriy Krivetskiy ^{1,*}, Konstantin Zamanskiy ² and Alina Krotova ¹

¹ Department of Chemistry, M.V. Lomonosov Moscow State University, Leninskie Gory 1/3, Moscow 119234, Russia; alinakrotova1996@mail.ru

² Faculty of Materials Sciences, M.V. Lomonosov Moscow State University, Leninskie Gory 1/3, Moscow 119234, Russia; zambahrs97@gmail.com

* Correspondence: vkrivetsky@inorg.chem.msu.ru

[†] Presented at the 8th GOSPEL Workshop. Gas Sensors Based on Semiconducting Metal Oxides: Basic Understanding & Application Fields, Ferrara, Italy, 20–21 June 2019.

Abstract: Convenient and scalable single step flame spray pyrolysis (FSP) synthesis of bimetal AuPd sensitized nanocrystalline SnO₂ for gas sensor application is reported. The materials chemical composition, structure and morphology has been studied by XRD, XPS, HAADFSTEM, BET, ICP-MS techniques as well as thermo-programmed reduction with hydrogen (TPR-H₂). Superior gas sensor response of bimetal modified SnO₂ towards wide concentration range of reducing (CO, CH₄, C₃H₈, H₂S, NH₃) and oxidizing (NO₂) gases compared to pure and monometallic modified SnO₂ is reported. The observed enhanced gas sensor performance is concluded to arise from combination of facilitated oxygen molecule spillover on gold particles and electronic effect of Fermi level control by reoxidizing Pd-PdO clusters, homogeneously distributed over SnO₂ particles surface.

Keywords: metal oxide; semiconductor; gas sensor; sensitization; bimetal; flame spray pyrolysis

1. Introduction

The use of bimetallic nanoparticles (NPs) in order to sensitize semiconductor metal oxide gas sensors attracts more and more attention lately [1]. Particularly gold-containing NPs with Pt-group metals have been reported to provide profound improvements in certain gases detection [2–6]. Currently bimetallic NPs functionalized semiconductor metal oxides are obtained in a two step process: either separately prepared bimetallic nanoparticles or noble metal precursors with further reduction are being deposited on the previously synthesized metal oxide matrix. Such procedure is time and labor consuming and bears risks if introduction of impurities in the final nanocomposite or deviations of NPs content. In this work we report superior gas sensing properties towards a wide spectrum of gases of bimetal—Au and Pd—modified nanocrystalline SnO₂, obtained in single step via flame spray pyrolysis (FSP) technique.

2. Experimental

The design of custom made apparatus for materials synthesis, as well as synthesis protocol were based on the earlier reports of pioneering researchers [7]. Materials were characterized by XRD, ICP MS, XPS, STEM with EDX mapping, BET, TPR-H₂ techniques. Gas sensor performance was tested towards reducing and oxidizing gases in flow through sensor cell in DC mode.

3. Results

Parameters of synthesized samples are summarized in Table 1. XPS indicate presence of both Au and Pd on the surface of SnO₂ in a metallic state, however most part of Pd exists in the oxidized Pd²⁺ form. EDX mapping shows uniform homogeneous distribution of modifiers over the surface of bimetal modified sample. This nanocomposite demonstrates significantly higher response values towards both reducing and oxidizing gases compared to monometallic modified nanocomposites (Figure 1a–h).

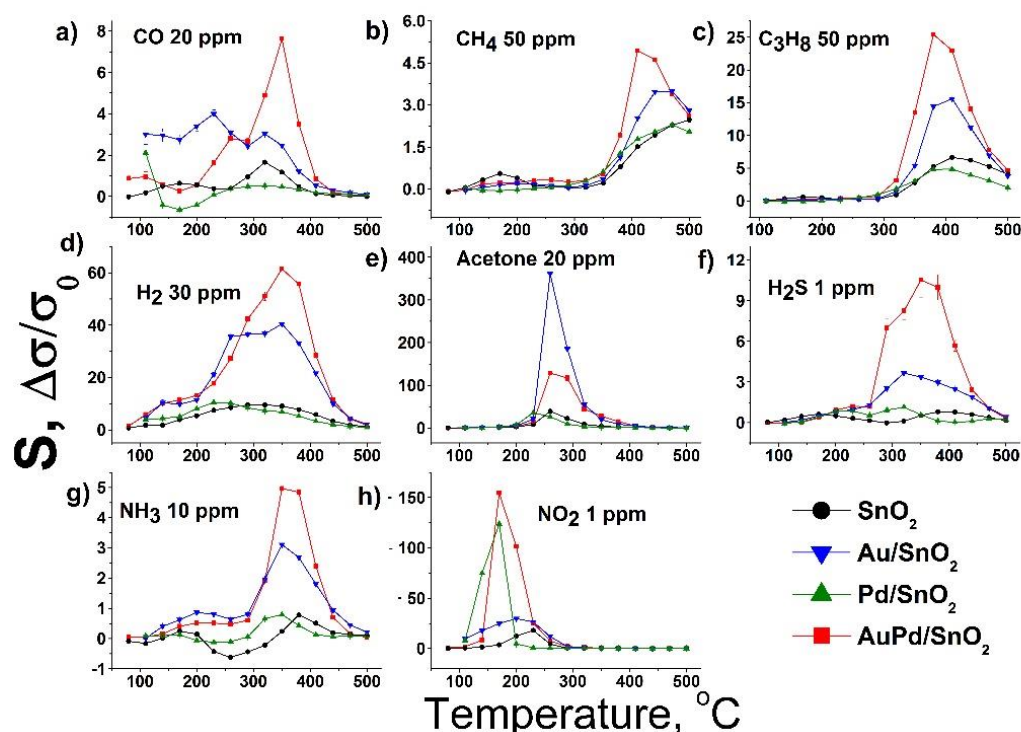


Figure 1. Dependence of gas sensor response of synthesized materials on sensor working temperature towards (a) CO 20 ppm, (b) CH₄ 50 ppm, (c) C₃H₈ 50 ppm, (d) H₂ 30 ppm, (e) acetone ppm, (f) H₂S 1 ppm, (g) NH₃ 10 ppm, (h) NH₃ 10 ppm in dry air.

Table 1. Parameters of synthesized nanocomposites.

Sample №	Sample Name	Au load		Pd Load %, mol	ICP MS, %mol		d, nm	S _{BET} , m ² /g
		%, mass	% mol		Au	Pd		
1	SnO ₂	--	--				14	52
2	Au/SnO ₂	0.4	0.31		0.29 ± 0.02		10	70
3	Pd/SnO ₂	--	--	0.31		0.29 ± 0.02	11	69
4	AuPd/SnO ₂	0.2	0.15	0.15	0.16 ± 0.01	0.15 ± 0.01	11	58

4. Conclusions

The homogeneous distribution of Au and Pd component over the structure of nanocrystalline SnO₂ based nanocomposites, achieved by flame spray pyrolysis synthesis technique, gives rise to a superior gas sensor performance of thus obtained material. The excellent gas sensor properties arise from synergistic combination of chemical catalytic effect of gold and electronic effect of Fermi level control by surface Pd clusters, prone to switch to PdO state in oxidizing conditions and back to Pd⁰ in the presence of reducing component. Besides being a highly effective in achieving of such synergistic effect, FSP is proven to be a convenient technique, which allows to obtain a bimetallic modification of SnO₂ with Au and Pd components in a single synthetic step with high level of content control.

Acknowledgments: The work was funded by Russian Science Foundation grant № 17-73-10491.

References

1. Kutukov, P.; Rummyantseva, M.; Krivetskiy, V.; Filatova, D.; Batuk, M.; Hadermann, J.; Khmelevsky, N.; Aksenenko, A.; Gaskov, A. Influence of Mono- and Bimetallic PtO_x, PdO_x, PtPdO_x Clusters on CO Sensing by SnO₂ Based Gas Sensors. *Nanomaterials* **2018**, *8*, 917, doi:10.3390/nano8110917.
2. Kim, S.; Park, S.; Park, S.; Lee, C. Acetone sensing of Au and Pd-decorated WO₃ nanorod sensors. *Sens. Actuators B Chem.* **2015**, *209*, 180–185, doi:10.1016/j.snb.2014.11.106.
3. Li, G.J.; Cheng, Z.X.; Xiang, Q.; Yan, L.M.; Wang, X.H.; Xu, J.Q. Bimetal PdAu decorated SnO₂ nanosheets based gas sensor with temperature-dependent dual selectivity for detecting formaldehyde and acetone. *Sens. Actuators B Chem.* **2019**, *283*, 590–601, doi:10.1016/j.snb.2018.09.117.
4. Ma, R.-J.; Li, G.-D.; Zou, X.X.; Gao, R.Q.; Chen, H.; Zhao, X. Bimetallic Pt–Au nanocatalysts decorated In₂O₃ nests composed of ultrathin nanosheets for Type 1 diabetes diagnosis. *Sens. Actuators B Chem.* **2018**, *270*, 247–255, doi:10.1016/j.snb.2018.05.028.
5. Fan, F.Y.; Zhang, J.J.; Li, J.; Zhang, N.; Hong, R.R.; Deng, X.C.; Tang, P.G.; Li, D.Q. Hydrogen sensing properties of Pt–Au bimetallic nanoparticles loaded on ZnO nanorods. *Sens. Actuators B Chem.* **2017**, *241*, 895–903, doi:10.1016/j.snb.2016.11.025.
6. Mutinati, G.C.; Brunet, E.; Koeck, A.; Steinhauer, S.; Yurchenko, O.; Laubender, E.; Urban, G.; Siegert, J.; Rohrer, K.; Schrank, F.; et al. Optimization of CMOS Integrated Nanocrystalline SnO₂ Gas Sensor Devices with Bimetallic Nanoparticles. *Procedia Eng.* **2014**, *87*, 787–790, doi:10.1016/j.proeng.2014.11.679.
7. Madler, L.; Sahm, T.; Gurlo, A.; Grunwaldt, J.-D.; Barsan, N.; Weimar, U.; Pratsinis, S.E. Sensing low concentrations of CO using flame-spray-made Pt/SnO₂ nanoparticles. *J. Nanopart. Res.* **2006**, *8*, 783–796, doi:10.1007/s11051-005-9029-6.



© 2019 by the authors. Licensee MDPI, Basel, Switzerland. This article is an open access article distributed under the terms and conditions of the Creative Commons Attribution (CC BY) license (<http://creativecommons.org/licenses/by/4.0/>).

Towards the Miniaturization of Electronic Nose as Personal Measurement Systems [†]

Jesús Lozano *, Félix Meléndez, Patricia Arroyo, José Ignacio Suárez, José Luis Herrero, Pablo Carmona and Juan Álvaro Fernández

Industrial Engineering School, University of Extremadura, Av. Elvas s/n, 06006 Badajoz, Spain; felixmv@unex.es (F.M.); parroyoz@unex.es (P.A.); jmarcelo@unex.es (J.I.S.); jherrero@unex.es (J.L.H.); pablo@unex.es (P.C.); jalvarof@unex.es (J.A.F.)

* Correspondence: jesuslozano@unex.es

† Presented at the 8th GOSPEL Workshop. Gas Sensors Based on Semiconducting Metal Oxides: Basic Understanding & Application Fields, Ferrara, Italy, 20–21 June 2019.

This study addresses the development of a miniaturized wireless sensing module (electronic nose) for a personal use in air quality detection. The proposed prototype has been developed as a test device for digital gas sensors and it includes 4 different: BME680 from Bosch Sensortech, CCS811 from Cambridge CMOS (ams), iAQ-Core from AppliedSensors (ams) and SGP30 from Sensirion. The core of the system is based on a high performance 32-bit microcontroller, model PIC32MM0256GPM048, from Microchip. The obtained data values are transmitted to the Smartphone through a Bluetooth communication module.

1. Introduction

As an alternative to classical analytical instruments, the combination of non-specific gas sensors with enhanced features (low cost, low power, low size) combined with pattern recognition methods could develop largely portable intelligent systems. This approach will allow for massive, distributed and ubiquitous measurements of atmospheric contaminants of the spatial and temporal resolution. This new generation of intelligent detection systems (based on the use of smartphones and other smart devices) will enable the citizens to monitor the quality of the surrounding atmosphere or use them as personal assistant to monitor diseases through the breath or test the quality of food and beverages; then, when necessary, taking measures in order to protect their health and wellness. In this sense, enhanced characteristics are required to the main components needed to develop these personal systems, e.g., low size and consumption sensors for the integration in very small and portable measurement systems, instrumentation and control systems with high precision and repeatability, low consumption and size with communication capabilities. Last but not less important, a machine learning system based on cloud or remote computing could be employed for signal and data processing of sensors and to save the computing power of smart devices used for control and monitoring.

In the last years, an important evolution of gas sensors has occurred from tube-type gas sensor of the 80's (Figaro and FIS among others) with a size higher than 17 mm diameter and a consumption of hundreds of mW to the latest commercial devices. Nowadays, MEMS based gas sensors (Figaro TGS1800, ams CCS801), Sgx Sensortech can be found in the market with a very low size (3 × 4 mm) and consumption (less than 15 mW). Other interesting sensors for integration in small and personal measurement systems are multisensor arrays with digital communication (via I2C or SPI interface). The main purpose of this work and of the device developed and showed in Figure 1 is to test these devices and analyze the response obtained from the digital sensors.

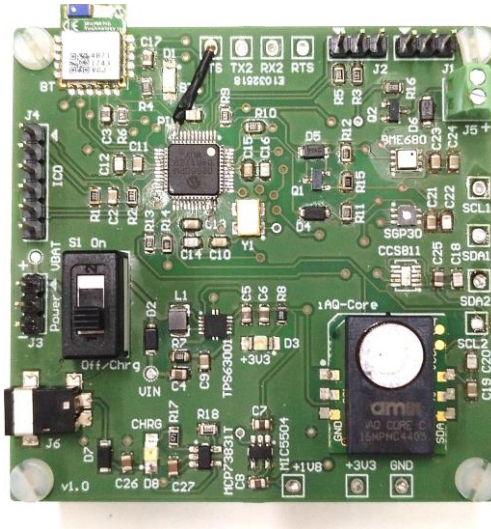


Figure 1. Image of the proposed electronic nose.

2. E-Nose Description

The sensor module is controlled by a microcontroller and it includes two power supplies (3.3 V and 1.8 V), a battery charger, a Bluetooth module and four digital sensors. It also has two UART ports (one of them to communicate to others 3.3 V devices and the other one to 5 V devices) and a terminal block for a solenoid valve connection. The block diagram of the module is depicted in Figure 2. The core of the system is based on a high performance 32-bit microcontroller, model PIC32MM0256GPM048, from Microchip. It has up to 24 analog to digital (A/D) 10/12-bit input channels, 256 Kbytes of program memory, 32 Kbytes of data memory, 9 Capture/Compare/PWM (CCP) modules, 3 Inter-Integrated Circuit (I2C) modules, 3 Universal Synchronous Asynchronous Receiver Transmitter (USART) modules, and a maximum operating speed of 25 MHz. The communications module is a Bluetooth 4.2 Low Energy module, the RN4871 from Microchip. Among its main features include UART Transparent Service for serial data applications, ASCII command interface API over UART and a compact form factor (9 mm × 11.5 mm) with an on-board ceramic chip antenna.

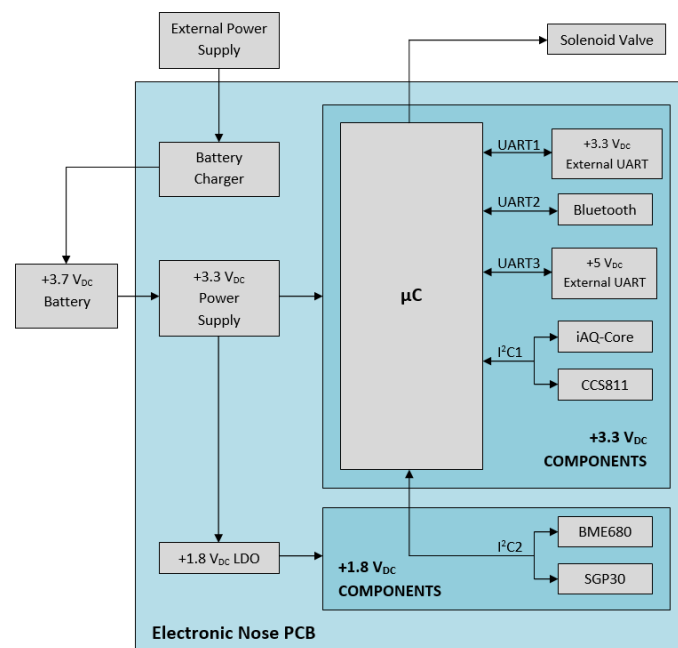


Figure 2. Block diagram of the electronic nose.

3. Results

Three of the sensors, CCS811, iAQ-Core and SGP30, return processed data of signals, but BME680 returns unprocessed data of signals, so additional processing of the signal is needed. As an example, different measurements with volatile organic compounds are made in order to test and analyze the response of the through I2C communication between the microcontroller and the sensor. These sensors provide the data in only one command communication. Depending on the model of the sensors, it sends the concentration of CO₂ (ppm), then the status of the sensor, the value of the sensor gas resistance (k Ω), and finally the concentration of volatile organic compounds (ppb), temperature, humidity or pressure data, and also some or all of them.



© 2019 by the authors. Licensee MDPI, Basel, Switzerland. This article is an open access article distributed under the terms and conditions of the Creative Commons Attribution (CC BY) license (<http://creativecommons.org/licenses/by/4.0/>).

Abstract

A Novel Modular System for Breath Analysis Using Temperature Modulated MOX Sensors [†]

Carsten Jaeschke ^{1,2,*}, Oriol Gonzalez ^{2,*}, Marta Padilla ^{2,*}, Kaylen Richardson ², Johannes Glöckler ¹, Jan Mitrovics ² and Boris Mizaikoff ¹

¹ Institute of Analytical and Bioanalytical Chemistry, University of Ulm, Albert-Einstein-Allee 11, 89081 Ulm, Germany; johannes.gloeckler@uni-ulm.de (J.G.); boris.mizaikoff@uni-ulm.de (B.M.)

² JLM Innovation GmbH, Vor dem Kreuzberg 17, 72070 Tuebingen, Germany;

kaylen.richardson@jlm-innovation.de (K.R.); jan.mitrovics@jlm-innovation.de (J.M.)

* Correspondence: carsten.jaeschke@jlm-innovation.de (C.J.); oriol.gonzalez@jlm-innovation.de (O.G.); marta.padilla@jlm-innovation.de (M.P.)

[†] Presented at the 8th GOSPEL Workshop. Gas Sensors Based on Semiconducting Metal Oxides: Basic Understanding & Application Fields, Ferrara, Italy, 20–21 June 2019.

Abstract: In this work, a new generation of gas sensing systems specially designed for breath analysis is presented. The developed system comprises a compact modular, low volume, temperature-controlled sensing chamber with three compartments that can host different sensor types. In the presented system, one compartment contains an array of 8 analog MOX sensors and the other two 10 digital MOX sensors each. Here, we test the system for the detection of low concentrations of several compounds.

Keywords: gas sensor array; MOX sensors; VOCs; breath analysis

1. Introduction

Breath analysis is becoming an important field of research, since it has been proved that some volatile organic compounds (VOCs) present in the human breath can be potential biomarkers for several diseases [1]. The analysis of breath can therefore be used as a diagnosis or a therapy progress monitoring method, being very convenient for the patient because breath sampling is not invasive and thus not painful [1]. Currently, the experimental techniques for detection of VOCs in exhaled breath is gas chromatography coupled to mass spectrometry (GC-MS) and proton-transfer reaction-mass spectrometry (PTR-MS). These techniques are very powerful, but they need highly skilled operating personnel, are time consuming and have high costs. As an alternative, breath analysis based on gas sensors would be fast, low cost, portable and easier to operate [2].

In this work, we present a novel sensor-based system for breath analysis—the Modular Breath Analyzer (MBA) and show results of initial tests aiming to detect low concentrations of several VOCs of interest.

2. Materials and Methods

The MBA contains a breath sampling unit for direct collection of the exhaled breath, and a compact modular, low volume, temperature-controlled sensing chamber with three exchangeable compartments capable of hosting up to 30 sensors. This versatile modular sensor system allows the combination of different sensor types within one device. The sensors can be commercial or experimental, only the circuitry of one compartment must be updated to incorporate a new sensor array to the MBA. Therefore, the MBA is an excellent platform for testing new sensor technologies applied to breath analysis. Figure 1 shows an external (a) and an internal view of the MBA with its components (b), as well as a list of the series of MOX sensors used; an array of 8 analog MOX sensors,

and two arrays with 10 digital MOX sensors each, 4 of which are modulated in temperature. Thus, a total of 36 sensors (real and virtual).

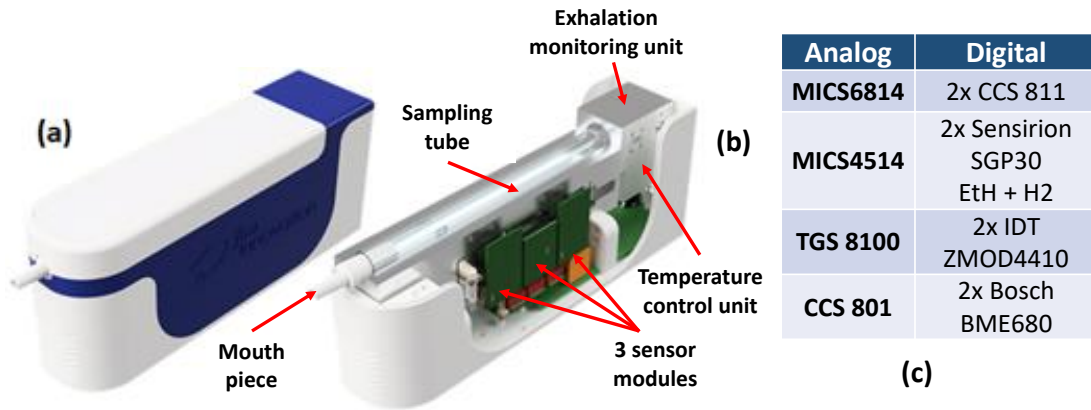


Figure 1. External (a) and internal view of the MBA system (b), and list of MOX sensors (c).

The breath sampling unit is designed to capture the deep portion of the exhaled breath (alveolar breath) which contains the VOCs biomarkers related to the disease of interest. In the two experiments shown here the breath sampling unit was excluded, thus the air sample is directly driven to the sensing chamber.

The aim is to test the MBA with samples similar to human breath: VOCs of interest at body temperature and high humidity. At this moment, two preliminary experiments have been performed; a first experiment to detect several VOCs at different low concentrations (isopropanol, isoprene, n-pentane from 5 to 10 ppm, and acetone from 80 to 500 ppb) under dry conditions, and a second experiment to detect acetone and ethanol (3 to 18 ppm) under moderate humidity conditions (22% RH). Before and after exposing the sensors to the analytes during 10 min, the sensors were cleaned with synthetic air during 10 min.

3. Results and Conclusions

Figure 2a shows some of the raw sensors signals and Figure 2b a scores plot of a Principal Component Analysis with first results, showing that the VOCs can be easily differentiated with the MBA. More experiments will be performed to test the MBA in real human breath conditions.

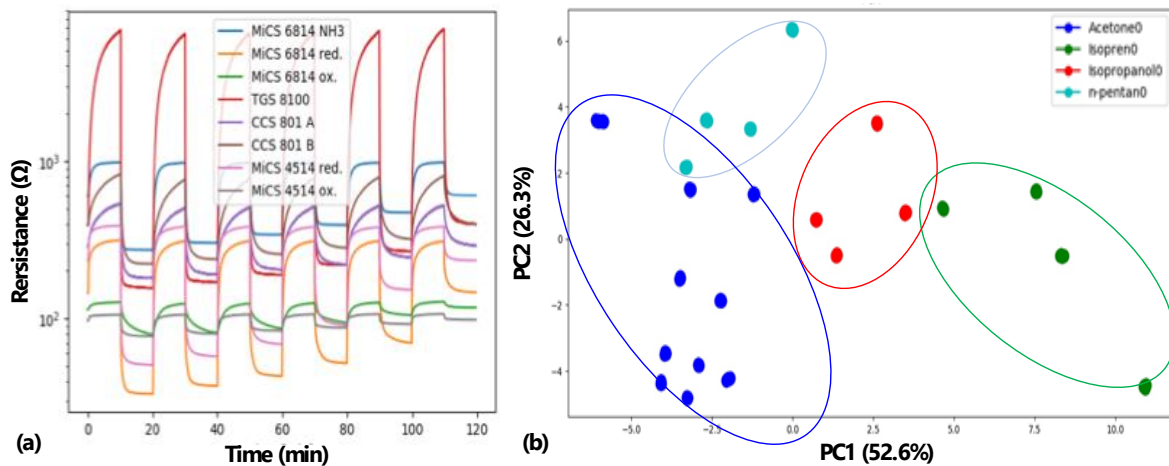


Figure 2. Raw signals from analog MOX sensors in one of the three compartments responding to several concentrations (3–18 ppm) of ethanol at 22% of RH and 45 °C (a), and PCA scores plot of 25 measurements from first experiment (b).

References

1. Miekisch, W.; Schubert, J.K.; Noeldge-Schomburg, G.F.E. Diagnostic potential of breath analysis—focus on volatile organic compounds. *Clin. Chim. Acta.* **2004**, *347*, 25–39.
2. Buszewski, B.; Keszy, M.; Ligor, T.; Amann, A. Human exhaled air analytics: Biomarkers of diseases. *Biomed. Chromatogr.* **2007**, *21*, 553–566.



© 2019 by the authors. Licensee MDPI, Basel, Switzerland. This article is an open access article distributed under the terms and conditions of the Creative Commons Attribution (CC BY) license (<http://creativecommons.org/licenses/by/4.0/>).

Abstract

Elaboration and Characterization of SnO₂ Doped TiO₂ Gas Sensors Deposited through Dip and Spin Coating Methods [†]

Zineb Essalhi ¹, Soufiane Krik ², Bouchaib Hartiti ¹, Andrea Gaiardo ², Abderrazak Lfakir ³, Matteo Valt ², Salah Fadili ¹, Barbara Fabbri ², Maryam Siadat ⁴, Vincenzo Guidi ² and Philippe Thevenin ⁵

¹ ERDyS Laboratory, MEEM&DD Team, Department of Physics, FSTM, University Hassan II Casablanca, Mohammedia, Morocco; zineb.essalhi@gmail.com (Z.E.)

² Department of Physics and Earth Sciences, University of Ferrara, 44122 Ferrara, Italy

³ Department of Physics, FSTB, University My Slimane, Béni Mellal, Morocco

⁴ LCOMS Laboratory, University of Lorraine, Metz, France

⁵ LMOPS Laboratory, University of Lorraine, Metz, France

[†] Presented at the 8th GOSPEL Workshop. Gas Sensors Based on Semiconducting Metal Oxides: Basic Understanding & Application Fields, Ferrara, Italy, 20–21 June 2019.

Abstract: Semiconductor functional materials play an increasingly important role in science and technology because of their unique optical, electrical, magnetic, catalytic and chemical properties. They are widely used in fields such as solar cell, photo-catalysts, optical coating, capacitors for large scale integrated devices, electrochromic systems and gas sensors. One important application for semiconductor gas sensors is the detection of pollutant gases for the control of the combustion process.

Nanostructured titanium dioxide (TiO₂) is a cheap, non-toxic and biodegradable materials that is widely used in industry. For gas sensing application, it can be used as sensing elements for chemoresistive gas sensors. The physical properties of such materials and their electrical performance largely depend on their methods of production. Nowadays, considerable efforts were dedicated to enhance the TiO₂ sensing performance, e.g., by adding dopants or metal/metal-oxide decorations in the sensing layer.

In this work, we used sol-gel method associated to spin and dip coating techniques to produce titanium dioxide mixed with tin dioxide (TiO₂/SnO₂) and pure TiO₂ thin films, the concentrations of SnO₂ used are 3 and 7%. The samples were mainly characterized by means of X-ray Diffraction (XRD) and Scanning Electron Microscopy (SEM).

The SEM characterization highlighted a nanostructured morphology of the films prepared and homogeneous layers of TiO₂ and TiO₂/SnO₂ deposited onto alumina substrates (Figure 1).

The electrical characterization of the sensors produced was performed for two different gases (Ethanol and Ethylene), both in dry air and in presence of different percentages of relative humidity.

Only TiO₂/SnO₂(7%) deposited using spin coating technique gave a good response in both dry and wet air, to different concentrations of ethanol (Figure 2). It can be seen from Figure 2 that the sensor gave relatively low gas sensing response to this gas target, but the sensor resulted to be not affected by the presence of the humidity, highlighting about the same response values both in dry and wet air.

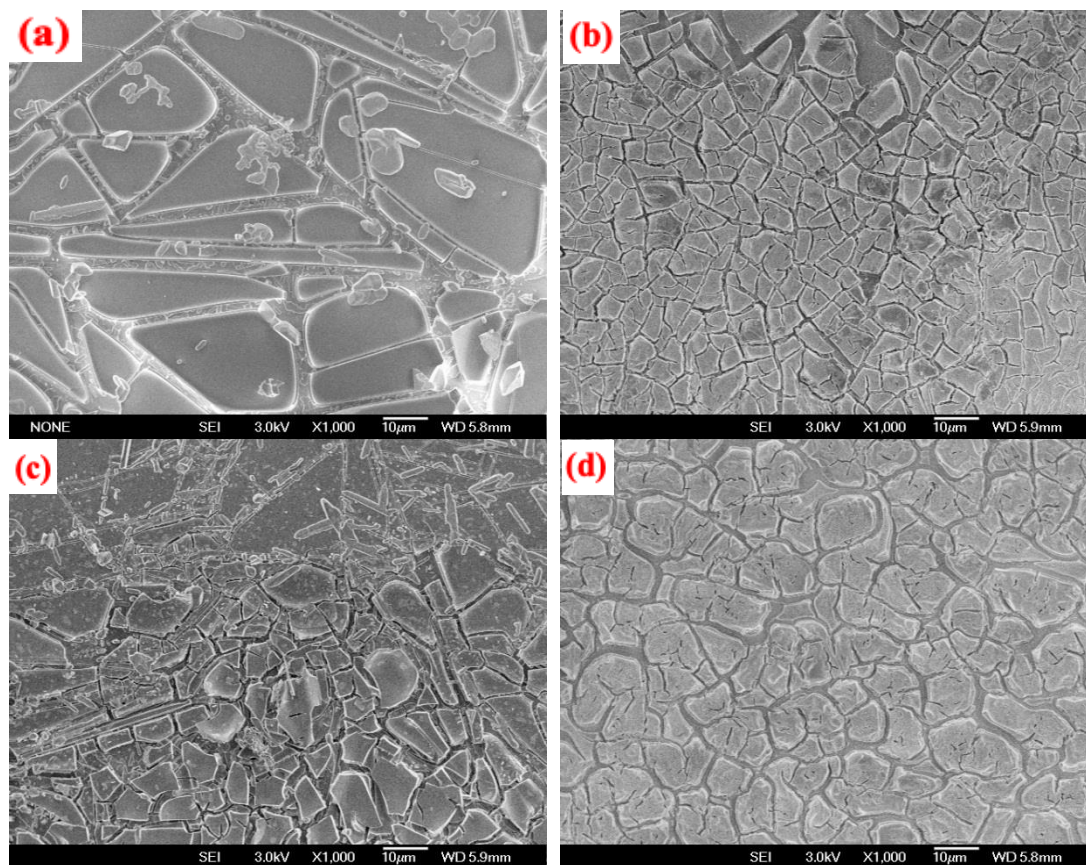


Figure 1. SEM images of synthesized samples ((a): Undoped TiO₂ using dip coating (b) SnO₂ doped TiO₂ using spin coating, (c) Undoped TiO₂ using spin coating and (d) SnO₂ doped TiO₂ using dip coating).

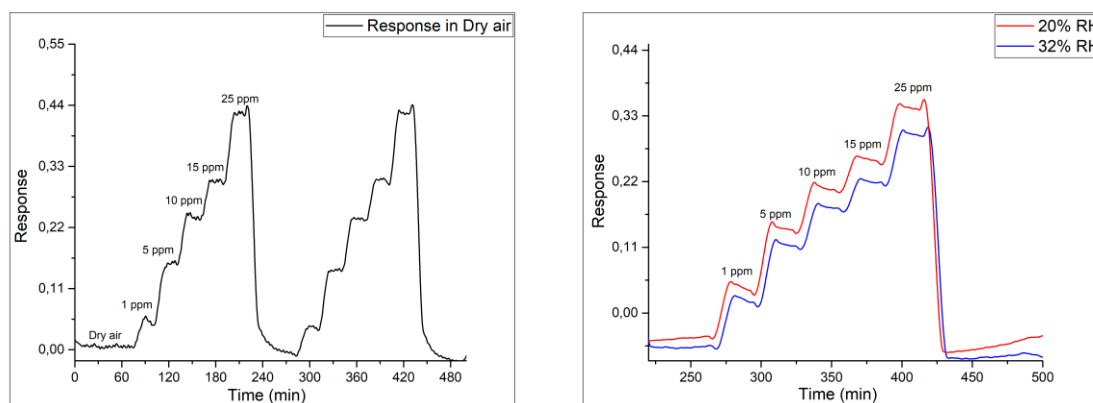


Figure 2. Response of TiO₂/SnO₂ to Ethanol in both dry air and in the presence of relative humidity with $Response = \frac{G_{gas} - G_{air}}{G_{air}}$.



© 2019 by the authors. Licensee MDPI, Basel, Switzerland. This article is an open access article distributed under the terms and conditions of the Creative Commons Attribution (CC BY) license (<http://creativecommons.org/licenses/by/4.0/>).

Influence of Oxygen Vacancies in Gas Sensors Based on Tin Dioxide Nanostructure: A First Principles Study [†]

Soufiane Krik ^{1,2,*}, Andrea Gaiardo ^{1,2}, Matteo Valt ¹, Barbara Fabbri ¹, Cesare Malagù ¹, Pierluigi Bellutti ² and Vincenzo Guidi ¹

¹ Department of Physics and Earth Sciences, University of Ferrara, 44122 Ferrara, Italy; andrea.gaiardo@unife.it (A.G.); matteo.valt@unife.it (M.V.); barbara.fabbri@unife.it (B.F.); malagu@fe.infn.it (C.M.); guidi@fe.infn.it (V.G.)

² Center of Materials and Microsystems, Bruno Kessler Foundation, 38128 Trento, Italy; bellutti@fbk.eu (P.B.)

* Correspondence: soufiane.krik@unife.it

[†] Presented at the 8th GOSPEL Workshop. Gas Sensors Based on Semiconducting Metal Oxides: Basic Understanding & Application Fields, Ferrara, Italy, 20–21 June 2019.

The use of computer simulations for performance predictions has become almost essential. In the gas sensing field, the simulation of the physical-chemical properties of (Metal Oxide) MOX semiconductors can be used to predict the performance of sensors based on the material studied.

Tin dioxide is a typical n-type semiconducting material with a wide band gap of 3.6 eV [1]. It has attracted the attention of many researchers due to its broad spectrum of physical-chemical properties, indeed it has been used in several fields such as optoelectronic devices, electrocatalysis, ceramics and gas sensors. SnO₂ is the most studied semiconductor as sensing layer for chemoresistive gas sensors production [2]. Then, it represents the best candidate for the innovative work here proposed.

So far, literature presents lacks of studies on how number and arrangement of oxygen vacancies affects the sensing performance of chemoresistive gas sensors, which usually needs a high operating temperature. Therefore, in order to enhance the behavior of SnO₂ as active element in gas sensors devices, we propose a study concerning the impact of oxygen vacancies on its physical-chemical properties. Structural, electronic and electrical properties of the stoichiometric SnO₂ and the reduced one were studied.

A series of first principles study was carried out using the Full Potential Linearized Augmented Plane Wave (FP-LAPW) method [3] within the framework of Density Functional Theory (DFT) as implemented in the Wien2k code [4]. The principle of DFT simulations is to calculate the physical-chemical properties by solving the Kohn and Sham equation.

The results showed a high electrical conductivity for samples with oxygen vacancies, which can give a decrease of the temperature that sensing material needs to be thermo-activated. The position of the impurity states is one of the important parameters, which involve the reactions on the material surface. Indeed, the arrangement of the impurities impact on the Energy that is necessary to ionize the impurity states.

Figure 1 illustrates the total density of state (DOS) of the stoichiometric SnO₂ and the reduced ones with two different concentration (3.125 and 9.375%) of oxygen vacancies. It can be seen from this figure that in the case of reduced compounds, the impurity states are found to be present in the energy gap regions and, by increasing the concentration of the defects studied the positions of these states change and the excitation of electrons from this level will need less energy then.

The simulated results show an important impact of the oxygen vacancies on the electronic and electrical properties of SnO₂, which lead to experimental investigations to modify and tailor MOX semiconductors for gas sensing applications.

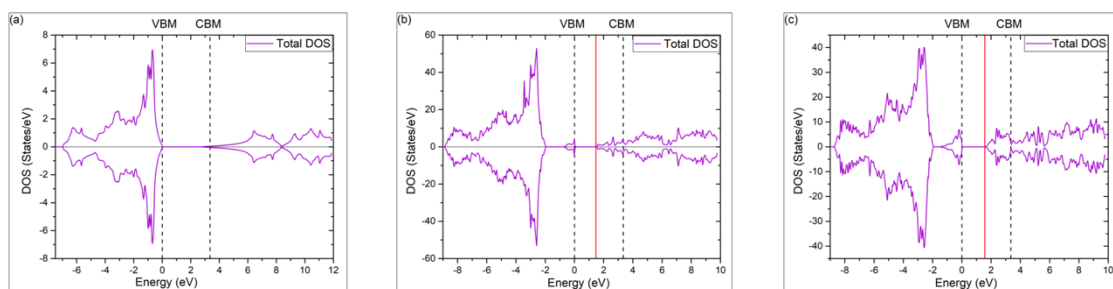


Figure 1. Total Density of States of (a): stoichiometric SnO₂ (b) and (c) are Reduced SnO₂ (Sn₁₆O₃₁ and Sn₁₆O₂₉, respectively).

References

1. Batzill, M.; Diebold, U. The surface and materials science of tin oxide. *Progress Surf. Sci.* **2005**, *79*, 47–154.
2. Wang, C.; Yin, L.; Zhang, L.; Xiang, D.; Gao, R. Metal oxide gas sensors: Sensitivity and influencing factors. *Sensors* **2010**, *10*, 2088–2106.
3. Andersen, O.K. Linear methods in band theory. *Phys. Rev. B* **1975**, *12*, 3060–3083.
4. Blaha, P.; Schwarz, K.; Madsen, G.; Kvasnicka, D.; Luitz, J. *WIEN2k, An Augmented Plane Wave Plus Local Orbitals Program for Calculating Crystal Properties*, 2nd ed.; Vienna University of Technology: Vienna, Austria 2001.



© 2019 by the authors. Licensee MDPI, Basel, Switzerland. This article is an open access article distributed under the terms and conditions of the Creative Commons Attribution (CC BY) license (<http://creativecommons.org/licenses/by/4.0/>).

Morphological Control of Metal Oxide for Semiconductor-Based Gas Sensor [†]

Takeshi Hashishin ¹, Jian Sun ², Kazuyoshi Sato ³ and Hiroshi Kubota ²

¹ Faculty of Advanced Science and Technology, Kumamoto University, 2-39-1 Kurokami, Chuo-ku, Kumamoto 860-8555, Japan

² Graduate School of Science and Technology, Kumamoto University, 2-39-1, Kurokami Chuo-ku, Kumamoto 860-8555, Japan; 186d8884@st.kumamoto-u.ac.jp (J.S.); kubota@cs.kumamoto-u.ac.jp (H.K.)

³ Graduate School of Science and Technology, Gunma University, 1-5-1 Tenjin-cho, Kiryu, Gunma 376-8515, Japan; kazuyoshi-sato@gunma-u.ac.jp

* Correspondence: hashishin@msre.kumamoto-u.ac.jp

[†] Presented at the 8th GOSPEL Workshop. Gas Sensors Based on Semiconducting Metal Oxides: Basic Understanding & Application Fields, Ferrara, Italy, 20–21 June 2019.

Morphological control of metal oxide (MO) is important for enhancement of sensing properties such as sensor response and response-recovery characteristics. Our research group has been developed MO based gas sensors fabricated by WO₃ and SnO₂ nanocrystals synthesized by hydrothermal method for high sensor response to NO₂ or H₂ [1,2]. On the other hand, shuttle-shape SnO₂ showed the sensor response to NO₂ and H₂S at room temperature.

The film sensor with cuboid-shape monoclinic WO₃ nanocrystal (Figure 1a) showed sensor response (R_g/R_a) of 10²–10⁴ to 0.05–1 ppm NO₂ at 200 °C (Figure 1c). In contrast, the sensor with hexagonal-shape hexagonal WO₃ nanocrystal (Figure 1b) showed sensor response lower one order of magnitude than that with cuboid-shape monoclinic WO₃ in above same detection condition (Figure 1d). This difference was related to surface states. XPS spectra of O1s showed that the content of OH⁻ was larger for hexagonal-shape hexagonal WO₃ (O²⁻/OH⁻/H₂O (in %) = 60.0/38.1/1.9, in Figure 1e) than for cuboid-shape monoclinic WO₃ (80.4/4.9/14.7, in Figure 1f). The results suggested that the high content of oxygen adsorbate (O²⁻) on the surface of WO₃ could be contributed to higher sensor response.

The SnO₂ nanocrystals were prepared by hydrothermal treatment with tetramethyl ammonium hydroxide (N(CH₃)₄OH; TMAH). The alkaline solutions of KOH and NaOH were also used instead of TMAH. The nanocrystals were grown at 150 °C for 24 h depending on the pH value. N(CH₃)₄⁺ adsorbed on the surface of SnO₂ nanocrystals. The size of the nanocrystals were finer than those grown with KOH and NaOH. The nanocrystals of Figure 2a had the cubic shape consisted in the (001) and (110) faces in the case of using TMAH as an alkaline solution. The film sensor with cuboid-shape tetragonal SnO₂ nanocrystal showed the sensor response (R_a/R_g) of 300 to 1000 ppm H₂ at 200 °C. This sensor response was 100 times higher than the film sensor with irregular-shape SnO₂ nanocrystal.

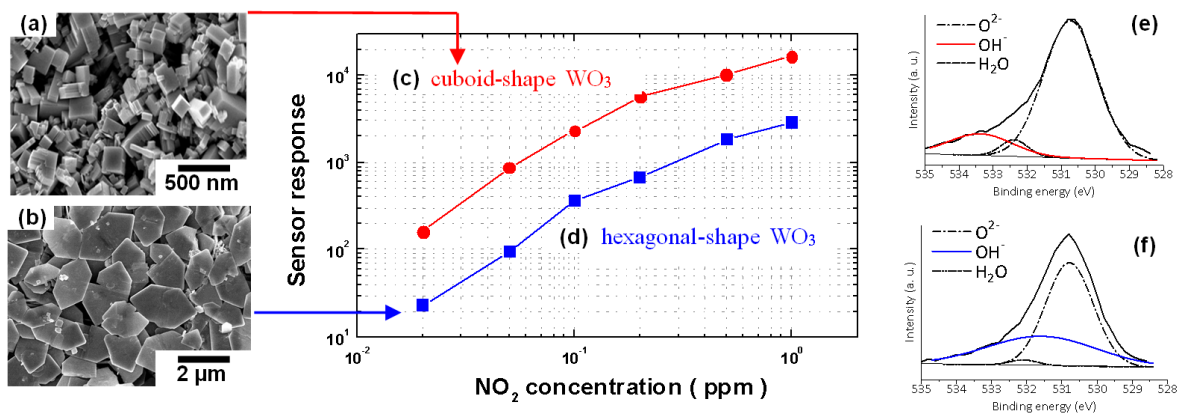


Figure 1. FE-SEM images of (a) cuboid-shape monoclinic WO₃ nanocrystal and (b) hexagonal-shape hexagonal WO₃ nanocrystal. Sensor response as a function of NO₂ concentration for (c) cuboid-shape WO₃ and (d) hexagonal-shape WO₃. XPS spectra of O 1s on the surface of (e) as-prepared cuboid-shape WO₃ and (f) hexagonal-shape WO₃.

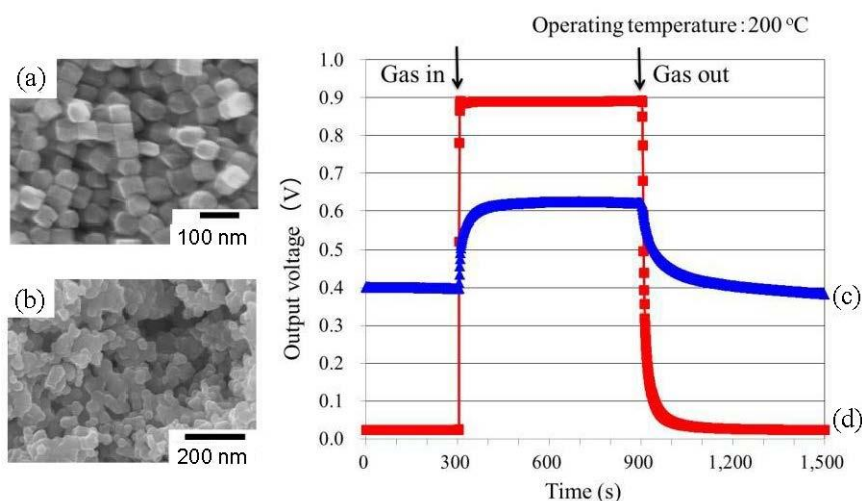


Figure 2. FE-SEM images of (a) SnO₂ nanocubes annealed at 250 °C for 3 h and (b) commercial SnO₂ nanoparticles calcined at 1100 °C. Response-recovery transients of (c,d) to respective gas mixture of 1000 ppm H₂ and air.

References

- Meng, Z.; Fujii, A.; Hashishin, T.; Wada, N.; Sanada, T.; Tamaki, J.; Kojima, K.; Haneoka, H.; Suzuki, T. Morphological and crystal structural control of tungsten trioxide for highly sensitive NO₂ gas sensors. *J. Mater. Chem. C* **2015**, *3*, 1134–1141.
- Sato, K.; Yokoyama, Y.; Valmalette, J.C.; Kuruma, K.; Abe, H.; Takarada, T. Hydrothermal Growth of Tailored SnO₂ Nanocrystals. *Cryst. Growth. Des.* **2013**, *13*, 1685–1693.



© 2019 by the authors. Licensee MDPI, Basel, Switzerland. This article is an open access article distributed under the terms and conditions of the Creative Commons Attribution (CC BY) license (<http://creativecommons.org/licenses/by/4.0/>).

ZnO Nanostructures for Gas Sensing Applications: From Tetrapods-Based Chemoresistive Devices to Carbon Fiber Integration [†]

Daive Calestani ^{*}, Marco Villani, Maurizio Culiolo, Nicola Coppedè and Andrea Zappettini

IMEM-CNR, Institute of Materials for Electronics and Magnetism, Parco Area delle Scienze 37/A, I-43124 Parma, Italy; marco.villani@imem.cnr.it (M.V.); Maurizio.culiolo@imem.cnr.it (M.C.); nicola.coppede@imem.cnr.it (N.C.); andrea.zappettini@imem.cnr.it (A.Z.)

^{*} Correspondence: daive.calestani@imem.cnr.it

[†] Presented at the 8th GOSPEL Workshop. Gas Sensors Based on Semiconducting Metal Oxides: Basic Understanding & Application Fields, Ferrara, Italy, 20–21 June 2019.

1. Introduction

Zinc oxide (ZnO) nanostructures can be grown in different morphologies by means of a wide range of techniques. Although the strong evidence of their gas sensing capabilities has been reported in several papers, not all of them are suitable for a large-scale or industrial scale production of gas sensor devices.

Among the several ZnO nanostructures that have been grown so far at IMEM-CNR Institute, we focused our attention on tetrapods (TPs), because a vapour phase growth process that can produce grams of these nanostructures have been designed and optimized in our laboratories. This quantity of nanostructures, produced in a small lab-scale reactor, is enough to prepare several thousands of gas sensing devices. Moreover, the produced ZnO-TPs are free-standing and not constrained to a growth substrate, and can be easily suspended in a liquid media.

The highly-porous entangled network of ZnO-TPs, which can be obtained by direct deposition on sensor substrate, demonstrated to efficiently work as chemoresistor, while its sensing properties (sensitivity, selectivity, ...) can be tuned or modified through the functionalization of TPs surface with other materials (noble metals, inorganic semiconductor nanoparticles, organic semiconductor layers).

At the same time, ZnO nanostructures and their multifunctional properties can be used to functionalize the surface of other materials and, eventually, add to them sensing capabilities. As a meaningful example, we can illustrate the adding of ZnO nanorods (ZnO-NRs) to the surface of carbon fibers with a wet chemical process that is easily scalable to a larger scale.

It has been recently demonstrated that two crossing ZnO-functionalized carbon fibers can be used to sense and transduce a piezoelectric signal or UV light, as well as a chemoresistive information.

2. Gas Sensors Based on ZnO Tetrapods

ZnO-TPs are obtained by evaporating cheap metallic zinc powders in a controlled stream of inert gas and oxygen. At the end of the process, a large veil of electrostatically bonded nanostructures can be easily collected from the growth reactor. By suspending these nanostructures in an alcoholic solution, it is possible then to deposit the nanostructures on different substrates with contacts for collecting the electric signal and heaters to control the sensing element temperature. Proper methods have been optimized and successfully tested for both simple alumina substrates and micromachined MEMS micro-membrane substrates. Dynamic responses are reported both for not-functionalized

ZnO-TPs and ZnO-TPs functionalized with cadmium sulphide (CdS) and titanyl-phthalocyanine (TiO-PC) to show and compare the original and modified sensing properties of these nanostructures.

3. Sensing by ZnO Nanorods Integrated in Carbon Fibers

Carbon fibers have been functionalized with a brush-like layer of ZnO-NRs, aligned perpendicularly to the fiber surface. The functionalization has been obtained thanks to a two-steps process. The first one is for the deposition of a ZnO seed layer by Silar-technique. The second one is for the growth of 1–2 μm long NRs by chemical bath deposition, dipping them in a closed reactor containing equimolar zinc acetate and hexamethylenetetramine aqueous solution (20 mM) at 90 °C for 4h, during which NWs grew.

To demonstrate the working principle, two 4 cm long carbon fibers, functionalized with ZnO-NWs only in their central part, were placed in a crossing configuration, touching each other in a single point in the middle. Electrically conductive carbon fibers were used to transduce the signal from that point, while ZnO-NRs were self-heated by Joule effect thanks to the flowing electrical current. A very fast response and high response is observed towards the testing volatile organic (ethanol). The peculiar response dynamic is a combination of resistance variation and temperature variation, because of the different current flowing through the intersection point.

These results can be then considered as the basis to turn a carbon fiber texture into a “smart” array of different micron-scale sensors.



© 2019 by the authors. Licensee MDPI, Basel, Switzerland. This article is an open access article distributed under the terms and conditions of the Creative Commons Attribution (CC BY) license (<http://creativecommons.org/licenses/by/4.0/>).